



# The Sizewell C Project

## 9.31 Storm Erosion Modelling of the Sizewell C Soft Coastal Defence Feature using XBeach-2D and XBeach-G

---

Revision: 3.0  
Applicable Regulation: Regulation 5(2)(q)  
PINS Reference Number: EN010012

---

September 2021

Planning Act 2008  
Infrastructure Planning (Applications: Prescribed  
Forms and Procedure) Regulations 2009



## BRITISH EDF ESTUARINE & MARINE STUDIES

|                                     |  |
|-------------------------------------|--|
| Technical Report Series:            | TR545: Storm erosion modelling of the Sizewell C Soft Coastal Defence Feature using the XBeach modelling suite |
| Sub-Contract Report Original Title: | Storm erosion modelling of the Sizewell C Soft Coastal Defence Feature using the XBeach modelling suite        |

### Summary of Purpose & Value to BEEMS

Cefas commissioned the Coastal Marine Applied Research (CMAR) Group at the University of Plymouth to provide an independent assessment of the erosion potential of the Soft Coastal Defence Feature (SCDF) proposed at Sizewell C. Whilst Cefas have reviewed and Quality Controlled Edition 1 of the report, it is a CMAR report. Citations to relevant BEEMS reports within this report were provided by Cefas to CMAR for purposes of aligning the report to the Development Consent Order (DCO) Application. These reports have not been reviewed by CMAR and therefore comments on these reports are owned by Cefas. Any interpretation of model results relating to engineering decisions regarding the design of the SCDF in this report are owned by Cefas and SZC Co. New modelling of the full decommissioning phase presented in Editions 2 and 3 of the report is conducted by CMAR, which was reviewed and Quality Controlled by Cefas, along with additional text written by Cefas and reviewed by CMAR. This new material was requested by Regulators as part of the Sizewell C Public Examination. No further modelling has been conducted for the operational phase and the conclusions of CMAR from Edition 1 remain unchanged.

Preliminary first stage modelling, by Cefas, developed a 1D sand model using XBeach-S to examine beach erosion under severe storms (BEEMS Technical Report TR531). This initial work assembled real-world storm erosion datasets for Sizewell and used them to undertake model calibration and validation against the present-day natural beach without the SCDF. The results are very conservative estimates of erosion for a severe storm (again for the natural beach only). Specifically, it examined the width and volume eroded for sections of the SZC frontage using the first and second storms (E1 and E2 in this report) in the Beast from the East storm sequence (hereafter referred to as BfE).

The purpose of the initial modelling was to provide preliminary estimates of the scale of erosion to be used to assess the SCDF volumes and provide data to set thresholds for when it needs to be recharged. The final thresholds will be set and incorporated into the Coastal Processes Monitoring and Mitigation Plan (CPMMP) (BEEMS Technical Report TR523), which also sets out the monitoring against which the triggers would be regularly tested.

Sizewell is a composite beach with a sandy subtidal, mixed sand-gravel (shingle) intertidal beach and a pebble supra-tidal beach. There is no single model capable of modelling a mixed sand-gravel beach, nor a more complex composite beach. Therefore, the final thresholds set in the CPMMP will be based on a holistic view of a range of individual sand and gravel models and sensitivity testing.

This report uses the XBeach storm erosion modelling suite (XBeach-Sand 1D & 2D and XBeach -Gravel 1D) to investigate the response of the proposed SCDF to storm wave conditions. The 2D XBeach-S model is used to assess loss (erosion) from the SCDF, whilst the 1D XBeach-S and XBeach-G models are used to investigate the sensitivity of the SCDF to differing sediment sizes. The modelling will inform decisions made in BEEMS Technical Report TR544 and the CPMMP on the recharge threshold, the typical expected recharge intervals (i.e., SCDF maintenance requirements) and the SCDF composition (particle sizes). The main benefit of the 2D modelling is it allows for the inclusion of longshore transport as well as the cross-shore transport, allowing for a more accurate prediction of erosion. Whilst XBeach is capable of modelling near term beach recovery the focus of this study is on storm erosion modelling to determine the maximum losses over individual severe storms. The natural recovery process, in which much or all of the sediment is expected to return, has not been modelled.

In Edition 1 of the report, a new calibration/validation process was undertaken by CMAR for this report and



represents a significant improvement over the preliminary modelling, undertaken and described in BEEMS Technical Report TR531, and more importantly provides a consistent calibration and validation for different storms with a single set of model settings.

Furthermore, this study included a wider range of scenarios to test the erosion potential of the SCDF. These included two distinct storms: (1) a constant storm wave height (equal to the instantaneous 1:20 year return interval wave height) over a single tidal cycle (low tide to low tide; 13 hours) and (2) the full BfE storm sequence (events E1 + E2 + E3, February/March 2018) which is a 1:107 year storm for cumulative power. Both these storms are used to estimate the volume lost during severe storms under present-day sea level and sea level rise (SLR) for 2069 and 2099.

These storm conditions were tested for the present-day shoreline as well as a future naturally severely receded shoreline adjacent to Sizewell C (north and south), which is based on the postulated shoreline at or toward the end of the decommissioning phase without an increase in sediment supply – see Section 7.7 of Volume 2, Appendix 20A of the Sizewell C Environmental Statement (SZC Co., 2020). This case was included because erosion pressure on the SCDF is expected to rise as the adjacent shorelines become more misaligned.

In Edition 2 of the report, further model runs were conducted extending the modelling to the end of the decommissioning phase in 2140. The SCDF is tested against SLR predictions of RCP4.5. The Adaptive Design is predicted to only be required during the decommissioning phase under RCP8.5 SLR conditions. As such, the Adaptive Design is tested against those conditions only. UKCP18 SLR predictions extend to 2100. For SLR rise projections beyond 2100, the UKCP18 exploratory sea level projections for the UK to 2300 have been used.

In addition to new model runs, the design of the HCDF has also been updated, but the position and crest elevation of the SCDF remain unchanged, thereby increasing the beach volume to the north and a reduction to the south. The spatial plots of the operational model runs, presented in Edition 1 will be revisited in a future version of this report. However, the 2D volumes presented in Table 3-1 from Edition 1 have been updated with respect to the new HCDF design to allow comparison with the decommissioning results. Gravel volumes remain unaffected as they are calculated in 1D over an unaffected section of the SCDF. As such the design changes will not affect the conclusions of Edition 1.

In Edition 3 of the report (this Edition), further model runs were conducted, testing the SCDF and the Adaptive Design against the 1:20 year SE storm and the BfE storm during the decommissioning phase, up to 2140. The SCDF is tested against SLR predictions of RCP4.5 with the 1:20 year SE and BfE storm. The Adaptive Design is predicted to only be required during the decommissioning phase under RCP8.5 SLR conditions. As such, the Adaptive Design is tested against those conditions only in relation to the BfE storm.

### **Results – for Editions 1, 2 and 3**

The volume losses for the present-day sea level under the full BfE storm sequence (which in energy terms has a 1:107 year return interval) would lead to an average loss of 16 m<sup>3</sup> of sediment per metre of north-south shoreline (expressed hereafter as m<sup>3</sup>/m). As expected, SLR increases erosion to 22 m<sup>3</sup>/m by 2069 and 27 m<sup>3</sup>/m by 2099. These volumes (present day and 2069) are significantly less than the preliminary stage 1 modelling (BEEMS Technical Report TR531) owing to refined model calibration, however they are still conservative in that they over predict erosion compared to observations.

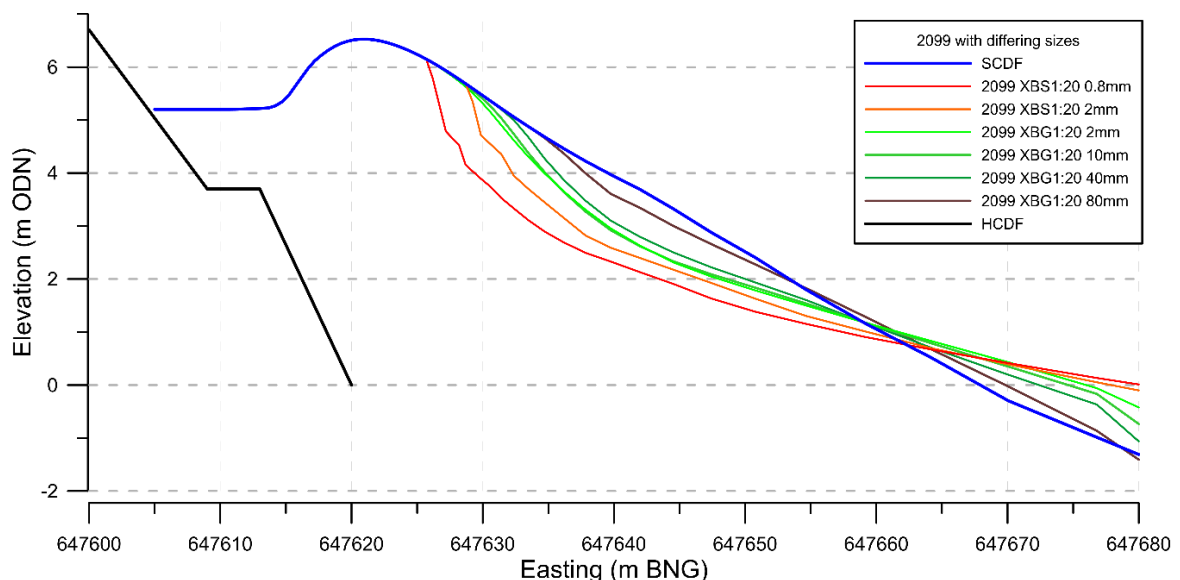
As expected, the model results show that the naturally, severely receded adjacent shorelines north and south of the Sizewell C frontage increase erosion pressure on the SCDF, although the degree of shoreline recession modelled is not expected until after the decommissioning phase. For the BfE storm sequence, the modelled mean erosion with SLR and receded adjacent shorelines is 35 m<sup>3</sup>/m in 2069 and 43 m<sup>3</sup>/m in 2099, but higher localised losses are observed at both ends of the SCDF due to higher wave angles and longshore transport gradients where the shoreline curves from the SCDF to the adjacent frontage. The greatest localised erosion (82 m<sup>3</sup>/m over a 5 m long stretch of frontage) occurred at the northern end of the SCDF under the combined 2099 SLR and receded shoreline model scenario, but even this still left ~70% of the pre-storm subaerial SCDF beach volume intact. Were the adjacent shorelines to become as severely eroded as those modelled, it is likely that the frequency of beach recharge would need to rise in

order to maintain the SCDF, albeit across relatively short sections (10s of metres) of frontage (this conclusion has not changed from Edition 1).

It is worth noting that the severely receded adjacent shorelines take no account of sediment supply to the neighbouring beaches from the eroding SCDF – the modelling indicates that sediment eroded from the SCDF was predicted to feed the beaches immediately north and south of the SCDF, highlighting a likely feedback loop i.e., that adjacent shoreline recession is likely to stimulate the SCDF to supply sediment at a faster rate, countering the natural erosion rate there (for as long as the SCDF is being maintained).

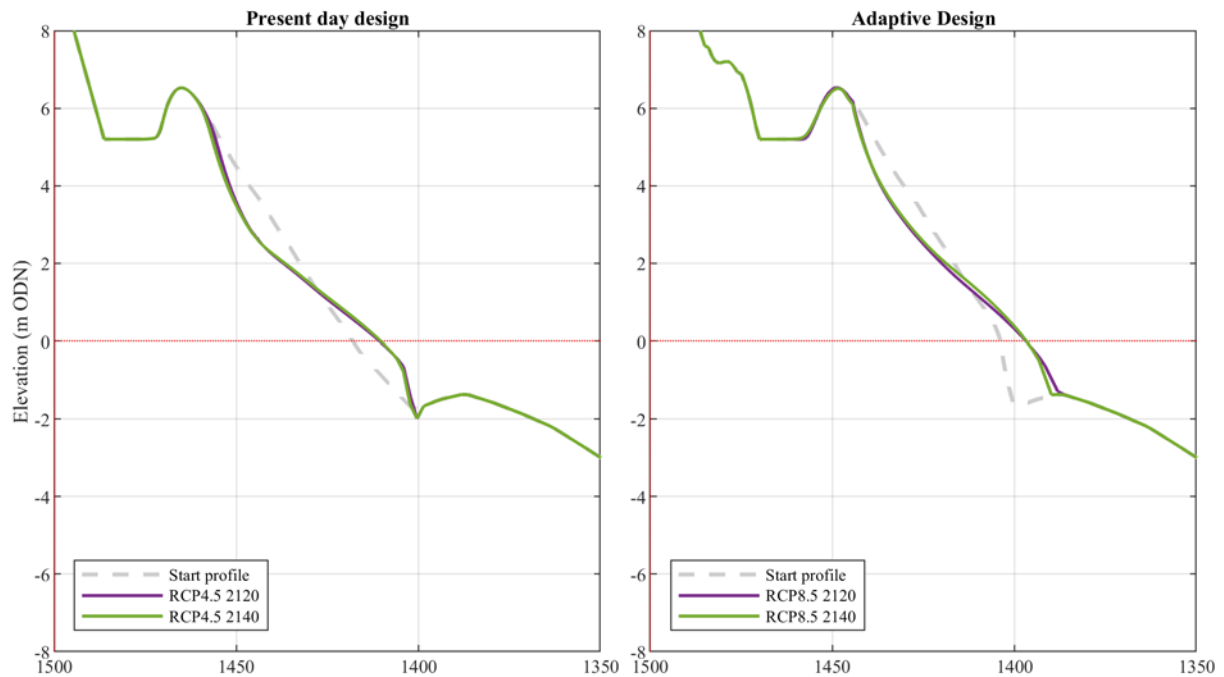
The scenarios modelled in the 1D grain size sensitivity tests indicate that using a larger particle size for the SCDF will increase its resilience to wave erosion arising from storms (see VAS Figure 1). Using very coarse sand/fine pebbles ( $D_{50} = 2 \text{ mm}$ ) resulted in 3-6 times less volumetric erosion of the SCDF (above 0 m ODN) than coarse sand ( $D_{50} = 0.8 \text{ mm}$ ), while medium pebbles ( $D_{50} = 10 \text{ mm}$ ) resulted in 3-9 times less SCDF erosion, and very coarse pebbles ( $D_{50} = 40 \text{ mm}$ ) resulted in 3-12 times less SCDF erosion. Although the design has not been finalised, the default position for SCDF particle size is to match the native size distribution, which has a model pebble size of approximately 10 mm diameter. Fine cobbles ( $D_{50} = 80 \text{ mm}$ ) show a dramatic increase in erosion resistance, with 18-35 times less erosion of the SCDF predicted than with coarse sand. For example, the storm erosion demand on the SCDF during the modelled 1-in-20 year NE storm (2099 sea level), was  $-37 \text{ m}^3/\text{m}$  with the coarse sand ( $D_{50} = 0.8 \text{ mm}$ ),  $-14 \text{ m}^3/\text{m}$  with very coarse sand/fine pebbles ( $D_{50} = 2 \text{ mm}$ ),  $-14 \text{ m}^3/\text{m}$  with medium pebbles ( $D_{50} = 10 \text{ mm}$ ),  $-12 \text{ m}^3/\text{m}$  with very coarse pebbles ( $D_{50} = 40 \text{ mm}$ ), and  $-2 \text{ m}^3/\text{m}$  with cobbles ( $D_{50} = 80 \text{ mm}$ ). These results show that an exposed cobble surface would have very different behaviour and sustain very low erosion rates, even at 2099 sea level rise predictions, compared to a coarse sand or pebble beach under an equivalent storm.

The wave runoff heights from the modelled storms indicate that the proposed SCDF feature is resistant to overtopping for nearly all of the cases investigated. However, under a 1-in-20 year storm from the NE at 2099 sea level and with storm surge, the highest swashes were predicted to reach the SCDF crest, although the modelled erosion was negligible, at  $< 1 \text{ cm}$ . In comparison, the natural beach to the north of the Sizewell C experienced overtopping, and breaching of the natural beach crest is predicted by the model to occur under these storm conditions (with and without the SCDF in the model). The degree of wave runoff and risk of SCDF overtopping reduces as the particle size is increased, due to increased porosity and hydraulic conductivity.



VAS Figure 1: Erosion sensitivity to particle size, at end of operational phase.





VAS Figure 2: North East 1-in-20 year storm, RCP4.5 2120 and 2140 sea levels (left) and RCP8.5 2120 and 2140 sea levels (right) – End of simulation profiles,  $D_{50} = 10$  mm.

## Conclusions

In all modelled cases under RCP4.5 (during the operational phase, up to 2099), the SCDF crest remained intact with a minimum of ~74% of subaerial beach volume remaining after the worst-modelled storm/shoreline/sea level combination. This indicates that the proposed SCDF is sufficient to withstand storm events of the magnitude of those modelled in this study, especially given that the 2D XBeach-S model over-predicted erosion in the calibration and validation cases by at least 2-3 times. Furthermore, volumetric losses are predicted to be up to an order of magnitude less for the coarser particles likely to constitute the SCDF: medium pebbles had 3-9 times less SCDF erosion, very coarse pebbles had 3-12 times less SCDF erosion, and fine cobbles had 18-35 times less erosion of the SCDF, compared to the coarse sand used in the XBeach-S model.


With sea level rise, the erosion demand on the SCDF is predicted to increase. Under the most extreme storm sequence modelled, up to 65% more erosion was predicted at 2099 sea level than at present sea level, and up to 158% more SCDF erosion was predicted with future eroded shorelines adjacent to the SCDF at 2099. Under 2140 SLR up to 242% more SCDF erosion was predicted with future eroded shorelines. However, these figures are highly conservative, as the simulations with coarse particles suggest that erosion demand will not increase as dramatically with SLR if medium or very coarse pebbles, and especially cobbles, are used for the SCDF rather than coarse sand.

Under RCP4.5 SLR conditions (the RCP scenarios used for the operation model runs), the HCDF is not exposed during the decommission phase but the SCDF crest height is reduced during the BfE storm only, from 6.4 m to 5.8 m ODN at 2140. However, it remains higher than the coastal path behind the SCDF crest and 48% of the pre-storm subaerial SCDF beach volume remains. Under RCP8.5 SLR scenarios, the SCDF crest of the Adaptive Design is predicted to be lowered by the 1:20 year NE storm, from 6.4 m to 6 m ODN at 2140 and 46% of the pre-storm subaerial SCDF beach volume remains (mean volumetric loss - 44  $\text{m}^3/\text{m}$  and maximum loss -141  $\text{m}^3/\text{m}$ ). However, with the BfE storm, the SCDF crest of the Adaptive Design is lowered to the edge of the coastal path behind at approximately 5.2 mODN with 18% of the pre-storm subaerial beach volume remaining. This is a conservative result as it is based on the XBeach-S (sand, modelled as  $D_{50} = 0.8$  mm) 2D model, which cannot take account of the much coarser pebbly

sediment (modelled as  $D_{50} = 10$  mm) that dominates the beach shingle and is more resistant to erosion. XBeach-G model runs for the modal pebble size ( $D_{50} = 10$  mm), showed that the SCDF remains intact with no crest lowering, for both the RCP4.5 and RCP8.5 scenarios with the 1:20 year NE storm, with 93% of the initial beach volume remaining in both scenarios.

The lateral ends of the SCDF are predicted to incur the greatest erosional losses during the simulated storms, and the northern half of the SCDF is predicted to be more vulnerable to storm erosion than the southern half during the shore-normal BfE storm sequence modelled. With this in mind, future recharge of the SCDF may require more frequent localised interventions at each end of the SCDF if the adjacent shoreline becomes severely receded in combination with the high sea level rises (2140) modelled in this report (this conclusion has not changed from Edition 1).

The volumetric erosion results from the report are used in BEEMS Technical Report TR544 – Preliminary design and maintenance requirements for the Sizewell C Soft Coastal Defence Feature (Version 4) – to further investigate SCDF performance and maintenance (most likely beach recharge) requirements with respect to sea level rise, receded adjacent shorelines and particle size.

|                            |  |
|----------------------------|--|
| Cefas Quality Assessor:    | Dr David Haverson  |
| Signature:                 |  |
| Position in Cefas / BEEMS: | BEEMS Modelling Lead   |
| Date of Evaluation:        | 28/09/2021   |

**Coastal Marine  
Applied Research**



# **Storm erosion modelling of the Sizewell C Soft Coastal Defence Feature using the XBeach modelling suite**



# **Storm erosion modelling of the Sizewell C Soft Coastal Defence Feature using the XBeach modelling suite**

Produced by Dr Christopher Stokes, Liane Brodie, and  
Professor Daniel Conley<sup>a</sup>

<sup>a</sup> Coastal Applied Marine Research (CMAR), University of Plymouth Enterprise Limited, School of Biological and Marine Sciences, University of Plymouth.



## Version, Quality Control, and Authorship

|                            | Version | Author     | Date       |
|----------------------------|---------|------------|------------|
| Draft                      | 0.01    | LB, CS     | 24/05/2021 |
| Internal QC & revision     | 0.02    | LB, CS, DC | 01/06/2021 |
| Cefas review               | 0.03    | DH, TD     | 08/06/2021 |
| CMAR revision              | 0.04    | LB, CS, DC | 16/06/2021 |
| Executive QC & Final Draft | 0.05    | DH, TD     | 18/06/2021 |
| EDF review                 | 0.06    | JR, SR     | 21/06/2021 |
| Revision                   | 0.07    | DH, TD, SL | 21/06/2021 |
| Submission to EDFE         | 1.00    |            | 21/06/2021 |
| Revision – new material    | 1.01    | DH         | 18/06/2021 |
| Internal & CMAR review     | 1.02    | CS, RB, PC | 19/06/2021 |
| Executive QC & Final Draft | 1.03    | SL         | 23/08/2021 |
| EDF review                 | 1.04    | SR         | 03/09/2021 |
| Submission to EDFE         | 2.00    |            |            |
| Revision – new material    | 2.01    | DH         | 21/01/2021 |
| Internal & CMAR review     | 2.02    | CS, TD     | 23/09/2021 |
| Executive QC & Final Draft | 2.03    | SL         | 24/09/2021 |
| EDF review                 | 2.04    | SR, JR     | 28/09/2021 |
| Submission to EDFE         | 3.00    |            |            |

This report was authored by Dr Christopher Stokes, Liane Brodie, and Professor Daniel Conley of CMAR (University of Plymouth). However, review and quality control of the report was undertaken throughout the project by Cefas. References to reports authored by BEEMS or NNB Generation Company that are cited in this report have been added by Cefas to provide additional context to the present report, but these reports have not been seen by CMAR and therefore comments on these reports are owned by Cefas. Any interpretation of model results relating to engineering decisions regarding the design of the Soft Coastal Defence Feature in this report are owned by Cefas.



**CMAR: Coastal Marine Applied Research**

CMAR is a research-informed consultancy group based in the School of Biological and Marine Sciences at the University of Plymouth, south west UK, and contract our services through the university's wholly owned commercial subsidiary, University of Plymouth Enterprise Limited (UoPEL). We focus on coastal processes and marine physics, and aim to provide a first-class data collection, analysis, modelling, and synthesis service to help address important issues in the coastal and marine environment. We strive to understand and predict the behaviour of coastal, marine and estuarine systems to support the appropriate management of resources and activities in these environments. Our team consists of highly qualified coastal scientists and engineers, and our research on coastal dynamics is published in international, peer-reviewed journals.

**DISCLAIMER**

Whilst UoPEL will use all reasonable endeavours to ensure the accuracy of the work performed and any information given, UoPEL makes no warranty, express or implied, as to accuracy and will not be held responsible for any consequence arising out of any inaccuracies or omissions unless such inaccuracies or omissions are the result of negligence on the part of UoPEL or its agents.

The obligations of UoPEL and its agents shall cease upon delivery of the report and no liability whatsoever either direct or indirect shall rest upon them for the effects of any product or process that may be produced or adopted by the client or any other party, notwithstanding that the formulation of such product or process may be based upon the findings of the report.

UoPEL shall not be liable for any death or injury unless it is caused by the negligence of UoPEL or its agents, nor shall it be liable for any loss or damage whatsoever unless it is caused by its wilful default or that of its agents.

All queries related to this document should be directed to:

CMAR, School of Biological and Marine Sciences, Reynolds Building, University of Plymouth, Drake  
Circus, Plymouth, Devon PL4 8AA

**Email:** [cmar@plymouth.ac.uk](mailto:cmar@plymouth.ac.uk)

**Telephone:** +44 1752 586177

**Web:** [www.plymouth.ac.uk/cmar](http://www.plymouth.ac.uk/cmar)

**Twitter:** @pu\_cmar

# Table of contents

|  |           |
|--|-----------|
| <b>Executive Summary.....</b>  | <b>19</b> |
| <b>1 Background.....</b>   | <b>24</b> |
| 1.1 Purpose.....   | 24        |
| 1.2 Aims and objectives .....  | 25        |
| 1.3 Modelling Approach .....   | 25        |
| <b>2 Methods.....</b>  | <b>26</b> |
| 2.1 Use of XBeach for a mixed sand-gravel beach.....                               | 26        |
| 2.2 2D XBeach model .....  | 27        |
| 2.2.1 2D Model Domain .....  | 28        |
| 2.2.2 Forcing Conditions.....  | 29        |
| 2.3 2D Calibration and Validation.....   | 33        |
| 2.3.1 Calibration and Validation Forcing Conditions.....                           | 33        |
| 2.3.2 Model Domain.....  | 34        |
| 2.3.3 Calibration and Validation Parameters .....                                  | 35        |
| 2.3.4 Calibration and Validation Results.....                                      | 37        |
| 2.4 1D XBeach gravel and sand model .....  | 43        |
| 2.5 Model Scenario Summary.....  | 45        |
| 2.5.1 Operational phase .....  | 45        |
| 2.5.2 Decommissioning phase and updates to the HCDF design .....                   | 48        |
| <b>3 Results.....</b>  | <b>51</b> |
| 3.1 Storm Erosion.....   | 52        |
| 3.1.1 SCDF Bed Elevation Change using the sand model.....                          | 52        |
| 3.1.2 SCDF compared with SCDF-receded future shorelines using the sand model ..... | 58        |
| 3.1.3 Volumetric change using the sand model.....                                  | 64        |
| 3.2 Variation due to particle size (gravel modelling) .....                        | 68        |
| 3.3 Wave Run-up and Overtopping.....   | 73        |
| 3.4 Decommissioning-phase modelling .....  | 74        |
| 3.4.1 Bed elevation change using the sand model.....                               | 74        |
| 3.4.2 Volumetric changes using the sand model.....                                 | 84        |
| 3.4.3 Variation due to particle size (gravel modelling).....                       | 90        |
| <b>4 Discussion .....</b>  | <b>94</b> |
| 4.1 Model parameters .....   | 94        |
| 4.2 General results.....   | 94        |
| 4.3 Sensitivity (wrt erosion).....   | 95        |
| 4.3.1 Wave obliquity.....  | 95        |
| 4.3.2 Particle size.....   | 95        |
| 4.4 Effect of sea level rise on SCDF erosion .....                                 | 96        |
| 4.5 Effect of laterally eroded shorelines on SCDF erosion .....                    | 97        |
| 4.6 SCDF design parameters recommendations.....                                    | 98        |
| 4.6.1 SCDF volumes.....  | 98        |
| 4.6.2 SCDF crest height and overtopping .....                                      | 98        |

4.6.3 Particle size recommendations..... 99

5 Conclusions ..... 100

6 References ..... 102



# List of Tables and Figures

## Tables

|   |    |
|---|----|
| Table 2-1 Final calibration model parameters .....  | 37 |
| Table 2-2 Calibrated model parameters for the 1D XBeach gravel-only model.....  | 45 |
| Table 2-3. 2D model scenario summary.....   | 46 |
| Table 2-4. 1D model scenario summary. The profile used in each 1D scenario (Figure 2-9) was taken from the centre of the SCDF DEM (location Y <sub>1</sub> , described in Section 3).....                           | 47 |
| Table 2-5. 2D model scenario summary for decommissioning phase. ....  | 50 |
| Table 2-6. 1D model scenario summary for decommissioning phase. The profile used in each 1D scenario (Figure 2-9) was taken from the centre of the SCDF DEM (location Y <sub>1</sub> , described in Section 3)..... | 50 |
| Table 3-1. Predicted volumetric change (above 0 m ODN) from the SCDF feature for each 2D XBeach-S simulation (to 1 <sup>st</sup> significant figure). ....  | 67 |
| Table 3-2. Predicted volumetric change (above 0 m ODN) from the SCDF feature for each 1D XBeach-S and XBeach-G simulation (to 1 significant figure). ....   | 72 |
| Table 3-3. Predicted volumetric change (above 0 m ODN) from the SCDF feature for each 2D XBeach-S simulation (to 1 <sup>st</sup> significant figure). ....  | 90 |
| Table 3-4. Predicted volumetric change (above 0 m ODN) from the SCDF feature for each 1D XBeach-G simulation (to 1 <sup>st</sup> significant figure).....   | 93 |

## Figures

|   |    |
|---|----|
| Figure 2-1. 2D Model Domain of the Baseline-2017 DEM, Case 1-SCDF DEM and Case 2-SCDF future eroded shoreline DEM (land on the left, sea on the right). ....  | 29 |
| Figure 2-2. Total water level timeseries used for the 1-in-20 year simulations (blue line, as measured on the 10 <sup>th</sup> Feb 2020 at the Sizewell tide gauge), consisting of a mean astronomical spring tidal cycle (red line), plus storm surge of up to 1 m coinciding with high tide. .... | 31 |
| Figure 2-3. BfE Event water level and wave forcing conditions. The period between the two red dotted lines indicates the period excluded from the simulations in order to reduce the record length and allow the model to run. ....   | 32 |
| Figure 2-4 Calibration (left) and Validation (right) starting model domains (land on the left, sea on the right). ....  | 35 |
| Figure 2-5. Model calibration ('May Storm') – topographic change from pre- to post-storm from the measured survey data (left), XBeach simulation (middle) and the difference between the measured and predicted changes (right).....  | 39 |
| Figure 2-6. Model calibration ('May Storm') – cross-sectional profiles of bed elevation pre- and post-storm from the measured survey (solid lines) and XBeach simulation (dashed lines). ....   | 40 |
| Figure 2-7. Model validation ('Storm Ciara') – topographic change from pre- to post-storm from the measured survey data (left), XBeach simulation (middle) and the difference between the measured and predicted changes (right).....   | 41 |
| Figure 2-8. Model validation ('Storm Ciara') – cross-sectional profiles of bed elevation pre- and post-storm from the measured survey (solid lines) and XBeach simulation (dashed lines). ....  | 42 |

|  |    |
|--|----|
| Figure 2-9. Model profile used in the gravel and sand versions of XBeach for the 1D grain size sensitivity tests. ....   | 44 |
| Figure 2-10. Plan overview of the difference between the updated HCDF design between V1 and V2 of this report. ....  | 48 |
| Figure 2-11. Comparison of the model domain used for the 1D gravel version of XBeach testing the SCDF for the HCDF and Adaptive Design. ....   | 49 |
| Figure 3-1. Average bed level along the SCDF frontage ( $Y_{average}$ , Section 3) at the start ('initial') and end of the three modelled storm events (present sea level). ....   | 52 |
| Figure 3-2. 2D change in bed elevation (coloured areas) along the SCDF frontage over the three modelled storm events (present sea level). ....   | 53 |
| Figure 3-3. Average bed level along the SCDF frontage ( $Y_{average}$ , Section 3) at the start ('initial') and end of the three modelled storm events (2069 sea level). ....  | 54 |
| Figure 3-4. 2D change in bed elevation (coloured areas) along the SCDF frontage over the three modelled storm events (2069 sea level). ....  | 55 |
| Figure 3-5. Average bed level along the SCDF frontage at the start ('initial') and end of the three modelled storm events (2099 sea level). ....   | 56 |
| Figure 3-6. 2D change in bed elevation (coloured areas) along the SCDF frontage over the three modelled storm events, at 2099 sea level. ....  | 57 |
| Figure 3-7. Comparison of 2D bed elevation changes (coloured areas) for the SCDF with present-day shoreline ('SCDF') and SCDF-with future receded shorelines ('SCDF future') cases, for the three modelled storms. ....  | 60 |
| Figure 3-8. Cross sections of bed level change for the North East 1-in-20 year storm, 2099 Sea Level (left panels) and South East 1-in-20 year storm, 2099 Sea Level (right panels) for the SCDF with present-day ('SCDF') and future eroded shorelines ('SCDF future'). ....  | 61 |
| Figure 3-9. Cross sections of bed level change for the BfE storm sequence, 2069 Sea Level (left panels) and BfE storm sequence, 2099 Sea Level (right panels) for the SCDF with present-day ('SCDF') and future eroded shorelines ('SCDF future'). ....  | 62 |
| Figure 3-10. North East 1-in-20 year storm, 2099 Sea Level – Pre-storm and post-storm profiles at the breach location ( $Y_{breach}$ ) north of the SCDF with present-day (top panel) and future eroded shorelines (middle panel). The bottom panel shows the difference in breach magnitude between the cases with present-day and future eroded shorelines. .... | 63 |
| Figure 3-11. BfE storm sequence, 2021, 2069, and 2099 Sea Levels – Mean volume eroded along the frontage of the SCDF (above 0 m ODN) during the storm at the three sea levels tested. ....   | 65 |
| Figure 3-12. Volumetric map of the SCDF frontage (above 0 m ODN), pre-storm (left), and remaining post-storm beach volume (middle) and percentage (right) for the worst-modelled storm scenario: BfE event, 2099 SLR, with future eroded shoreline position. ....  | 66 |
| Figure 3-13. North East 1-in-20 year storm, 2021, 2069, and 2099 Sea Levels – End of simulation profiles (top panels) and profile changes (bottom panels) for various grain sizes. Simulations were run using both the XBeach sand surfbeat formulations (labelled 'XBeach-S') and the XBeach gravel non-hydrostatic formulations (labelled 'XBeach-G'). ....      | 70 |
| Figure 3-14. North East 1-in-20 year storm, 2021, 2069, and 2099 Sea Levels – intertidal volumetric change (above 0 m ODN and seaward of the SCDF crest) through time over the simulation for various grain sizes. ....  | 71 |
| Figure 3-15. North East 1-in-20 year storm, 2021, 2069, and 2099 Sea Levels – Predicted volume eroded from the intertidal beach (above 0 m ODN and seaward of the SCDF crest) during the storm at the three sea levels tested. ....  | 71 |

- Figure 3-16. Average bed level along the SCDF frontage ( $Y_{\text{average}}$ , Section 3) at the start ('initial') and end of the two modelled storm events with SCDF-with future receded shorelines. Upper panel: 1:20 year NE storm with RCP4.5 SLR 2120. Lower panel: 1:20 year NE storm with RCP4.5 SLR 2120. In each panel, the solid red line shows the vertical difference in the pre- and post-storm profiles. .... 75
- Figure 3-17. 2D change in bed elevation (coloured areas) along the SCDF frontage over the two modelled storm events with the SCDF-with future receded shorelines. Contour lines show starting bed elevation (m ODN), with 0 m contour line shown in bold for reference. The thick line on the supratidal beach represents the approximate location of the HCDF toe which is stylistic only and the HCDF is not included in the model domain as a hard non-erodible feature. .... 76
- Figure 3-18. Average bed level along the SCDF frontage ( $Y_{\text{average}}$ , Section 3) at the start ('initial') and end of the two modelled storm events with Adaptive Design - with future receded shorelines. Upper panel: 1:20 year NE storm with RCP8.5 SLR 2120. Lower panel: 1:20 year NE storm with RCP8.5 SLR 2120. In each panel, the solid red line shows the vertical difference in the pre- and post-storm profiles. .... 77
- Figure 3-19. 2D change in bed elevation (coloured areas) along the SCDF frontage over the two modelled storm events with the Adaptive Design - with future receded shorelines and RCP8.5 sea levels. Contour lines show starting bed elevation (m ODN), with 0 m contour line shown in bold for reference. The thick line on the supratidal beach represents the approximate location of the HCDF toe. .... 78
- Figure 3-20 Average bed level along the SCDF frontage ( $Y_{\text{average}}$ , Section 3) at the start ('initial') and end of the two modelled storm events with SCDF-with future receded shorelines. Upper panel: 1:20 year SE storm with RCP4.5 SLR 2120. Lower panel: 1:20 year SE storm with RCP4.5 SLR 2120. In each panel, the solid red line shows the vertical difference in the pre- and post-storm profiles. .... 79
- Figure 3-21 2D change in bed elevation (coloured areas) along the SCDF frontage over the two modelled storm events with the SCDF-with future receded shorelines. Contour lines show starting bed elevation (m ODN), with 0 m contour line shown in bold for reference. The thick line on the supratidal beach represents the approximate location of the HCDF toe which is stylistic only and the HCDF is not included in the model domain as a hard non-erodible feature. .... 80
- Figure 3-22 Average bed level along the SCDF frontage ( $Y_{\text{average}}$ , Section 3) at the start ('initial') and end of the two modelled storm events with SCDF-with future receded shorelines. Upper panel: BfE storm with RCP4.5 SLR 2120. Lower panel: BfE storm with RCP4.5 SLR 2120. In each panel, the solid red line shows the vertical difference in the pre- and post-storm profiles. .... 81
- Figure 3-23 2D change in bed elevation (coloured areas) along the SCDF frontage over the two modelled storm events with the SCDF-with future receded shorelines. Contour lines show starting bed elevation (m ODN), with 0 m contour line shown in bold for reference. The thick line on the supratidal beach represents the approximate location of the HCDF toe which is stylistic only and the HCDF is not included in the model domain as a hard non-erodible feature. .... 82
- Figure 3-24 Average bed level along the SCDF frontage ( $Y_{\text{average}}$ , Section 3) at the start ('initial') and end of the modelled BfE storm with RCP8.5 SLR 2140 with the Adaptive Design -with future receded shorelines. The solid red line shows the vertical difference in the pre- and post-storm profiles. The dashed red line shows the HCDF. .... 83
- Figure 3-25 2D change in bed elevation (coloured areas) along the SCDF frontage over the modelled BfE storm event with the Adaptive Design - with future receded shorelines and RCP8.5 sea levels. Contour lines show starting bed elevation (m ODN), with 0 m contour line shown in bold for reference. The thick line on the supratidal beach represents the approximate location of the HCDF toe. .... 84



|   |    |
|---|----|
| Figure 3-26. Volumetric map of the SCDF frontage (above 0 m ODN), remaining post-storm beach volume (left) and percentage (right) for the 1:20 year NE storm with RCP4.5 SLR 2140, with future eroded shoreline position. ....  | 86 |
| Figure 3-27 Volumetric map of the SCDF frontage (above 0 m ODN), remaining post-storm beach volume (left) and percentage (right) for the BfE storm with RCP4.5 SLR 2140, with future eroded shoreline position. ....  | 87 |
| Figure 3-28. Volumetric map of the Adaptive Design frontage (above 0 m ODN), remaining post-storm beach volume (left) and percentage (right) for the 1:20 year NE storm with RCP8.5 SLR 2140, with future eroded shoreline position. ....   | 88 |
| Figure 3-29 Volumetric map of the Adaptive Design frontage (above 0 m ODN), remaining post-storm beach volume (left) and percentage (right) for the BfE storm with RCP8.5 SLR 2140, with future eroded shoreline position. The 5 m polygon bins visible in the middle and right panels were used to calculate volumetric changes over the SCDF frontage for all 2D simulations run (Table 2-5)..... | 89 |
| Figure 3-30. North East 1-in-20 year storm, RCP4.5 2120 and 2140 sea levels (left) and RCP8.5 2120 and 2140 sea levels (right) – End of simulation profiles (top panels) and profile changes (bottom panels) for 10 mm grain size. Simulations were run using the XBeach gravel non-hydrostatic formulations.....   | 92 |
| Figure 4-1. Example increase in significant wave height, averaged along the frontage of the SCDF, between 2021 and 2069 for a south-easterly 1-in-20 year storm event. It should be noted that this uplift in wave height is purely a result of higher sea level. ....  | 97 |

## Executive Summary

A Soft Coastal Defence Feature (SCDF) has been proposed for the beach frontage at Sizewell C. The SCDF is a maintained and volumetrically enlarged beach, seaward of the hard coastal defence feature (HCDF), that is designed to prevent exposure of hard coastal defences (BEEMS Technical Report TR544). It uses a “working with nature” approach where the release and transport of SCDF sediment in the coastal system is determined by natural coastal processes (erosion by storm waves), some of which would deposit on adjacent shorelines. To prevent HCDF exposure by progressive, unmitigated, natural erosion, the SCDF would be maintained or ‘topped up’ (primarily by recharge) once the beach volume reduces to a threshold value, which will be set in the Coastal Processes Monitoring and Mitigation Plan (BEEMS Technical Report TR523).

This report uses the XBeach storm erosion modelling suite to investigate the response of the proposed SCDF to storm wave conditions. The modelling will inform decisions made in BEEMS Technical Report TR544 on the recharge threshold, the typical expected recharge intervals and SCDF composition (particle sizes).

The calibrated XBeach-S 2D model<sup>1</sup> is used to investigate how present and future conditions affect SCDF erosion during severe storms. Whilst XBeach is capable of modelling near term beach recovery (Pender and Karunaratna, 2013) the focus of this study is on storm erosion modelling to determine the maximum losses over individual severe storms. The natural recovery process, in which much or all of the sediment is expected to return, has not been modelled. This modelling is appropriate for testing viability of the SCDF but the losses quoted are for storms only without recovery, and do not equate to the real-world losses, which with natural recovery are expected to be small, incremental and driving the net patterns of shoreline change and SCDF volumetric loss over periods of years – decades.

As summarised in Figure i, volume losses for the present-day sea level under the Beast from the East (BfE) storm sequence (which in energy terms has a 1:107 year return interval) would lead to a loss of -16 m<sup>3</sup> of sediment per metre of north-south shoreline<sup>2</sup> (expressed hereafter as m<sup>3</sup>/m). As expected, sea level rise (SLR) increases erosion to -22 m<sup>3</sup>/m by 2069 and -27 m<sup>3</sup>/m by 2099<sup>3</sup>.

The modelling also considered a future severely receded shoreline adjacent to Sizewell C (north and south), based on the postulated shoreline at or toward the end of the decommissioning phase without an increase in sediment supply<sup>4</sup> – see Section 7.7 of Volume 2, Appendix 20A of the Sizewell C Environmental Statement (NNB Generation Company (SZC) Limited, 2020). This case was included because erosion pressure on the SCDF is expected to rise as the alignment with adjacent shorelines changes.

As expected, the model shows that severely receded adjacent shorelines increase erosion pressure on the SCDF, although the level of shoreline recession modelled is not expected until late in, or beyond, the end of the 21<sup>st</sup> century. For the BfE storm sequence, the modelled mean erosion with SLR and receded adjacent

---

<sup>1</sup> XBeach-S is a sandy beach erosion model that has both 1D (i.e., a beach profile) and 2D (i.e., a beach area) versions. The benefit of the 2D version is that it is also able to resolve longshore transport, which is important at Sizewell as most storm waves approach the coast at an angle, meaning that a component of their energy moves sediment along the coast (as well as up and down the beach profile).

<sup>2</sup> The 16 m<sup>3</sup>/m volumetric loss is less than the 31 m<sup>3</sup>/m predicted by preliminary storm modelling (BEEMS Technical Report TR531) owing to the incorporation of longshore transport in the 2D model and further optimisation of model parameters.

<sup>3</sup> Sea level rises scenarios are expressed with respect to the year 2020 using the intermediate RCP4.5 95<sup>th</sup> percentile climate change scenario. This gives a sea level rise of 0.4 m for 2069 and 0.7 m for 2099. 2069 and 2099 were specified by Cefas as they are approximately midway and slightly after the end of the planned Sizewell C operation phase.

<sup>4</sup> This is a conservative case as sediment supply is expected to increase downdrift of soft cliffs with rising sea levels owing to increased cliff erosion (Brooks, S. M. and Spencer, T. 2012. Shoreline retreat and sediment release in response to accelerating sea level rise: Measuring and modelling cliffline dynamics on the Suffolk Coast, UK. *Global and Planetary Change*, **80-81**, 166-179.)

shorelines is  $-35 \text{ m}^3/\text{m}$  in 2069 and  $-43 \text{ m}^3/\text{m}$  in 2099 (Figure i), but higher localised losses are observed at both ends of the SCDF due to higher wave angles and longshore transport gradients where the shoreline curves from the SCDF to the adjacent frontage. The greatest localised erosion ( $-82 \text{ m}^3/\text{m}$ ) occurred at the northern end of the SCDF under the combined 2099 SLR and receded shoreline scenario, but still left 65-70% of the pre-storm subaerial SCDF beach volume intact. Were the adjacent shorelines to become as severely eroded as those modelled, it is likely that the frequency of beach recharge would need to rise in order to maintain the SCDF, albeit across relatively short (10s of metres) sections of frontage.

In all the operational phase modelled cases, the SCDF crest remained intact with a minimum of 65-70% of subaerial beach volume remaining after the worst-modelled storm. This indicates that the proposed SCDF is sufficient to withstand storm events of the magnitude of those modelled in this study, especially given that the 2D XBeach-S model over-predicted erosion in the calibration and validation cases by at least 2-3 times. Furthermore, volumetric losses are predicted to be up to an order of magnitude less for coarser particles, with medium pebbles (8 – 16 mm)<sup>5</sup> resulting in 3-9 times less SCDF erosion, very coarse pebbles (32 – 64 mm)<sup>6</sup> resulting in 3-12 times less SCDF erosion, and fine cobbles (64 – 128 mm)<sup>7</sup> resulting in 18-35 times less erosion of the SCDF, compared to the coarse sand used in the XBeach-S model<sup>8</sup>.

Whilst the XBeach-S 2D model has the benefit of incorporating longshore transport, it is a sand model (the median sediment size used was 0.8 mm diameter), while in reality the subaerial beach (above low tide) sediments are primarily pebble-sized (median diameter of 10mm). As the real-world performance of the SCDF will be affected by particle size, additional modelling was undertaken to test the SCDF's erosion sensitivity to different particle sizes using XBeach-G<sup>9</sup>, to give some qualitative contrast to the XBeach-S 2D model and to inform the target particle size.

Tests using the 1D XBeach-S (calibrated for Sizewell) and 1D XBeach-G (semi-calibrated through best alignment with calibrated models for similar beaches from literature) models were conducted on pebbles ranging from 2 – 80 mm (Figure ii). The results indicate that the 10 mm and 40 mm pebbles produce similar results to each other for the present-day sea level, however as sea level rise progresses, particle size becomes increasingly important to erosion resistance – for example, erosion volume is 24% higher for the 10 mm pebbles in 2099 than the 40 mm pebbles. The 80 mm fine cobble sediment class is predicted to give a substantive performance increase compared to the pebbles, with effectively no losses for the present-day and 2069 cases, and minimal losses ( $2.5 \text{ m}^3/\text{m}$ ) in 2099. The default position for SCDF particle size is to match the native size distribution, which has a model pebble size of approximately 10 mm diameter.

Finally, wave run-up and overtopping were also investigated because overtopping can lead to degradation of the SCDF crest. The modelled runup heights using XBeach-S indicate that the proposed SCDF feature is resistant to overtopping for nearly all the cases investigated. However, under the 1-in-20 year NE storm scenario with 2099 SLR, the highest swashes were predicted to reach the SCDF crest, although the predicted topographic change at the crest was small ( $< 1 \text{ cm}$ ). The same conditions are predicted to cause natural overtopping and breaching of the south Minsmere shingle ridge, just north of Sizewell C –overtopping and breaching is predicted to occur there with, and without, the presence of the SCDF, demonstrating it is a natural process. In contrast, no SCDF overtopping was observed for natural pebble sized sediments (and fine cobbles) using XBeach-G, which is more accurate as it resolves individual wave crests and includes the processes of infiltration and exfiltration that control runup on coarse beaches. Overall, these results show that SCDF overtopping is unlikely to be a concern over the operational phase, but that natural overtopping and breaching is increasingly likely on the southern Minsmere frontage toward the end of the century. That

---

<sup>5</sup> Modelled as 10 mm diameter particles.

<sup>6</sup> Modelled as 40 mm diameter particles.

<sup>7</sup> Modelled as 80 mm diameter particles.

<sup>8</sup> It is not the intention to construct the SCDF of fine cobbles. However, a design option includes a layer of fine cobbles deep within the pebbly SCDF matrix that would reduce risks of HCDF exposure in the unlikely event that it became exposed.

<sup>9</sup> XBeach-G is a 1D model for gravel sized sediments, ranging from 2 – 80 mm. Whilst the XBeach-S model is calibrated to observations of the existing beach at Sizewell, the XBeach-G model is not strictly calibrated to Sizewell or the SCDF as data does not exist, for example for hydraulic conductivity (the ability of water to infiltrate and exfiltrate through the gravel beach). However, the model is parameterised based on suitable published calibration studies.

prospect may be avoided by decades of deposition of SCDF sediments, which is not accounted for in the model but was assessed as a potential benefit of the SCDF (see Section 2.15 of NNB Generation Company (SZC) Limited, 2021a).

## **Updates to Edition 2**

Edition 1 of this report investigated the response of the proposed SCDF to storm wave conditions up to the end of the operational phase in 2099. Edition 2 of this report extends the modelling to the end of the decommissioning phase in 2140<sup>10</sup>. The SCDF is tested against SLR predictions of RCP4.5 95<sup>th</sup> percentile<sup>11</sup>. The Adaptive Design is predicted to only be required during the decommissioning phase under the higher RCP8.5 95<sup>th</sup> percentile SLR conditions. As such, it is tested against those conditions only. The modelling also considered both the SCDF and the Adaptive Design with the future severely receded shoreline adjacent to Sizewell C (north and south) as used in Edition 1 of this report.

In addition to new model runs, the design of the HCDF has also been updated, in line with details provided in the Sizewell C Coastal Defences Design Report [REP2-116], consisting of the paring back of the BLF abutment to the north and the Sizewell B tie-in the southern end of the HCDF. The position and crest elevation of the SCDF remain unchanged, therefore the geometry of the HCDF increases the beach volume at the north of the SCDF and reduces it at the south of the SCDF. The spatial plots of the operational model runs, presented in Edition 1, will be revisited in the next version of this report. The 2D volumes in the text and presented in Table 3-1 from Edition 1 have been updated with respect to the new HCDF design to allow comparison with the decommissioning results. However, the design changes do not affect the conclusions of Edition 1. Under the modelled storms with RCP4.5 SLR conditions (the RCP scenarios used for the operation-phase model runs) the HCDF is not exposed during the decommissioning phase nor is the SCDF crest height reduced, showing the SCDF is still robust during the operational phase.

Details of the change to the HCDF are discussed in Section 2.5.2. A summary of the new model runs are presented in Table 2-5 and Table 2-6 in Section 2.5.2. The new results are presented in Section 3.4. Minor text edits were made to the Executive Summary, Section 4 Discussion and Section 5 Conclusions, where appropriate. The remainder of the report remains unchanged.

As shown with the future receded shoreline during the operational phase, the model continues to show into the decommissioning phase that the severely receded adjacent shorelines increase erosion pressure on the northern and southern ends of SCDF and HCDF along with the Adaptive Design of the HCDF. For the 1:20 year NE storm with RCP4.5 SLR, the modelled mean erosion is -26 m<sup>3</sup>/m in 2120 and -27 m<sup>3</sup>/m in 2140, but higher localised losses are observed at both ends of the SCDF due to higher wave angles and longshore transport gradients where the shoreline curves from the SCDF to the adjacent frontage. For the 1:20 year NE storm with RCP8.5 SLR against the Adaptive Design, the modelled mean erosion is -40 m<sup>3</sup>/m in 2120 and -44 m<sup>3</sup>/m in 2140. The greatest localised erosion (-141 m<sup>3</sup>/m) occurred at the northern end of the SCDF under the RCP8.5 2140 SLR and receded shoreline scenario, but this still left 46% of the pre-storm subaerial SCDF beach volume intact.

Under the RCP4.5 SLR scenarios, the SCDF crest remained intact with a minimum of 74% of subaerial beach volume remaining after the worst-modelled storm. This indicates that the proposed SCDF is sufficient to withstand storm events of the magnitude of those modelled in this study. Under the 1:20 year NE storms with the RCP8.5 SLR scenario for 2140, the SCDF crest of the Adaptive Design is predicted to lower from 6.4 m to 6 m ODN. However, it remains higher than the coastal path behind the SCDF crest and 46% of the pre-storm subaerial SCDF beach volume remains. This indicates that the proposed SCDF is still sufficient to withstand storm events of the magnitude of those modelled in this study, especially given that the 2D XBeach-S model over-predicted erosion in the calibration and validation cases by at least 2-3 times.

---

<sup>10</sup> UKCP18 SLR predictions extend to 2100. For SLR rise projections beyond 2100, the UKCP18 Exploratory sea level projections for the UK to 2300 have been used.

<sup>11</sup> Representative Concentration Pathway (RCP) specify the concentrations of greenhouse gases that would result in the target amounts of radiative forcing at the top of the atmosphere by 2100, relative to preindustrial levels.

Furthermore, volumetric losses are predicted to be less for coarser particles, with medium pebbles ( $D_{50} = 10$  mm) resulting in 3-4 times less SCDF erosion.

### **Updates to Edition 3**

Edition 3, this report, extends the modelling to the end of decommissioning phase in 2140 using the 1:20 year SE storm and the BfE storm. A summary of the new model runs is presented in Table 2-5 in Section 2.5.2. The new results are presented in Section 3.4. Minor text edits were made to the Executive Summary, Section 4 Discussion and Section 5 Conclusions, where appropriate. The remainder of the report remains unchanged.

As shown with the 1:20 year NE storm, the sand model continues to show into the decommissioning phase that the severely receded adjacent shorelines increase erosion pressure on the northern and southern ends of the SCDF. For the BfE storm with RCP4.5 SLR, the modelled mean erosion is  $-51 \text{ m}^3/\text{m}$  in 2120 and  $-56 \text{ m}^3/\text{m}$  in 2140, but higher localised losses are observed at both ends of the SCDF due to higher wave angles and longshore transport gradients where the shoreline curves from the SCDF to the adjacent frontage. For the BfE storm with RCP8.5 SLR against the Adaptive Design, the modelled mean erosion is  $-101 \text{ m}^3/\text{m}$  in 2140. The greatest localised erosion ( $-188 \text{ m}^3/\text{m}$ ) occurred at the southern end of the SCDF under the RCP8.5 2140 SLR and receded shoreline scenario, but this still left 50% of the pre-storm subaerial SCDF beach volume intact at this location. The beach section that had the smallest remaining beach volume as a percentage of the starting volume was to the north at 18%.

Under the RCP4.5 SLR scenarios, the SCDF crest remained intact under the 1:20 year NE and SE storms, but lowered under the BfE storm. The SCDF crest is predicted to lower from 6.4 m to 5.8 m ODN at 2140. However, it remains higher than the coastal path behind the SCDF crest and 48% of the pre-storm subaerial SCDF beach volume remains. This indicates that the proposed SCDF is sufficient to withstand storm events of the magnitude of those modelled in this study. Under the BfE storms with RCP8.5 SLR scenarios, the SCDF crest of the Adaptive Design is predicted to lower from 6.4 m to the edge of the coastal path at approximately 5.2 m ODN at 2140. On average 54% of the pre-storm subaerial SCDF beach volume remains. This indicates that the proposed SCDF is still sufficient to withstand storm events of the magnitude of those modelled in this study, especially given that the 2D XBeach-S (sand) model over-predicted erosion in the calibration and validation cases by at least 2-3 times. For example, for the 1:20 year NE storm with RCP8.5 2140 SLR against the Adaptive Design, the modelled mean erosion is  $-44 \text{ m}^3/\text{m}$  with Xbeach-S (sand) and  $13 \text{ m}^3/\text{m}$  with XBeach-G (gravel).

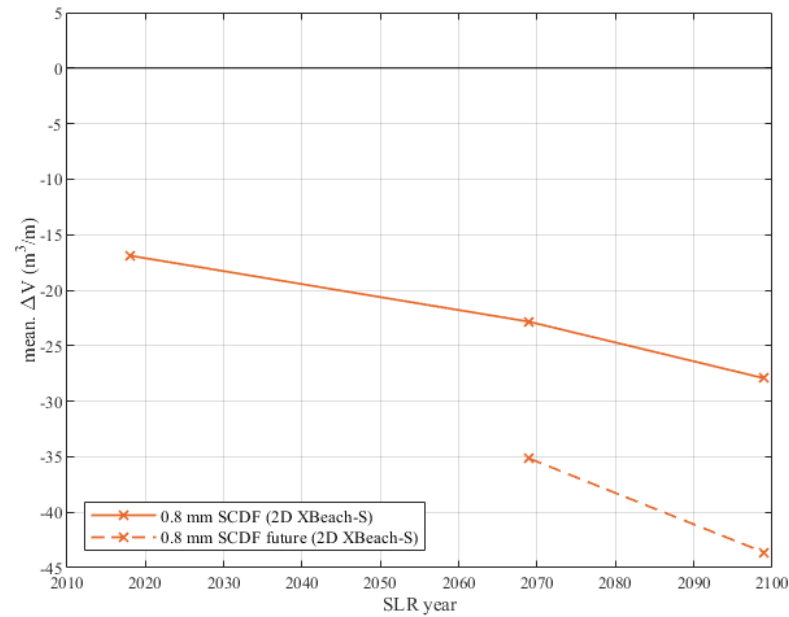


Figure i. Beast from the East storm sequence, 2021, 2069, and 2099 Sea Levels – Mean volume eroded along the frontage of the SCDF (above 0 m ODN) during the storm at the three sea levels tested. Note that model data only exists for years 2021, 2069, and 2099 and is shown for XBeach-S simulations only.

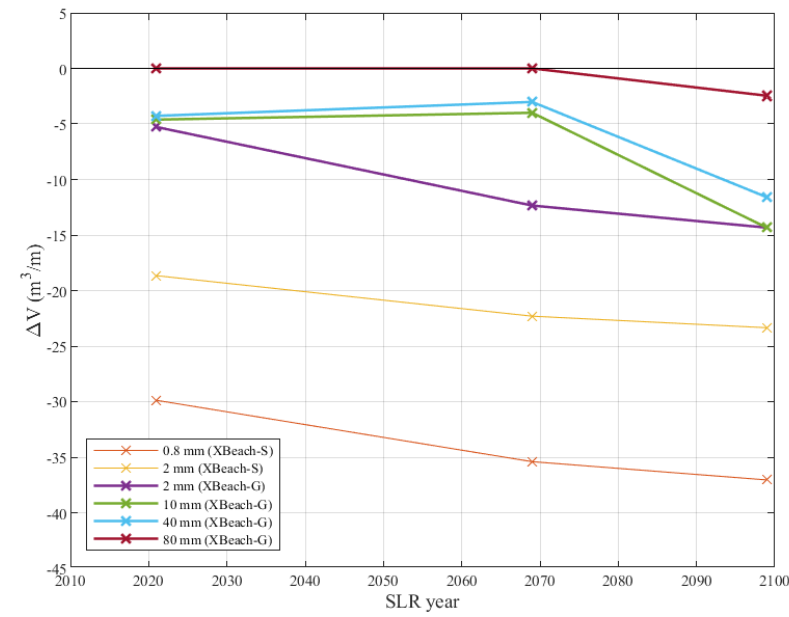


Figure ii. North East 1-in-20 year storm, 2021, 2069, and 2099 Sea Levels – Maximum volume eroded from the intertidal beach (above 0 m ODN and seaward of the SCDF crest). Note that model data only exists for years 2021, 2069, and 2099. Simulations were run using both the XBeach sand surfbeat model (labelled 'XBeach-S') and the XBeach gravel non-hydrostatic model (labelled 'XBeach-G').

# 1 Background

---

## 1.1 Purpose

---

At Sizewell C, a hard coastal defence feature (HCDF) is proposed to be constructed along the eastern (seaward) flank. It is the primary defence against coastal flooding during extreme waves and water levels, and is required for site integrity. It would be constructed in the terrestrial environment and would be separated from the sea by a shingle soft coastal defence feature (SCDF). The SCDF would be constructed between the HCDF and Mean High Water Spring (MHWS) level to increase back-beach volume.

The SCDF is a maintained and volumetrically enlarged beach seaward of the hard coastal defence feature (HCDF) that is designed to prevent exposure of hard coastal defences (BEEMS Technical Report TR544). It uses a “working with nature” approach where the release and transport of SCDF sediment in the coastal system is determined by natural coastal processes (erosion by storm waves), some of which would deposit on adjacent shorelines (and potentially reduce erosion rates there). To prevent HCDF exposure by progressive, unmitigated, natural erosion, the SCDF would be maintained or ‘topped up’ (primarily by recharge) once the beach volume reduces to a threshold value, which will be set in the Coastal Processes Monitoring and Mitigation Plan (CPMMP) (BEEMS Technical Report TR523).

Preliminary first stage modelling developed a 1D sand model using XBeach to examine beach erosion under severe storms (BEEMS Technical Report TR531). This initial modelling undertook calibration and validation against the present-day natural beach without the SCDF and provides more conservative estimates of erosion for a severe storm (again for the natural beach only). Specifically, it examined the width and volume eroded for sections of the SZC frontage using the first and second storms (E1 and E2 in this report) in the Beast from the East storm sequence (hereafter BfE).

The purpose of the initial modelling was to provide preliminary estimates of the scale of erosion to be used to assess the SCDF volumes and set thresholds for when it needs to be recharged. The final thresholds will be set and incorporated into the Coastal Processes Monitoring and Mitigation Plan (CPMMP) (BEEMS Technical Report TR523), which also sets out the monitoring against which the triggers would be regularly tested.

Sizewell is a composite beach with a sandy subtidal, mixed sand-gravel (shingle) intertidal beach and a pebble supra-tidal beach (with low sand content)<sup>12</sup>. There is no single model capable of modelling a mixed sand-gravel beach, nor a complex composite beach. Therefore, the final thresholds set in the CPMMP will be based on a holistic view of a range of individual sand and gravel models and sensitivity testing.

This report develops further 1D and 2D sand models using XBeach Sand (herein, ‘XBeach-S’) as well as a 1D XBeach gravel model (herein, ‘XBeach-G’). These models will investigate both the baseline natural beach profiles as well as the inclusion of the SCDF under present day conditions, sea level rise conditions and a future eroded shoreline.

Whilst XBeach is capable of modelling near term beach recovery (Pender and Karunaratna, 2013) the focus of this study is on storm erosion modelling to determine the maximum losses over individual severe storms. The natural recovery process, in which much or all of the sediment is expected to return, has not been modelled. This modelling is appropriate for testing viability of the SCDF but the losses quoted are for storms only without recovery, and do not equate to the real-world losses, which with natural recovery are expected to be small, incremental and driving the net patterns of shoreline change and SCDF volumetric loss over periods of years – decades.

---

<sup>12</sup> The sedimentological terms for sediment size grades, classes and fractions (sand, pebbles, fine cobbles) used in this report derive from the modified Udden-Wentworth classification (Blair, T. C. and McPherson, J. G. 1999. Grain-size and textural classification of coarse sedimentary particles. *Journal of Sedimentary Research*, **69**, (1), 6-19.), which can be found in Appendix A.



## 1.2 Aims and objectives

---

The primary aim of this modelling study is to investigate the response of the proposed SCDF under storm wave conditions. To achieve this aim, the following objectives have been identified:

1. Develop a numerical model, calibrated to reproduce the natural response of Sizewell Beach to storm waves as closely as possible.
2. Simulate beach and shoreline change to understand and quantify the erosional response of the SCDF under storm wave conditions.
3. Investigate the sensitivity of SCDF erosion to the grain size used to build and maintain the SCDF.

## 1.3 Modelling Approach

---

This report uses the XBeach storm erosion modelling suite to investigate the response of the proposed SCDF to storm wave conditions. XBeach simulates hydrodynamic and morphodynamic processes on the time scale of storms. A 2D XBeach-S model is calibrated against real world data of partial beach profile evolution for two distinct storms. It then models two distinct types of storms: a 1:20 year return interval peak storm wave height over a single tidal cycle (low tide to low tide) and the full BfE storm sequence (events E1 + E2 + E3, February/March 2018) which represents a 1:107 year storm sequence in terms of cumulative wave power.

Both these storms are used to estimate the volume lost during severe storms under present-day sea level and sea level rise (SLR). Two SLR conditions are investigated: 0.4 m and 0.7 m. 0.4 m is the SLR between a baseline year of 2020 and UKCP18 climate predictions for the year 2069 (RCP4.5, 95<sup>th</sup> percentile), which is approximately halfway through the operation phase of the power station. 0.7 m is the SLR between a baseline year of 2020 and UKCP18 climate predictions for the year 2099 (RCP4.5, 95<sup>th</sup> percentile), which is approximately the end of the operational phase. The modelled conditions considered can thus be considered as representative of real storm events both with and without SLR.

For the 1:20 year storm, the SLR conditions are also further extended to 2120 and 2140<sup>13</sup>, with 2140 representing the end of the SZC decommissioning phase. The SCDF is tested against UKCP18 climate predictions from RCP4.5 95<sup>th</sup> percentile. During the decommissioning phase, the HCDF is predicted to be required to be upgraded to the Adaptive Design, only under RCP8.5 95<sup>th</sup> percentile conditions. Therefore, the Adaptive Design is also tested against these conditions for 2120 and 2140.

The modelling also considers a future severely receded shoreline adjacent to Sizewell C (north and south), based on the postulated shoreline at or toward the end of the decommissioning phase without an increase in sediment supply – see Section 7.7 of Volume 2, Appendix 20A of the Sizewell C Environmental Statement (NNB Generation Company (SZC) Limited, 2020). This case was included because erosion pressure on the SCDF is expected to rise as the alignment with adjacent shorelines changes.

Whilst the XBeach-S 2D model used in this report has the benefit of incorporating longshore transport, it is a sand model (the median sediment size used was 0.8 mm diameter), while in reality the subaerial beach (above low tide) sediments are primarily pebble-sized (median diameter of 10mm). As the real-world performance of the SCDF will be affected by particle size, additional modelling was undertaken to test the SCDF's erosion sensitivity to different particle sizes using XBeach-G, a 1D model for gravel sized sediments ranging from 2 – 80 mm, to give some qualitative contrast to the XBeach-S 2D model and to inform the target particle size.

---

<sup>13</sup> UKCP18 SLR predictions extend to 2100. For SLR rise projections beyond 2100, the UKCP18 Exploratory sea level projections for the UK to 2300 have been used, but these results are considered experimental by UKCP.

## 2 Methods

---

For this project, the process-based numerical model XBeach has been identified by Cefas as the preferred modelling platform. XBeach can simulate the propagation of incident and infragravity waves, wave-induced currents, sediment transport and morphological changes, solving the time-dependent short wave action-balance equations, roller energy equations, the non-linear shallow water equations of mass and momentum, sediment transport formulations and bed updating (Roelvink *et al.*, 2010). Wave dissipation is modelled (Roelvink, 1993; Daly *et al.*, 2012), and a roller model (Svendsen, 1984; Nairn *et al.*, 1991; Roelvink and Reniers, 2011) is used to represent the momentum carried after wave breaking. Radiation stress gradients (Longuet-Higgins and Stewart, 1962, 1964) then drive infragravity motion and unsteady currents in the model, which are solved with the non-linear shallow water equations (Phillips, 1977). XBeach was developed to model storm impacts on beaches, and therefore is not designed to simulate beach dynamics over large temporal and spatial scales. It is limited to storm-event time scales (days-weeks) and spatial scales on the order of kms. It is also not designed to model beach recovery between storm events.

Since its initial development for sandy beach-dune systems, XBeach-S has proved effective in reproducing measured hydrodynamics and beach response under a wide range of scenarios (Roelvink *et al.*, 2009; Van Dongeren *et al.*, 2009; McCall *et al.*, 2010; Bolle *et al.*, 2011; Splinter and Palmsten, 2012). XBeach has since been expanded to include gravel beach dynamics (XBeach-G; Masselink *et al.*, 2014; McCall *et al.*, 2014; McCall *et al.*, 2015) by solving intra-wave flow and surface elevation variations of incident waves, gravel transport equations, and groundwater mechanics, including infiltration and exfiltration of groundwater that exerts important controls on how gravel beaches erode. The model's morpho- and hydro-dynamics have previously been validated for use on pure gravel beaches using physical model data and field measurements (McCall *et al.*, 2014).

Given the varied beach sediment sizes under investigation and the mixed sand-gravel composition of Sizewell Beach (Section 2.1), the objectives of this project (Section 1.2) require two different modelling methodologies. The two methodologies and purposes are detailed below:

- ▶ A 2D XBeach-S model was developed to investigate the potential volume loss from the SCDF during storms. Calibration and validation was undertaken on the 2D XBeach-S model to verify its suitability for this purpose.
- ▶ A 1D XBeach domain was also developed to test the sensitivity of the SCDF response to grain size, and run using XBeach-S and XBeach-G separately.

Details of the developed models and calibration/validation are provided below.

### 2.1 Use of XBeach for a mixed sand-gravel beach

---

While the sand and gravel versions of XBeach have both proven highly effective at reproducing measured storm response, no numerical model has yet been developed (in XBeach or otherwise) that can adequately capture the complex processes that occur on a mixed sand-gravel beach such as Sizewell. Therefore, separate XBeach-S and XBeach-G models were developed in the present study to investigate the probable range of beach and SCDF response at Sizewell. The main differences between the two models within XBeach are:

- ▶ XBeach-S resolves wave action on the timescale of the infragravity wave envelope ('surfbeat'/wave groups) which is suitable at shallow sloping beaches where the surf-zone is saturated due to depth limited breaking. The 'non-hydrostatic' XBeach-G resolves individual wave crests and troughs, as incident wave motion dominates the wave signal at the shore of steep sloping beaches.
- ▶ XBeach-S includes formulations for bed load and suspended load sediment transport, whereas XBeach-G only includes bed load formulations because suspended load transport is negligible at gravel beaches.

- ▶ XBeach-G includes groundwater effects (groundwater level, infiltration, exfiltration) as water exchange with the beach face plays an important role in influencing wave uprush and backwash velocities at gravel beaches as well as the sediment transport and morphological response (McCall, 2015). XBeach-S assumes the beach face is impermeable as such processes are unimportant at sandy beaches.

Additionally, the XBeach-S model used assumes that the seabed has a uniform layer composed of coarse sand. In reality, the subaerial beach at Sizewell has a mixed sand and gravel (pebble size class) composition, with sand content with elevation on the supra-tidal beach. From a modelling perspective the assumption that the beach is sandy is conservative, as beach erosion under storm conditions is likely to be more pronounced for sand as opposed to mixed and coarser seabed compositions (Sutherland *et al.*, 2005). However, wave runup in XBeach-S is assumed to be dominated by infragravity motion, while on steeper beaches incident wave motion dominates the water level signal, and can lead to significantly higher wave runup height (Poate *et al.*, 2016). Therefore, potential wave runup heights are investigated in this report using both XBeach-S and XBeach-G.

Based on the sand fraction of sediment samples collected at Sizewell, typical sand grain properties of the beach face are:  $D_{15} = 0.29$  mm,  $D_{50} = 0.40$  mm and  $D_{90} = 0.52$  mm. However, the pebble dominant subaerial beach has a median size of around 10 mm, including larger particles up to 50-60 mm diameter. To account for the mixed sand-gravel nature of Sizewell beach in the 2D XBeach-S model, values for the sediment grain size were set to the largest recommended values for the sand-only model of  $D_{50} = 0.8$  mm and  $D_{90} = 1.5$  mm (see Section 3.1). For the 1D XBeach model runs, sensitivity to grain size was explored further by using median grain sizes of up to 2 mm in XBeach-S, and up to 80 mm in XBeach-G (see Section 3.2).

## 2.2 2D XBeach model

---

A 2D XBeach-S model was developed using measured bathymetric and topographic data, and was calibrated and validated against measured topographic field data before being used to simulate a number of scenarios (detailed in Section 2.5).

The model was forced with wave conditions uniformly along the seaward boundary, and all wave driven currents within the model were computed by XBeach. Water levels were varied using measured tidal data (detailed in 2.2.2.2). The 2D model was run in 'Surfbeat' mode, whereby waves are resolved in the model on the timescale of individual wave groups. This is the default mode of operation for XBeach-S and has previously been shown to replicate the primary hydro- and morpho-dynamics occurring on sandy beaches during energetic wave conditions (Roelvink *et al.*, 2009; Van Dongeren *et al.*, 2009; McCall *et al.*, 2010; Bolle *et al.*, 2011; Splinter and Palmsten, 2012; McCarroll *et al.*, 2015).

There are limitations in using an XBeach-S model for the mixed sand-gravel beach at Sizewell. The key limitations can be summarised as:

- ▶ The sand model used is limited in the grain sizes that can be simulated. The largest grain sizes at Sizewell are larger than those within the sand model used.
- ▶ The sand model used assumes that grain sizes are uniformly distributed across the beach face. The mixed sand-gravel beach at Sizewell displays notable grading in grain size in the cross-shore direction with mostly sand in the subtidal but considerable fractions of gravel (mainly medium and coarse pebbles) occurring on the upper beach.
- ▶ The sand model uses sediment transport equations developed for sand, which are not expected to perform well for the coarser fractions of sediment at Sizewell.
- ▶ The sand model used does not account for any infiltration or exfiltration of water from the beach face, while in reality, areas of coarser sediment at Sizewell may allow this to occur.

Despite these limitations, calibration of the XBeach-S model (Section 2.3) achieved a reasonable agreement with the measured storm response at Sizewell, and the calibrated model is deemed to provide an acceptable model for the present aims.

### 2.2.1 2D Model Domain

In order to determine the effects and response of the SCDF, a number of topographic Digital Elevation Models (DEMs) were developed by Cefas to represent the SCDF with present-day and potential-future shoreline positions, as well as a baseline domain representing the present day morphology (without the SCDF) for comparison. A description of each model domain is given below.

- ▶ **Baseline – 2017 DEM:** This model domain represents the Baseline “As Now” case. This domain is made up of the 2017 LIDAR data in the intertidal areas and 2017 Titan Bathymetry offshore. It represents the most recent co-incident terrestrial and subtidal elevation data. These combined data have a resolution of 1 m.
- ▶ **Case 1 – SCDF:** Cefas constructed the DEM of the coast with the proposed SCDF geometry merged with the Baseline DEM (present-day shoreline) for this model domain (BEEMS Technical Report TR544). The SCDF was based on the specifications set out in Section 3.7 of NNB Generation Company (SZC) Limited (2021b). The SCDF’s seaward facing slope is approximately 8.3°, which is the spatio-temporal averaged slope for the Sizewell C frontage, as described in BEEMS Technical Report TR544.
- ▶ **Case 2 – SCDF receded future shorelines:** Cefas also constructed the DEM for the proposed SCDF geometry with severely receded shorelines north and south of SZC. This model domain was based on the postulated shoreline at or toward the end of SZC’s decommissioning phase with present-day sediment supply<sup>14</sup> – see Section 7.7 of Volume 2, Appendix 20A of the Sizewell C Environmental Statement (NNB Generation Company (SZC) Limited, 2020).

The SCDF-future DEM was informed by the principle that the SCDF feature will be maintained throughout its lifetime, effectively holding the line along the frontage, and therefore it is expected that some degree of ‘outflanking’ may occur at the southern and northern ends of the SCDF in future. This is because the natural coastline either side of the SCDF would be free to retreat landward with sea level rise (Bruun, 1954; Kinsela *et al.*, 2017; McCarroll *et al.*, 2021), while the maintained frontage of the SCDF would not retreat landward. The expected result is therefore a shoreline that bends inland at the northern and southern ends of the SCDF in future. Within this version of the report, only the Baseline, SCDF and SCDF-future simulations have been modelled.

The 2D domains were developed with a total alongshore length of 4.5 km, centred on the proposed SCDF, which was deemed sufficient to capture any potential up- and down-drift hydrodynamic disturbances caused by the SCDF and would ensure model boundary effects (including lateral boundary wave shadows) would not influence the region of primary interest at the SCDF. The model has a cross-shore extent of 1.6 km. For both domains, the origin ( $x=0, y=0$ ) of the model grid is located at the most northerly, offshore location. Increasing southward distances are shown as positive values and increasing onshore distances are shown as positive values (Figure 2-1). To align the grid’s x-axis perpendicular to the shore at Sizewell, the XBeach model domain is rotated by one degree clockwise from north.

The offshore boundary of the model domain was initially placed to coincide with a water depth similar to that at the location of the Sizewell waverider buoy, used to provide forcing scenarios for the model. The buoy is located seaward of the Sizewell-Dunwich sandbank, in approximately 10 m water depth at mid tide. However, to ensure the model domain was of a size that could be feasibly managed in XBeach, the offshore boundary was actually placed landward of the Sizewell-Dunwich sandbank, at the equivalent water depth. Some frictional dissipation and even breaking of the largest waves would occur over the sandbank (-5.8 m ODN crest elevation), but is not accounted for in this study as the sandbank is not present in the model domain. Therefore, the beach response predicted by the model is considered to be conservative (i.e. more erosive than in reality), as the cumulative wave energy reaching the shore is likely to be larger than in reality under storm wave conditions. As per the recommended XBeach guidelines (<https://xbeach.readthedocs.io>), an artificial offshore slope to a depth of 20 m was added at the offshore boundary of the model domain,

---

<sup>14</sup> This is a conservative case as sediment supply is expected to increase downdrift of soft cliffs with rising sea levels owing to increased cliff erosion (Brooks, S. M. and Spencer, T. 2012. Shoreline retreat and sediment release in response to accelerating sea level rise: Measuring and modelling cliff line dynamics on the Suffolk Coast, UK. *Global and Planetary Change*, 80-81, 166-179.)



(Figure 2-1) to ensure wave breaking could not occur at the forcing boundary, and additional lateral and seaward model grid cells were implemented to remove any near-boundary gradients.

The model grid was developed with a variable resolution. In the area of primary interest, 800m around the proposed SCDF, the cross-shore and alongshore resolution was fixed at 2 m. North and south of this, the alongshore resolution gradually decreases to 20 m at the lateral boundaries. The cross-shore resolution was varied as a function of the water depth and offshore wave conditions, with a minimum resolution of 2 m in the vicinity of the SCDF, and maximum of 30 m at the offshore boundary. For this purpose, the Courant condition (Courant *et al.*, 1928) was used to find the optimal grid size at each depth, in terms of sufficiently resolving physical processes as well as yielding maximum computational efficiency and grid smoothness.

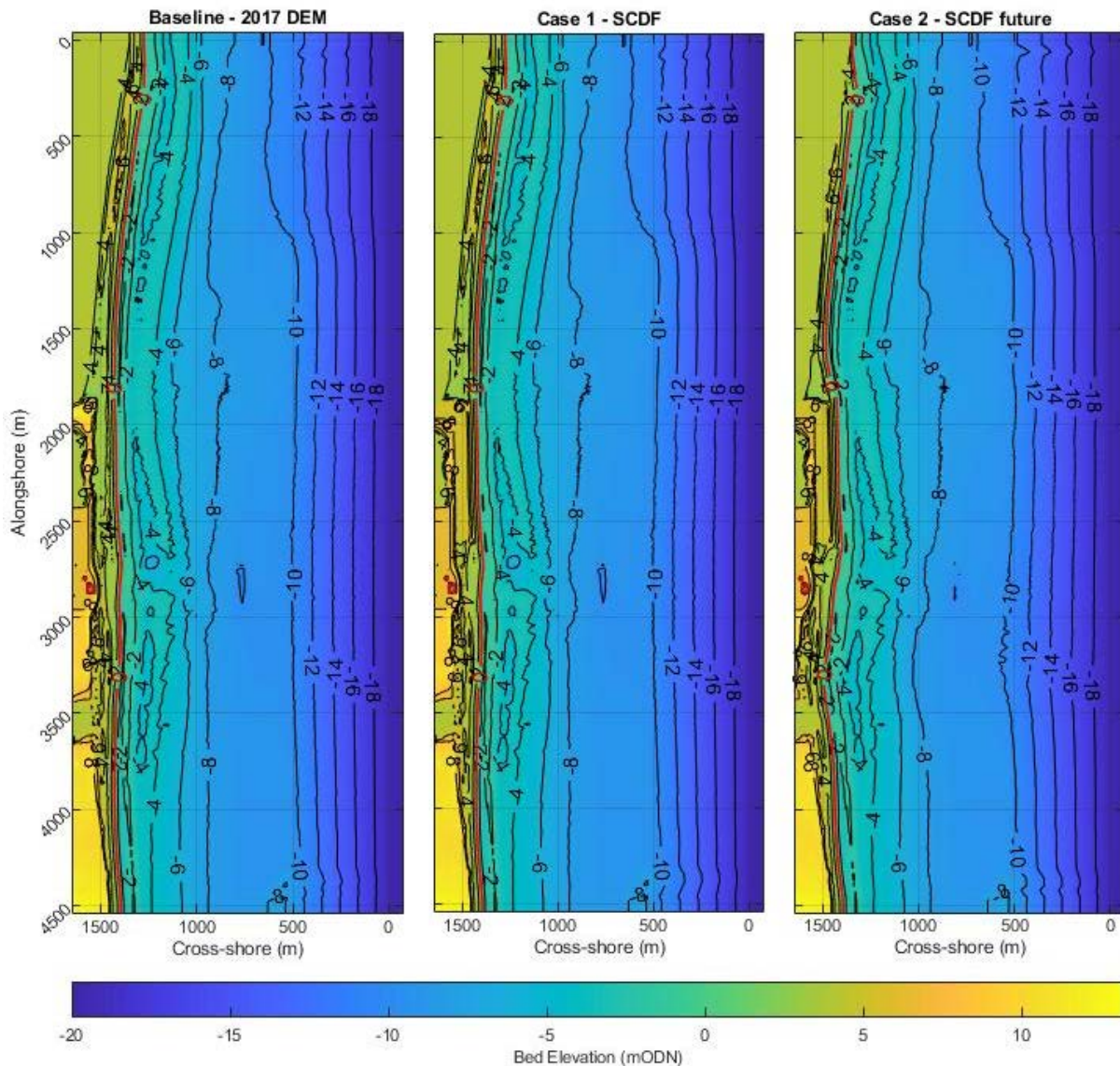


Figure 2-1. 2D Model Domain of the Baseline-2017 DEM, Case 1-SCDF DEM and Case 2-SCDF future eroded shoreline DEM (land on the left, sea on the right). Contour lines and colour show bathymetric depth from ODN. The red contour line shows the 0 m contour for reference.

## 2.2.2 Forcing Conditions

### 2.2.2.1 Waves

Observed wave conditions and water levels were used to provide boundary conditions for the model. The wave conditions were obtained from the Sizewell Waverider buoy, located at 52°12.62'N, 001°41.12'E. As the Waverider measurements were recorded near the model domain and in similar water depths (Section

2.2.1), the observed wave conditions were used to force the XBeach model directly, with the values of the significant wave height ( $H_s$ ), peak period ( $T_p$ ), and wave approach angle ( $D_p$ ) being updated hourly.

Three wave forcing conditions were used for the model scenarios, detailed below. All wave conditions were input to XBeach as JONSWAP spectra<sup>15</sup>:

- ▶ 1-in-20 year return period instantaneous wave height from the north east (herein, 1-in-20 NE) Event -  $H_s = 3.18$  m,  $T_p = 10.71$  s,  $D_p = 77^\circ$ , directional spread =  $18^\circ$  (as used in BEEMS Technical Report TR543).
- ▶ 1-in-20 year return period instantaneous wave height from the south east (herein, 1-in-20 SE) Event -  $H_s = 2.90$  m,  $T_p = 7.52$  s,  $D_p = 129^\circ$ , directional spread =  $18^\circ$  (as used in BEEMS Technical Report TR543).
- ▶ Beast from the East (BfE) Event - wave forcing conditions were those measured during the BfE storm sequence, (23<sup>rd</sup> Feb – 21<sup>st</sup> Mar 2018, Figure 2-3.) at the wave buoy offshore of the site. The event consists of three significant easterly storms in succession, with maximum  $H_s$  and  $T_p$  of 4.31 m and 11.8 s, respectively, and a combined return period of 1-in-107 years in terms of cumulative wave power (Appendix B, BEEMS Technical Report TR531). 9 days of low wave conditions were removed from the middle of the 26 day forcing timeseries (Figure 2-3.) to make computation of the three storm peaks feasible, including only periods where wave height remained  $> 1$  m. Removal of these periods is expected to have minimal impact on the final predicted beach morphology as beach evolution under such conditions is small.

In addition to the above model scenarios, two storm events were used for the calibration and validation of the 2D XBeach model, detailed in Section 2.3.1.

#### 2.2.2.2 Water levels

Tidal elevations were obtained from the Sizewell tide gauge, located on the Sizewell B intake navigation marker, and were updated in the model every 10 minutes.

- ▶ The timeseries in the 1-in-20 events represents a measured 13-hour mean spring tidal cycle centred over high tide (from low water to low water, observed 10th Feb 2020) with the addition of a measured storm surge curve that peaks at 1 m of surge at high tide, providing a maximum total water level of 2.1 m ODN (Figure 2-2). This magnitude of the surge component was selected based on the template curve predicted by the Environment Agency for Lowestoft and applicable between Winterton-on-Sea to Aldeburgh (McMillan *et al.*, 2011). This is in line with the Coastal Flood Boundary recommendations for design tide and storm surge height in this location.
- ▶ For the BfE Event, the water level timeseries measured during the event was used (Figure 2-3). Where a period of low waves was removed from the middle of the BfE sequence (Section 2.2.2.1), the two time periods were cropped and joined at the same low water tidal depth to avoid any sudden changes in water level.

---

<sup>15</sup> with default peak enhancement factor of 3.3 applied

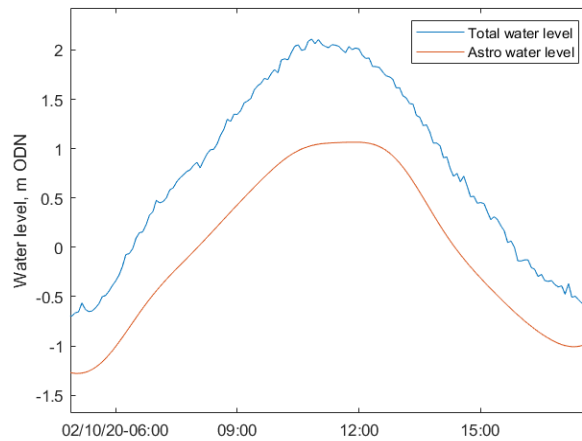


Figure 2-2. Total water level timeseries used for the 1-in-20 year simulations (blue line, as measured on the 10<sup>th</sup> Feb 2020 at the Sizewell tide gauge), consisting of a mean astronomical spring tidal cycle (red line), plus storm surge of up to 1 m coinciding with high tide.



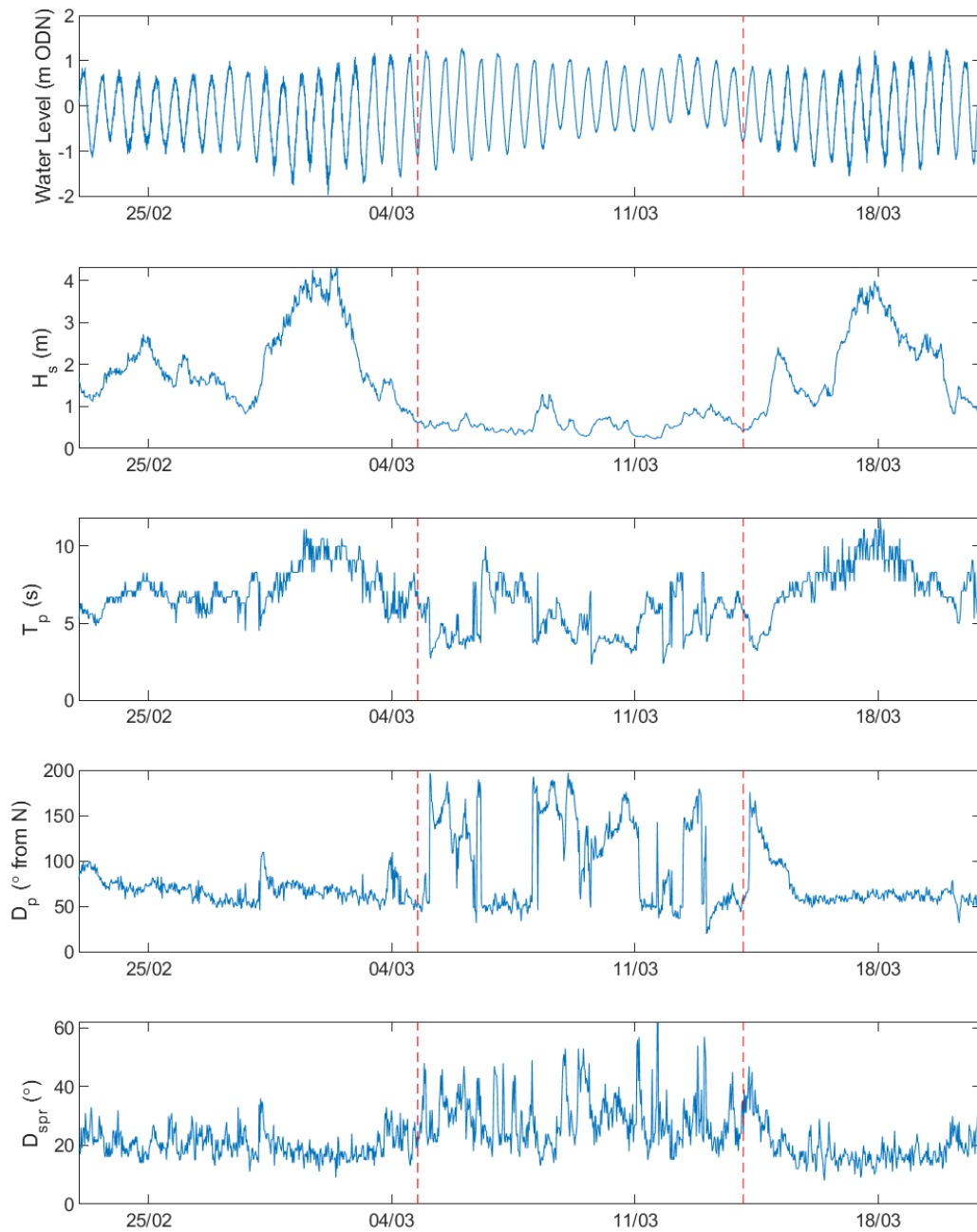


Figure 2-3. BfE Event water level and wave forcing conditions. The period between the two red dotted lines indicates the period excluded from the simulations in order to reduce the record length and allow the model to run.

### 2.2.2.3 Sea Level Rise

For model scenarios representing future conditions, sea level rise (SLR) was applied to the water levels (Section 2.2.2.2) using UKCP18 RCP4.5 95<sup>th</sup> percentile SLR projections. Table 2-3 and Table 2-4 detail the SLR applied to each model scenario. As measured water levels were used in each scenario, the amount of SLR applied differed depending on the year the water level timeseries was measured, and the future year being simulated. Therefore, the 1-in-20 year and BfE events differ slightly in SLR amount for a given future scenario as the BfE event occurred in 2018, whereas the representative 1-in-20 year water level timeseries was measured in 2020. For the hypothetical 1-in-20 year present-day scenarios, a UKCP18 SLR correction between 2020 and 2021 was applied, whereas the BfE scenario used the water level as measured in 2018.

## 2.3 2D Calibration and Validation

---

Model calibration was undertaken to provide the best possible accuracy of the model while validation was used to check that the calibrated XBeach model could reproduce other storm events. Given the mixed sand-gravel composition of the beach, perfect model performance was not expected to be achieved, and while skill scores were used to guide the tuning of model parameters, focus was placed on best reproducing the location and magnitude of measured erosion at Sizewell.

As XBeach is primarily a storm response model, the length of the model runs are on the order of the storm length. As such, calibration/validation beach topography data is needed as close to the start of the storm and immediately after, to ensure that the post-storm data only includes the influence of the storm and not any beach recovery under more benign conditions. Due to the mobilisation time (under COVID rules<sup>16</sup>), storms with predicted wave heights above 2 m for a duration of 12 hours were targeted.

The following storm events were selected for model calibration and validation:

- ▶ Calibration was performed on the 'May Storm' from 7<sup>th</sup> May 2020 to 15<sup>th</sup> May 2020.
- ▶ Validation was performed on 'Storm Ciara' from 6<sup>th</sup> February 2020 to 14<sup>th</sup> February 2020.

The dates of the start and end of the two simulations were limited to when surveys were undertaken pre- and post-storm, and therefore cover a longer period of time than the storm events themselves.

### 2.3.1 Calibration and Validation Forcing Conditions

Timeseries plots showing the measured hydrodynamic conditions for the calibration and validation events are provided in Appendix B.

#### 2.3.1.1 Waves

For both the calibration and validation events, the time varying wave forcing conditions were those measured during each storm at the Sizewell wave buoy offshore of the site (Section 2.2.2.1). The peak wave conditions of the two storms were:

- ▶ Calibration – 'May Storm'; max.  $H_s = 3.02$  m, max.  $T_p = 11.1$  s, median  $D_p = 52^\circ$ .
- ▶ Validation – 'Storm Ciara'; max.  $H_s = 3.63$  m, max.  $T_p = 10$  s, median  $D_p = 146^\circ$ .

#### 2.3.1.2 Water Levels

For both calibration and validation, water levels used to force the model were those measured during each storm at the Sizewell tide gauge (Section 2.2.2.2).

The calibration, "May Storm" simulation has a maximum water level of 1.52 mODN. The validation, 'Storm Ciara' simulation has a maximum water level of 2.10 mODN.

---

<sup>16</sup> Due to the unforeseeable impact of COVID-19, strict limitations for safely deploying the Cefas RPA during the winter storm conditions in early 2020 and the 2020/21 winter were in place, which restricted the number of storms that could be captured.

### **2.3.2 Model Domain**

Figure 2-4 shows the starting model domains used in the calibration and validation runs. The model domains were made up of the following data:

- ▶ Remote Piloted Aircraft (RPA) survey data in the intertidal region close to the site before and after each storm, created using the Structure from Motion (SfM) technique
- ▶ 2019 LiDAR data north and south of the site; and
- ▶ 2017 BEEMS bathymetry data offshore.

The topography of the RPA DSM equates to the visual surface seen in the photography. In the case of bare sediment, soil, grazed vegetation and walking/vehicle tracks, RPA, RTK-GPS and LiDAR will estimate the same elevation surface, however where there is tall vegetation, such as dune grasses, bushes and trees, elevation estimates may differ. That is, where RPA pixels cannot 'see' the bare earth beneath, the elevation of the vegetated surface will be estimated. This is similar to LiDAR, except that the pixel resolution of the Sizewell RPA surveys is too coarse to see through some grasses and gorse bushes to bare earth beneath<sup>17</sup>. The comparison of the RPA DSMs assumes no or negligible change in the height of the dune grasses, although volumetric interpretation will bear these points in mind.

As the model domain extends in the marine environment, the beach topography is combined at the water line with the multibeam bathymetry from 2017. Whilst in reality storm conditions will alter the inner and outer longshore bars along the Sizewell frontage over time, the 2017 bathymetry is the most recent and accurate data available relative to the selected storms, and is deemed to represent the position of the inner and outer longshore bars sufficiently to achieve the aims of the present modelling activity.

---

<sup>17</sup> This is effectively what Lidar does, though more effectively because of the smaller laser footprint. However, for dense ground vegetation, both methods are likely to suffer from the same issue of not being able to 'see' the bare ground.

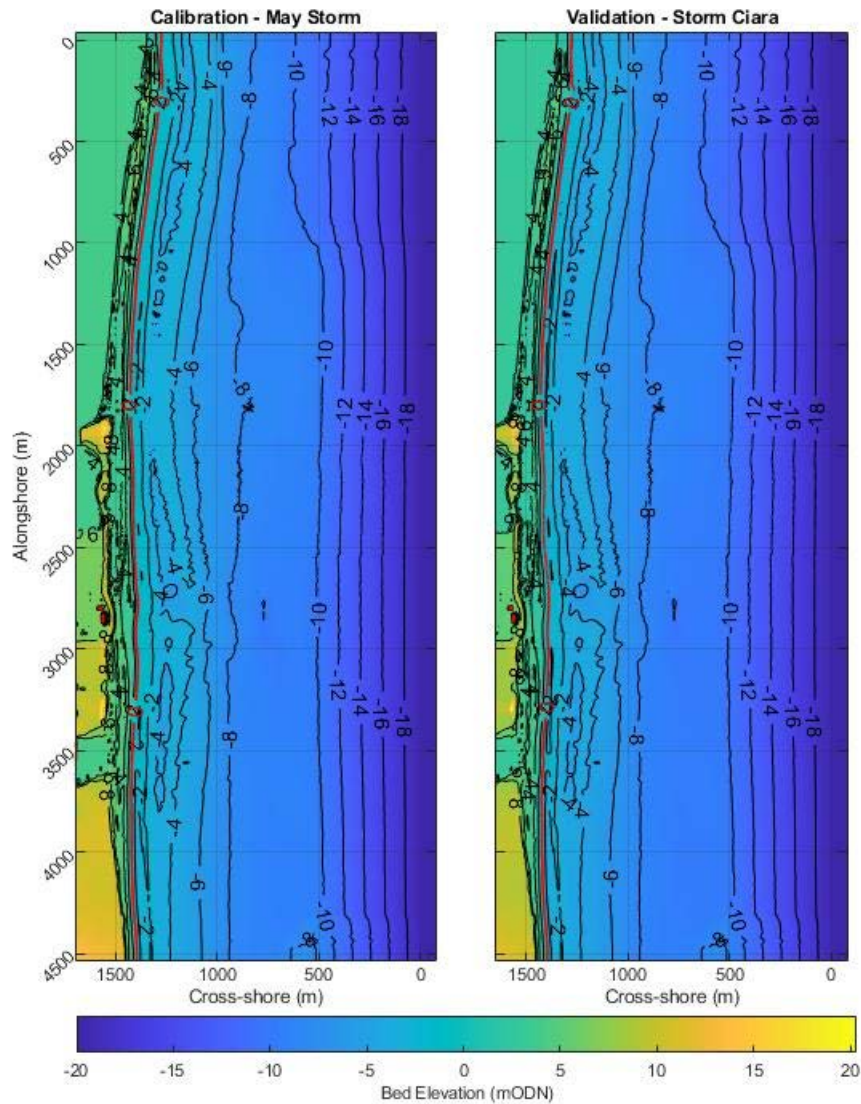


Figure 2-4 Calibration (left) and Validation (right) starting model domains (land on the left, sea on the right). The subaerial topography was obtained from an RPA survey on the 7<sup>th</sup> May 2020 for the calibration and the 6<sup>th</sup> February 2020 for the validation. Contour lines and colour show bathymetric depth from ODN. The red contour line shows the 0 m contour for reference.

### 2.3.3 Calibration and Validation Parameters

Model parameters that resulted in optimal model performance were explored during the calibration process. This process aimed to tune the XBeach settings in order to best reproduce observed morphodynamic changes at Sizewell during two different storm events, described previously. Preliminary 1D XBeach-S modelling in BEEMS Technical Report TR531 also provided a calibrated and validated model for Sizewell beach; however, the calibration and validation in this report is new (although using some of the same source data) and provides a significantly improved validation against field measurements over the original calibration in report TR531.

Following the extensive scientific literature on XBeach model calibration (Vousdoukas *et al.*, 2012; Nederhoff *et al.*, 2015; Elsayed and Oumeraci, 2017; Schambach *et al.*, 2018; Simmons *et al.*, 2019), the following key tuning parameters in XBeach were optimised to calibrate the 2D sand model in this study:

- ▶ **Facua** - the parameterized wave asymmetry sediment transport component.

This parameter determines the balance between offshore and onshore sediment transport, and is a key morphological tuning parameter in XBeach. On steep beaches wave asymmetry becomes more important and since the default facua parameter in XBeach was determined for Dutch beaches, calibration is needed (Nederhoff *et al.*, 2015). Higher values of facua cause the model to simulate a stronger onshore sediment transport component (Roelvink *et al.*, 2010).

- ▶ **Bed friction** - influences the bed stability and the sediment transport via the formulation of the bed shear stress.

The bed friction coefficient becomes very important in cases of overwashing, where higher bed friction values result in less sediment transport on top of the barrier (Nederhoff *et al.*, 2015), but also influences processes in the nearshore that impact the flow near the bed.

- ▶ **Gamma** - the random wave equivalent of the breaker index in the wave dissipation model (Simmons *et al.*, 2019), used to determine the proportion of broken waves at a given water depth.

- ▶ **Grain size** – distribution of sediment sizes, characterised using the median ( $D_{50}$ ) and 90<sup>th</sup> percentile ( $D_{90}$ ) sediment sizes.

While grain size is not usually considered a tuning parameter in XBeach, it was varied within this study in order to explore which representative (sand) grain size distribution best reproduced the observed (mixed sand-gravel) morphodynamic response at Sizewell.

Secondary tuning parameters that were also used in this study include:

- ▶ **Morfac** – This is used to reduce computation time by accelerating the morphological response within the model relative to the hydrodynamic forcing, yet has negligible effects on the morphological outcome.

In previous studies, morfac values of up to 20 have been found to have little effect on the results of an XBeach simulation, despite providing a considerable reduction in the computational time required (Lindemer *et al.*, 2010; McCall *et al.*, 2010). Therefore, using Morfac of 10 (acceleration used in this study) produces erosion volumes that are negligibly different to those obtained with Morfac of 1 (no acceleration), but incurs 10 times less computational effort.

- ▶ **Wetslp** - critical bed slope for the slumping of sandy material in the wet area of the model.

Table 2-1 Final calibration model parameters

| Parameter          | Definition   | Range  | Default   | Selected  |
|--------------------|--|--|---|---|
| <i>facua</i>       | Wave asymmetry sediment transport component          | 0 - 1  | 0.1   | 0.3   |
| <i>bedfriccoef</i> | Bed friction coefficient using the Chezy formulation | 20 - 100   | 55  | 40  |
| <i>gamma</i>       | random wave equivalent of the breaker index          | 0.4 - 0.9  | 0.55  | 0.4   |
| <i>grain size</i>  | Size and distribution of sandy beach sediment        | D <sub>15</sub> : 0.1 - 0.8 mm<br>D <sub>50</sub> : 0.1 - 0.8 mm<br>D <sub>90</sub> : 0.1 - 1.5 mm | D <sub>15</sub> : 0.15 mm<br>D <sub>50</sub> : 0.2 mm<br>D <sub>90</sub> : 0.3 mm | D <sub>15</sub> : 0.15 mm<br>D <sub>50</sub> : 0.8 mm<br>D <sub>90</sub> : 1.5 mm |
| <i>morfac</i>      | Morphological acceleration factor                    | 0 - 1000   | 1   | 10  |
| <i>wetslp</i>      | critical wet slope for avalanching                   | 0.1 - 1  | 0.3   | 0.2   |

### 2.3.4 Calibration and Validation Results

The difference between the start and predicted end topography of the calibration simulation was spatially plotted (in 2D) alongside the difference in the pre and post storm measured surveys to assess the performance of the model (Figure 2-5 – calibration and Figure 2-7 – validation). Additionally, five cross-sectional profiles were extracted from the 2D model and measured data, at locations used previously in the preliminary 1D modelling (BEEMS Technical Report TR531) to help assess the model performance. Profile locations are indicated in Figure 2-5 and Figure 2-7. Figure 2-6 shows the cross-sectional comparison plots for the calibration May Storm simulation. Figure 2-8 shows the cross-sectional comparison plots for the validation Storm Ciara simulation.

For both the calibration and validation simulations, the location of erosion occurs at a similar position on the beach face to that of the observed erosion (Figure 2-6 and Figure 2-8). The divergence of the beach profile from the initial starting condition occurs at a similar point on the measured and modelled post-storm profiles, indicating that the landward extent of beach erosion is being reproduced by the model. For both the calibration and validation storms, erosion volume is overestimated using the chosen model parameters by at least 2-3 times compared to the observed erosion. With other (sub-optimal) combinations of the tuning parameters (in particular, *facua*, Section 2.3.3) erosion was either severely overestimated, or too much onshore transport of sediment occurred resulting in unrealistic beach face accretion. The measured erosion during Storm Ciara (Figure 2-8) is significantly lower than that of the May storm (Figure 2-6), and the chosen model parameters reproduce this proportionally in the predicted beach response, albeit with proportional overestimation of the erosion in both cases.

There is a limitation to the extent the model can be calibrated due to measured data only being available on the subaerial beach, i.e., in areas visible at low tide, which is a commonly encountered situation. For this reason, it is difficult to determine fully how the model is performing in terms of erosion and accretion on the subtidal beach face. From the observed lower beach response, and due to the over prediction of erosion higher on the beach face, it is likely that accretion in the subtidal is overestimated by the calibrated model. In the measured data, conspicuous berm/ridge buildup is visible at places on the supra-tidal beach (Figure 2-5 to Figure 2-8), in addition to beach erosion on the intertidal profile. This is a typical response seen on beaches with coarse material (Almeida *et al.*, 2015; McCall *et al.*, 2015) but is not reproduced by the

calibrated XBeach-S model, which is not expected to recreate the behaviour of the coarsest particles at Sizewell.

The chosen parameters provide the best qualitative match with regards to the location and approximate magnitude of observed storm response. They also provided the best model skill scores when assessed with Brier Skill (BSS) and Root-Mean-Squared-Error (RMSE) of the parameters tested. However, due to the limitations with regards to mixed sand-gravel beaches and the conservative over-estimation of storm erosion, BSS was classed as 'poor' ( $<0.3$ ) for all tested combinations of model settings (Table B-1). RMSE, assessed using the difference between the post-storm modelled and measured bed elevations, was 1.04 m and 1.44 m for the calibration and validation model predictions, respectively. Despite the performance of the calibrated model being poor when assessed with BSS, the fact that it is qualitatively able to reproduce the location and cross-shore extent of storm erosion, and provide conservative erosion volumes with average bed level accuracy on the order of 1 m, means the calibrated model is fit for the purposes of the present study.

The chosen model settings are therefore deemed to provide the best match possible to the observed beach response, given the limitations of the model with regards to mixed sand-gravel beaches. The calibrated model is deemed suitable for the present modelling study, as it reproduces the location and cross-shore extents of erosion, and importantly, provides conservative estimates of the magnitude of storm erosion at Sizewell beach with which to determine the SCDF volume loss (including SCDF sediment transported away from SZC to adjacent frontages) during storm events.



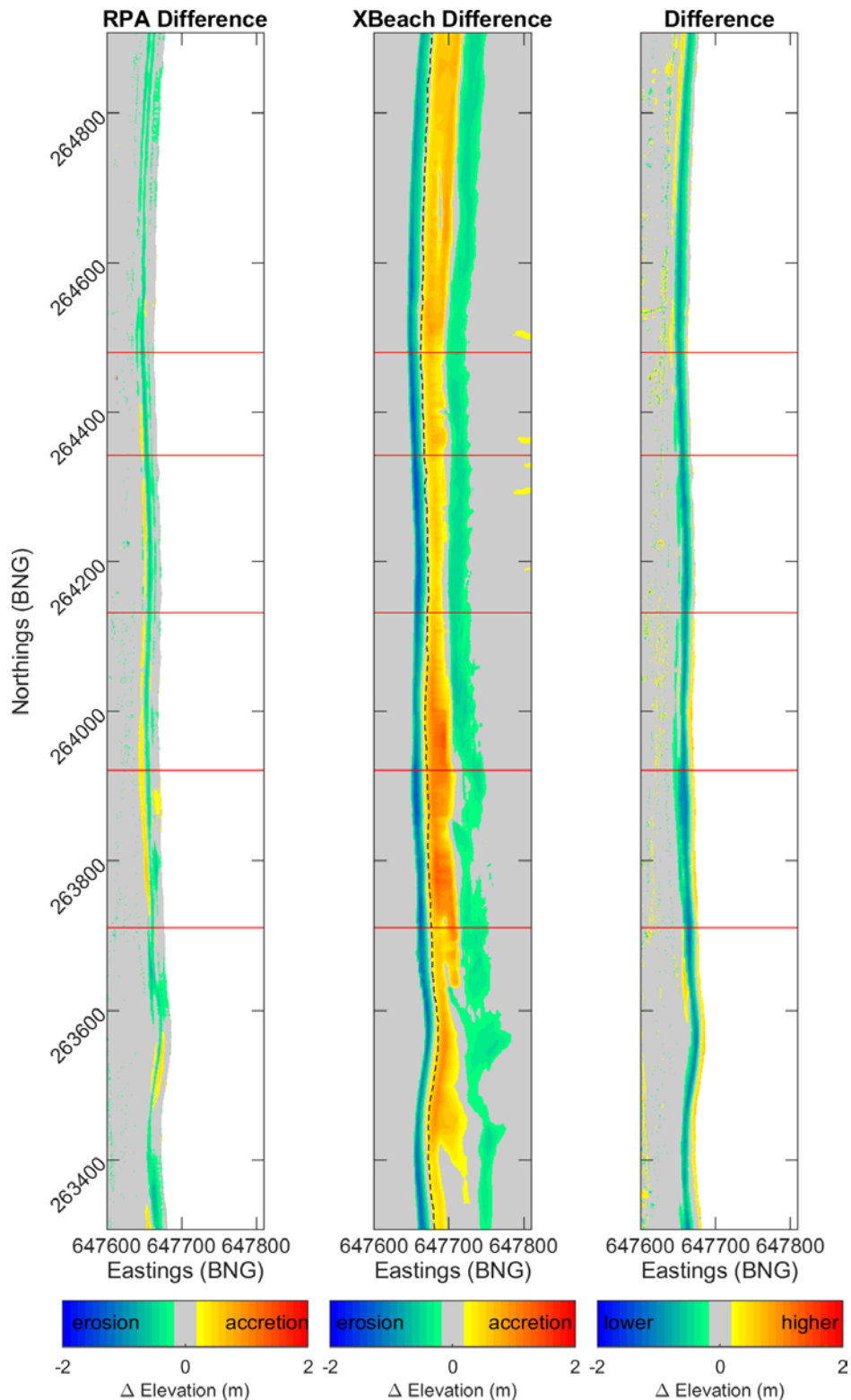


Figure 2-5. Model calibration ('May Storm') – topographic change from pre- to post-storm from the measured survey data (left), XBeach simulation (middle) and the difference between the measured and predicted changes (right). The right panel shows where the modelled beach surface is lower (blue/green) or higher (yellow/red) than the measured beach surface at the end of the storm. The red lines indicate the location of the cross-sections plotted in Figure 2-6. The black dotted line in the middle panel indicates the seaward extent of the measured data. Sizewell C is between 263,745 m N and 264,508 m N (BNG).

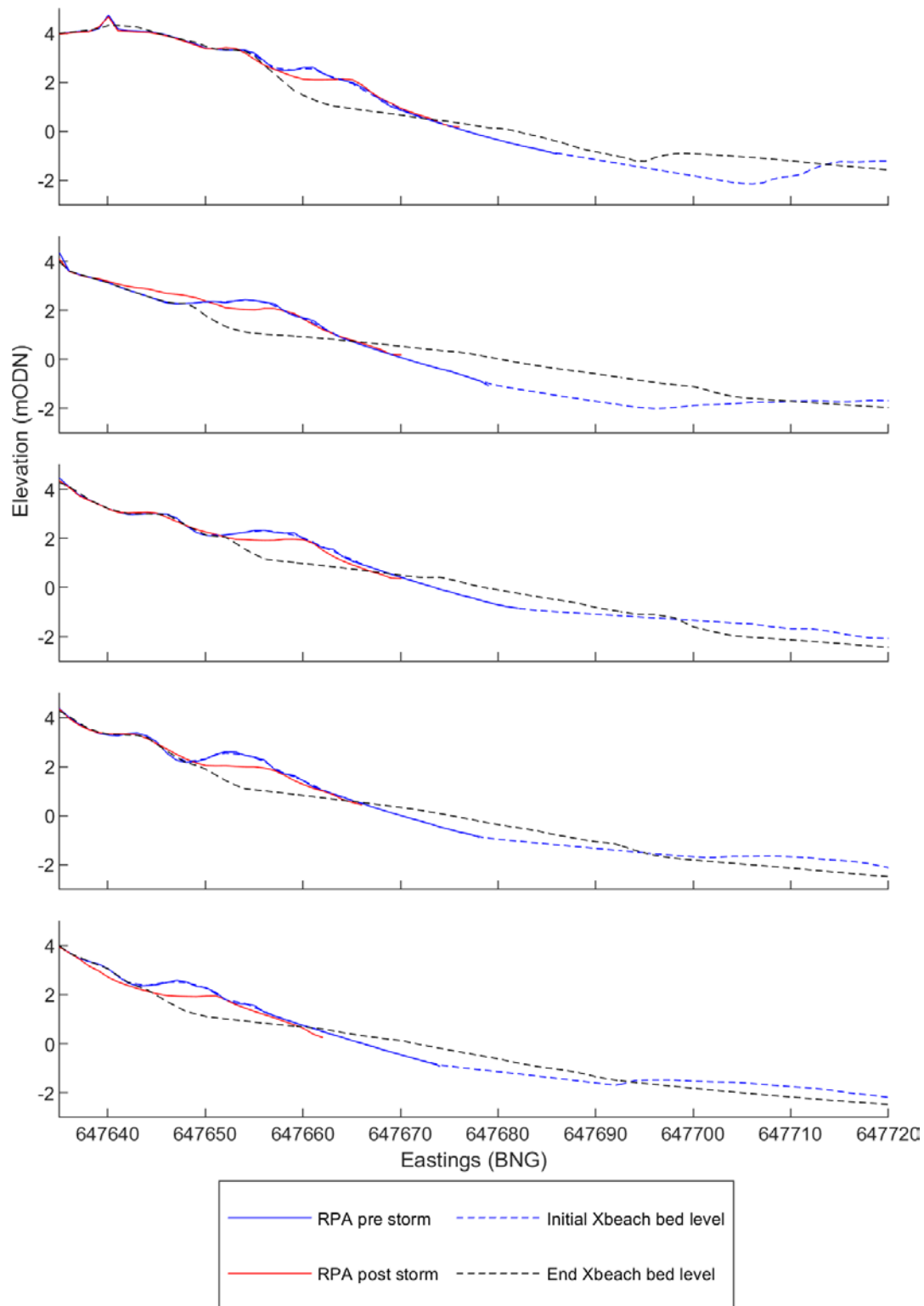


Figure 2-6. Model calibration ('May Storm') – cross-sectional profiles of bed elevation pre- and post-storm from the measured survey (solid lines) and XBeach simulation (dashed lines). Profiles are located at 263710.5 N (top), 263921.1 N (second from top), 264131.6 N (middle), 264342.1 N (second from bottom) and 264480.0 N (bottom).

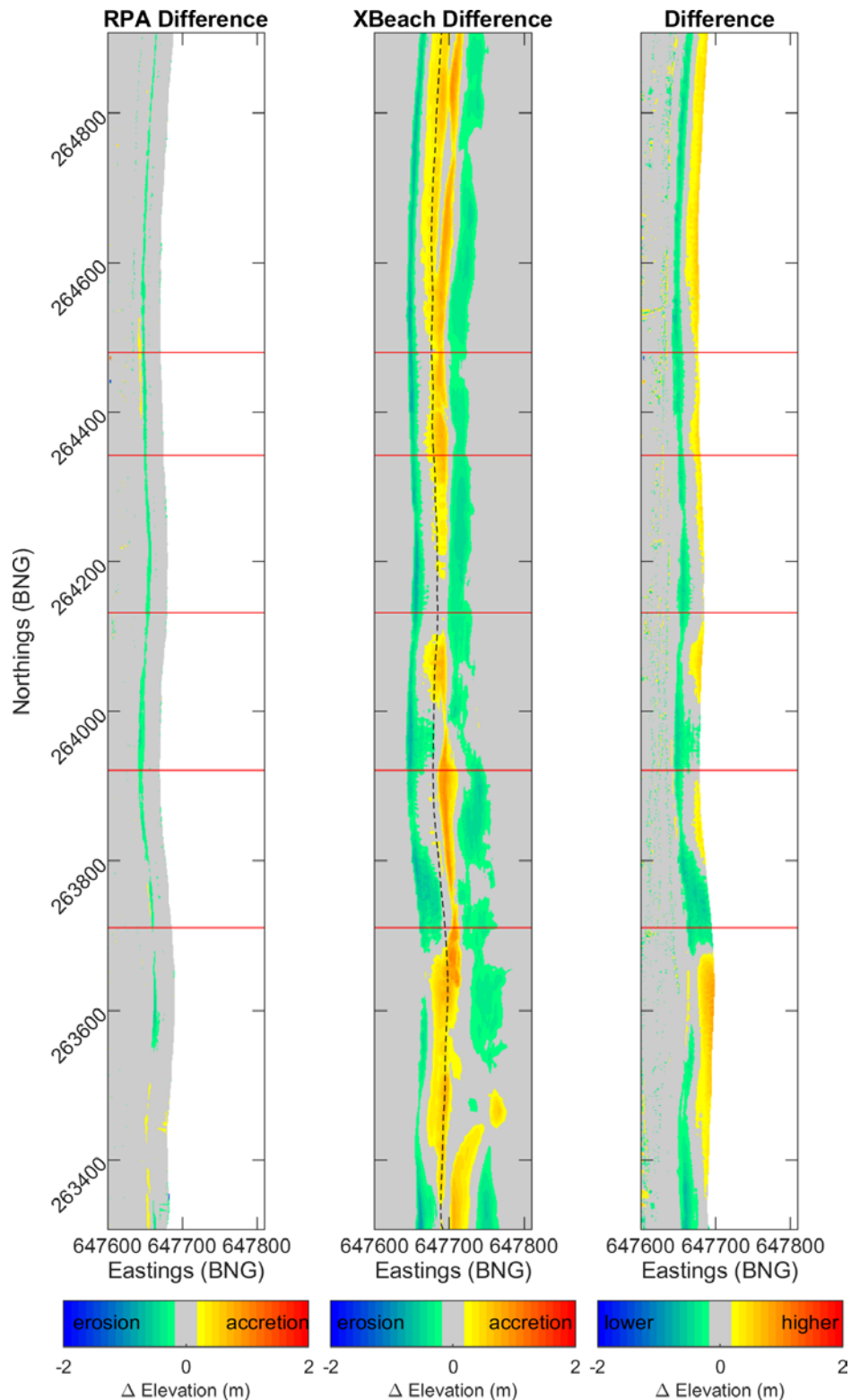


Figure 2-7. Model validation ('Storm Ciara') – topographic change from pre- to post-storm from the measured survey data (left), XBeach simulation (middle) and the difference between the measured and predicted changes (right). The right panel shows where the modelled beach surface is lower (blue/green) or higher (yellow/red) than the measured beach surface at the end of the storm. The red lines indicate the location of the cross-sections plotted in Figure 2-8. The black dotted line in the middle panel indicates the seaward extent of the measured data. Sizewell C is between 263,745 m N and 264,508 m N (BNG).

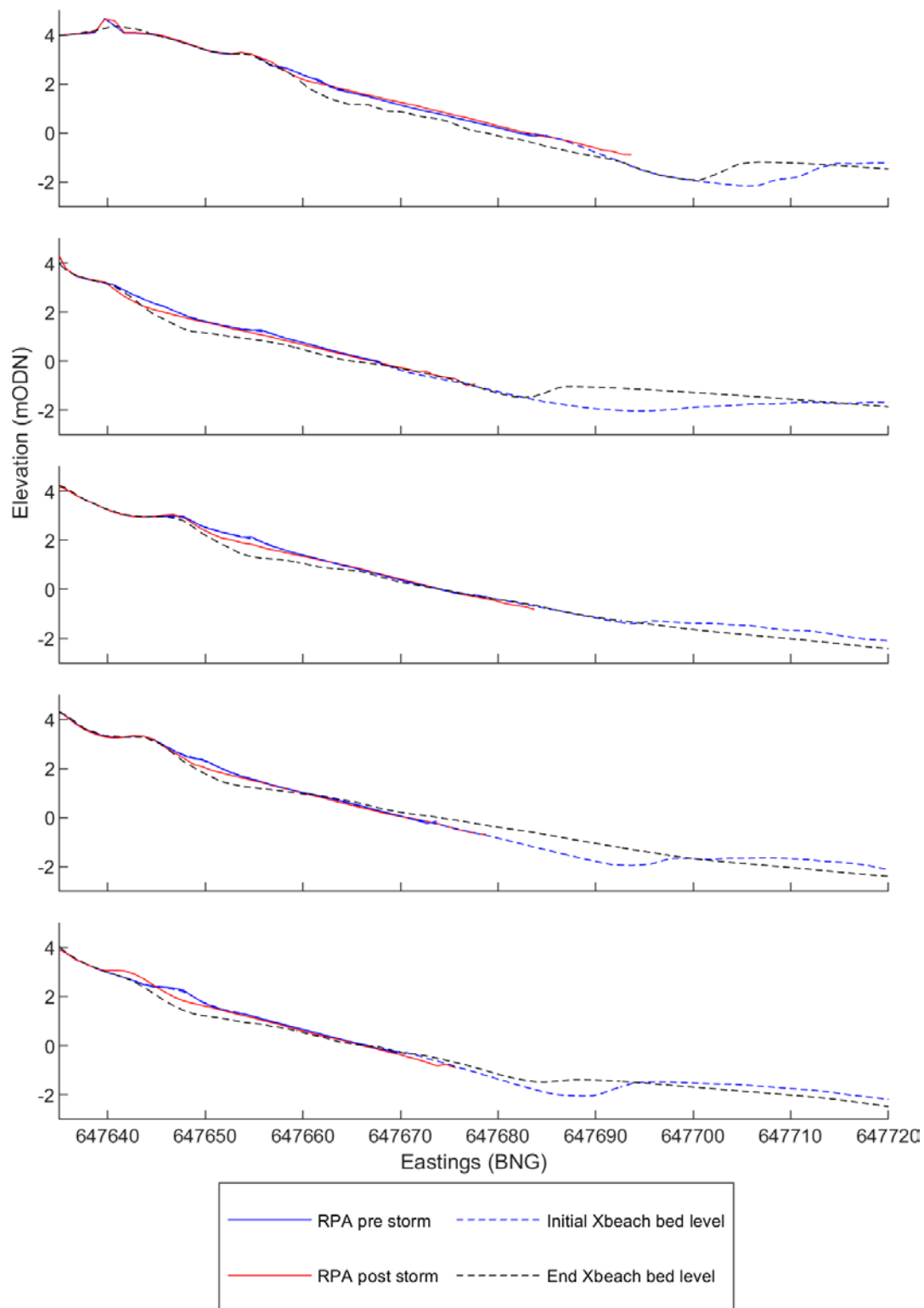


Figure 2-8. Model validation ('Storm Ciara') – cross-sectional profiles of bed elevation pre- and post-storm from the measured survey (solid lines) and XBeach simulation (dashed lines). Profiles are located at 263710.5 N (top), 263921.1 N (second from top), 264131.6 N (middle), 264342.1 N (second from bottom) and 264480.0 N (bottom).

## 2.4 1D XBeach gravel and sand model

A 1D model domain was developed in XBeach to test the sensitivity of the SCDF's storm response to the grain size used for the SCDF. As discussed in Section 2.1, no formulations exist yet within XBeach (or any other process-based numerical models) specifically for mixed sand-gravel beach dynamics. Therefore, the 1D model was run using both XBeach-S (with calibrated parameters from Section 2.3.3) and XBeach-G separately, enabling the morphological behaviour of a wide range of grain sizes – from very coarse sand to fine cobbles – to be explored.

Running simulations in XBeach-G is important in this study because:

- ▶ The erosional behaviour of the gravel fraction (pebble and cobble size classes) is different to that of sand. In particular, the higher fall velocity of coarse particles makes them less mobile than sand and the higher permeability of coarse particles influences wave runup and backwash velocities.
- ▶ Wave runup at steep coarse-grained beaches (such as the designed SCDF) is significantly higher than wave runup at shallow sandy beaches due to the incident wave signal remaining at the shore of steep beaches (Poate et al., 2016).

Therefore, XBeach-G is required to reproduce the incident wave signal that drives the high runup heights at steep beaches, allowing erosion to be better reproduced and potential overtopping to be more reliably identified. Further to the XBeach-S limitations identified in Section 2.2, there are also limitations in using an XBeach-G model for the mixed sand-gravel beach at Sizewell. The key limitations can be summarised as:

- ▶ The gravel model assumes that only bed-load transport occurs, and therefore suspended transport of the finer sand fractions is ignored. The finest naturally-occurring grain sizes at Sizewell are therefore smaller than those that can be simulated reliably in the gravel model, but the pebbles (and potentially fine cobbles) that are likely to be used for the SCDF are well within the suitable size limits of the gravel model.
- ▶ The gravel model used assumes that grain sizes are uniformly distributed across the beach face. The mixed sand-gravel beach at Sizewell displays notable grading in grain size in the cross-shore direction with mostly sand in the subtidal, a varying, gravel-dominant, sand-gravel mixture in the intertidal and a gravel supra-tidal (with low volumes of sand) beach. The SCDF will most likely be constructed medium – coarse pebbles or larger particles.
- ▶ The gravel model accounts for infiltration and exfiltration of water from the beach face, but in reality this is likely to be inhibited to some degree on the natural mixed sand-gravel parts of the beach (i.e. the intertidal beach) due to pore spaces being filled with finer sand.

As the finer sediment contained in the subtidal bars and offshore region at Sizewell cannot be reliably modelled in the gravel version of XBeach, the seabed at Sizewell was made non-erodible within the 1D XBeach model runs seaward of the inner trough of the inner bar ( $x < 1400$ , Figure 2-9). The effect of this is that the movement of the finer sediment contained in the bars and offshore region are not simulated, meaning that only the dynamics of the subaerial beach/SCDF (pebbles/cobbles) were modelled ( $x > 1400$ , Figure 2-9).

### 2.4.1 1D Model Profile

For the 1D simulations, a single cross-shore profile was extracted from the 2D SCDF model domain (Figure 2-1, centre panel) at Northing 264105, which lies at the centre of the SCDF. The 1D XBeach-S domain used the same optimised cross-shore resolution as the 2D domain (minimum resolution of 2 m at the coast, and maximum of 30 m at the offshore boundary), while the 1D XBeach-G simulations were performed on the same profile but with an increased cross-shore resolution (minimum resolution of 0.1 m at the coast, and maximum of 6.3 m at the offshore boundary), required for the non-hydrostatic computations<sup>18</sup>. The 1D

---

<sup>18</sup> Non-hydrostatic computations require a fine resolution between computational nodes to fully discretise the individual wave lengths. In practice this means the resolution must be increased relative to a 'surf-beat' XBeach-S model.

domain has the same cross-shore extent as the 2D domain (1.6 km), and contains the same artificial slope at the offshore boundary down to 20 m depth for model stability.

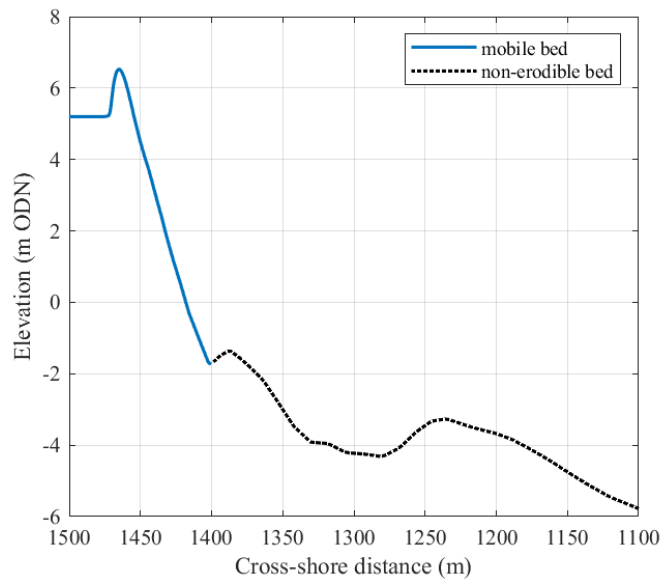


Figure 2-9. Model profile used in the gravel and sand versions of XBeach for the 1D grain size sensitivity tests. The extent shown is zoomed in on the SCDF and inner bars, while the full DEM cross-shore extent (Figure 2-1) was used in the models. The solid line indicates the mobile seabed within the model, while the dotted line shows the seabed that was made non-erodible in the model.

## 2.4.2 Forcing Conditions

A single storm scenario was used for the 1D grain size sensitivity simulations. The forcing conditions for the 1-in-20 year NE event (Section 2.2.2) were used, including the same water levels, and UKCP18 RCP4.5 sea level rise scenarios for 2021, 2069, and 2099 (Table 2-4). This event was chosen for these tests as it is the more shore-normal of the two 1-in-20 year events and is therefore more appropriate for a 1D model. The BfE storm sequence, although shore-normal, consists of three storm events spanning at least 17 days (Section 2.2.2) and when tested in XBeach-G it was not possible for the non-hydrostatic 1D XBeach-G model to successfully complete the full BfE sequence.

## 2.4.3 Grain Size

Five different grain sizes were tested in the 1D XBeach models. Grain size was varied between  $D_{50} = 0.8$  mm (coarse sand) and 2 mm (very coarse sand/fine gravel) in the XBeach-S, and  $D_{50} = 2$  mm, 10 mm (medium pebbles), 40 mm (very coarse pebbles), and 80 mm (fine cobbles) in the gravel model (Blair and McPherson, 1999). The gravel sizes were chosen to coincide with those tested during the development of XBeach-G, and for which measured ground water hydraulic conductivity values were available (McCall, 2015). A summary of the grain size settings for each 1D model scenario are provided in Table 2-4.

The very coarse sand/granule size ( $D_{50} = 2$  mm) tested is slightly coarser than the recommended maximum for the XBeach-S ( $D_{50} = 0.8$  mm), but is at the boundary between the sand and gravel fractions, and is therefore a useful comparison case that can be run in both the sand and gravel models. Cobble sizes larger than 80 mm may be suitable for the construction of the SCDF, but have not previously been validated in XBeach and were therefore not simulated in these tests. The default position for SCDF particle size is to match the native size distribution, which has a model pebble size of approximately 10 mm diameter.

## 2.4.4 Model parameters

The 1D XBeach-S simulations were run using the same model parameters as those selected following the 2D model calibration exercise (Table 2-1). The 1D XBeach-S model is therefore also considered to be a calibrated model when run with these settings and  $D_{50}$  of 0.8 mm, as the key tuning parameters control



cross-shore dominant processes only (Section 2.3.3) such as onshore vs offshore transport (*facua*), wave breaking (*gamma*), bed friction, and profile slumping (*wets/p*), which will transfer directly to a 1D simulation.

The 1D XBeach-G model has not specifically been calibrated for use at Sizewell, or for the SCDF in question, but where possible, model settings from previously calibrated gravel XBeach models were applied (McCall *et al.*, 2014; McCall, 2015; McCall *et al.*, 2015). It is therefore semi-calibrated through best possible alignment with calibrated models for similar beaches from the scientific literature. The primary parameters (Table 2-2) controlling beach response in the gravel formulations within XBeach are:

- ▶ **Hydraulic conductivity,  $K$** , which determines the ability of water to infiltrate and exfiltrate through the gravel beach. Higher values of  $K$  allow faster transmission of water through the beach face.

The  $K$  value used in this study (Table 2-4) was observed through field measurements to occur at beaches with grain size of  $D_{50} = 2$  mm, but is lower than the  $K$  values observed in the field at pure gravel beaches with 10 – 80 mm grain sizes (McCall *et al.*, 2014; McCall, 2015; McCall *et al.*, 2015). However, the chosen value is still significantly permeable, and was the maximum value recommended by the developers of XBeach-G (members of both Deltares and University of Plymouth, via personal communication) for numerical stability, due to the high groundwater velocities that can occur otherwise. This is expected to result in conservative erosion and runup values (i.e. higher than may occur in reality), as the lower  $K$  values used will primarily increase uprush and backwash relative to a higher  $K$  value (McCall, 2015), promoting higher runup and increased offshore directed transport, respectively.

- ▶ **Transport formula, *form***. Various bed-load transport formulae can be selected for gravel in XBeach, and each has related coefficients determining the transport rate.

Of the various transport formulations available for gravel within XBeach, the formula of McCall-Van Rijn (Van Rijn, 2007a, b; McCall *et al.*, 2015) has been found to provide the best comparison to measured storm response at gravel beaches (McCall, 2015), and was therefore selected for this study.

- ▶ **Transport calibration coefficient, *sedcal***. Following previous studies (Van Rijn, 2007a; McCall, 2015; McCall *et al.*, 2015), we set the McCall-Van Rijn calibration coefficient to 0.5.

Table 2-2 Calibrated model parameters for the 1D XBeach gravel-only model.

| Parameter     | Definition                              | Range       | Default         | Selected        |
|---------------|---|-------------|-----------------|-----------------|
| $K$           | Hydraulic conductivity                  | 1e-05 - 0.1 | 0.0001          | 0.01            |
| <i>form</i>   | Gravel transport formulation            | various     | McCall-Van Rijn | McCall-Van Rijn |
| <i>sedcal</i> | McCall-Van Rijn calibration coefficient | any         | 1               | 0.5             |

## 2.5 Model Scenario Summary

### 2.5.1 Operational phase

Table 2-3 details each of the 2D model runs undertaken including the Model Domain used, Storm condition and sea level rise applied to each scenario during the operational phase of SZC.

Table 2-4 details each of the 1D model runs undertaken including the Model Domain used, Storm condition and sea level rise applied to each scenario during the operational phase of SZC.

Table 2-3. 2D model scenario summary.

| Scenario | Description                        | Model Domain    | Storm | SLR Year | SLR correction (m) |
|----------|------------------------------------|-----------------|-------|----------|--------------------|
| 10       | BfE storm, E, present SL           | SCDF DEM        | BfE   | 2018     | 0.000              |
| 2        | 1-in-20 year storm, NE, present SL | SCDF DEM        | NE    | 2021     | 0.007              |
| 4        | 1-in-20 year storm, SE, present SL | SCDF DEM        | SE    | 2021     | 0.007              |
| 13       | BfE storm, E, 2069 SLR             | SCDF DEM        | BfE   | 2069     | 0.413              |
| 14       | BfE storm, E, 2069 SLR             | SCDF-future DEM | BfE   | 2069     | 0.413              |
| 15       | 1-in-20 year storm, NE, 2069 SLR   | SCDF DEM        | NE    | 2069     | 0.400              |
| 16       | 1-in-20 year storm, SE, 2069 SLR   | SCDF DEM        | SE    | 2069     | 0.400              |
| 11       | BfE storm, E, 2099 SLR             | SCDF DEM        | BfE   | 2099     | 0.714              |
| 12       | BfE storm, E, 2099 SLR             | SCDF-future DEM | BfE   | 2099     | 0.714              |
| 5        | 1-in-20 year storm, NE, 2099 SLR   | SCDF DEM        | NE    | 2099     | 0.701              |
| 7        | 1-in-20 year storm, SE, 2099 SLR   | SCDF DEM        | SE    | 2099     | 0.701              |
| 6        | 1-in-20 year storm, NE, 2099 SLR   | SCDF-future DEM | NE    | 2099     | 0.701              |
| 8        | 1-in-20 year storm, SE, 2099 SLR   | SCDF-future DEM | SE    | 2099     | 0.701              |

Table 2-4. 1D model scenario summary. The profile used in each 1D scenario (Figure 2-9) was taken from the centre of the SCDF DEM (location Y<sub>1</sub>, described in Section 3).

| Scenario | Description                                 | Grain size (mm)                                | Hydraulic conductivity (m/s) | Storm | SLR Year | SLR correction (m) |
|----------|---|--|------------------------------|-------|----------|--------------------|
| 1-1D     | 1-in-20 year storm, NE, 2021 SLR (XBeach-S) | D <sub>50</sub> = 0.8<br>D <sub>90</sub> = 1.5 | n/a                          | NE    | 2021     | 0.007              |
| 2-1D     | 1-in-20 year storm, NE, 2021 SLR (XBeach-S) | D <sub>50</sub> = 2<br>D <sub>90</sub> = 3     | n/a                          | NE    | 2021     | 0.007              |
| 3-1D     | 1-in-20 year storm, NE, 2021 SLR (XBeach-G) | D <sub>50</sub> = 2<br>D <sub>90</sub> = 3     | 0.01                         | NE    | 2021     | 0.007              |
| 4-1D     | 1-in-20 year storm, NE, 2021 SLR (XBeach-G) | D <sub>50</sub> = 10<br>D <sub>90</sub> = 15   | 0.01                         | NE    | 2021     | 0.007              |
| 5-1D     | 1-in-20 year storm, NE, 2021 SLR (XBeach-G) | D <sub>50</sub> = 40<br>D <sub>90</sub> = 60   | 0.01                         | NE    | 2021     | 0.007              |
| 6-1D     | 1-in-20 year storm, NE, 2021 SLR (XBeach-G) | D <sub>50</sub> = 80<br>D <sub>90</sub> = 120  | 0.01                         | NE    | 2021     | 0.007              |
| 7-1D     | 1-in-20 year storm, NE, 2069 SLR (XBeach-S) | D <sub>50</sub> = 0.8<br>D <sub>90</sub> = 1.5 | n/a                          | NE    | 2069     | 0.400              |
| 8-1D     | 1-in-20 year storm, NE, 2069 SLR (XBeach-S) | D <sub>50</sub> = 2<br>D <sub>90</sub> = 3     | n/a                          | NE    | 2069     | 0.400              |
| 9-1D     | 1-in-20 year storm, NE, 2069 SLR (XBeach-G) | D <sub>50</sub> = 2<br>D <sub>90</sub> = 3     | 0.01                         | NE    | 2069     | 0.400              |
| 10-1D    | 1-in-20 year storm, NE, 2069 SLR (XBeach-G) | D <sub>50</sub> = 10<br>D <sub>90</sub> = 15   | 0.01                         | NE    | 2069     | 0.400              |
| 11-1D    | 1-in-20 year storm, NE, 2069 SLR (XBeach-G) | D <sub>50</sub> = 40<br>D <sub>90</sub> = 60   | 0.01                         | NE    | 2069     | 0.400              |
| 12-1D    | 1-in-20 year storm, NE, 2069 SLR (XBeach-G) | D <sub>50</sub> = 80<br>D <sub>90</sub> = 120  | 0.01                         | NE    | 2069     | 0.400              |
| 13-1D    | 1-in-20 year storm, NE, 2099 SLR (XBeach-S) | D <sub>50</sub> = 0.8<br>D <sub>90</sub> = 1.5 | n/a                          | NE    | 2099     | 0.701              |
| 14-1D    | 1-in-20 year storm, NE, 2099 SLR (XBeach-S) | D <sub>50</sub> = 2<br>D <sub>90</sub> = 3     | n/a                          | NE    | 2099     | 0.701              |
| 15-1D    | 1-in-20 year storm, NE, 2099 SLR (XBeach-G) | D <sub>50</sub> = 2<br>D <sub>90</sub> = 3     | 0.01                         | NE    | 2099     | 0.701              |
| 16-1D    | 1-in-20 year storm, NE, 2099 SLR (XBeach-G) | D <sub>50</sub> = 10<br>D <sub>90</sub> = 15   | 0.01                         | NE    | 2099     | 0.701              |
| 17-1D    | 1-in-20 year storm, NE, 2099 SLR (XBeach-G) | D <sub>50</sub> = 40<br>D <sub>90</sub> = 60   | 0.01                         | NE    | 2099     | 0.701              |
| 18-1D    | 1-in-20 year storm, NE, 2099 SLR (XBeach-G) | D <sub>50</sub> = 80<br>D <sub>90</sub> = 120  | 0.01                         | NE    | 2099     | 0.701              |

### 2.5.2 Decommissioning phase and updates to the HCDF design

As part of version 2 of this report, new model scenarios are considered for the decommissioning phase of SZC. Additionally, the design of the HCDF has also been updated, in line with details provided at Deadline 5 [REP5-015]. The two main changes are the paring back of the BLF abutment to the north and the deviation of the last 200 m of the southern end of the HCDF away from the main line of the HCDF. The new HCDF is also 70 m with a rounded end. The position and crest elevation of the SCDF remain unchanged as a result of the HCDF changes. The result of these HCDF changes, therefore, is to increase the beach volume at the north end of the SCDF and reduce beach volume at the south end of the SCDF.

As noted on their captions, maps of elevation change from the XBeach-s 2D model feature the former and outdated version of the HCDF toe location. These maps were not updated in order to meet Sizewell C Examination delivery deadlines, but they will be updated should any additional modelling take place as a result of consultation with the Marine Technical Forum. In all cases, the updated HCDF [REP5-015] is not exposed and indeed the erosion pressure is greatest for the higher levels of the decommissioning phase (2140), which has included the correct HCDF toe location and does not show exposure anywhere along the SCDF frontage.

The new HCDF design is included in the decommissioning model runs. The models runs associated with the operational phase will be revisited in the next version of this report. However, the design changes will not affect the conclusions of the results presented in Sections 3.1 to 3.3 as the SCDF has not changed location.

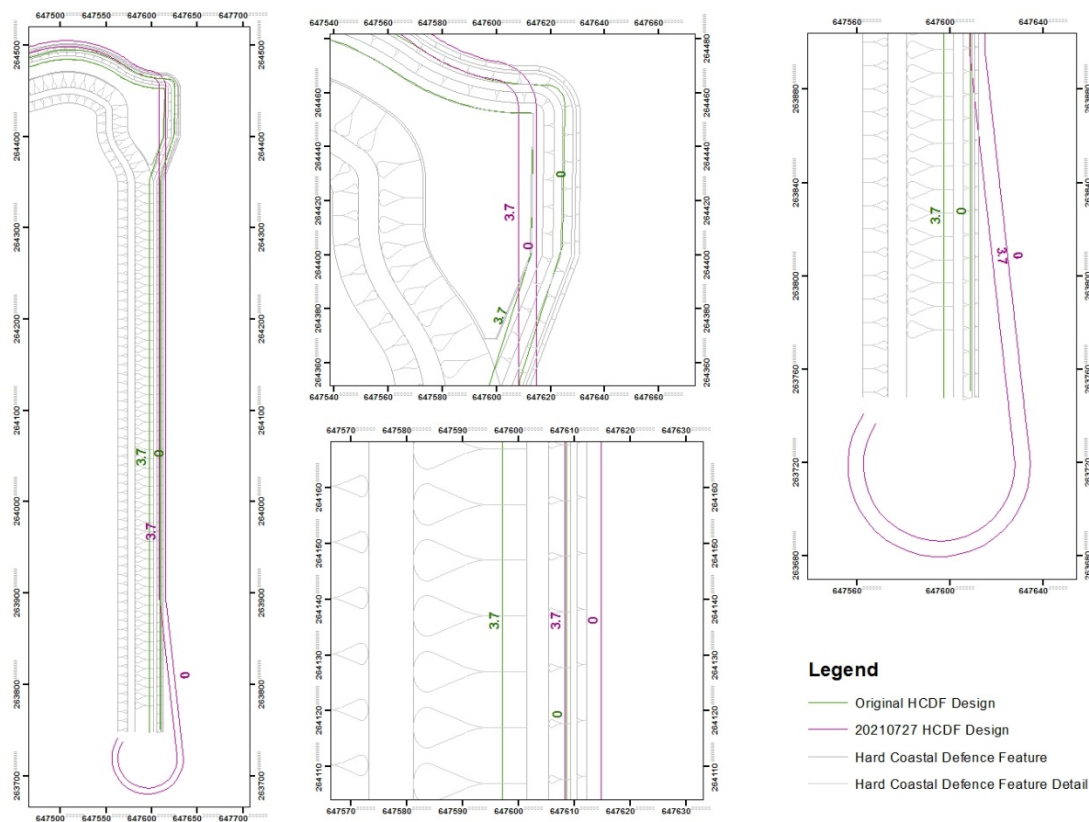


Figure 2-10. Plan overview of the difference between the updated HCDF design between V1 and V2 of this report.

The Adaptive Design is larger than the original HCDF, with a higher overall crest height and the HCDF toe more seaward. As a result, the SCDF crest, associated with the Adaptive Design only, is pushed seaward by ~17 m. A comparison of the 1D profile used in the XBeach-G runs is shown in Figure 2-11.

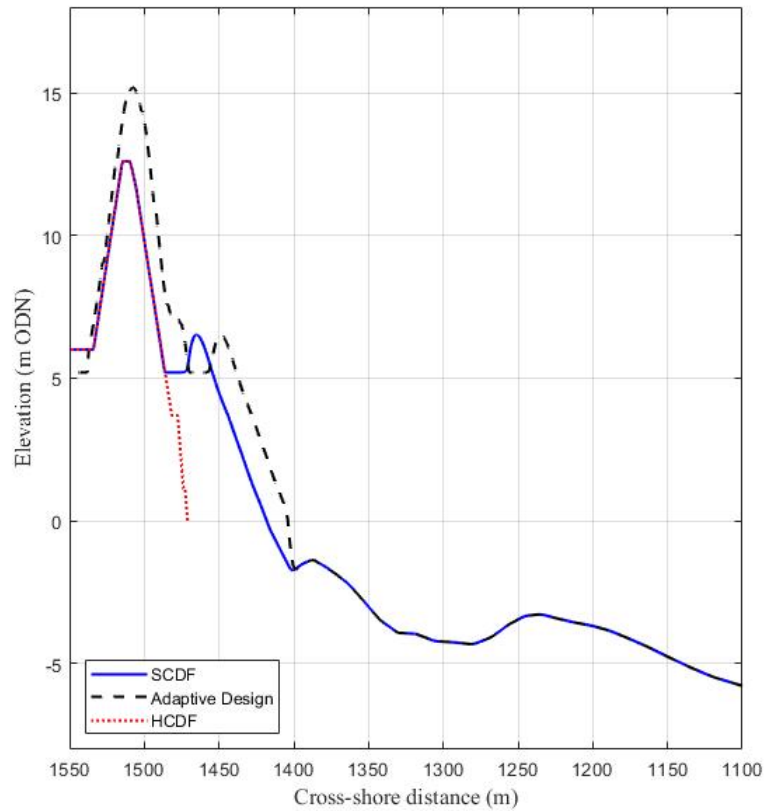


Figure 2-11. Comparison of the model domain used for the 1D gravel version of XBeach testing the SCDF for the HCDF and Adaptive Design.

Table 2-5 details each of the 2D model runs undertaken including the Model Domain used, Storm condition and sea level rise applied to each scenario during the decommissioning phase of SZC.

Table 2-6 details each of the 1D model runs undertaken including the Model Domain used, Storm condition and sea level rise applied to each scenario during the decommissioning phase of SZC.

Table 2-5. 2D model scenario summary for decommissioning phase.

| Scenario | Description                             | Model Domain        | Storm | SLR Year | SLR correction (m) |
|----------|---|---------------------|-------|----------|--------------------|
| 1-2D     | 1-in-20 year storm, NE, RCP4.5 2120 SLR | SCDF-future DEM     | NE    | 2120     | 0.885              |
| 2-2D     | 1-in-20 year storm, NE, RCP4.5 2140 SLR | SCDF-future DEM     | NE    | 2140     | 1.088              |
| 3-2D     | 1-in-20 year storm, NE, RCP8.5 2120 SLR | Adaptive Design DEM | NE    | 2120     | 1.313              |
| 4-2D     | 1-in-20 year storm, NE, RCP8.5 2140 SLR | Adaptive Design DEM | NE    | 2140     | 1.661              |
| 5-2D     | 1-in-20 year storm, SE, RCP4.5 2120 SLR | SCDF-future DEM     | SE    | 2120     | 0.885              |
| 6-2D     | 1-in-20 year storm, SE, RCP4.5 2140 SLR | SCDF-future DEM     | SE    | 2140     | 1.088              |
| 7-2D     | BfE storm sequence, RCP4.5 2120 SLR     | SCDF-future DEM     | BfE   | 2120     | 0.885              |
| 8-2D     | BfE storm sequence, RCP4.5 2140 SLR     | SCDF-future DEM     | BfE   | 2140     | 1.088              |
| 9-2D     | BfE storm sequence, RCP8.5 2140 SLR     | Adaptive Design DEM | BfE   | 2140     | 1.661              |

Table 2-6. 1D model scenario summary for decommissioning phase. The profile used in each 1D scenario (Figure 2-9) was taken from the centre of the SCDF DEM (location Y<sub>1</sub>, described in Section 3).

| Scenario | Description                             | Grain size (mm)                              | Model Domain        | Storm | SLR Year | SLR correction (m) |
|----------|---|--|---------------------|-------|----------|--------------------|
| 1-1D     | 1-in-20 year storm, NE, RCP4.5 2120 SLR | D <sub>50</sub> = 10<br>D <sub>90</sub> = 15 | SCDF-future DEM     | NE    | 2120     | 0.885              |
| 2-1D     | 1-in-20 year storm, NE, RCP4.5 2140 SLR | D <sub>50</sub> = 10<br>D <sub>90</sub> = 15 | SCDF-future DEM     | NE    | 2140     | 1.088              |
| 3-1D     | 1-in-20 year storm, NE, RCP8.5 2120 SLR | D <sub>50</sub> = 10<br>D <sub>90</sub> = 15 | Adaptive Design DEM | NE    | 2120     | 1.313              |
| 4-1D     | 1-in-20 year storm, NE, RCP8.5 2140 SLR | D <sub>50</sub> = 10<br>D <sub>90</sub> = 15 | Adaptive Design DEM | NE    | 2140     | 1.661              |



### 3 Results

The following sections (Sections 3.1 - 3.3) describe model results for bed elevation changes, volumetric change, variation due to particle size, and run-up estimates at and near the SCDF site during the operational phase of SZC up to 2099. The section is structured as follows:

- ▶ Storm erosion – presents the results of the change in bed elevation for the SCDF case, compares the results of the SCDF with present and future eroded shorelines, and presents volumetric change results on the beach in the location of the SCDF.
- ▶ Variation due to particle size – details the sensitivity of the SCDF with regards to the grain size used.
- ▶ Wave run-up and overtopping – presents wave run-up values in relation to SCDF and natural shingle ridge crest heights to help identify possible cases where overtopping and crest lowering could occur now and in the future.

Results are first presented in 2D spatial plots, showing the frontage of the SCDF and surrounding beach area, up to 350 m north and south of the SCDF frontage, and up to 250 m seaward of the SCDF. The spatial plots each show a birds eye view of the topographic contours (m ODN) at the start of each simulation, and overlay a colour map showing the magnitude of a model output parameter (e.g. end of simulation bed level, bed level change, etc.). Some of the spatial plots have vectors overlaid on the colour map showing the direction of an additional parameter (e.g. wave direction, such as Figure E-1) or the direction and magnitude of a parameter (e.g. sediment flux direction and magnitude, such as Figure E-7). The location of the 0 m ODN contour line and the location of the SCDF crest are shown in the spatial plots as thicker contour lines, for reference.

Morphodynamic models are not expected to accurately model erosion/deposition at a fixed point in space where quasi-random processes heavily affect the processes, but have been shown to do a good job of reproducing the general trends of morphological response along sections of beach. For that reason, we provide both deterministic results (by showing effects at specific profiles) to give an indication of the scale of localised response which may be expected, but also provide section averages (averaged along the SCDF frontage) to clarify the general beach response.

Cross-sections of the 2D model data are plotted at three alongshore locations;  $Y_1$  (250 m north of the SCDF),  $Y_2$  (at the centre of the SCDF), and  $Y_3$  (250 m south of the SCDF). Note,  $Y_1$  and  $Y_3$  are not presented in the Results section but shown in Appendix E. During the 2099 1-in-20 year NE simulations a potential breach location, north of the SZC site, was predicted (at  $Y_{\text{breach}}$ ); for these simulations, additional cross-sectional profiles were extracted. To understand the general trend along the area of the SCDF feature, alongshore averaged cross-sectional results ( $Y_{\text{average}}$ ) are also presented along the immediate frontage of the SCDF. Locations of  $Y_1$ ,  $Y_2$ ,  $Y_3$  and  $Y_{\text{breach}}$  are shown in each relevant 2D plot. The Northing of each of these locations are:

- ▶  $Y_1 = 264542$  N
- ▶  $Y_2 = 264105$  N
- ▶  $Y_3 = 263502$  N
- ▶  $Y_{\text{breach}} = 264502$  N
- ▶  $Y_{\text{average}} = \text{Average between } 263755 \text{ N and } 264455 \text{ N.}$

In Sections 3.1 and 3.2, the results are focussed on the morphological change predicted during each simulation. In sections 3.3 the results are focussed on wave run-up and overtopping. Appendix E presents additional hydrodynamic model results from the 2D model runs showing wave height and direction, current velocities, bed shear stress and sediment flux, temporally averaged over each simulation.

Section 3.4 describes model results for bed elevation changes, volumetric change and variation due to particle size, during the decommissioning phase of SZC, up to 2140.

### 3.1 Storm Erosion

#### 3.1.1 SCDF Bed Elevation Change using the sand model

##### 3.1.1.1 Present Sea Level

Under the three modelled storm cases, a cut and fill beach response is seen with sediment losses on the supratidal beach face and gains on the subtidal beach face (Figure 3-1 and Figure 3-2). For the three modelled storms, vertical bed level change (erosion) along the supratidal SCDF frontage is on the order of 1-2 m (Figure 3-2), with similar magnitudes of vertical beach accretion in the subtidal.

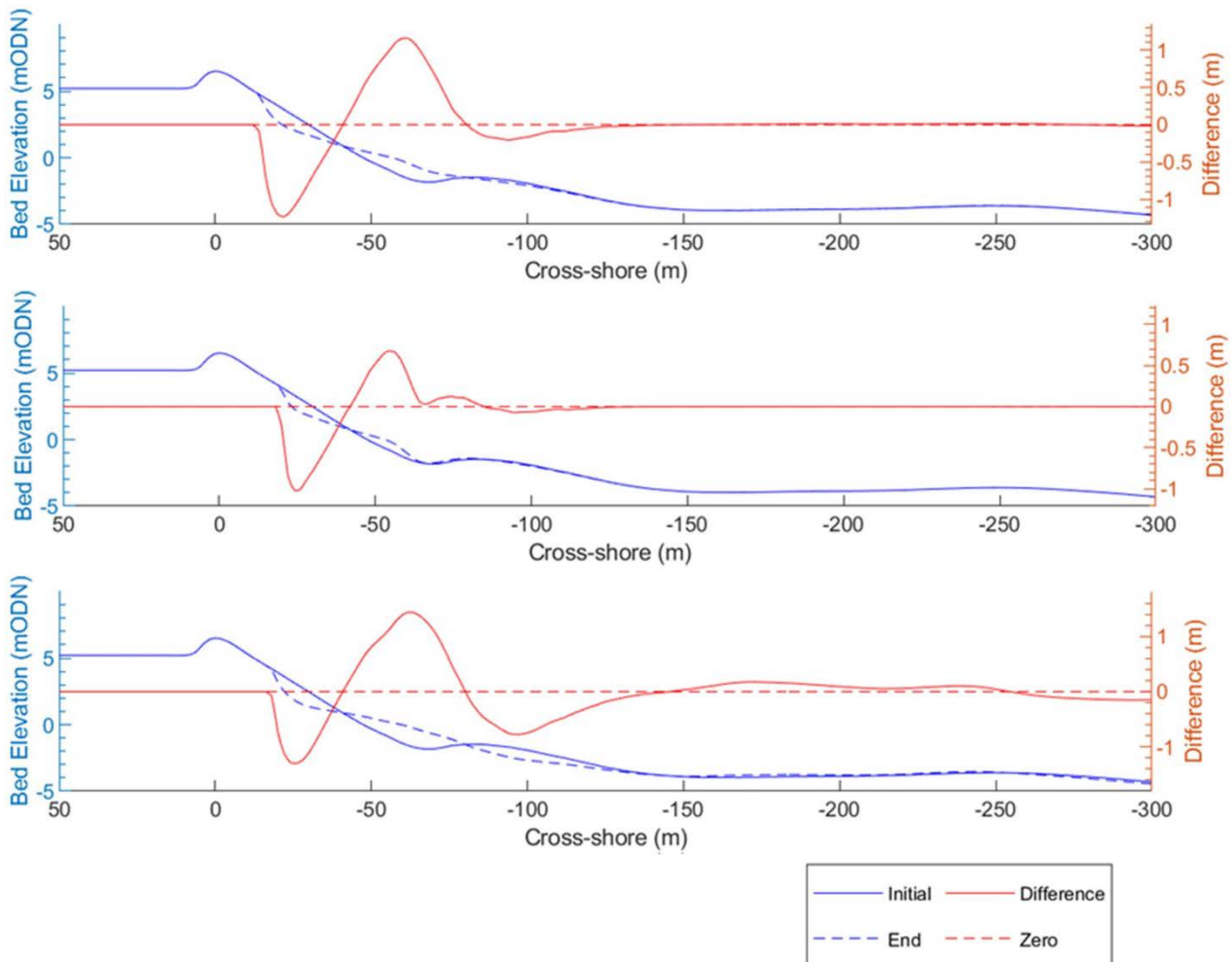


Figure 3-1. Average bed level along the SCDF frontage ( $Y_{average}$ , Section 3) at the start ('initial') and end of the three modelled storm events (present sea level). Upper panel: 1:20 year NE storm. Middle panel: 1:20 year SE storm. Lower panel: BfE storm. In each panel, the solid red line shows the vertical difference in the pre- and post-storm profiles.

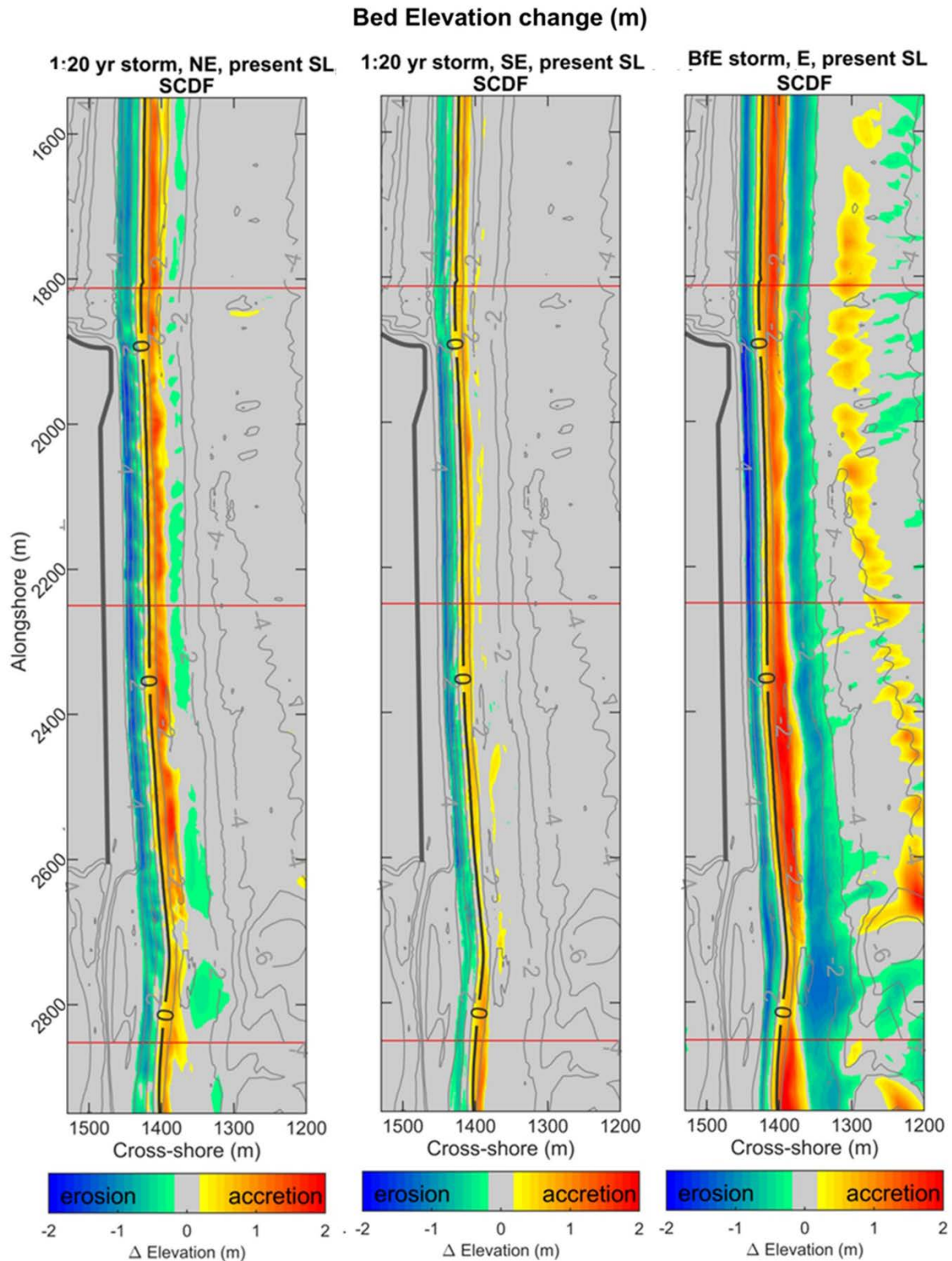


Figure 3-2. 2D change in bed elevation (coloured areas) along the SCDF frontage over the three modelled storm events (present sea level). Contour lines show starting bed elevation (m ODN), with 0 m contour line shown in bold for reference. The thick line on the supratidal beach represents the approximate location of the HCDF toe (superseded but with no implications for toe exposure, see Section 2.5.2). The red lines indicate the locations of Y<sub>1</sub>, Y<sub>2</sub>, and Y<sub>3</sub>, for visual reference.

### 3.1.1.2 2069 Sea Level

Under the three modelled storm cases, a cut and fill beach response is seen with sediment losses on the supratidal beach face and gains on the subtidal beach face (Figure 3-3 and Figure 3-4). For the three modelled storms, vertical bed level change (erosion) along the supratidal SCDF frontage is on the order of -1-2 m (Figure 3-4), with similar magnitudes of vertical beach accretion in the subtidal. Averaged along the SCDF frontage, the BfE and NE 1:20 year storms are predicted to incur approximately -1-1.2 m of supratidal bed level erosion, while the SE 1:20 year storm is predicted to incur < -1 m of supratidal bed level erosion (Figure 3-3). No erosion of the SCDF crest is predicted to occur during the three modelled storm events at 2069 sea level.

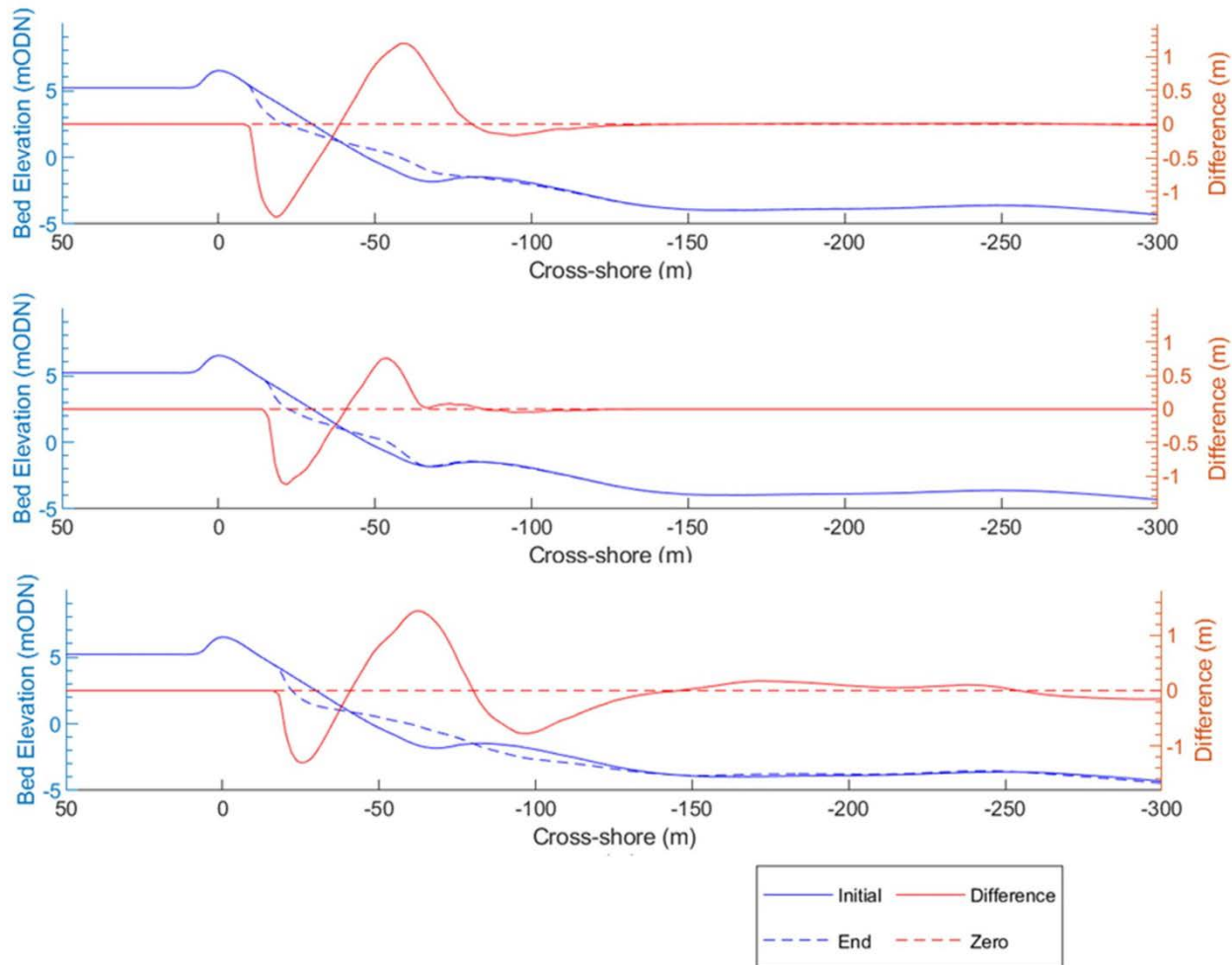


Figure 3-3. Average bed level along the SCDF frontage ( $Y_{average}$ , Section 3) at the start ('initial') and end of the three modelled storm events (2069 sea level). Upper panel: 1:20 year NE storm. Middle panel: 1:20 year SE storm. Lower panel: BfE storm. In each panel, the solid red line shows the vertical difference in the pre- and post-storm profiles.



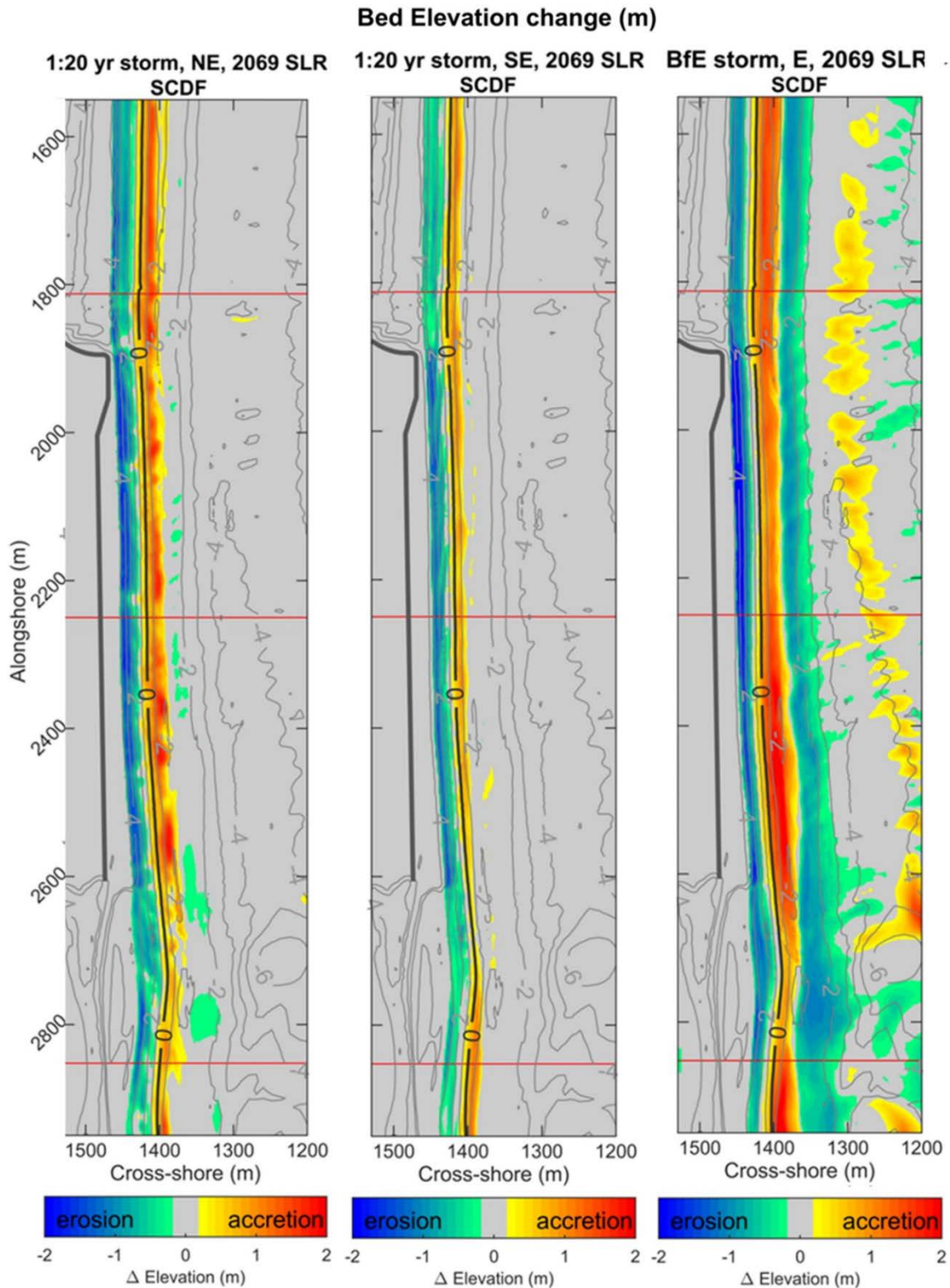


Figure 3-4. 2D change in bed elevation (coloured areas) along the SCDF frontage over the three modelled storm events (2069 sea level). Contour lines show starting bed elevation (m ODN), with 0 m contour line shown in bold for reference. The thick line on the supratidal beach represents the approximate location of the HCDF toe (superseded but with no implications for toe exposure, see Section 2.5.2). The red lines indicate the locations of Y<sub>1</sub>, Y<sub>2</sub>, and Y<sub>3</sub>, for visual reference.

### 3.1.1.3 2099 Sea Level

Under the three modelled storm cases, a cut and fill beach response is seen with sediment losses on the supratidal beach face and gains on the subtidal beach face (Figure 3-5 and Figure 3-6). For the NE and SE 1:20 year storm events, vertical bed level change (erosion) along the supratidal SCDF frontage is on the order of -1-2 m (Figure 3-6), while the BfE event incurs supratidal bed level erosion in places > 2 m. Similar magnitudes of vertical beach accretion are predicted in the subtidal in each case. Averaged along the SCDF frontage, the BfE and NE 1:20 year storms are predicted to incur approximately -1.2-1.5 m of supratidal bed level erosion, while the SE 1:20 year storm is predicted to incur < -1 m of supratidal bed level erosion (Figure 3-5).

From the averaged bed level results (Figure 3-5), the supratidal face of the SCDF is predicted to erode back horizontally almost as far as the crest position during the NE 1:20 year storm and BfE storm sequence. However, the SCDF crest height is not predicted to be lowered during either event at 2099 sea level. Erosion was less severe during the SE 1:20 year storm event and did not erode the SCDF back to the crest position.

During the NE 1:20 year storm event, natural overtopping and breaching of the south Minsmere shingle ridge, just north of Sizewell C (SZC), is predicted to occur (Figure 3-6). Breaching is predicted to occur there with and without the presence of the SCDF, demonstrating it is a natural process. Although the BfE storm sequence represents a higher total amount of wave power than the 1:20 year events, the total water level is lower in the BfE event than in the 1:20 year storm events (Section 2.2.2), which is why similar breaching is not predicted during the BfE event. Breaching is not predicted during the SE 1:20 event, likely due to the lower wave height and period compared to the NE 1:20 year event (Section 2.2.2).

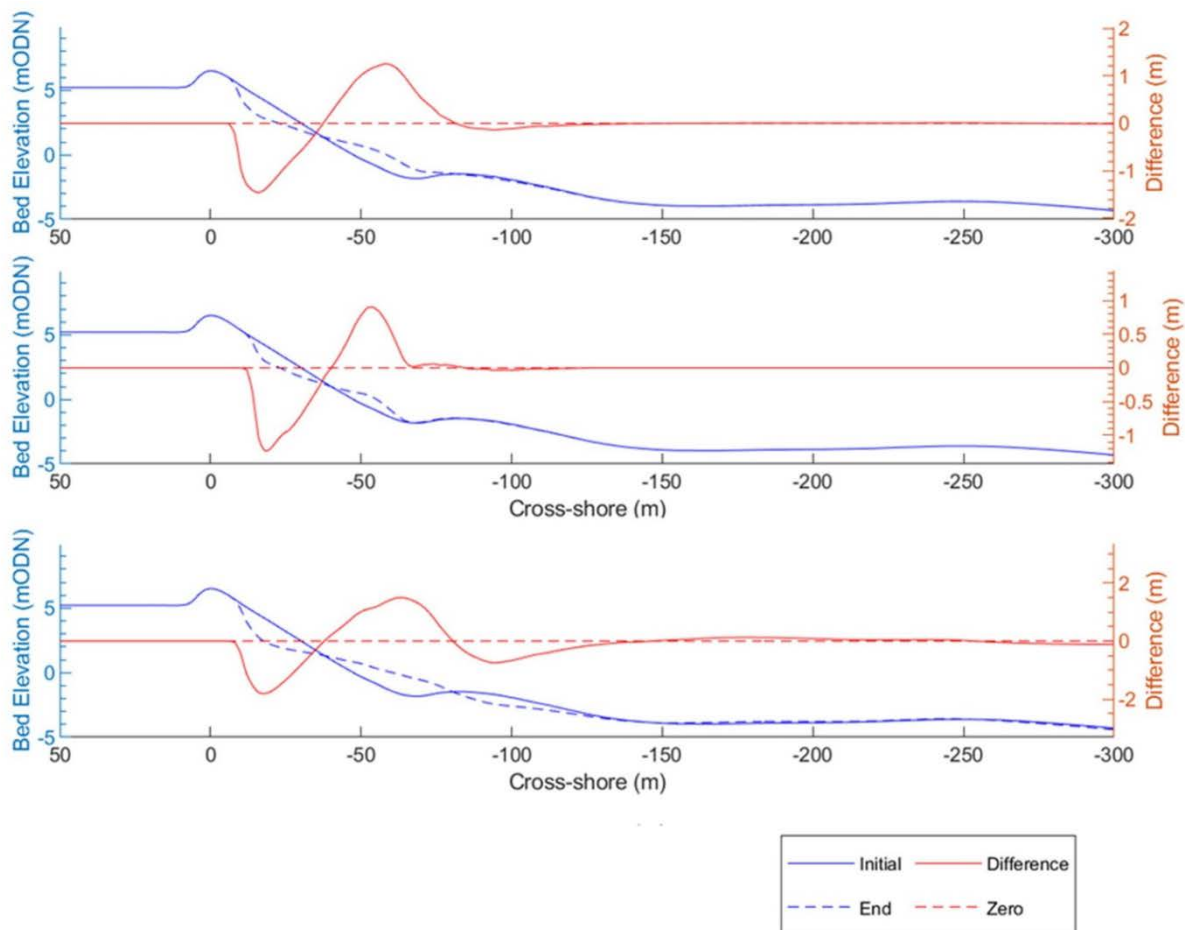


Figure 3-5. Average bed level along the SCDF frontage at the start ('initial') and end of the three modelled storm events (2099 sea level). Upper panel: 1:20 year NE storm. Middle panel: 1:20 year SE storm. Lower panel: BfE storm. In each panel, the solid red line shows the vertical difference in the pre- and post-storm profiles.



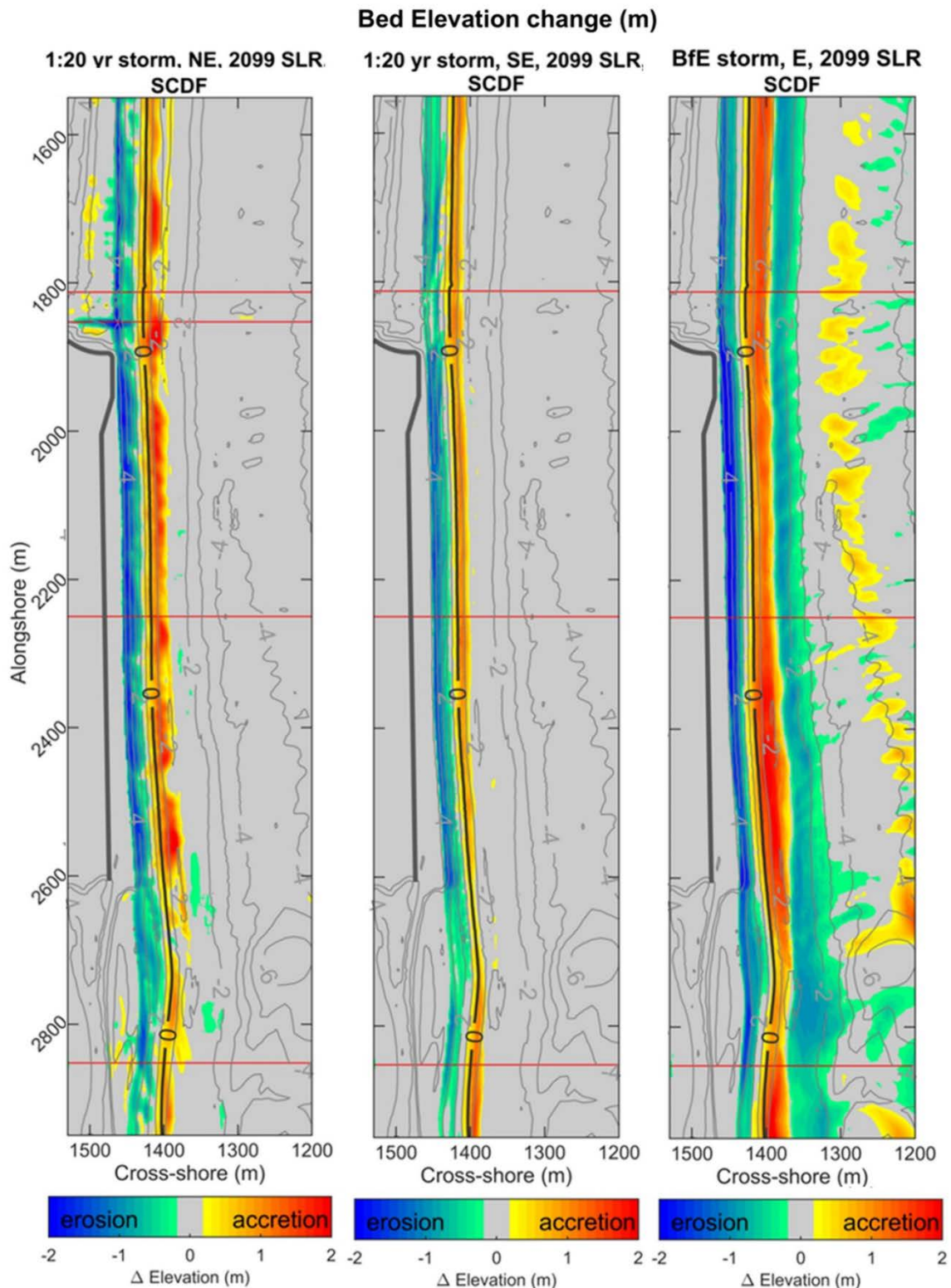


Figure 3-6. 2D change in bed elevation (coloured areas) along the SCDF frontage over the three modelled storm events, at 2099 sea level. Contour lines show starting bed elevation (m ODN), with 0 m contour line shown in bold for reference. The thick line on the supratidal beach represents the approximate location of the HCDF toe (superseded but with no implications for toe exposure, see Section 2.5.2). The red lines indicate the locations of Y1, Y2, and Y3, for visual reference, and an additional red line is plotted at  $Y_{\text{breach}}$ .

### 3.1.2 SCDF compared with SCDF-receded future shorelines using the sand model

In addition to the effects of SLR, recession of the shorelines adjacent to SZC is likely to increase erosion pressure on the SCDF. Whilst the degree of recession shown in Section 7.7 of Volume 2, Appendix 20A of the Sizewell C Environmental Statement NNB Generation Company (SZC) Limited (2020) is not expected during the operation phase modelled in this report, it has been incorporated as a precaution. This section assessed the combined effects of 2099 SLR with severely receded adjacent shorelines. In order to isolate the contribution of the receded shorelines it also makes comparisons of each SLR case with and without the severely receded shorelines. For the BfE storm sequence, which incurs the greatest SCDF erosion of the modelled cases, an additional scenario is tested with 2069 SLR and severely receded adjacent shorelines.

#### 3.1.2.1 2069 and 2099 Sea Level

During the three storm events tested with 2099 sea level, areas of erosion and accretion are observed in similar locations for both the SCDF case and the SCDF with future eroded shorelines (Figure 3-7). In both scenarios, a cut and fill beach response is seen with sediment losses on the supratidal SCDF beach face and gains on the subtidal beach face.

With future receded shorelines, supratidal erosion along the SCDF frontage is only negligibly increased during the NE and SE 1:20 year storm events, with an average of ~0.05-0.1 m more supratidal bed level erosion with future receded shorelines than with present-day shoreline position (Figure 3-8). Vertical accretion on the subtidal SCDF beach face is also predicted to be reduced by ~0.1-0.2 m with future receded shorelines for the NE and SE 1:20 year storms. However, erosion at both the north and south lateral ends of the SCDF is predicted to increase with future eroded shorelines, compared to the case with present day shorelines, although the losses are still of the same order of magnitude as the main frontage of the SCDF.

North and south of the SCDF, differences in erosion and accretion patterns are visible on the adjacent shorelines during the NE 1:20 year storm (Figure 3-7), and in particular, supratidal erosion is reduced and subtidal accretion is increased to the north of the SCDF with future receded shorelines. This is likely to be due to a combination of littoral currents (Appendix E) slowing down where the coastline begins to curve around the SCDF allowing sediment transported from the north to be deposited, and sediment eroded from the SCDF feeding the adjacent shoreline. To the south of the SCDF, subtidal accretion is also slightly increased in places with future eroded shorelines during this storm. During the SE 1:20 year storm, the future eroded shorelines are predicted to cause similar changes in erosion and accretion to the shorelines adjacent to the SCDF, but to a lesser degree than the NE 1:20 storm.

During the NE 1:20 year storm, a breach of the natural shingle ridge is predicted to occur just north of the SCDF with present-day and future eroded shorelines (Figure 3-10). The breach occurs in the same place with future eroded shorelines as with present-day shoreline position. Additionally, the accretion of sediment on the subtidal beach beneath the breach in the SCDF case appears to be inhibited with future eroded shorelines, likely due to an alongshore transport gradient at the lateral end of the SCDF frontage where the shoreline straightens (i.e. becomes more oblique to the NE wave approach). Note that the same breach also occurred under the NE 1:20 year storm at 2099 sea level without the presence of the SCDF (Section 3.1.1.3), indicating it is a natural process and not directly caused by the SCDF.

For the BfE storm sequence, the effect of future receded shorelines is predicted to be greater than in the 1:20 year storm simulations (Figure 3-7). With 2069 SLR, the future eroded shorelines adjacent to the SCDF increase the magnitude of supratidal erosion along the frontage of the SCDF by an average of ~0.4 m, but also reduce accretion on the subtidal beach face by ~0.3 m, compared to the SCDF with present-day shoreline position (Figure 3-9). With 2099 SLR, the enhancement of supratidal erosion and subtidal accretion along the SCDF by the future receded shorelines increases to ~0.5 m. The northern and southern lateral end-points of the SCDF erode more readily with future eroded shorelines, and this effect is amplified at 2099 sea level compared to 2069 sea level for the BfE storm sequence. The losses are still of the same order of magnitude as the main frontage of the SCDF, but the erosion affects a wider area and occurs higher on the supratidal beach face, especially at the northern lateral end-point (Figure 3-7).

The future receded shoreline appears to make the shingle ridge to the north of the SCDF more vulnerable. While a breach of the shingle ridge north of the SCDF is not predicted by the model, erosion is predicted to

influence the crest of the ridge to some extent (at the same location as  $Y_{\text{breach}}$  in the NE 1:20 year storm with 2099 SLR, Figure 3-7).



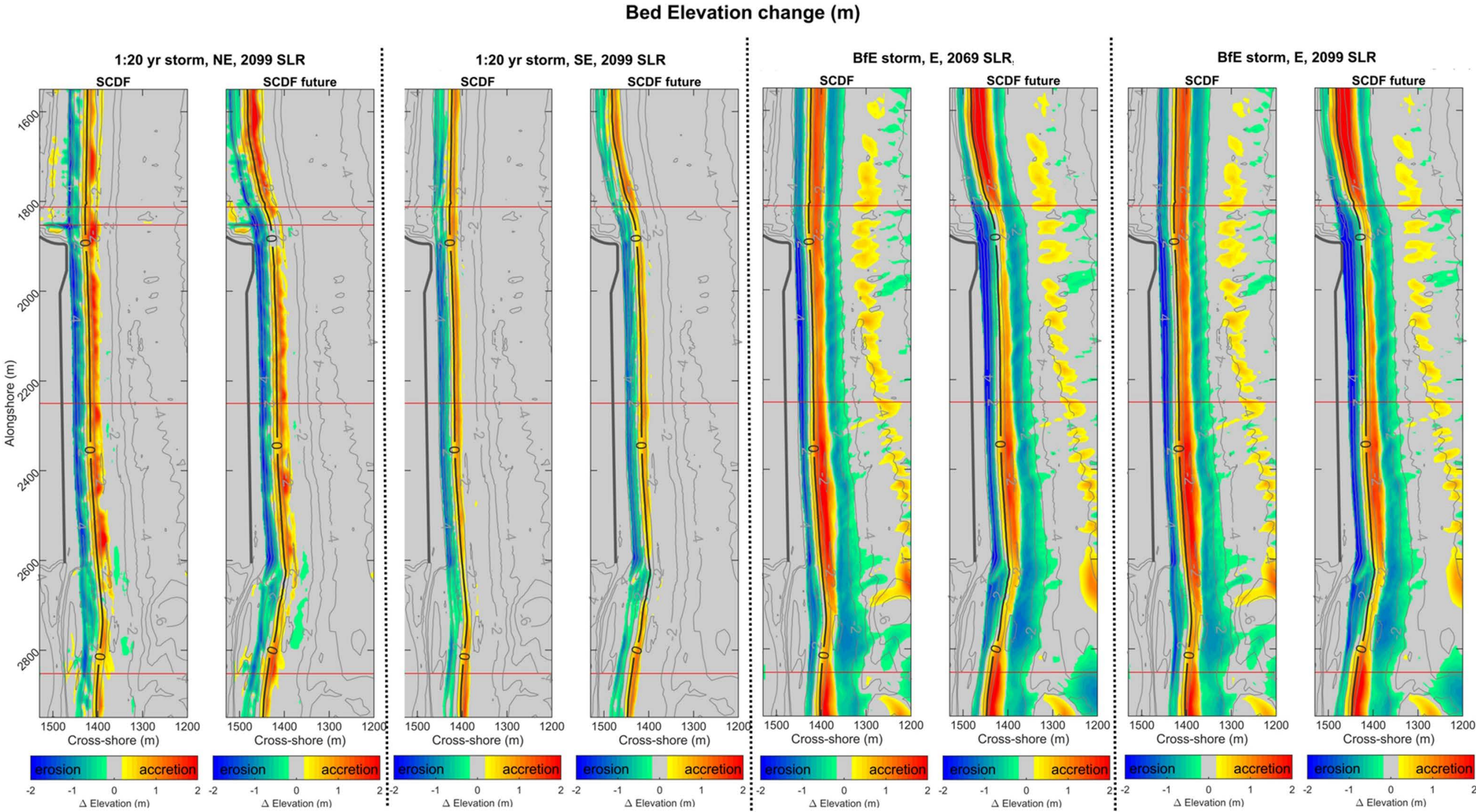


Figure 3-7. Comparison of 2D bed elevation changes (coloured areas) for the SCDF with present-day shoreline ('SCDF') and SCDF-with future receded shorelines ('SCDF future') cases, for the three modelled storms. Dotted lines divide the four cases tested: North East 1-in-20 year storm, 2099 Sea Level (left two panels), South East 1-in-20 year storm, 2099 Sea Level (third and fourth from left), Beast from the East storm, 2069 Sea Level (fifth and sixth from left) and Beast from the East storm, 2099 sea level (right two panels). Contour lines show starting bed elevation (m ODN), with 0 m contour line shown in bold for reference. The thick line on the supratidal beach represents the approximate location of the HCDF toe (superseded but with no implications for toe exposure, see Section 2.5.2). The red lines indicate the locations of  $Y_1$ ,  $Y_2$ , and  $Y_3$ , for visual reference.



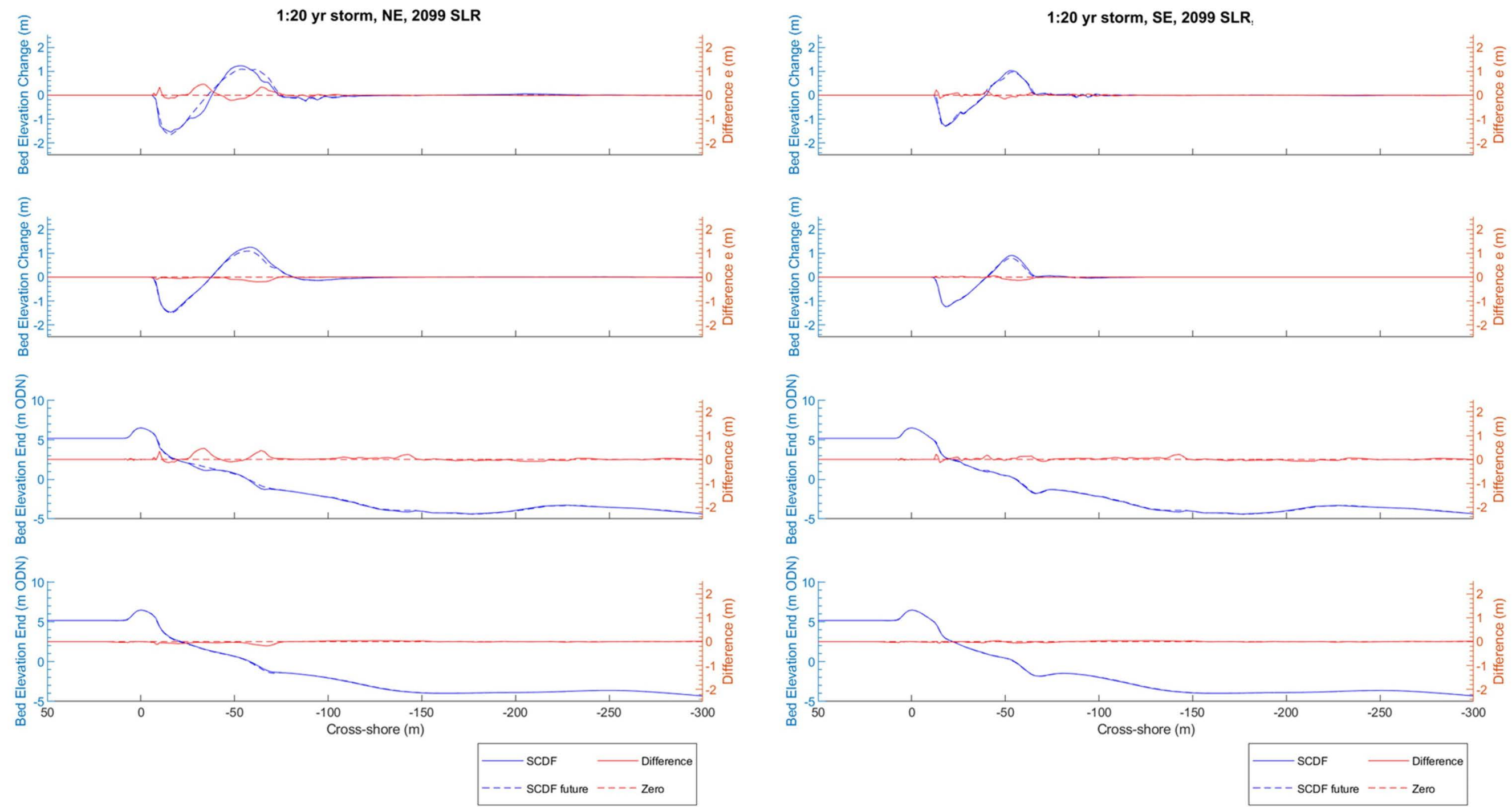


Figure 3-8. Cross sections of bed level change for the North East 1-in-20 year storm, 2099 Sea Level (left panels) and South East 1-in-20 year storm, 2099 Sea Level (right panels) for the SCDF with present-day ('SCDF') and future eroded shorelines ('SCDF future'). Top panels: Comparison of changes in bed elevation during the simulated storms at the middle of the SCDF frontage ( $Y_2$ ). Second from top panels: Comparison of changes in bed elevation during the simulated storms averaged along the SCDF frontage ( $Y_{average}$ ). Third from top panels: Comparison of post-storm bed elevations during the simulated storms at the middle of the SCDF frontage ( $Y_2$ ). Bottom panels: Comparison of post-storm bed elevations averaged along the SCDF frontage ( $Y_{average}$ ). The red solid line in each panel shows the difference between the cases with present-day and future eroded shorelines.

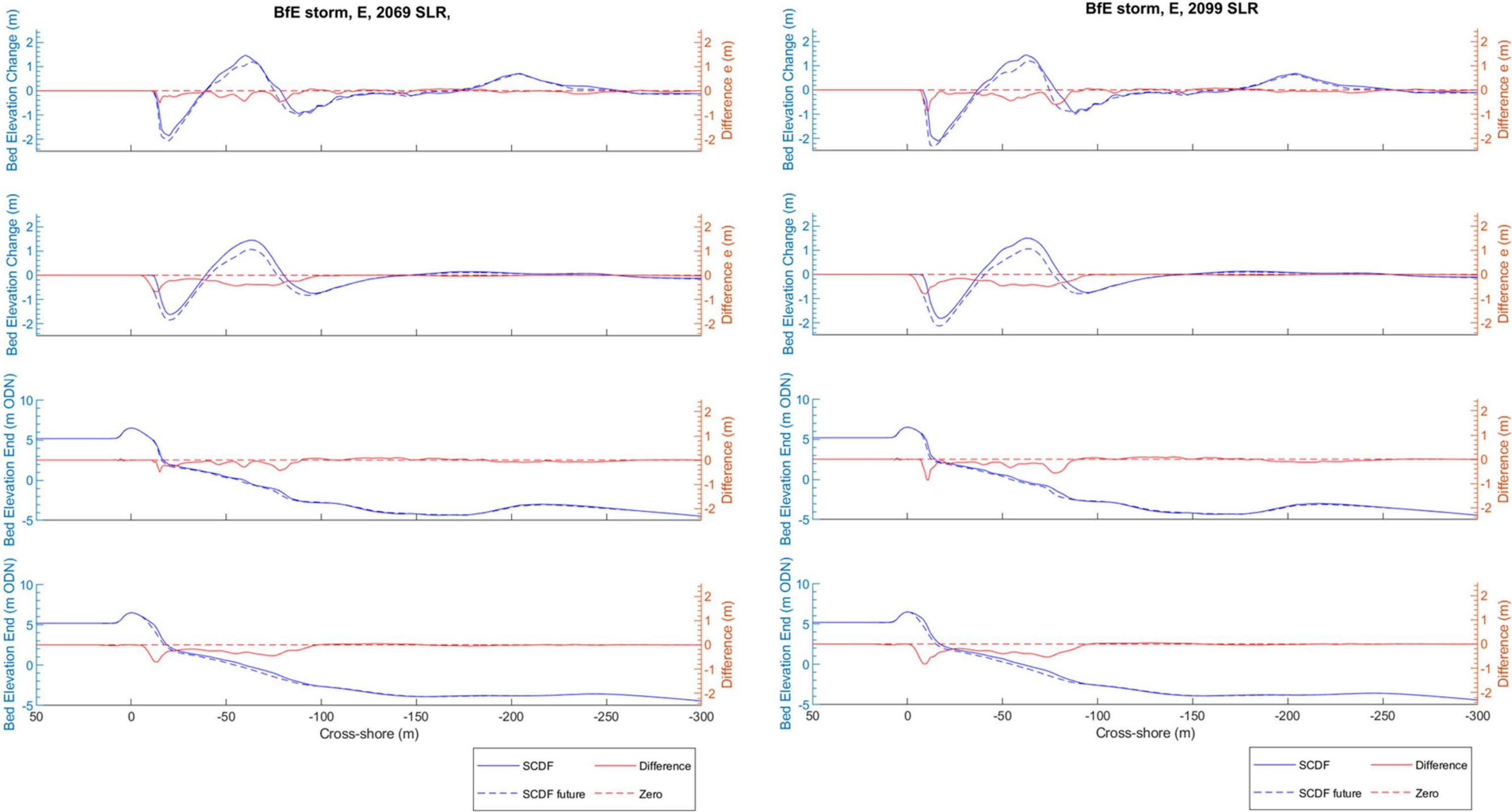


Figure 3-9. Cross sections of bed level change for the BfE storm sequence, 2069 Sea Level (left panels) and BfE storm sequence, 2099 Sea Level (right panels) for the SCDF with present-day ('SCDF') and future eroded shorelines ('SCDF future'). Top panels: Comparison of changes in bed elevation during the simulated storms at the middle of the SCDF frontage ( $Y_2$ ). Second from top panels: Comparison of changes in bed elevation during the simulated storms averaged along the SCDF frontage ( $Y_{average}$ ). Third from top panels: Comparison of post-storm bed elevations at the middle of the SCDF frontage ( $Y_2$ ). Bottom panels: Comparison of post-storm bed elevations averaged along the SCDF frontage ( $Y_{average}$ ). The red solid line in each panel shows the difference between the cases with present-day and future eroded shorelines.



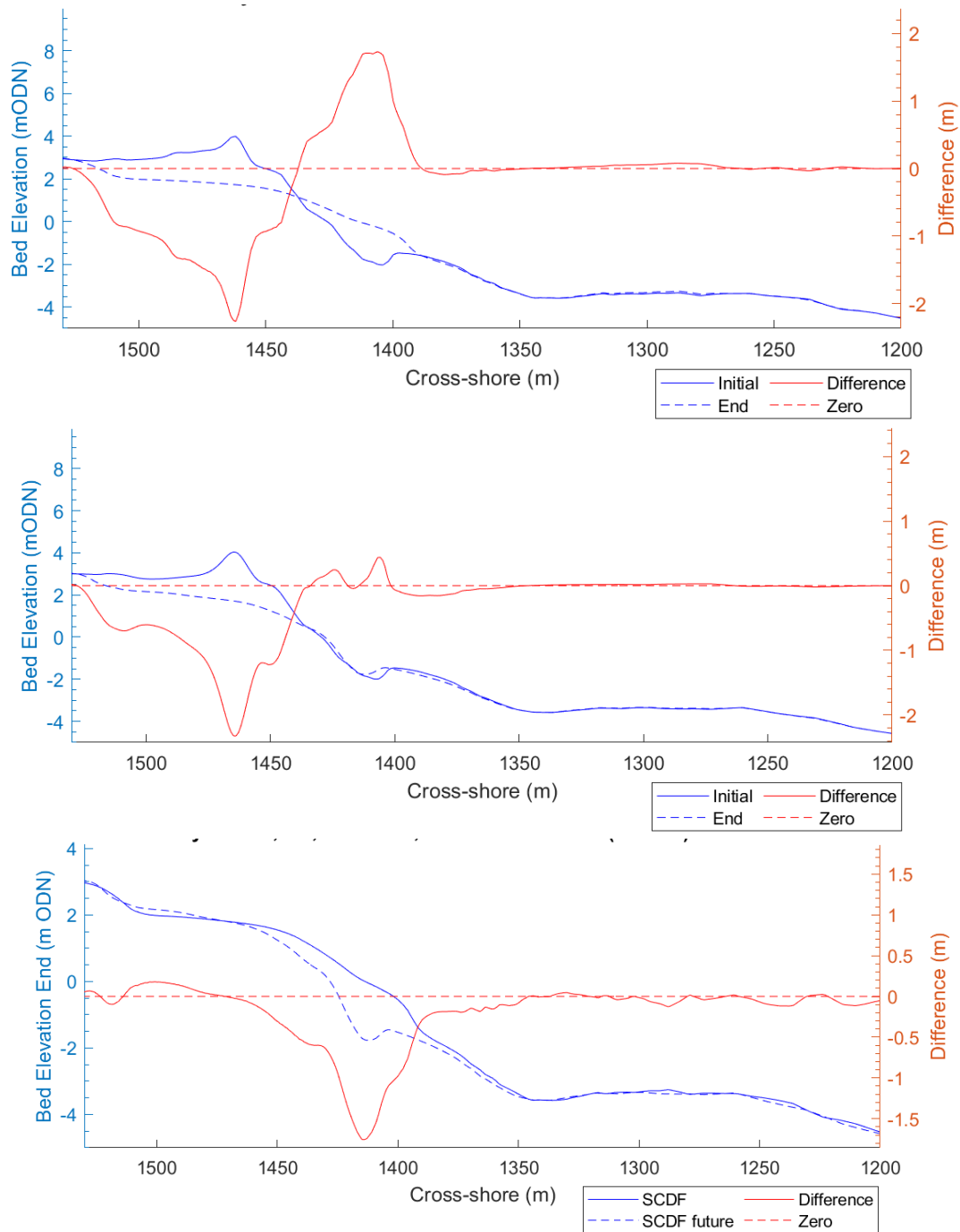


Figure 3-10. North East 1-in-20 year storm, 2099 Sea Level – Pre-storm and post-storm profiles at the breach location ( $Y_{\text{breach}}$ ) north of the SCDF with present-day (top panel) and future eroded shorelines (middle panel). The bottom panel shows the difference in breach magnitude between the cases with present-day and future eroded shorelines. The red line in each panel shows the change in bed level over the storm (top two panels) and the difference in post-storm bed level (bottom panel).

### 3.1.3 Volumetric change using the sand model

Volumetric change was calculated within 151 polygons across the SCDF frontage using the bed levels at the beginning and end of each 2D simulation. Each polygon covers 5 m alongshore and covers the SCDF down to approximately 0 m ODN in the cross-shore direction. From the total volumetric change within each polygon, the volumetric loss was calculated and expressed per metre of alongshore beach length ( $\text{m}^3/\text{m}$ ). Maps depicting the volume loss per m along the frontage of the SCDF are presented in Appendix C. Table 3-1 summarises the average volume loss per m, the minimum and maximum volumetric loss alongshore, and the total loss across all 5 m polygons. Volumetric changes from the 2D simulations are summarised in this section of the report, while volumetric changes from the 1D simulations with various SCDF grain sizes are presented in Section 3.2.

Following the release of Edition 1 of this report, the HCDF design has been updated, as detailed in Section 2.5.1. As a result, the polygons used to define the volume calculations have been altered to allow direct comparison with the decommissioning phase simulations which take account for the new HCDF design. The volumes stated in the text along with summary of the volumes for each operational model simulation provided in Table 3-1 has been updated in Edition 2 of this report, although the changes are small. However, the spatial plots have not been updated yet with the new HCDF line, such as in Figure 3-2 and Figure 3-12. These will be updated in the next version of the report, as the changes are stylistic and do not alter the original conclusions of Edition 1.

The BfE storm sequence resulted in the highest volume lost from the SCDF, followed by the 1-in-20 year NE storm and the 1-in-20 year SE storm (Table 3-1). For each storm, volumetric losses are predicted to be greater with future eroded shorelines than with present-day shoreline position and, as expected, volumetric losses from the SCDF are predicted to increase with sea level rise (Figure 3-11). From Table 3-1, mean losses across the SCDF frontage for the various storm scenarios range from  $-10 \text{ m}^3/\text{m}$  to  $-43 \text{ m}^3/\text{m}$ . However, the northern half of the SCDF feature appears to be more vulnerable to erosion than the southern half, and the peak losses along the SCDF frontage were as high as  $-82 \text{ m}^3/\text{m}$  under the most extreme storm tested (BfE storm 2099 SLR with future eroded shorelines, Figure 3-12).

As expected, the model shows that severely receded adjacent shorelines increase erosion pressure on the SCDF. For the BfE storm sequence, the modelled mean erosion along the SCDF frontage ( $Y_{\text{average}}$ ) with SLR and receded adjacent shorelines is  $35 \text{ m}^3/\text{m}$  in 2069 and  $43 \text{ m}^3/\text{m}$  in 2099 (Figure 3-11), but higher localised losses are observed at both ends of the SCDF, due to higher wave angles and longshore transport gradients where the shoreline curves from the SCDF to the adjacent frontage. In contrast, with present day shoreline position, the SCDF is predicted to lose  $-22 \text{ m}^3/\text{m}$  and  $-27 \text{ m}^3/\text{m}$  at 2069 and 2099 sea level, respectively.

For the NE 1:20 year storm at 2099 sea level, the SCDF feature loses slightly more sediment with future eroded shorelines than with present-day shoreline position. Averaged along the SCDF frontage, volume losses above 0 m ODN are  $-24 \text{ m}^3/\text{m}$  with future eroded shorelines, compared to  $-22 \text{ m}^3/\text{m}$  with present-day shorelines. For the SE 1:20 year storm, the average volume loss per m of SCDF frontage is the same (rounded to the nearest  $\text{m}^3$ ) with present-day and future eroded shorelines, with  $-18 \text{ m}^3/\text{m}$  lost under both scenarios.

Even in the most affected areas of the SCDF, the volume eroded by the simulated storms is still less than the available beach volume with the SCDF, and at no alongshore location along the SCDF frontage was all of the subaerial volume removed by any of the simulated storms. The worst-modelled storm scenario in terms of erosional losses was the BfE storm with 2099 SLR and future eroded shorelines (Figure 3-12), where the peak loss was  $82 \text{ m}^3/\text{m}$ , centred in a 100 m long section at the north of the SCDF with continuous losses  $> 70 \text{ m}^3/\text{m}$ . The peak losses in this area still left  $> 120 \text{ m}^3/\text{m}$  of sediment on the beach face (65-70% of initial beach volume).

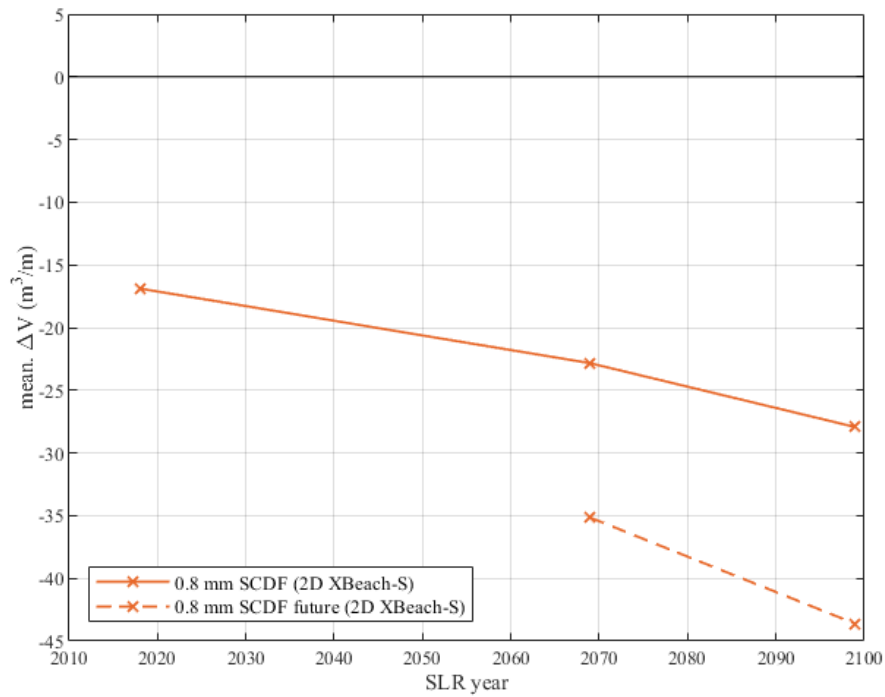


Figure 3-11. BfE storm sequence, 2021, 2069, and 2099 Sea Levels – Mean volume eroded along the frontage of the SCDF (above 0 m ODN) during the storm at the three sea levels tested. Both the SCDF with present-day shoreline position (solid line) and SCDF with future eroded shorelines (dashed line) are presented. Note that model data only exists for years 2021, 2069, and 2099.

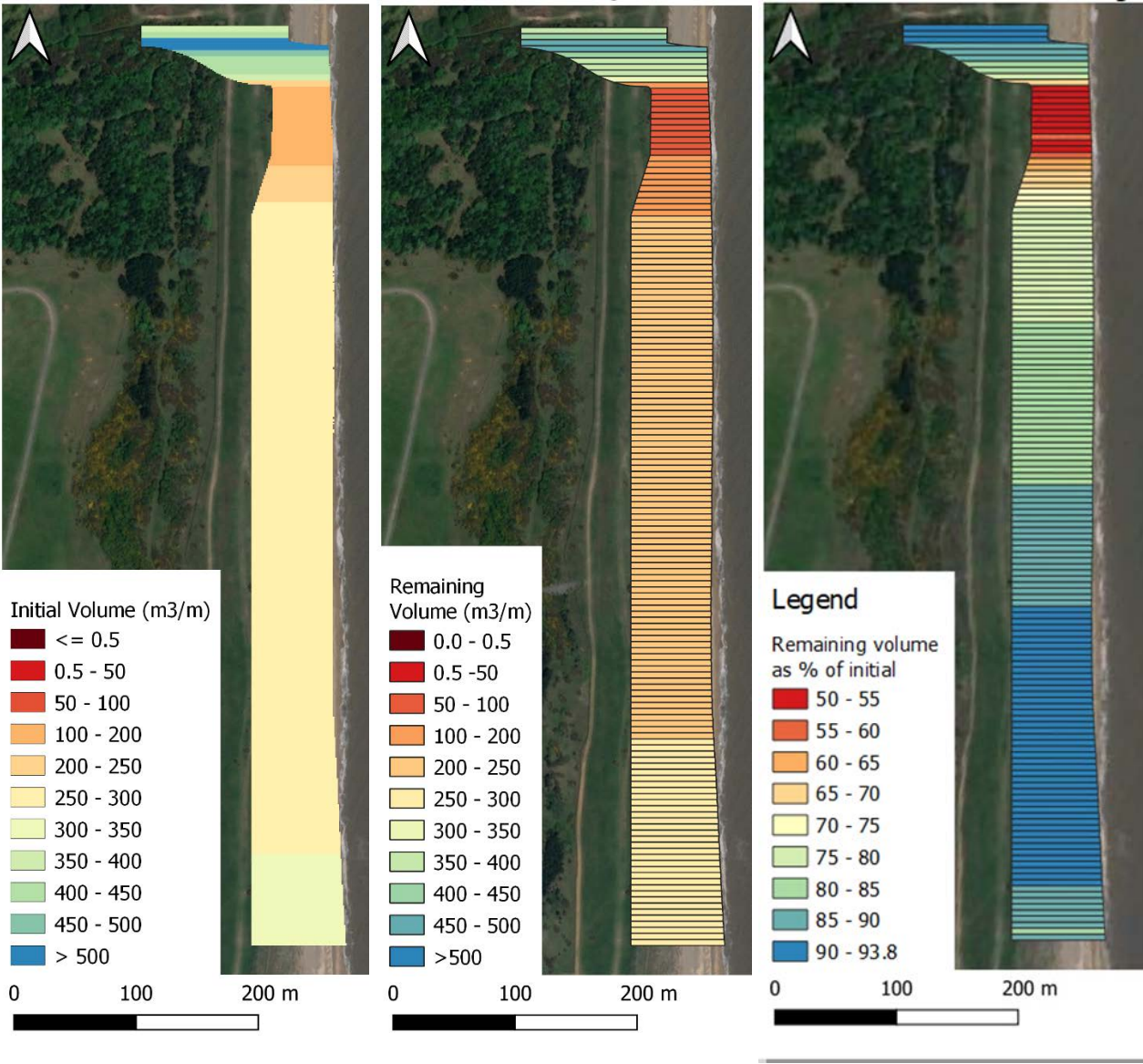


Figure 3-12. Volumetric map of the SCDF frontage (above 0 m ODN), pre-storm (left), and remaining post-storm beach volume (middle) and percentage (right) for the worst-modelled storm scenario: BfE event, 2099 SLR, with future eroded shoreline position. The 5 m polygon bins visible in the middle and right panels were used to calculate volumetric changes over the SCDF frontage for all 2D simulations run (Table 3-1).

Table 3-1. Predicted volumetric change (above 0 m ODN) from the SCDF feature for each 2D XBeach-S simulation (to 1<sup>st</sup> significant figure).

| Scen.<br>No. | Description                                   | Mean<br>loss per<br>m<br><br>(m <sup>3</sup> /m) | Min<br>loss per<br>m<br><br>(m <sup>3</sup> /m) | Max<br>loss per<br>m<br><br>(m <sup>3</sup> /m) | Total<br>loss<br>over<br>SCDF<br><br>(m <sup>3</sup> ) |
|--------------|---|--|---|---|--|
| 10           | BfE storm, E, present SL, SCDF                | -16  | 0   | -28   | -13,359  |
| 2            | 1-in-20 year storm, NE, present SL, SCDF      | -18  | 0   | -26   | -14,716  |
| 4            | 1-in-20 year storm, SE, present SL, SCDF      | -12  | 0   | -18   | -10,034  |
| 13           | BfE storm, E, 2069 SLR, SCDF                  | -22  | 0   | -38   | -18,023  |
| 14           | BfE storm, E, 2069 SLR, SCDF Future           | -35  | 0   | -69   | -28,167  |
| 15           | 1-in-20 year storm, NE, 2069 SLR, SCDF        | -20  | 0   | -31   | -16,316  |
| 16           | 1-in-20 year storm, SE, 2069 SLR, SCDF        | -15  | 0   | -22   | -12,277  |
| 11           | BfE storm, E, 2099 SLR, SCDF                  | -27  | 0   | -45   | -22,130  |
| 12           | BfE storm, E, 2099 SLR, SCDF Future           | -43  | 0   | -82   | -34,927  |
| 5            | 1-in-20 year storm, NE, 2099 SLR, SCDF        | -22  | 0   | -40   | -17,888  |
| 7            | 1-in-20 year storm, SE, 2099 SLR, SCDF        | -18  | 0   | -24   | -14,196  |
| 6            | 1-in-20 year storm, NE, 2099 SLR, SCDF future | -24  | 0   | -38   | -19,697  |
| 8            | 1-in-20 year storm, SE, 2099 SLR, SCDF future | -18  | 0   | -29   | -14,481  |

### 3.2 Variation due to particle size (gravel modelling)

Using the 1D XBeach-S and XBeach-G models (Section 2.4), the response of the SCDF to the 1-20-year storm (NE<sup>19</sup>) was investigated with various SCDF grain sizes at 2021, 2069, and 2099 sea levels. The results of the simulations are summarised in Figure 3-13 – Figure 3-15. Table 3-2 shows the predicted volume change from the SCDF, above 0 m ODN.

The profile change over both the 1D XBeach-S and XBeach-G simulations shows primarily a cut and fill beach response, decreasing in magnitude as particle size increases (Figure 3-13), similar to that seen in the 2D simulations. The cut and fill was significantly reduced for the largest particle size ( $D_{50} = 80$  mm), which showed very little change in profile shape. The crest of the SCDF was not predicted to be eroded or lowered under the simulated 1-in-20 year NE storm in any of the simulations, regardless of grain size or sea level.

Periods of subaerial accretion and erosion appear to occur during the tidal cycle in the XBeach-G simulations (Figure 3-14), but this is actually caused by the location of the cut and fill moving up the profile during the rising tide, resulting in more of the eroded subaerial sediment being deposited above 0 m ODN at high tide (6.5 hours into the simulation; Figure 3-14) than during the rising tide (< 6.5 hours). During the falling tide (> 6.5 hours), the subaerial erosion starts to deposit sediment below the 0 m contour again, and net losses (above 0 m ODN) are therefore seen by the end of the simulation (Figure 3-14). In all but the coarsest grain size ( $D_{50} = 80$  mm) the volume loss was greatest at the end of each simulated storm.

Under the modelled 1-in-20 year NE storm event, the coarser grain sizes tested were more resilient to erosion than the finer grain sizes. In the XBeach-G model,  $D_{50}$  grain sizes of 2, 10, 40, and 80 mm showed reducing net subaerial erosion with increasing grain size (from -5 to 0 m<sup>3</sup>/m at 2021 sea level, Table 3-2), and showed lower gross transport on any part of the profile with increasing grain size. The erosion predicted in the XBeach-G model runs was lower than in the XBeach-S simulations.

The 2 mm grain size, tested in both the 1D XBeach-S and XBeach-G models, was eroded more readily in the XBeach-S model than in the XBeach-G model. This grain size is exactly at the boundary of what is feasible to model in XBeach-S and XBeach-G<sup>20</sup>, and the difference in predicted erosion is likely to be due to shortcomings in both models at this boundary grain size: the lack of groundwater infiltration in XBeach-S means that erosion may be overestimated for 2 mm particles, as on a gravel beach infiltration slows backwash velocity and reduces erosion. Conversely, XBeach-G may underestimate erosion for this particle size as the lack of suspended sediment transport (which may still be relevant to particles of this size) in XBeach-G could mean offshore transport is under-predicted. For the tested  $D_{50}$  grain sizes of 10 mm and greater, suspended sediment transport is expected to be negligible, and therefore XBeach-G is not expected to under-predict erosion for the coarser particle sizes.

As sea level increases, the volume lost above 0 m ODN during a 1-in-20 year storm is predicted to increase in a relatively linear manner for  $D_{50} = 0.8$  and 2 mm (Figure 3-15). However, for  $D_{50} = 10, 40$  and 80 mm grain sizes, the effect of sea level rise is more complex: the storm erosion above 0 m ODN is predicted to remain the same, or even reduce, between 2021 and 2069 under the simulated storm. This is because, with higher sea levels, more of the eroded subaerial sediment is deposited above the 0 m ODN contour, and therefore erosion appears to reduce as sea level rises. In reality, the volume of sediment eroded from the subaerial beach (i.e. above *mean sea level*, rather than 0 m ODN) will probably steadily increase with sea level rise. By 2099, erosion above 0 m ODN is predicted to have increased for all grain sizes tested, due to the diminishing ability of the subtidal bars and beach face (which, conservatively, do not adjust with SLR in this model) to dissipate wave energy through bed friction and breaking. The XBeach-G model predicts that by 2099, erosion above 0 m ODN during a 1-in-20 year storm will range from -14 m<sup>3</sup>/m to -2 m<sup>3</sup>/m for  $D_{50}$

<sup>19</sup> The modelling in this section is 1D, meaning that alongshore sediment transport is neglected and obliquely arriving waves are reduced in energy according to Snell's law for refraction. The wave height condition used is that of the 1:20 year return interval from the NE sector, which is the larger of the two primary wave directional sectors.

<sup>20</sup> Differences between the models are described in more detail in Section 2.4.

grain sizes of 2-80 mm (Table 3-2), which is significantly less than that predicted by the 2D sand model (Table 3-1).

The  $D_{50} = 10$  and 40 mm grain sizes (pebbles), representing the modal and coarser sediments in the natural distribution, retain the cut and fill pattern (albeit it with lesser change than the sandy sizes) but show very similar patterns to one another. In comparison, the  $D_{50} = 80$  mm grain size (cobbles) was the most resilient to storm erosion at all sea levels, with predicted volume change above 0 m ODN during the simulated 1-in-20 year storm of  $+2 \text{ m}^3/\text{m}$  at 2099 sea level. The model predicted that the cobbles would actually exhibit slightly more onshore directed transport than offshore transport at 2021 and 2069 sea levels, resulting from minor reshaping of the subtidal beach face step and little erosion of the subaerial beach. However, offshore transport of the cobbles is predicted to overcome onshore transport at the 2099 sea level, resulting in  $2 \text{ m}^3/\text{m}$  volume loss during the simulated storm.



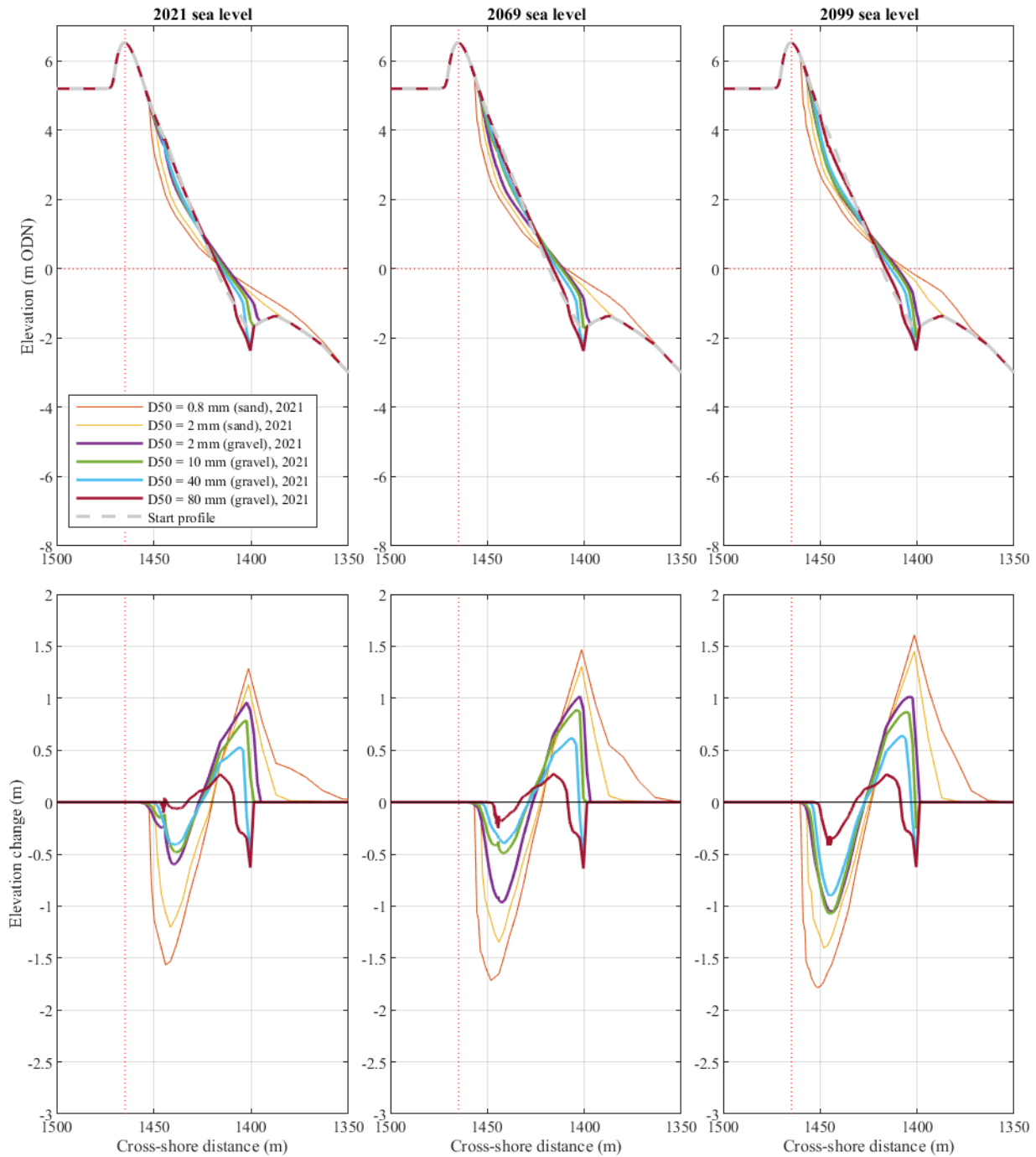


Figure 3-13. North East 1-in-20 year storm, 2021, 2069, and 2099 Sea Levels – End of simulation profiles (top panels) and profile changes (bottom panels) for various grain sizes. Simulations were run using both the XBeach sand surfbeat formulations (labelled 'XBeach-S') and the XBeach gravel non-hydrostatic formulations (labelled 'XBeach-G').

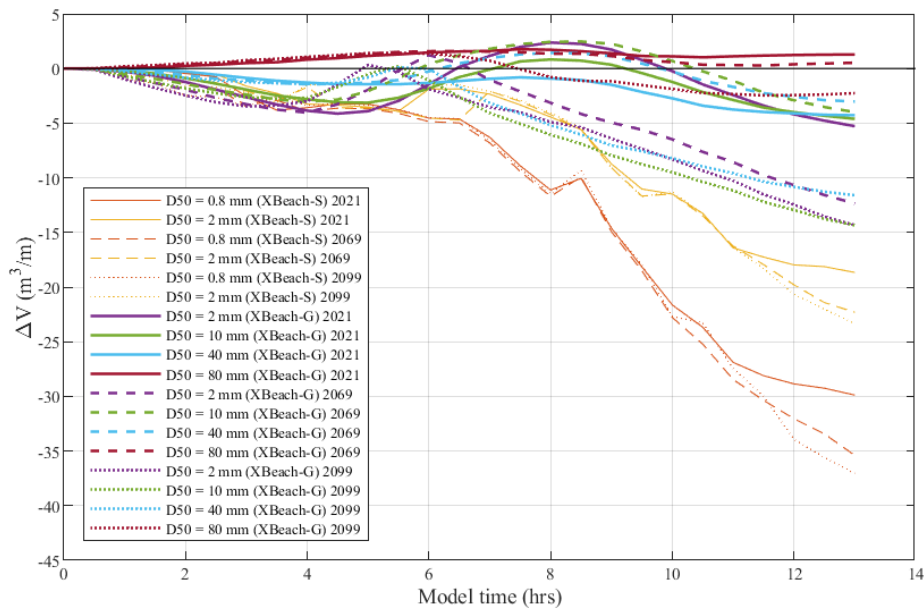


Figure 3-14. North East 1-in-20 year storm, 2021, 2069, and 2099 Sea Levels – intertidal volumetric change (above 0 m ODN and seaward of the SCDF crest) through time over the simulation for various grain sizes. Simulations were run using both the XBeach sand surfbeat model (labelled 'XBeach-S') and the XBeach gravel non-hydrostatic model (labelled 'XBeach-G').

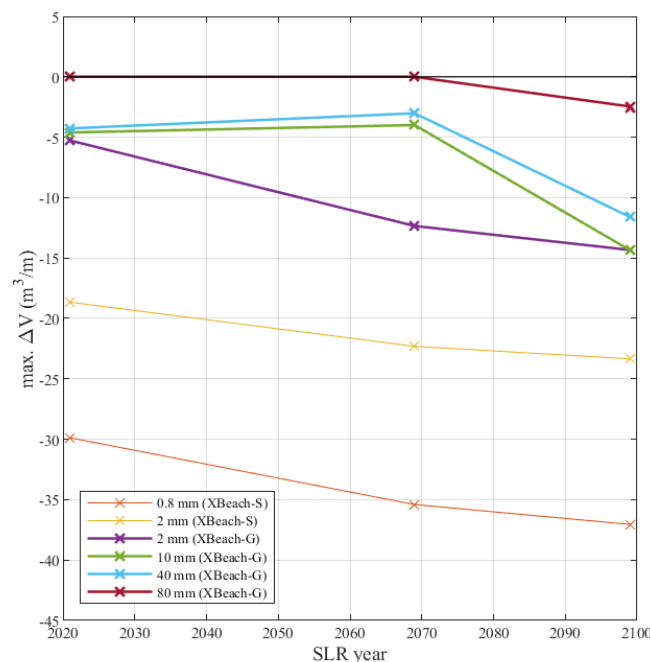


Figure 3-15. North East 1-in-20 year storm, 2021, 2069, and 2099 Sea Levels – Predicted volume eroded from the intertidal beach (above 0 m ODN and seaward of the SCDF crest) during the storm at the three sea levels tested. Note that the maximum eroded volume during the simulation is shown for each case, and that model data only exists for years 2021, 2069, and 2099. Simulations were run using both the XBeach sand surfbeat model (labelled 'XBeach-S') and the XBeach gravel non-hydrostatic model (labelled 'XBeach-G').

Table 3-2. Predicted volumetric change (above 0 m ODN) from the SCDF feature for each 1D XBeach-S and XBeach-G simulation (to 1 significant figure).

| Scen. No. | Description                      | Model    | Grain size (mm)                  | Net volume change ( $m^3/m$ ) | Max loss during run ( $m^3/m$ ) |
|-----------|----------------------------------|----------|----------------------------------|-------------------------------|---------------------------------|
| 1-1D      | 1-in-20 year storm, NE, 2021 SLR | XBeach-S | $D_{50} = 0.8$<br>$D_{90} = 1.5$ | -30                           | -30                             |
| 2-1D      | 1-in-20 year storm, NE, 2021 SLR | XBeach-S | $D_{50} = 2$<br>$D_{90} = 3$     | -19                           | -19                             |
| 3-1D      | 1-in-20 year storm, NE, 2021 SLR | XBeach-G | $D_{50} = 2$<br>$D_{90} = 3$     | -5                            | -5                              |
| 4-1D      | 1-in-20 year storm, NE, 2021 SLR | XBeach-G | $D_{50} = 10$<br>$D_{90} = 15$   | -5                            | -5                              |
| 5-1D      | 1-in-20 year storm, NE, 2021 SLR | XBeach-G | $D_{50} = 40$<br>$D_{90} = 60$   | -4                            | -4                              |
| 6-1D      | 1-in-20 year storm, NE, 2021 SLR | XBeach-G | $D_{50} = 80$<br>$D_{90} = 120$  | +1                            | 0                               |
| 7-1D      | 1-in-20 year storm, NE, 2069 SLR | XBeach-S | $D_{50} = 0.8$<br>$D_{90} = 1.5$ | -35                           | -35                             |
| 8-1D      | 1-in-20 year storm, NE, 2069 SLR | XBeach-S | $D_{50} = 2$<br>$D_{90} = 3$     | -22                           | -22                             |
| 9-1D      | 1-in-20 year storm, NE, 2069 SLR | XBeach-G | $D_{50} = 2$<br>$D_{90} = 3$     | -12                           | -12                             |
| 10-1D     | 1-in-20 year storm, NE, 2069 SLR | XBeach-G | $D_{50} = 10$<br>$D_{90} = 15$   | -4                            | -4                              |
| 11-1D     | 1-in-20 year storm, NE, 2069 SLR | XBeach-G | $D_{50} = 40$<br>$D_{90} = 60$   | -3                            | -3                              |
| 12-1D     | 1-in-20 year storm, NE, 2069 SLR | XBeach-G | $D_{50} = 80$<br>$D_{90} = 120$  | +0.5                          | 0                               |
| 13-1D     | 1-in-20 year storm, NE, 2099 SLR | XBeach-S | $D_{50} = 0.8$<br>$D_{90} = 1.5$ | -37                           | -37                             |
| 14-1D     | 1-in-20 year storm, NE, 2099 SLR | XBeach-S | $D_{50} = 2$<br>$D_{90} = 3$     | -23                           | -23                             |
| 15-1D     | 1-in-20 year storm, NE, 2099 SLR | XBeach-G | $D_{50} = 2$<br>$D_{90} = 3$     | -14                           | -14                             |
| 16-1D     | 1-in-20 year storm, NE, 2099 SLR | XBeach-G | $D_{50} = 10$<br>$D_{90} = 15$   | -14                           | -14                             |
| 17-1D     | 1-in-20 year storm, NE, 2099 SLR | XBeach-G | $D_{50} = 40$<br>$D_{90} = 60$   | -12                           | -12                             |
| 18-1D     | 1-in-20 year storm, NE, 2099 SLR | XBeach-G | $D_{50} = 80$<br>$D_{90} = 120$  | -2                            | -2                              |

### 3.3 Wave Run-up and Overtopping

---

Appendix D details the wave run-up heights predicted in the model simulations.  $R_{2\%}$  (98<sup>th</sup> percentile) and  $R_{\max}$  (maximum) values are provided, which represent the height exceeded by the largest 2% of swashes ( $R_{2\%}$ ) and the single highest swash height reached during the simulation ( $R_{\max}$ ).  $R_{2\%}$  is a commonly used runup metric in the scientific literature as it describes the height exceeded by the largest swashes, and therefore helps identify which point on the beach will be vulnerable to impact or overwashing.  $R_{\max}$  is less commonly used as it may only be reached by a single swash and represents a point on the beach that is, for the most part, unaffected by swashes. However, both  $R_{\max}$  and  $R_{2\%}$  are useful for the present purpose of predicting if any of the simulated conditions are likely to lead to overtopping of the SCDF.

For overtopping of the SCDF crest to happen,  $R_{\max}$  would have to reach the SCDF crest height at some point during the simulation, whilst more severe overtopping would occur if  $R_{2\%}$  was to reach the crest height, as this would mean a greater number of larger individual swashes were reaching the crest height. As XBeach-G includes infiltration and resolves water level fluctuations for each individual wave crest, while XBeach-S only resolves the wave group envelope, wave runup predictions from XBeach-G are expected to be more accurate than those from XBeach-S<sup>21</sup> for the  $D_{50} = 2 - 80$  mm particles tested (Poate *et al.*, 2016).

Increasing SCDF particle size has the effect of reducing the predicted wave runup height, as more infiltration of water into the beach face can occur with larger grains. From the XBeach-G simulations,  $R_{2\%}$  wave runup height was 0.48 m lower for  $D_{50} = 80$  mm (fine cobbles) than for  $D_{50} = 2$  mm (coarse sand/fine pebbles) at present sea level, and was 0.13 m and 0.37 m lower than the coarse sand with  $D_{50} = 10$  mm and  $D_{50} = 40$  mm pebbles, respectively. With  $D_{50} = 2$  mm (very coarse sand/fine pebbles), the 1D XBeach-G model suggests that  $R_{\max}$  may exceed the crest height of the SCDF under the NE 1-in-20 year storm at 2099 sea level (Scenario 15-1D, Table D-2).  $R_{2\%}$  for this event is 1.4 m lower than the crest height, however, so only the very largest swashes (approaching  $R_{\max}$ ) would exceed the crest of the SCDF. The equivalent 2D XBeach-S simulations (Scenarios 5 and 17, Table D-2) suggests that there is also risk of overtopping north of SZC (on the natural beach frontage at  $Y_1$ ) under the same North East 1-in-20 year storm (2099 sea level) with both  $R_{2\%}$  and  $R_{\max}$  exceeding the height of the natural beach there. This overtopping risk exists with and without the SCDF in place. None of the other modelled scenarios were predicted to result in any overtopping at the location of the SCDF ( $Y_2$ ) or along the natural beach ( $Y_1$  and  $Y_3$ ).

---

<sup>21</sup> Differences between the models are described in more detail in Section 2.4.

### 3.4 Decommissioning-phase modelling

---

For the decommissioning phase of SZC, two SLR conditions, 2120 and 2140, are tested against two HCDF designs. RCP4.5 is used for the SCDF and HCDF design from the start of the project with the future receded shoreline, whereas RCP8.5 is used for the Adaptive Design. Note that the RCP8.5 scenario was designed by climate scientists with the intention of exploring an unlikely high risk future. RCP4.5 is not tested against the Adaptive Design as it will only be built if SLR trends follow the RCP8.5 predictions. It will not be built if trends follow the RCP4.5 predictions.

#### 3.4.1 Bed elevation change using the sand model

##### 3.4.1.1 1:20 year NE storm

Under the two modelled SLR cases during decommissioning phase with future shorelines with the 1:20 year NE storm, a cut and fill beach response is seen with sediment losses on the supratidal beach face and gains on the subtidal beach face (Figure 3-16 and Figure 3-17). For the two modelled storms with RCP4.5 SLR scenarios, vertical bed level change (erosion) along the supratidal SCDF frontage is of the order of -1 to -2 m (Figure 3-17), with similar magnitudes of vertical beach accretion in the subtidal. Averaged along the SCDF frontage, the NE 1:20 year storms are predicted to incur approximately -1.6 to -1.8 m of supratidal bed level erosion, for 2120 and 2140 respectively (Figure 3-16). No erosion of the SCDF crest is predicted to occur during either of the modelled storm events at the 2120 and 2140 sea level.

The inclusion of the HCDF line in Figure 3-17 is stylistic only and the HCDF is not included in the model domain as a hard non-erodible feature. However, this does not present an issue as the HCDF is not exposed. The modelled SCDF is the same as that used in Section 3.1.2. As such, it has not been extended south in this modelling to account for the 70 m southerly extension of the updated HCDF as the designs were not available when the modelling commenced. The present day natural topography has been used in this area, which has a lower volume than the SCDF would (i.e., and has increased from a minimum of 105 m<sup>3</sup>/m to 185 m<sup>3</sup>/m with the SCDF present). Although this is conservative (the beach modelled has less sediment than it would in reality), the SCDF will be updated and re-modelled in the next version of the report.

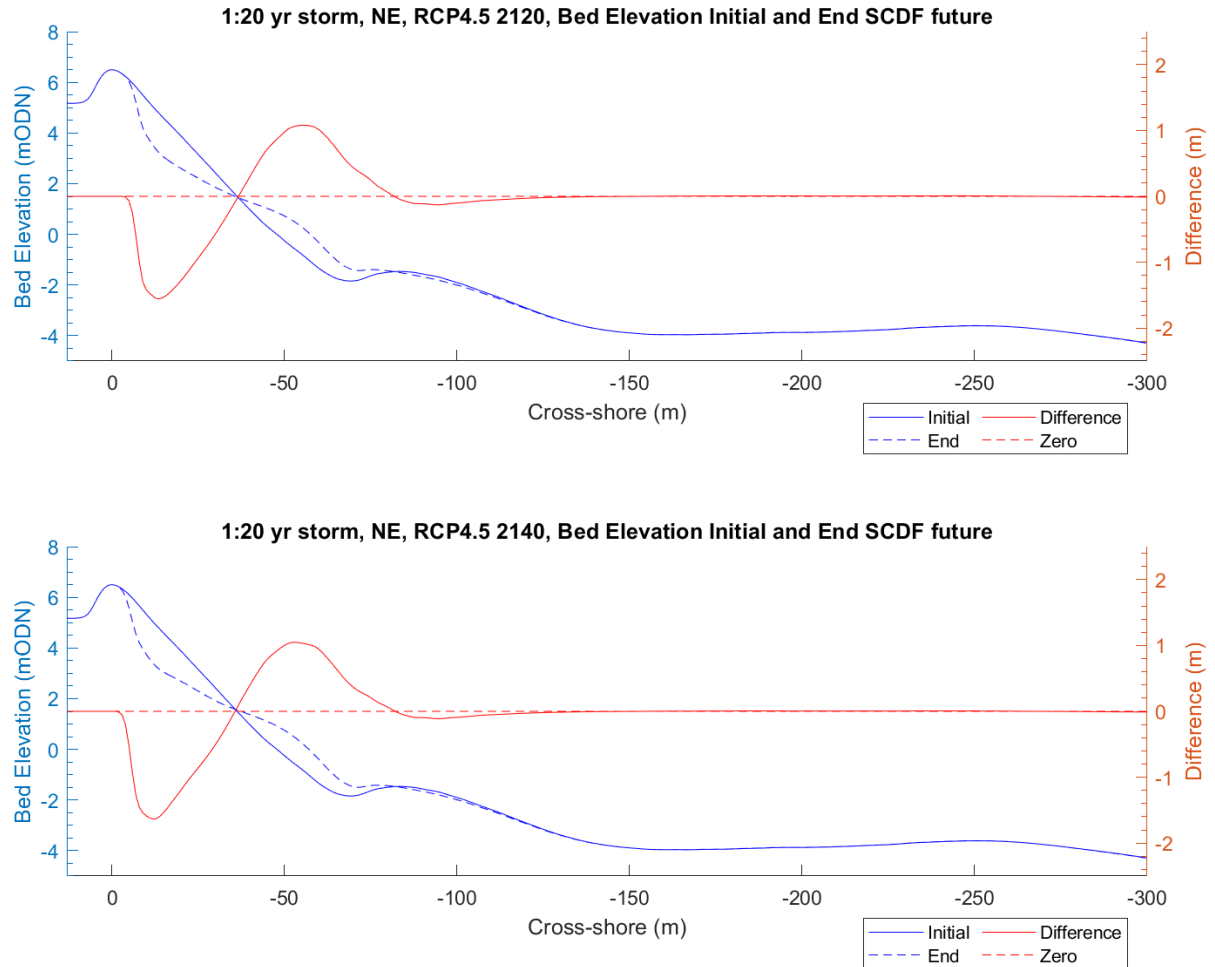


Figure 3-16. Average bed level along the SCDF frontage ( $Y_{average}$ , Section 3) at the start ('initial') and end of the two modelled storm events with SCDF-with future receded shorelines. Upper panel: 1:20 year NE storm with RCP4.5 SLR 2120. Lower panel: 1:20 year NE storm with RCP4.5 SLR 2140. In each panel, the solid red line shows the vertical difference in the pre- and post-storm profiles.

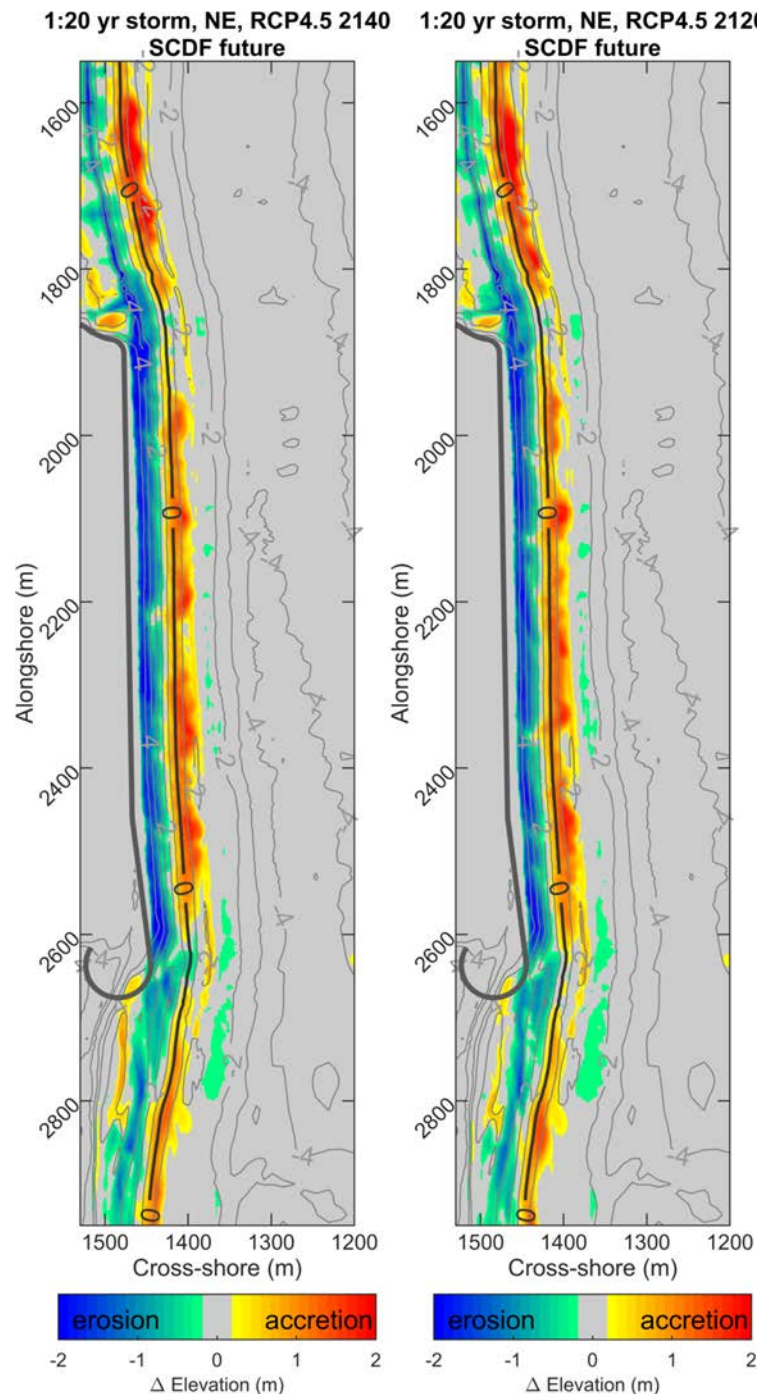


Figure 3-17. 2D change in bed elevation (coloured areas) along the SCDF frontage over the two modelled storm events with the SCDF-with future receded shorelines. Contour lines show starting bed elevation (m ODN), with 0 m contour line shown in bold for reference. The thick line on the supratidal beach represents the approximate location of the HCDF toe which is stylistic only and the HCDF is not included in the model domain as a hard non-erodible feature.

Under the two RCP8.5 SLR cases modelled for the Adaptive Design with future shorelines, a cut and fill beach response is seen with sediment losses on the supratidal beach face and gains on the subtidal beach face (Figure 3-18 and Figure 3-19). For the two modelled storms, vertical bed level change (erosion) along the supratidal SCDF frontage is of the order of -2 to -3 m (Figure 3-19), with similar magnitudes of vertical beach accretion in the subtidal. Averaged along the SCDF frontage, the NE 1:20 year storms are predicted to incur approximately -2.0 to -2.2 m of supratidal bed level erosion, for 2120 and 2140 respectively (Figure 3-18). Erosion of the SCDF crest is predicted to occur with RCP8.5 SLR during both of the modelled storm



events at 2120 and 2140 sea levels. During the 2140 SLR, the crest height was reduced from 6.4 m ODN to approximately 6 m ODN, but still remained higher than the crest elevation of the coastal path behind the SCDF crest.

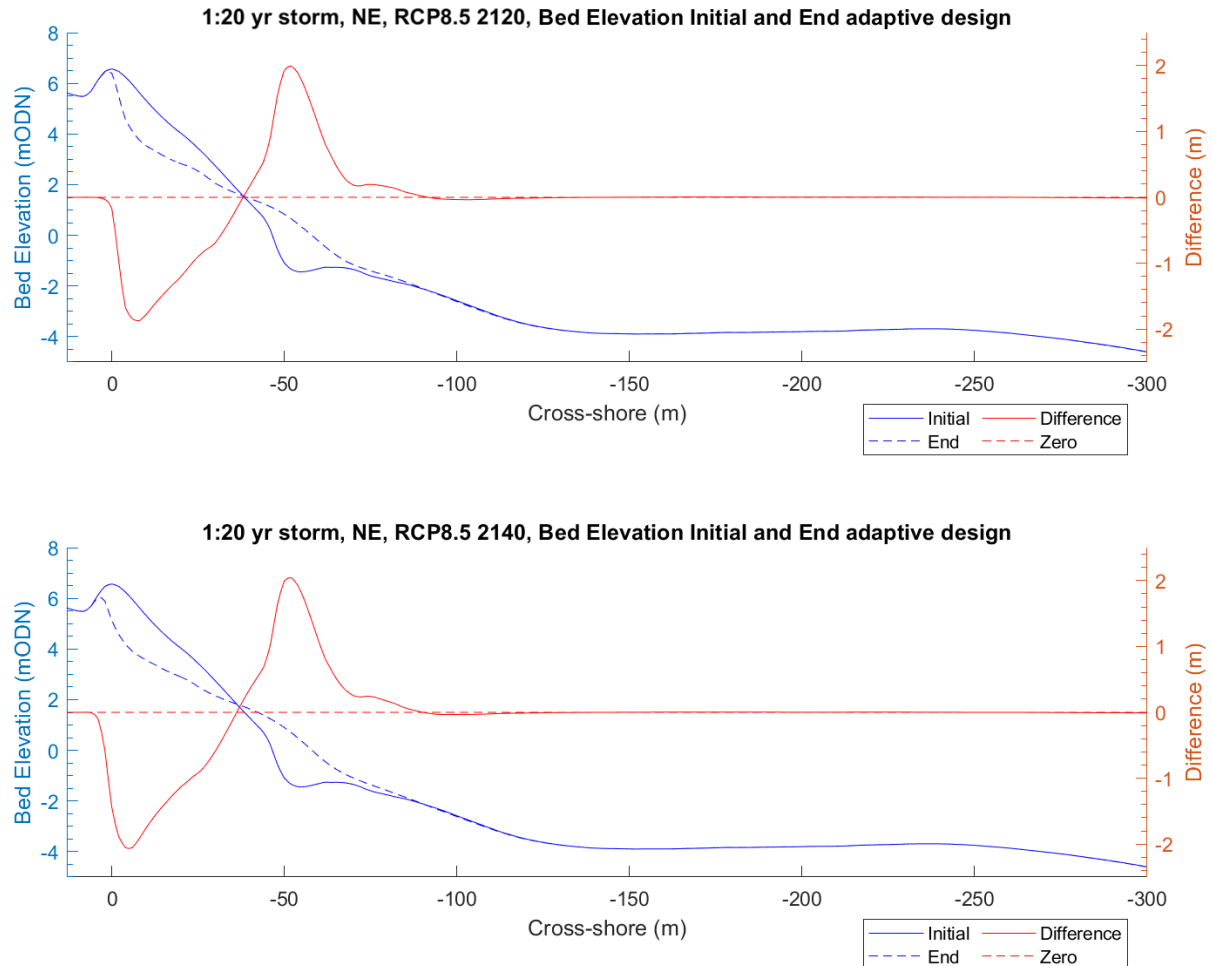


Figure 3-18. Average bed level along the SCDF frontage ( $Y_{average}$ , Section 3) at the start ('initial') and end of the two modelled storm events with Adaptive Design - with future receded shorelines. Upper panel: 1:20 year NE storm with RCP8.5 SLR 2120. Lower panel: 1:20 year NE storm with RCP8.5 SLR 2140. In each panel, the solid red line shows the vertical difference in the pre- and post-storm profiles.

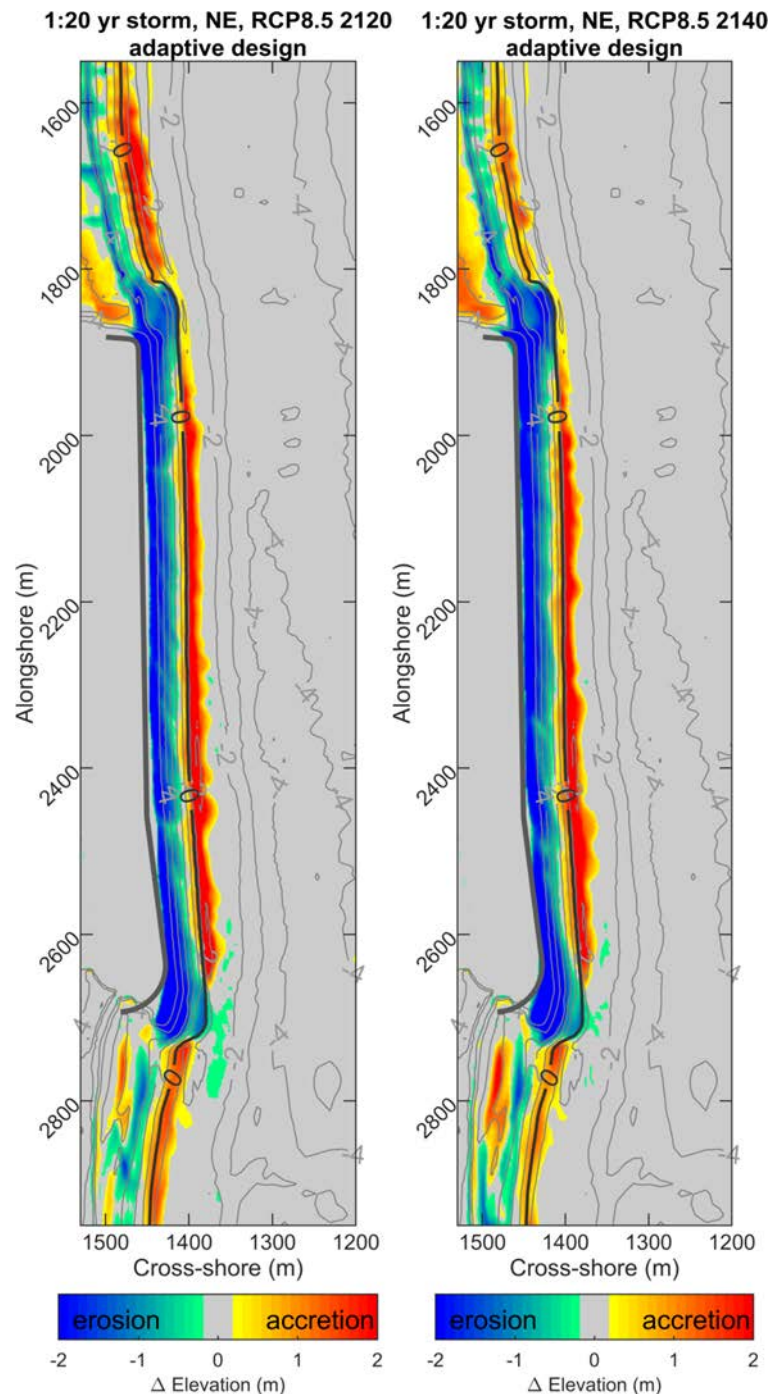


Figure 3-19. 2D change in bed elevation (coloured areas) along the SCDF frontage over the two modelled storm events with the Adaptive Design - with future receded shorelines and RCP8.5 sea levels. Contour lines show starting bed elevation (m ODN), with 0 m contour line shown in bold for reference. The thick line on the supratidal beach represents the approximate location of the HCDF toe.

#### 3.4.1.2 1:20 year SE storm

Under the two modelled SLR cases during the decommissioning phase with the future shorelines with the 1:20 year SE storm, a cut and fill beach response is seen with sediment losses on the supratidal beach face and gains on the subtidal beach face (Figure 3-20 and Figure 3-21). For the two modelled storms with RCP4.5 SLR scenarios, vertical bed level change (erosion) along the supratidal SCDF frontage is on the order of -1 to -2 m (Figure 3-21), with similar magnitudes of vertical beach accretion in the subtidal.

Averaged along the SCDF frontage, the SE 1:20 year storms are predicted to incur approximately -1.6 m of supratidal bed level erosion, for 2120 and 2140 respectively (Figure 3-20). No erosion of the SCDF crest is predicted to occur during either of the modelled storm events at 2120 and 2140 sea level for the SE event.

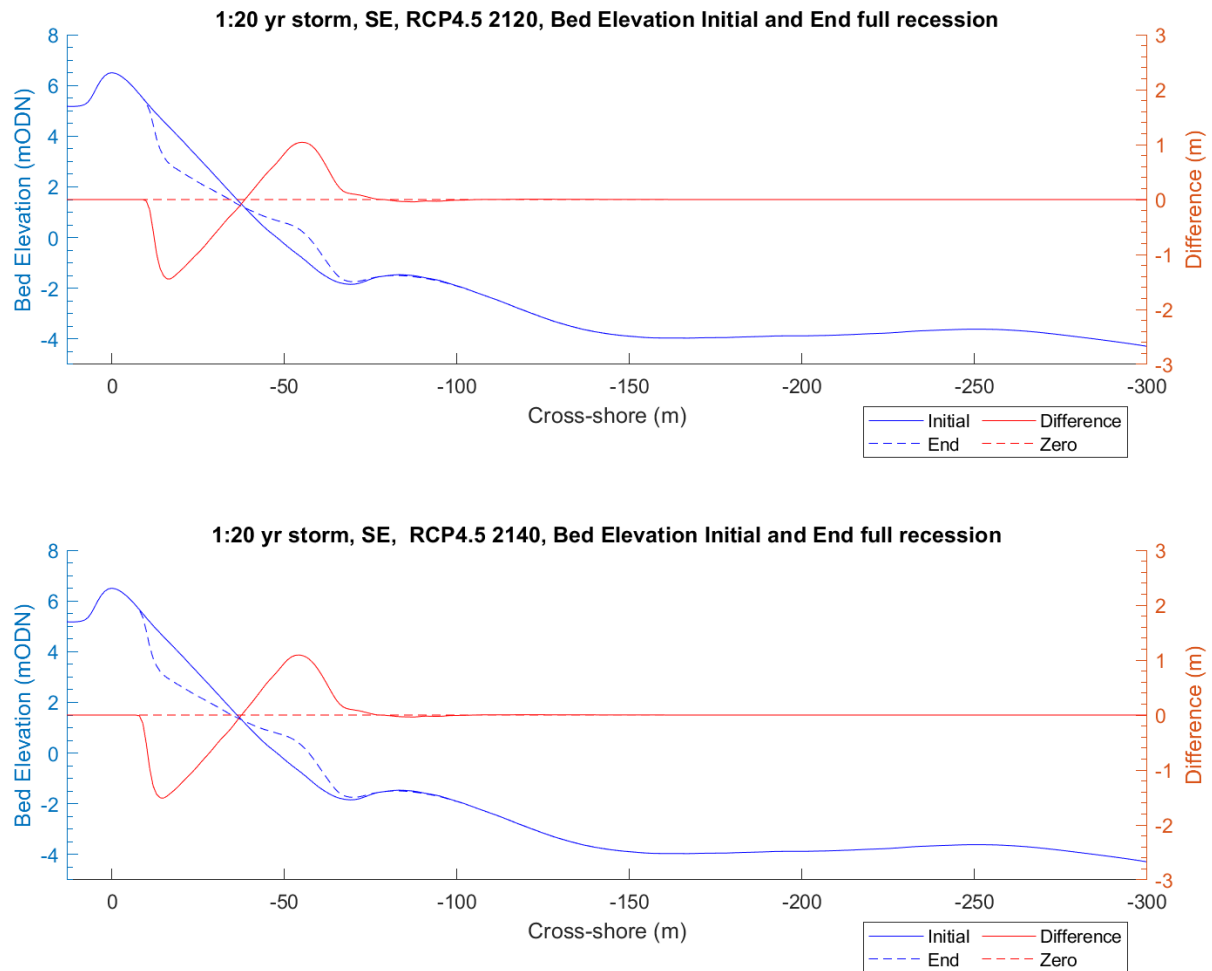


Figure 3-20 Average bed level along the SCDF frontage ( $Y_{average}$ , Section 3) at the start ('initial') and end of the two modelled storm events with SCDF-with future receded shorelines. Upper panel: 1:20 year SE storm with RCP4.5 SLR 2120. Lower panel: 1:20 year SE storm with RCP4.5 SLR 2140. In each panel, the solid red line shows the vertical difference in the pre- and post-storm profiles.

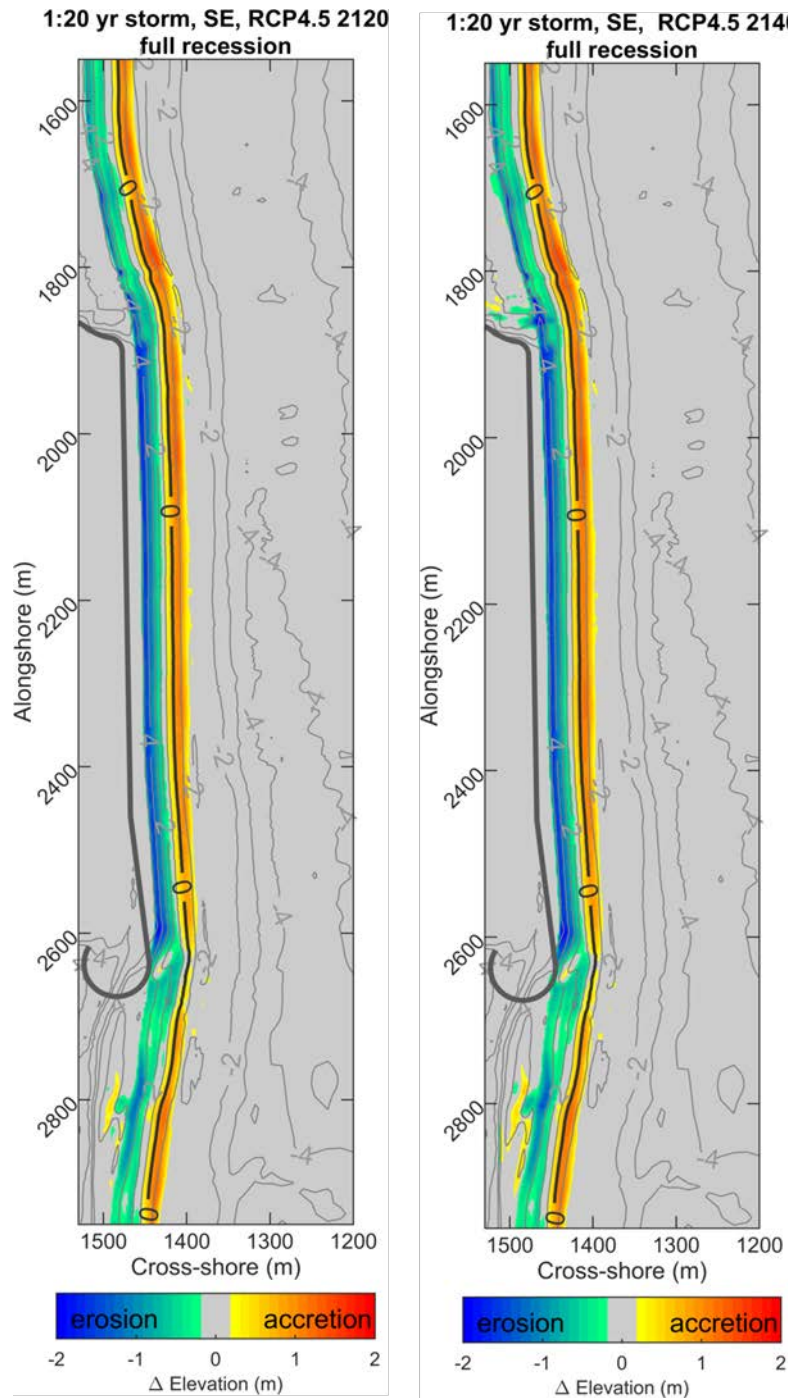


Figure 3-21 2D change in bed elevation (coloured areas) along the SCDF frontage over the two modelled storm events with the SCDF-with future receded shorelines. Contour lines show starting bed elevation (m ODN), with 0 m contour line shown in bold for reference. The thick line on the supratidal beach represents the approximate location of the HCDF toe which is stylistic only and the HCDF is not included in the model domain as a hard non-erodible feature.

### 3.4.1.3 *Beast from the East* storm sequence

Under the two modelled SLR cases during the decommissioning phase with future shorelines with the BfE storm, a cut and fill beach response is seen with sediment losses on the supratidal beach face and gains on the subtidal beach face (Figure 3-22 and Figure 3-23). For the two modelled storms with RCP4.5 SLR scenarios, vertical bed level change (erosion) along the supratidal SCDF frontage is on the order of -2 to -3 m (Figure 3-23), with similar magnitudes of vertical beach accretion in the subtidal. Averaged along the SCDF frontage, the BfE storms are predicted to incur approximately -2.5 to -3.0 m of supratidal bed level erosion, for 2120 and 2140 respectively (Figure 3-22). Erosion of the SCDF crest is predicted to occur during the BfE storm with RCP4.5 SLR for both of the modelled storm events at 2120 and 2140 sea levels. During the 2140 SLR, the crest height was lowered from 6.4 m ODN to approximately 5.8 m ODN, but still remained higher than the crest elevation of the coastal path behind the SCDF crest.

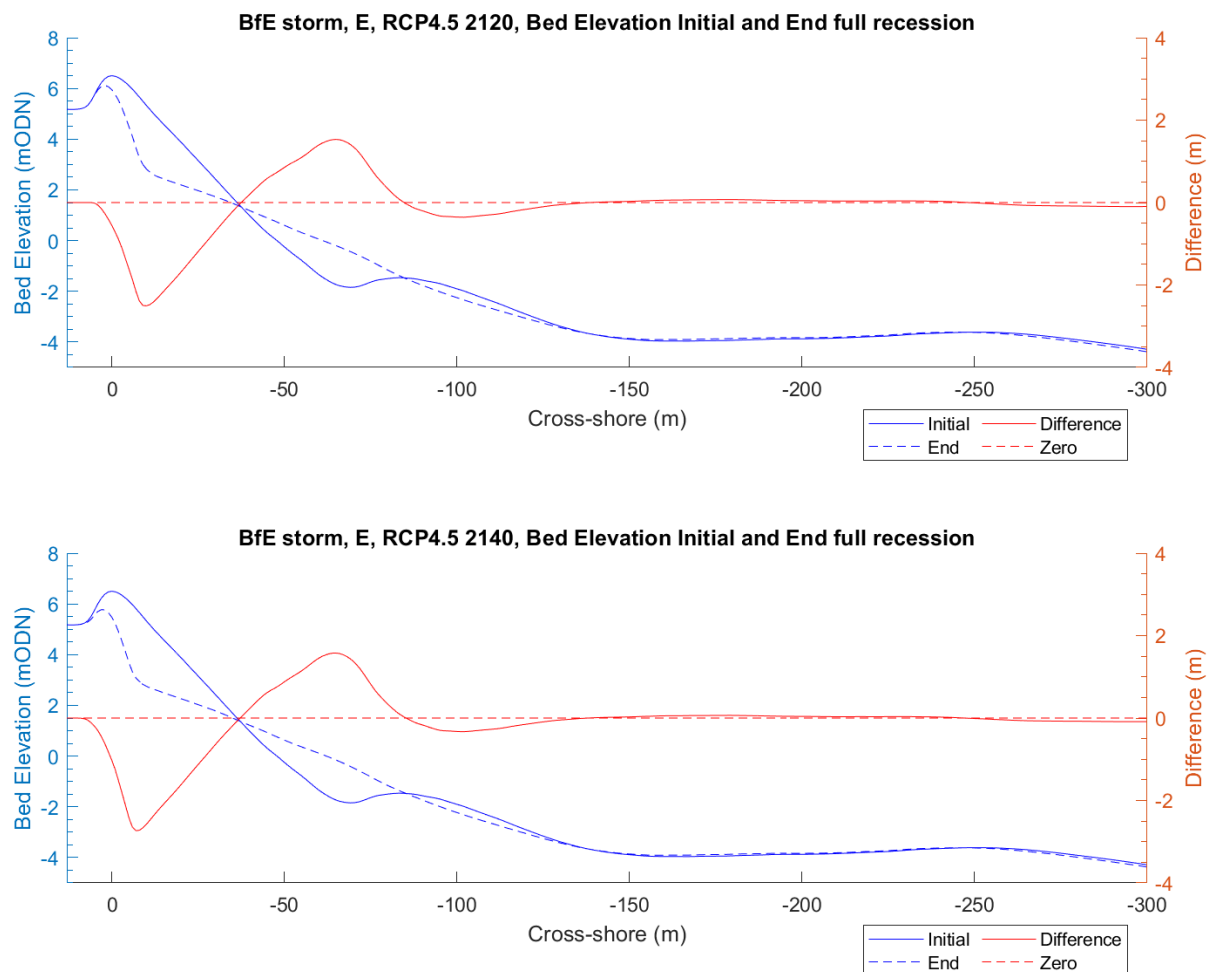


Figure 3-22 Average bed level along the SCDF frontage ( $Y_{average}$ , Section 3) at the start ('initial') and end of the two modelled storm events with SCDF-with future receded shorelines. Upper panel: BfE storm with RCP4.5 SLR 2120. Lower panel: BfE storm with RCP4.5 SLR 2140. In each panel, the solid red line shows the vertical difference in the pre- and post-storm profiles.



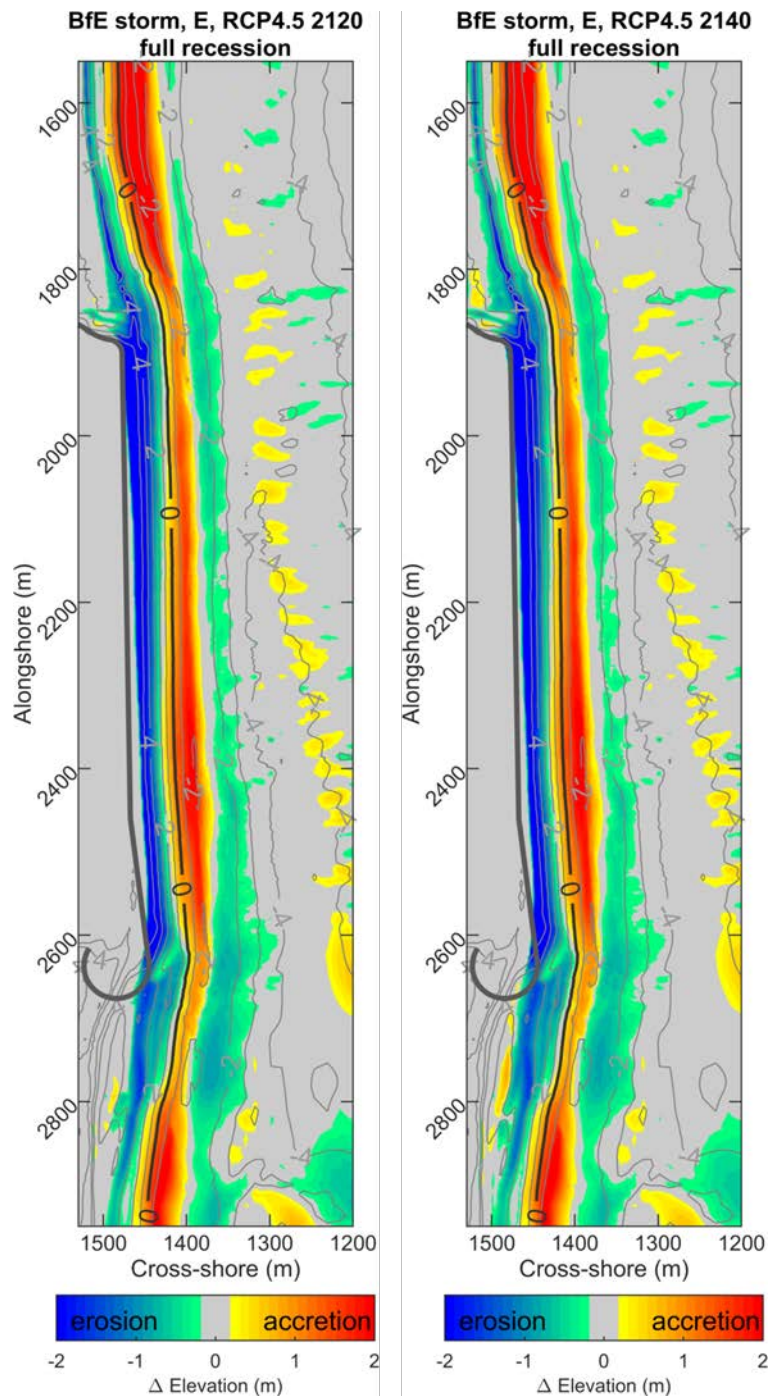


Figure 3-23 2D change in bed elevation (coloured areas) along the SCDF frontage over the two modelled storm events with the SCDF-with future receded shorelines. Contour lines show starting bed elevation (m ODN), with 0 m contour line shown in bold for reference. The thick line on the supratidal beach represents the approximate location of the HCDF toe which is stylistic only and the HCDF is not included in the model domain as a hard non-erodible feature.

Under the RCP8.5 2140 SLR case modelled for the Adaptive Design with future shorelines, a cut and fill beach response is seen with sediment losses on the supratidal beach face and gains on the subtidal beach face (Figure 3-24 and Figure 3-25). For the modelled storm, vertical bed level change (erosion) along the supratidal SCDF frontage is of the order of -2 to -4 m (Figure 3-25, with smaller magnitudes of vertical beach accretion in the subtidal). Averaged along the SCDF frontage, the BfE storm is predicted to incur approximately -3.5 m of supratidal bed level erosion, for 2140 (Figure 3-24). Erosion of the SCDF crest is predicted to occur with RCP8.5 SLR during the storm events at 2140 sea levels. During the 2140 SLR, the



crest height was reduced from 6.4 m ODN to the edge of the coastal path behind the SCDF crest at approximately 5.2 m ODN. However, this sand modelling ( $D_{50} = 0.8$  mm) is conservative as the beach and SCDF would be dominated by the modal pebble sizes of  $D_{50} = 10$  mm, which are modelled in Section 3.4.3 and show the beach is more resistant to erosion.

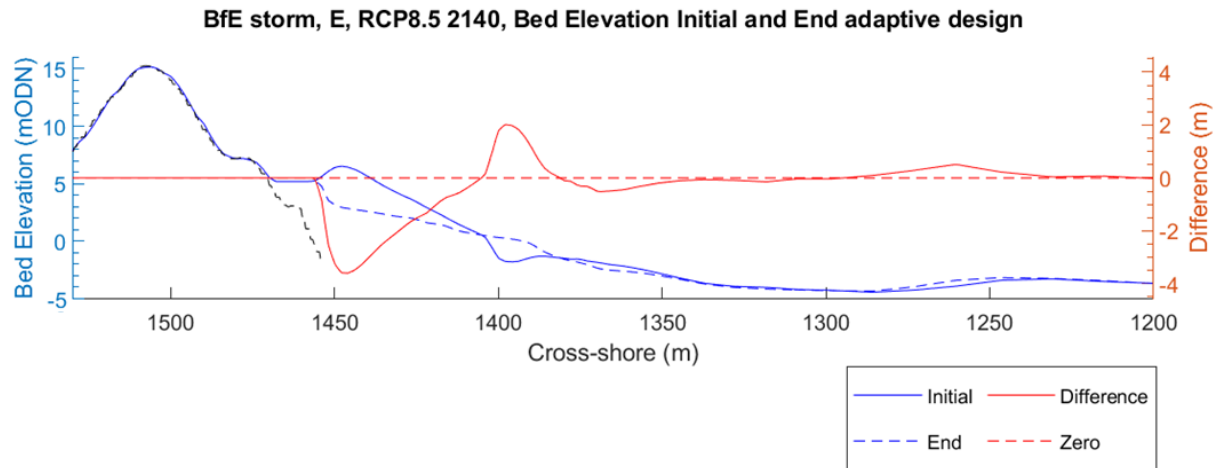


Figure 3-24 Average bed level along the SCDF frontage ( $Y_{average}$ , Section 3) at the start ('initial') and end of the modelled BfE storm with RCP8.5 SLR 2140 with the Adaptive Design -with future receded shorelines. The solid red line shows the vertical difference in the pre- and post-storm profiles. The dashed red line shows the HCDF.

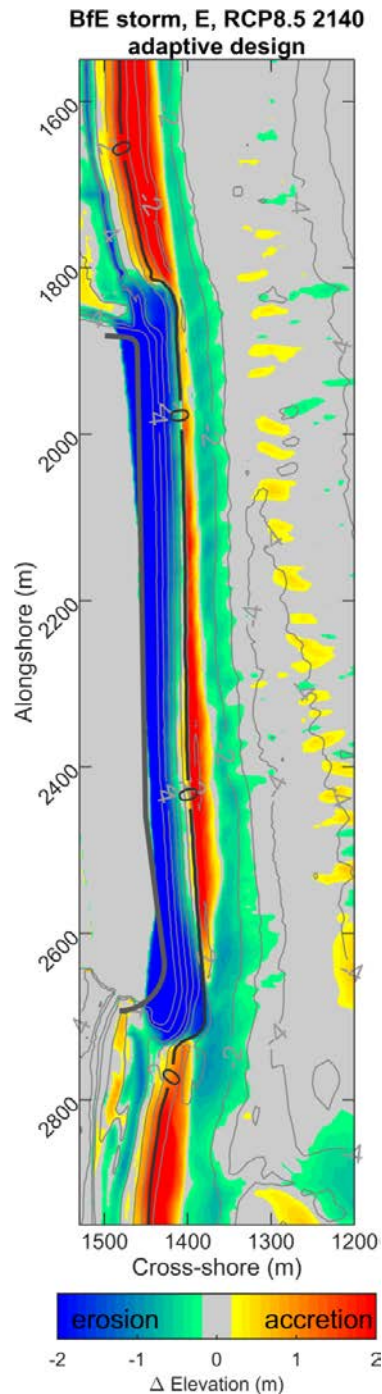


Figure 3-25 2D change in bed elevation (coloured areas) along the SCDF frontage over the modelled BfE storm event with the Adaptive Design - with future receded shorelines and RCP8.5 sea levels. Contour lines show starting bed elevation (m ODN), with 0 m contour line shown in bold for reference. The thick line on the supratidal beach represents the approximate location of the HCDF toe.

### 3.4.2 Volumetric changes using the sand model

For the SCDF with future eroded shoreline, the volumetric change using the 2D sand model was calculated within 151 polygons, following the methodology in Section 3.1.3, across the SCDF frontage using the bed levels at the beginning and end of each 2D simulation. For the adaptive design, the most shoreward edge of the polygons was adjusted to account for the different toe location. For both scenarios, each polygon still covers 5 m alongshore and covers the SCDF down to approximately 0 m ODN in the cross-shore direction.

From the total volumetric change within each polygon, the volumetric loss was calculated and expressed per metre of alongshore beach length ( $\text{m}^3/\text{m}$ ). Maps depicting the volume loss per m along the frontage of the SCDF are presented in Appendix C. Table 3-3 summarises the average volume loss per m, the minimum and maximum volumetric loss alongshore, and the total loss across all 5 m polygons. Volumetric changes from the 2D decommissioning simulations are summarised in this section of the report, while volumetric changes from the 1D decommissioning simulations with 10 mm grain size are presented in Section 3.4.3.

As expected, the higher SLR conditions of RCP8.5 resulted in the highest volume lost from the SCDF, followed by the RCP4.5 SLR (Table 3-3). From Table 3-3, mean losses across the SCDF frontage for the various storm scenarios range from  $-20 \text{ m}^3/\text{m}$  to  $-101 \text{ m}^3/\text{m}$  using the 2D sand model. The BfE storm with RCP8.5 SLR and the Adaptive Design resulted in the highest mean losses, along the peak loss at a single volumetric cell along the SCDF frontage of  $188 \text{ m}^3/\text{m}$ , Figure 3-29.

As seen with the future eroded shoreline used during the operational phase simulations, the decommissioning simulations show that the severely receded adjacent shorelines increase erosion pressure on the SCDF. For the 1:20 yr NE storm, the modelled mean erosion along the SCDF frontage ( $Y_{\text{average}}$ ) with RCP4.5 SLR and receded adjacent shorelines is  $-26 \text{ m}^3/\text{m}$  in 2120 and  $-27 \text{ m}^3/\text{m}$  in 2140, but higher localised losses are observed at both ends of the SCDF ( $60$  and  $80 \text{ m}^3/\text{m}$ ), due to higher wave angles and longshore transport gradients where the shoreline curves from the SCDF to the adjacent frontage. In contrast, with RCP8.5, the SCDF of the Adaptive Design is predicted to lose  $-40 \text{ m}^3/\text{m}$  and  $-44 \text{ m}^3/\text{m}$  at 2120 and 2140 sea level, respectively.

For the BfE storm, the modelled mean erosion along the SCDF frontage ( $Y_{\text{average}}$ ) with RCP4.5 SLR and receded adjacent shorelines is  $-51 \text{ m}^3/\text{m}$  in 2120 and  $-56 \text{ m}^3/\text{m}$  in 2140, but higher localised losses are observed at both ends of the SCDF ( $73$  and  $112 \text{ m}^3/\text{m}$ ), due to higher wave angles and longshore transport gradients where the shoreline curves from the SCDF to the adjacent frontage. In contrast, with RCP8.5, the SCDF of the Adaptive Design is predicted to lose  $-101 \text{ m}^3/\text{m}$  at 2140 sea level, but higher localised losses are observed at both ends of the SCDF ( $176$  and  $188 \text{ m}^3/\text{m}$ ).

Even in the most affected areas of the SCDF, the volume eroded by the simulated storms is still less than the available beach volume with the SCDF, and at no location along the SCDF frontage was all of the subaerial volume removed by any of the simulated storms – that is, the HCDF is not exposed in all the models run. The worst-modelled storm scenario in terms of erosional losses was the BfE storm, RCP8.5 2140 SLR with the Adaptive Design and future eroded shorelines (Figure 3-29), where the peak loss was  $-188 \text{ m}^3/\text{m}$ , centred in a 25 m long section at the south of the SCDF with continuous losses greater than  $-150 \text{ m}^3/\text{m}$ . The peak losses in this area still left  $180 \text{ m}^3/\text{m}$  of subaerial sediment on the beach face (50% of initial beach volume). The smallest remaining beach volume was to the north with  $38 \text{ m}^3/\text{m}$  (18% of initial beach volume). On average 54% of the pre-storm subaerial SCDF beach volume remains. This indicates that the proposed SCDF is still sufficient to avoid exposure of the HCDF, especially given that the 2D XBeach-S (sand) model over-predicted erosion in the calibration and validation cases by at least 2-3 times. For example, for the 1:20 year NE storm with RCP8.5 2140 SLR against the Adaptive Design, the modelled mean erosion is  $-44 \text{ m}^3/\text{m}$  with Xbeach-S (sand) and  $13 \text{ m}^3/\text{m}$  with XBeach-G (gravel).

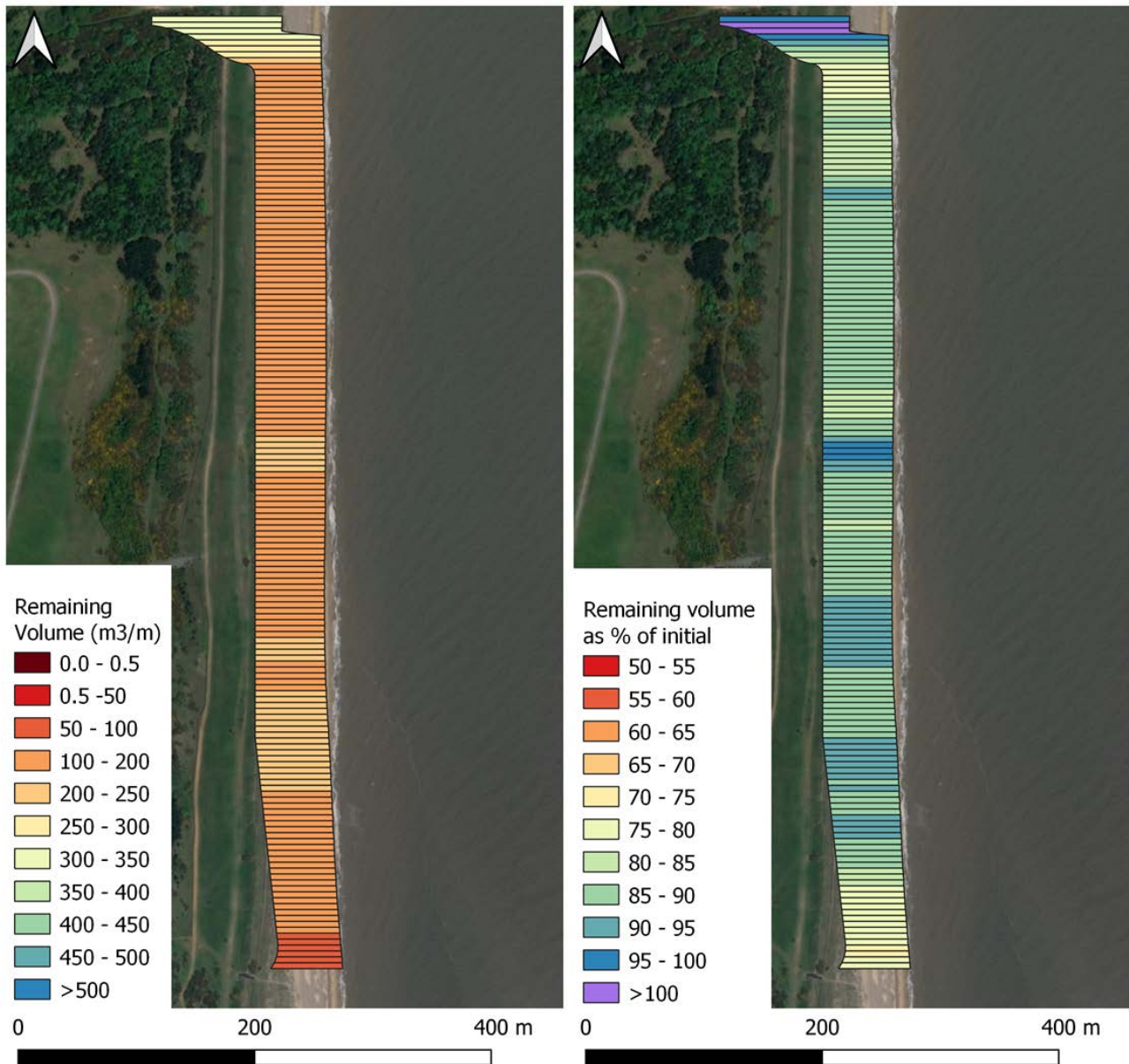


Figure 3-26. Volumetric map of the SCDF frontage (above 0 m ODN), remaining post-storm beach volume (left) and percentage (right) for the 1:20 year NE storm with RCP4.5 SLR 2140, with future eroded shoreline position. The 5 m polygon bins visible in the middle and right panels were used to calculate volumetric changes over the SCDF frontage for all 2D simulations run (Table 2-5).

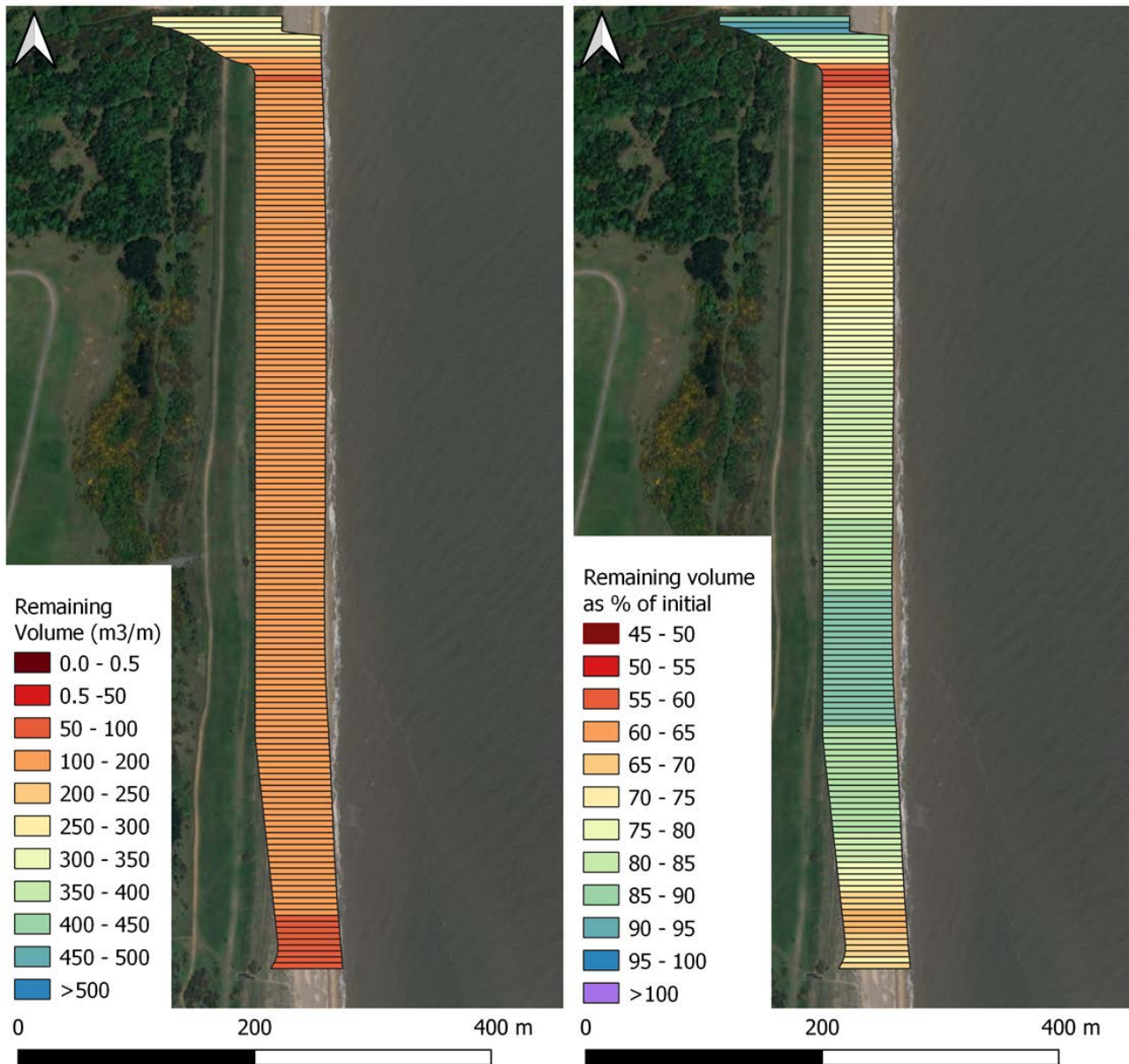


Figure 3-27 Volumetric map of the SCDF frontage (above 0 m ODN), remaining post-storm beach volume (left) and percentage (right) for the BfE storm with RCP4.5 SLR 2140, with future eroded shoreline position. The 5 m polygon bins visible in the middle and right panels were used to calculate volumetric changes over the SCDF frontage for all 2D simulations run (Table 2-5).



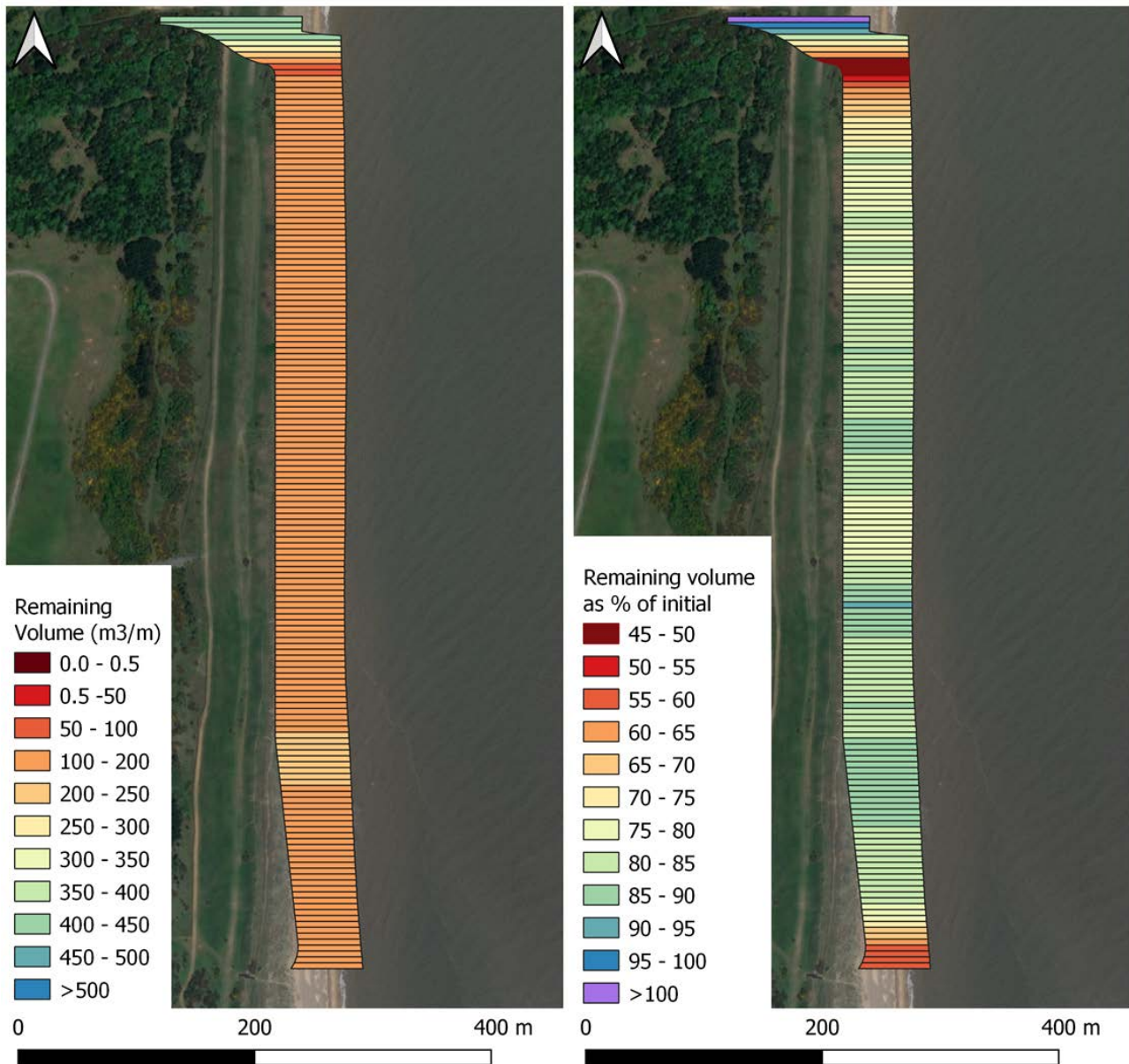


Figure 3-28. Volumetric map of the Adaptive Design frontage (above 0 m ODN), remaining post-storm beach volume (left) and percentage (right) for the 1:20 year NE storm with RCP8.5 SLR 2140, with future eroded shoreline position. The 5 m polygon bins visible in the middle and right panels were used to calculate volumetric changes over the SCDF frontage for all 2D simulations run (Table 2-5).



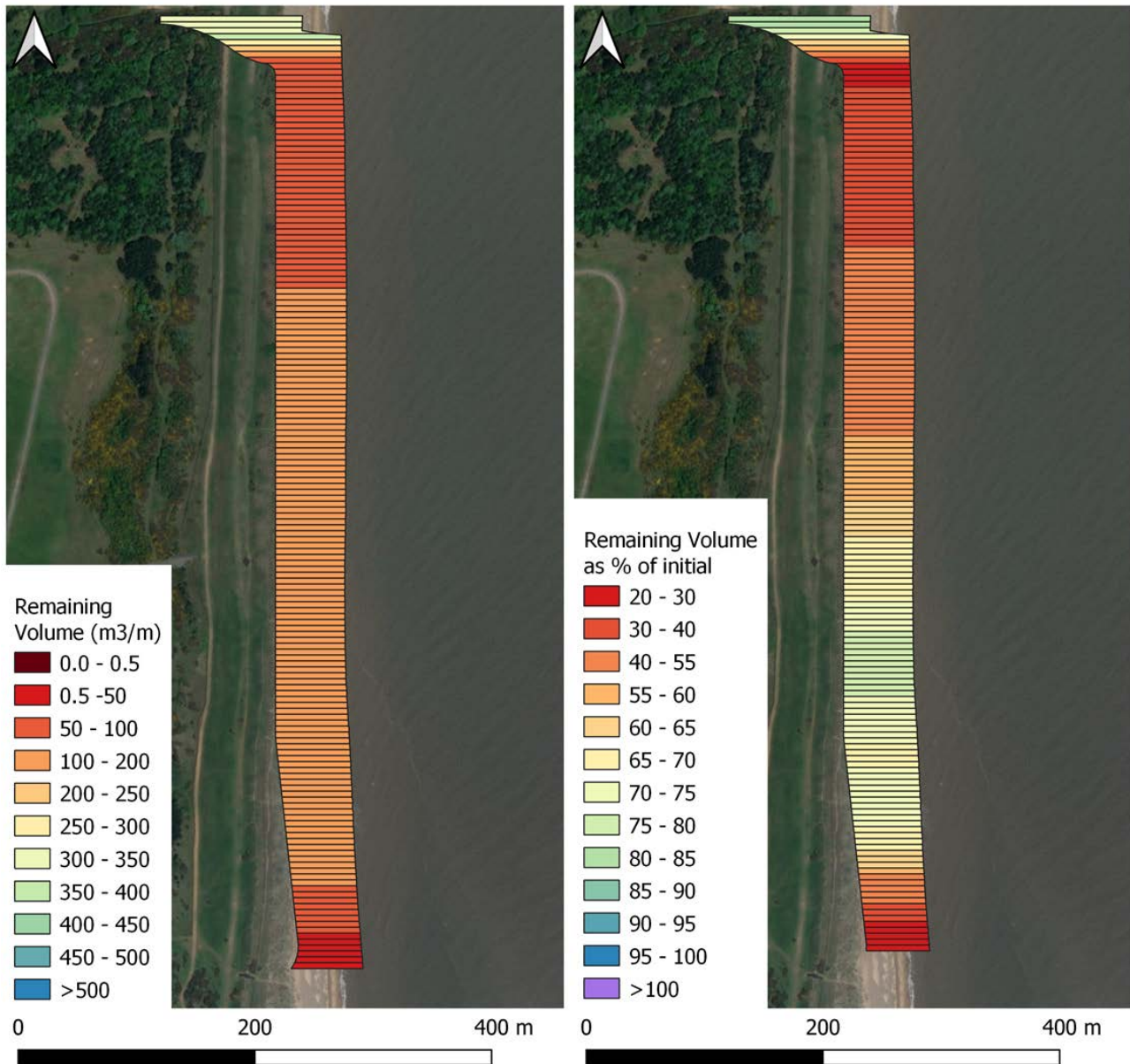


Figure 3-29 Volumetric map of the Adaptive Design frontage (above 0 m ODN), remaining post-storm beach volume (left) and percentage (right) for the BfE storm with RCP8.5 SLR 2140, with future eroded shoreline position. The 5 m polygon bins visible in the middle and right panels were used to calculate volumetric changes over the SCDF frontage for all 2D simulations run (Table 2-5).

Table 3-3. Predicted volumetric change (above 0 m ODN) from the SCDF feature for each 2D XBeach-S simulation (to 1<sup>st</sup> significant figure).

| Scen. No. | Description   | Mean loss per m<br>(m <sup>3</sup> /m) | Min loss per m<br>(m <sup>3</sup> /m) | Max loss per m<br>(m <sup>3</sup> /m) | Total loss over SCDF<br>(m <sup>3</sup> ) |
|-----------|---|--|---------------------------------------|---------------------------------------|---|
| 1-2D      | 1-in-20 year storm, NE, RCP4.5 2120 SLR, SCDF with receded shorelines                 | -26                                    | 0                                     | -41                                   | -21,187                                   |
| 2-2D      | 1-in-20 year storm, NE, RCP4.5 2140 SLR, SCDF with receded shorelines                 | -27                                    | 7                                     | -51                                   | -22,113                                   |
| 3-2D      | 1-in-20 year storm, NE, RCP8.5 2120 SLR, adaptive design SCDF with receded shorelines | -40                                    | 22                                    | -105                                  | -32,462                                   |
| 4-2D      | 1-in-20 year storm, NE, RCP8.5 2140 SLR, adaptive design SCDF with receded shorelines | -44                                    | 31                                    | -141                                  | -36,027                                   |
| 5-2D      | 1-in-20 year storm, SE, RCP4.5 2120 SLR, SCDF with receded shorelines                 | -20                                    | 0                                     | -31                                   | -16,581                                   |
| 6-2D      | 1-in-20 year storm, SE, RCP4.5 2140 SLR, SCDF with receded shorelines                 | -22                                    | 0                                     | -35                                   | -17,864                                   |
| 7-2D      | BfE storm sequence, RCP4.5 2120 SLR, SCDF with receded shorelines                     | -51                                    | 0                                     | -103                                  | -41,256                                   |
| 8-2D      | BfE storm sequence, RCP4.5 2140 SLR, SCDF with receded shorelines                     | -56                                    | 0                                     | -112                                  | -45,638                                   |
| 9-2D      | BfE storm sequence, RCP8.5 2140 SLR, adaptive design SCDF with receded shorelines     | -101                                   | 0                                     | -188                                  | -81,693                                   |

### 3.4.3 Variation due to particle size (gravel modelling)

Using the 1D XBeach-G model setup (as described in Section 2.4), the response of the SCDF and the Adaptive Design to the 1-20-year storm (NE) was investigated with a 10 mm grain size at 2120 and 2140 for RCP4.5 and RCP8.5 sea levels (for the Adaptive Design only). A grain size of 10 mm was chosen for the decommissioning phase model runs as it is the modal grain size of the gravel fraction of the Sizewell beach and results in Section 3.2 showed the SCDF was resilient up to 2099 with that grain size. The update of the HCDF design does not affect the volume calculations for the gravel runs, as the volumes are calculated over a central profile (which is unaffected by the HCDF update) rather than using the polygons as described for the 2D volume calculations. The results of the simulations are summarised in Figure 3-30. Table 3-4 shows the predicted volume change from the SCDF and adaptive design, above 0 m ODN.

The profile change over both RCP4.5 and RCP8.5 XBeach-G simulations shows primarily a cut and fill beach response, as seen in Section 3.2, increasing in magnitude as SLR increases (Figure 3-13), similar to that seen in the 2D simulations. The cut and fill volume was significantly reduced for the pebble particle size ( $D_{50} = 10$  mm), compared to the corresponding 2D sand models. The crest of the SCDF was not predicted to be eroded or lowered under the simulated 1-in-20 year NE storm in any of the simulations, regardless of SCDF design or sea level.

As sea level increases, the volume lost above 0 m ODN during a 1-in-20 year storm is predicted to increase in a relatively linear manner for RCP4.5 between 2069 and 2140. However, for RCP8.5, the effect of sea level rise is more complex: the storm erosion above 0 m ODN is predicted to reduce for 2140 compared to 2120 under the simulated storm. This is because, with higher sea levels, more of the eroded subaerial sediment is deposited above the 0 m ODN contour, and therefore erosion appears to reduce as sea level rises. In reality, the volume of sediment eroded from the subaerial beach (i.e. above *mean sea level*, rather than 0 m ODN) will probably steadily increase with sea level rise. The XBeach-G model predicts that by the end of decommissioning in 2140, erosion above 0 m ODN during a 1-in-20 year storm will range from -13 m<sup>3</sup>/m to -17 m<sup>3</sup>/m for D<sub>50</sub> grain size of 10 mm (Table 3-4), which is significantly less than that predicted by the 2D sand model (Table 3-3).

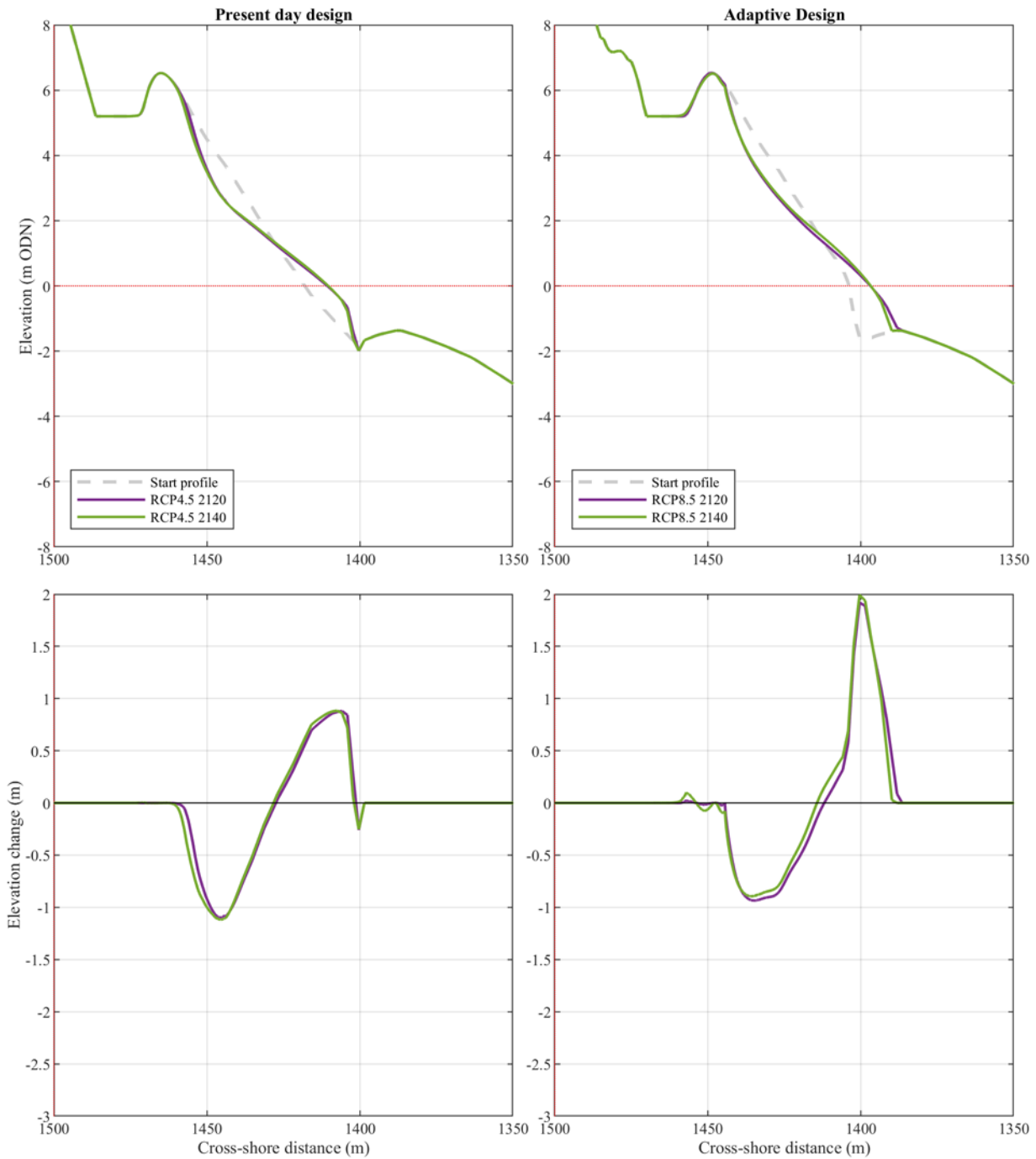


Figure 3-30. North East 1-in-20 year storm, RCP4.5 2120 and 2140 sea levels (left) and RCP8.5 2120 and 2140 sea levels (right) – End of simulation profiles (top panels) and profile changes (bottom panels) for 10 mm grain size. Simulations were run using the XBeach gravel non-hydrostatic formulations.

Table 3-4. Predicted volumetric change (above 0 m ODN) from the SCDF feature for each 1D XBeach-G simulation (to 1<sup>st</sup> significant figure).

| <b>Scen. No.</b> | <b>Description</b>   | <b>Model</b> | <b>Grain size (mm)</b>         | <b>Net volume change (<math>m^3/m</math>)</b> | <b>Max loss during run (<math>m^3/m</math>)</b> |
|------------------|--|--------------|--------------------------------|---|---|
| 1-1D             | 1-in-20 year storm, NE, RCP4.5<br>2120 SLR, SCDF                 | XBeach-G     | $D_{50} = 10$<br>$D_{90} = 15$ | -15   | -15   |
| 2-1D             | 1-in-20 year storm, NE, RCP4.5<br>2140 SLR, SCDF                 | XBeach-G     | $D_{50} = 10$<br>$D_{90} = 15$ | -16   | -16   |
| 3-1D             | 1-in-20 year storm, NE, RCP8.5<br>2120 SLR, adaptive design SCDF | XBeach-G     | $D_{50} = 10$<br>$D_{90} = 15$ | -17   | -17   |
| 4-1D             | 1-in-20 year storm, NE, RCP8.5<br>2140 SLR, adaptive design SCDF | XBeach-G     | $D_{50} = 10$<br>$D_{90} = 15$ | -13   | -13   |

## 4 Discussion

---

### 4.1 Model parameters

---

The 2D XBeach-S parameter settings chosen in this study ultimately represent the settings that best reproduced the response of the mixed sand-gravel beach at Sizewell, despite the calibration being performed using the sand version of XBeach only. Differences in response between a beach comprised entirely of sand and one comprised entirely of gravel at Sizewell are explored in Section 2.1 of this report.

Section 2.3.3 provides a summary of the XBeach parameter settings that were found to best reproduce the observed morphological changes at Sizewell during the calibration and validation storm events. Of most interest are the following parameter choices:

- ▶ A higher than default value for *facua* (wave asymmetry) was required to reproduce the magnitude of beach erosion observed in the calibration and validation events. Lower and higher values resulted in over- and under-prediction of the erosion magnitude, respectively. The requirement for a higher *facua* was expected given the relatively steep slope of Sizewell beach compared to Dutch beaches and is in line with previous findings from the literature for beaches with similar slopes (Elsayed and Oumeraci, 2017). Higher values of *facua* resulted in too much onshore transport of sediment from the nearshore bars.
- ▶ A lower than default value for the *bed friction coefficient* was required in order to reproduce the location and magnitude of the observed beach erosion. Altering the coefficient was found to alter the profile shape and magnitude of beach erosion.
- ▶ A lower than default value of *gamma* (wave breaker criterion) was required in order to reproduce the location and magnitude of the observed beach erosion. Lower and higher values of *gamma* were found to alter the cross-shore location of peak erosion and to a lesser degree the magnitude of erosion; however, the magnitude of erosion was predominantly controlled by *facua*.

### 4.2 General results

---

In all scenarios, both from XBeach-S and XBeach-G, a dominant cut and fill beach response to the modelled storm conditions is predicted, with sediment losses on the subaerial SCDF beach face and gains on the subtidal beach. However, this response does not represent a loss of sediment to the system. Intervening mild conditions, i.e., less energetic non-storm conditions (which are not modelled in this study) are expected to return most, if not all, of the sediment deposited on the subtidal part of the profile to the subaerial beach face. However, XBeach is a storm erosion model and as it does not accurately simulate the beach recovery process, the model was not run for the longer, post-storm, beach recovery period.

The model results show that the SCDF is successfully withstanding each storm event modelled, with the HCDF not exposed under any scenario. The BfE storm sequence only shows a small amount of SCDF crest lowering for the RCP4.5 SLR 2120 and 2140 and slightly more lowering for the Adaptive Design under the 1:20 year NE storms (RCP8.5 SLR) but crest elevations do not fall below 5.8 m ODN. However, for the Adaptive Design under the BfE (RCP8.5 SLR) the SCDF crest is eroded back to the edge of the coastal path, at approximately 5.2 m ODN.

Even in the most affected areas of the SCDF, the volume eroded by the simulated storms is always less than the available beach volume. Under the worst-modelled storm scenario during the operational phase, the most affected parts of the SCDF still had greater than 120 m<sup>3</sup>/m of sediment on the subaerial beach face (74% of initial beach volume) following the storm, and on other parts of the SCDF a considerably larger proportion of subaerial volume remained (Section 3.1.3). The worst-modelled storm for 2140 at the end of the decommissioning phase, had 37 m<sup>3</sup>/m of sediment on the subaerial beach (18%), and on other parts of the SCDF a considerably larger proportion of subaerial volume remained (100-160 m<sup>3</sup>/m (Section 3.4.2). This is a conservative result as it is based on the XBeach-S (sand, modelled as D<sub>50</sub> = 0.8 mm) 2D model, which cannot take account of the much coarser pebbly sediment (modelled as D<sub>50</sub> = 10 mm) that dominates the beach shingle and is more resistant to erosion.



### 4.3 Sensitivity (wrt erosion)

#### 4.3.1 Wave obliquity

Three primary wave directions have been explored in this study, using oblique storm events from the northeast and southeast (1-in-20 year events) and a shore normal storm sequence from the east (1-in-107 year return period in terms of cumulative wave power, 'Beast from the East'). While the events are not directly comparable due to differences in the magnitude of wave height, period, degree of wave obliquity and storm duration, the following can be observed regarding the effect of wave obliquity on the erosion of the SCDF from the model simulations:

- ▶ Wave obliquity increased the strength of alongshore oriented currents and alongshore sediment flux (Appendix E) along the frontage of the SCDF.
- ▶ Wave obliquity altered the pattern of sediment erosion along the SCDF frontage to some degree.
- ▶ Under the shore-normal wave approach in the BfE event, the greatest erosion of the SCDF occurred along the northern half of the SCDF frontage. It is not completely clear why this is the case, but it is hypothesised that the orientation and geometry of the subtidal sandbars, which curve naturally toward the coast along the northern half of the SCDF, allows marginally more wave energy to reach the shore there under shore-normal waves.

#### 4.3.2 Particle size

The scenarios modelled in the 1D grain size sensitivity tests indicate that using a larger particle size for the SCDF will increase its resilience to storm wave erosion. Using very coarse sand/fine pebbles ( $D_{50} = 2$  mm; which is finer than the native particle size mode) resulted in 3-6 times less volumetric erosion of the SCDF (above 0 m ODN) than coarse sand ( $D_{50} = 0.8$  mm), while medium pebbles ( $D_{50} = 10$  mm; the modal particle size) resulted in 3-9 times less SCDF erosion, and very coarse pebbles ( $D_{50} = 40$  mm) resulted in 3-12 times less SCDF erosion. With fine cobbles ( $D_{50} = 80$  mm) 18-35 times less erosion of the SCDF was predicted than with coarse sand. For example, the storm erosion demand on the SCDF during the modelled 1-in-20 year NE storm (2099 sea level), was  $-37$  m<sup>3</sup>/m with the coarse sand ( $D_{50} = 0.8$  mm),  $-14$  m<sup>3</sup>/m with very coarse sand/fine pebbles ( $D_{50} = 2$  mm),  $-14$  m<sup>3</sup>/m with modal medium pebbles ( $D_{50} = 10$  mm),  $-12$  m<sup>3</sup>/m with very coarse pebbles ( $D_{50} = 40$  mm), and  $-2$  m<sup>3</sup>/m with fine cobbles ( $D_{50} = 80$  mm). These results indicate that the optional internal layer of fine cobbles within the SCDF, if exposed, would have very different behaviour and sustain comparably very low erosion rates, even at 2099 sea level, than a coarse sand or pebble beach under an equivalent storm.

While erosion is noticeably reduced at 2069 sea levels for the medium pebbles ( $D_{50} = 10$  mm) compared to the very coarse sand/fine pebbles (Figure 3-15), it is notable that the coarse end of the naturally occurring grain size spectrum ( $D_{50} = 40$  mm) has surprisingly little performance improvement. The medium pebbles were predicted to have at most a 2 m<sup>3</sup>/m difference in eroded volumes compared to the very coarse pebbles ( $D_{50} = 40$  mm) for the tested storm scenario at three different sea levels (present day, 2069 and 2099). This is surprising given that the coarse pebbles tested are four times larger than the medium pebbles and would therefore be expected to be considerably less mobile. However, more detailed calibration of the model against field data or, ideally, full scale physical modelling would be needed to better understand the potential benefit of increasing SCDF particle size within the coarse end of the naturally occurring grain size spectrum (i.e. between  $D_{50} = 10$  mm and 40 mm).

Coarse sand ( $D_{50} = 0.8$  mm) was simulated in the 2D XBeach-S simulations; however, the SCDF would be constructed with much larger particles ( $D_{50} = 10$  mm), keeping its sediment in line with the native particle size distribution. Therefore, it is very likely that the volumetric losses from the 2D model runs (Table D-2) are highly conservative estimates of the erosion demand that the SCDF will experience, and the 1D XBeach-G simulations indicate that erosion volumes are likely to be at least 3 times lower based on the likely SCDF particle size matching to the native size distribution. The modelling of cobbles indicates that if a fine cobble layer were used and temporarily exposed (before recharge with shingle), its erosion to modelled conditions would be an order of magnitude lower. Further tests with the medium pebbles ( $D_{50} = 10$  mm) were run up to the end of decommissioning (2140) which showed the SCDF was still resilient to storm wave erosion, with no crest lowering predicted to occur. Erosion of the present day SCDF under RCP4.5 SLR, with a  $D_{50} =$

10 mm, is predicted to increase from -14 m<sup>3</sup>/m in 2099 to -16 m<sup>3</sup>/m in 2140. Under the larger RCP8.5 2140 SLR, for the Adaptive Design, the net volume eroded was 17 m<sup>3</sup>/m.

The increased runup height and decreased erosion predicted in the D<sub>50</sub> = 2-80 mm XBeach-G simulations compared to the D<sub>50</sub> = 0.8-2 mm XBeach-S simulations illustrates the importance of considering processes relevant to steeper beaches with coarse grains. Primarily, the computation of the full short wave timeseries in XBeach-G results in wave runup heights that reached much higher than in XBeach-S, where only the infragravity signal is considered (Table D-2). This reflects previous findings in the literature that show that wave runup elevations on steeper beaches, often composed of gravel, can far exceed wave runup on shallow sloping sandy beaches (Poate *et al.*, 2016). However, because of the lower mobility of coarse particles, as well as increased infiltration and exfiltration of water, erosion rates and wave runup heights for larger particles are predicted to be lower than that of coarse sand or fine pebbles. Therefore, increasing particle size plays an important role in reducing both erosion demand and wave runup, meaning that far more effective coastal protection can be provided by the SCDF if it is composed of coarser pebbles or if it includes a fine cobble layer, compared to sand. The default position for SCDF particle size is to match the native size distribution, which has a model pebble size of approximately 10 mm diameter.

#### **4.4 Effect of sea level rise on SCDF erosion**

With sea level rise, the erosion demand on the SCDF is predicted (and expected) to increase (Figure 3-11 and Figure 3-15). The predicted increases in erosion with increasing sea level results from larger waves acting higher on the shore of the SCDF due to a greater depth of water near the coast (for example, Figure 4-1). It should be noted that the uplift in wave height is purely a result of higher sea level and does not account for any future increases or decreases in wave height caused by potential modified storminess, which is not considered in this study.

From the XBeach-S simulations, the average erosion along the frontage of the SCDF, during the operational and decommissioning phase, under a 1-in-20 year storm event is predicted to increase from -18 m<sup>3</sup>/m in 2021, to -20 m<sup>3</sup>/m by 2069 (11% more erosion than present sea level), to -22 m<sup>3</sup>/m by 2099 (22% more erosion than present sea level), to -26 m<sup>3</sup>/m by 2120 (44% more erosion than present sea level) and then to -27 m<sup>3</sup>/m by 2140 (50% more erosion than present day) under a north east 1-in-20 year storm. For a south east 1-in-20 year storm, similar increases in erosion demand are expected; from -12 m<sup>3</sup>/m in 2021, to -15 m<sup>3</sup>/m by 2069 (25% more erosion than present sea level), to -18 m<sup>3</sup>/m by 2099 (50% more erosion than present sea level), to -20 m<sup>3</sup>/m by 2120 (66% more erosion than present sea level) and then to -22 m<sup>3</sup>/m by 2140 (83 % more erosion than present day).

Under an extreme sequence of shore normal (easterly) storms, here characterised by the BfE storm sequence, the erosion demand is predicted to increase more dramatically as sea levels rise. The erosion demand from the BfE sequence is predicted to increase from -16m<sup>3</sup>/m in 2021, to -22 m<sup>3</sup>/m by 2069 (38% more erosion than present sea level), to -27 m<sup>3</sup>/m by 2099 (69% more erosion than present sea level) to -51 m<sup>3</sup>/m by 2120 (319% more erosion than present sea level) and then to -56 m<sup>3</sup>/m by 2140 (350% more erosion than present day). However, despite the larger erosion demand at higher sea levels, the SCDF is predicted to retain a minimum of 74% of initial beach volume (above 0 m ODN) after the 1:107 year (in terms of cumulative wave power) storm sequence (Figure 3-12). These results were predicted using the calibrated XBeach-S model and are considered conservative given the calibration results (Section 2.3.3) and likelihood of coarser particles being used to construct the SCDF. These values also do not consider the effect of coastal retreat occurring either side of the SCDF, which is explored further in Section 4.5.

The exact geometry of the future shoreline and potential for breaching along the natural shingle ridge north of SZC are currently unknown. While the present modelling study is not expected to predict precisely if or when breaches may occur, the simulations do suggest that breaching north of the SZC is increasingly likely at sea levels approaching the modelled 2099 sea level. However, the simulations also suggest that sediment from the SCDF will feed the shorelines north and south of the SCDF, and as erosion of the SCDF is predicted to increase with SLR, it is also probable that the additional supply of sediment introduced by the SCDF to the wider beach will increase. The SCDF is therefore expected to act as a source of sediment available to reinforce both the SCDF frontage and the adjacent natural beaches.

From the XBeach-G grain size sensitivity tests, the effect of sea level rise on an SCDF constructed with coarse particles is perhaps more complex than the XBeach-S simulations suggest. As sea level increases, the location of erosion on the gravel beaches was seen to move up the beach profile, resulting in sediment eroded from the subaerial beach being deposited on the intertidal beach, above 0 m ODN. Therefore, the erosion of sediment above 0 m ODN (the metric specified for this study) appears to remain the same, or even reduce, between 2021 and 2069 under the simulated storm. In reality, the volume of sediment eroded from the subaerial beach (i.e. above *mean sea level*, rather than 0 m ODN) will probably steadily increase with sea level rise. By 2099, erosion above 0 m ODN is predicted to have increased for all grain sizes tested, due to the diminishing ability of the subtidal bars and beach face (which, conservatively, do not adjust with SLR in this model) to dissipate wave energy through bed friction and breaking. The XBeach-G model predicts that by 2099, erosion above 0 m ODN during a 1-in-20 year storm will range from -14 m<sup>3</sup>/m to -2 m<sup>3</sup>/m for D<sub>50</sub> grain sizes of 2-80 mm, with the modal grain size (D<sub>50</sub> = 10 mm) sitting at the lower end of this range (-14 m<sup>3</sup>/m). Furthermore, XBeach-G model predicts that by 2140, erosion above 0 m ODN during a 1-in-20 year storm will range from -16 m<sup>3</sup>/m to -13 m<sup>3</sup>/m for RCP4.5 and RCP8.5 respectively, with the modal grain size (D<sub>50</sub> = 10 mm).

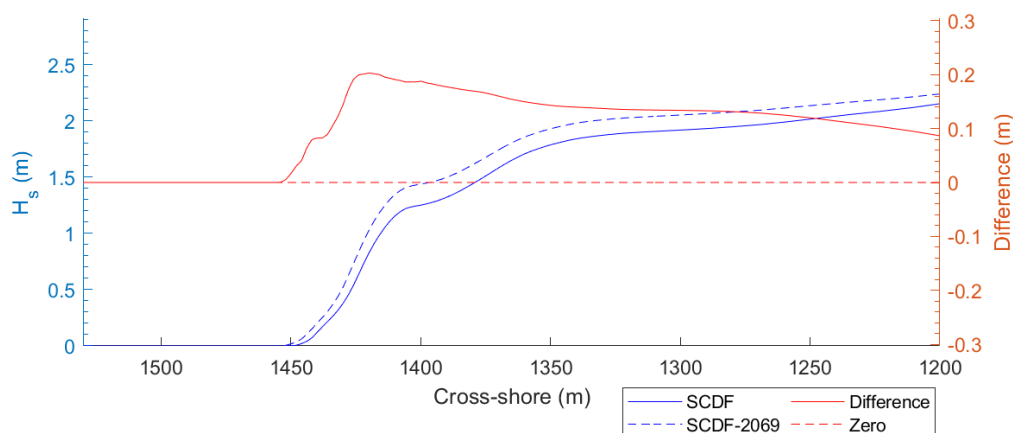


Figure 4-1. Example increase in significant wave height, averaged along the frontage of the SCDF, between 2021 and 2069 for a south-easterly 1-in-20 year storm event. It should be noted that this uplift in wave height is purely a result of higher sea level.

#### 4.5 Effect of laterally eroded shorelines on SCDF erosion

Under the 1-in-20 year storm events from the SE and NE, the effect of the receded shoreline on the majority of the SCDF frontage is minimal. Along the present-day SCDF frontage, the predicted cut and fill response to the storms results in bed level changes on the order of 1 m, while the receded shoreline causes bed levels along the SCDF frontage to deviate on average by around 10-20 cm from this. The effect of adjacent receded shorelines does, however, have a larger effect on the lateral ends of the SCDF than in the centre of the SCDF. The receded shorelines cause little difference in the predicted SCDF volumetric loss for the 1-in-20 year storm events. For example, the total losses along the frontage for the SE and NE event (2099 sea level) with the present-day shoreline position are -14,196 m<sup>3</sup> and -17,888 m<sup>3</sup>, respectively, while the same events run with a receded shoreline result in total SCDF losses of -14,481 m<sup>3</sup> and -19,697 m<sup>3</sup>.

During the more extreme BfE sequence, the effect of the receded shoreline on the SCDF frontage is more pronounced. The receded shoreline adjacent to the SCDF appears to increase the volumetric erosion demand on the SCDF by at least 1.5 times for the BfE event. The total volume loss along the SCDF frontage (2099 sea level) with the present-day shoreline position is -22,130 m<sup>3</sup>, while the same event run with a receded shoreline results in a loss in volume of -34,927 m<sup>3</sup>. When the SLR is extended to the end of the decommissioning phase (2140) the total volumetric loss with the receded shoreline is -45,638 m<sup>3</sup> with RCP4.5 and -81,693 m<sup>3</sup> with RCP8.5.

In all simulations with a receded future shoreline, enhanced storm erosion is predicted to occur at the northern and southern tips of the SCDF frontage as a result of the receded shoreline. Wave and current plots in Appendix E indicate that this is associated with localised wave focussing at the lateral tips of the SCDF frontage where the changes in shoreline orientation occur, as well as gradients in longshore sediment transport associated with changes in the orientation of the shoreline. This suggests that any future recharge of the SCDF may require greater volumes of sediment, or more frequent interventions, at each end of the SCDF if the adjacent shoreline becomes highly receded (i.e., as modelled). The simulations indicate that this extra eroded sediment would contribute to accretion north and south of the SCDF to some degree, but to properly quantify the magnitude of this effect and its contribution to long-term shoreline evolution, adjacent to the SCDF, would require longshore transport modelling over multi-annual timescales.

## **4.6 SCDF design parameters recommendations**

---

### **4.6.1 SCDF volumes**

Volume losses to the SCDF are expected during storms, and observed within the results, showing the need for beach recharge in order to maintain the SCDF into the future. Due to the XBeach-S model being calibrated and run with sand rather than gravel, all results relating to erosion volumes are likely to be highly conservative, and therefore an over-prediction of what is expected to occur in reality. With this in mind, the volume of the proposed SCDF is considered to be sufficient to withstand storm events of the magnitude of those modelled in this study, especially given that the 2D XBeach-S model over-predicted erosion volume by at least 2-3 times in the calibration and validation tests. Furthermore, volumetric losses are predicted to be up to an order of magnitude less for coarser particles, with medium pebbles ( $D_{50} = 10$  mm) resulting in 3-9 times less SCDF erosion, very coarse pebbles ( $D_{50} = 40$  mm) resulting in 3-12 times less SCDF erosion, and fine cobbles ( $D_{50} = 80$  mm) resulting in 18-35 times less erosion of the SCDF, compared to the coarse sand used in the 2D simulations.

The lateral ends of the SCDF are predicted to incur the greatest erosional losses during the simulated storms with future eroded shorelines, and the northern half of the SCDF is predicted to erode more readily than the southern half of the SCDF during the shore-normal BfE event. With this in mind, future recharge of the SCDF may require greater or more frequent volumes of sediment to be replenished at each end of the SCDF as the adjacent shoreline recedes with sea level rise, as well as along the northern half of the SCDF following shore-normal storm events.

### **4.6.2 SCDF crest height and overtopping**

While overtopping rates have not been specifically investigated in this study, the wave runup heights from the modelled storms indicate that the proposed SCDF feature is resistant to overtopping for nearly all of the cases investigated. However, under the NE 1-in-20 year storm tested, the highest swashes are predicted to reach the crest elevation of the SCDF by the XBeach-G model from 2099 onwards. The overtopping of the SCDF feature under this event is, however, only predicted to occur when the SCDF is composed of very coarse sand/fine pebbles, and for larger particle sizes maximum runup heights did not reach the SCDF crest height.

Under this same event, the 2D XBeach-S model identified that wave runup is also likely to reach the crest height of the natural shingle ridge to the north of SZC (predicted at position  $Y_1$ , for example) and that the natural shingle ridge immediately to the north of SZC (at position  $Y_{breach}$ ) is vulnerable to breaching under this event. The breaching north of SZC is predicted to occur with or without the SCDF in place, and hence is not caused by the SCDF. As the natural shingle ridge north of SZC is not solely composed of coarse sand (as assumed by the 2D model) and features coarser particles across the profile, especially on the supratidal beach, further assessment of runup and likelihood of breaching there is needed to better understand the likelihood (and degree) of breaching. This is because the effects of infiltration (acting to reduce runup) and incident wave swash (acting to increase runup), which are important at steep beaches with coarse particles, are not considered by the XBeach-S model. Such an assessment could, for example, employ a similar approach as that applied here to the SCDF runup heights at position  $Y_2$ , by using a 1D XBeach-G model with varying particle sizes at the most vulnerable alongshore location north of SZC (at  $Y_{breach}$ , for example) to more confidently predict the range of probable runup heights and likelihood of breaching.

While the SCDF is predicted to be resilient to erosion under the modelled storm events, overtopping may occur with finer particles ( $D_{50} \leq 2$  mm). However, fine size grain sizes will not be used to construct the SCDF, the default position for SCDF particle size is to match the native size distribution, which has a modal pebble size of approximately 10 mm diameter. It is recommended that further wave overtopping analysis is undertaken for the SCDF design, including a range of combined wave events and water levels (e.g. at least 1-in-50 year and 1-in-100 year return periods), either using a 1D XBeach-G model (phase-resolving) or using empirical wave runup formulae from the literature appropriate to gravel beach settings (Poate *et al.*, 2016). Such assessment may, for example, identify that a higher SCDF crest height is required to ensure resilience of the SCDF crest to overtopping/overwashing under extreme combinations of waves and water levels. Likewise, it would also give further confidence to assess future sea levels that are likely to increase overtopping – such information could inform the Coastal Processes Monitoring and Mitigation Plan (BEEMS Technical Report TR523). For example, further model runs of the Adaptive Design under RCP8.5 SLR conditions during the decommissioning phase showed lowering of the SCDF crest elevation, albeit it was still higher than the crest elevation of the coastal path behind it.

#### **4.6.3 Particle size recommendations**

Particle size is a very important consideration in the design of the SCDF. Not only has the model demonstrated that the reduced mobility of larger particles (pebbles, and especially fine cobbles) resists storm erosion far more effectively than coarse sand, it has also shown that large particles reduce wave runup elevation by increasing infiltration and exfiltration of water from the beach face.

While erosion is noticeably reduced by using modal medium pebbles ( $D_{50} = 10$  mm) rather than coarse sand ( $D_{50} = 0.8$  mm), it is notable that the model suggests relatively modest benefits by coarsening the SCDF to  $D_{50} = 40$  mm, which is within the native particle size distribution. Although these grain sizes were only predicted to have 2 m<sup>3</sup>/m difference in eroded volume or less (1:20 year storm scenario at three different sea levels), it does appear that performance improves as sea level and erosion pressure rises. As this is preliminary modelling of only one storm scenario (1:20 year NE storm), and as the XBeach-G model was only semi-calibrated by aligning tuning parameters as closely as possible with settings from the literature, it is recommended that if a decision is to be made regarding the use of these particular grain sizes, that further numerical modelling or, ideally, full scale physical modelling is undertaken to provide a better understanding of the potential benefit of increasing SCDF particle size within the coarse end of the naturally occurring grain size spectrum (i.e. between  $D_{50} = 10$  mm and 40 mm).

The exceptional resistance to storm erosion and runup predicted for the fine cobbles ( $D_{50} = 80$  mm) has also recently been reported from a laboratory scale physical modelling study where a cobble berm feature was tested under storm wave conditions (Bayle *et al.*, 2020). While the cobbles in the laboratory study were found to be dynamic, and exchanged readily from the front to the back of the feature being tested, the net change in the cobble berm volume was minimal and it maintained a consistent global shape. The study also found that using cobbles allowed roll over and adjustment to sea level rise as the cobble berm moved upward and landward under water level rise.

The benefits of coarsening within the native size distribution and the utility of a buried layer of fine cobbles have been demonstrated with respect to SCDF resilience and reducing the risks of exposing the HCDF. It is recommended to retain the native particle sizes ( $D_{50} = 10$  mm) or coarsening the sediments as these options produce a viable SCDF across the life of the station and reduce risks of HCDF exposure. The benefit of retaining the native sizes is retention of natural processes as much as possible, and it is understood that this is the preferred option of many Interested Parties as it reduces uncertainty.



## 5 Conclusions

The present modelling study aimed to investigate the response of the proposed SCDF under storm wave conditions for five sea level scenarios across the operation (2021, 2069, 2099) and decommissioning phases (2120 and 2140) and included a case with severely receded shorelines adjacent to Sizewell C's maintained frontage that increases erosion pressure on the SCDF. The decommissioning phase models were also run for the more extreme RCP8.5 SLR scenario with the Adaptive Design which would only be required under such high sea levels. From the simulations the following conclusions can be drawn:

- ▶ The calibrated 2D XBeach-S model reproduces the location and cross-shore extents of measured storm erosion at Sizewell, and importantly, provides conservative estimates of the magnitude of storm erosion.
- ▶ Running additional 1D simulations in XBeach-G is important in this study because not only is the erosional behaviour of pebbles/cobbles different to that of sand, but XBeach-G also provides more accurate predictions of wave runup height at steep beaches such as that of the designed SCDF.
- ▶ The SCDF is predicted to have a minimal influence (order of 10s of cm) on wave heights for all storm scenarios modelled. The influence on average current velocities, bed shear stress and sediment flux show no clear trends, with the SCDF inducing spatially variable and low magnitude responses in the flows.
- ▶ Areas of erosion and accretion from the simulated storms are predicted to occur in similar locations for the Baseline, SCDF and Adaptive Design cases. In all scenarios, a dominant cut and fill beach response is predicted with sediment losses on the subaerial beach face and gains on the subtidal beach face. Most of the sediment deposited on the subtidal part of the profile is expected to return to the subaerial beach face during intervening mild conditions (which is not simulated in this study).
- ▶ The volume of the proposed SCDF is predicted to be sufficient to withstand storm events of the magnitude of those modelled in this study, especially given that the 2D XBeach-S model over-predicted erosion volume by at least 2-3 times in the calibration and validation tests. Furthermore, volumetric losses are predicted to be up to an order of magnitude less for coarser particles, with medium pebbles ( $D_{50} = 10$  mm) resulting in 3-9 times less SCDF erosion, very coarse pebbles ( $D_{50} = 40$  mm) resulting in 3-12 times less SCDF erosion, and fine cobbles ( $D_{50} = 80$  mm) resulting in 18-35 times less erosion of the SCDF, compared to the coarse sand used in the XBeach-S model.
- ▶ With sea level rise, the erosion demand on the SCDF is predicted to increase. Under the most extreme storm sequence modelled, up to 65% more erosion was predicted at 2099 sea level than at present sea level, and up to 158% more SCDF erosion was predicted with future eroded shorelines adjacent to the SCDF at 2099. Under 2140 SLR up to 242% more SCDF erosion was predicted with future eroded shorelines. However, these figures are highly conservative as the simulations with coarse particles suggest that erosion demand will not increase as dramatically with SLR if medium or very coarse pebbles, and especially cobbles, are used for the SCDF rather than coarse sand.
- ▶ The lateral ends of the SCDF are predicted to incur the greatest erosional losses during the simulated storms, and the northern half of the SCDF is predicted to be more vulnerable to storm erosion than the southern half during the shore-normal BfE storm sequence modelled. With this in mind, future recharge of the SCDF may require more frequent localised interventions at each end of the SCDF if the adjacent shoreline becomes severely receded several decades or more into the future and with the degree of sea level rise modelled in this report. The degree of recession of adjacent shorelines modelled is not expected during the operation phase – see Section 7.7 of Volume 2, Appendix 20A of the Sizewell C Environmental Statement NNB Generation Company (SZC) Limited (2020) for details of the receded shoreline modelled.
- ▶ The wave runup heights from the modelled storms indicate that the proposed SCDF feature is resistant to overtopping for nearly all of the cases investigated. However, under a 1-in-20 year storm from the NE with storm surge, the highest swashes were predicted to reach the SCDF crest with SLR from 2099 to 2140. Along the natural beach to the north of the SCDF, overtopping and potential breaching of the natural beach crest is predicted to occur under these storm conditions (which also occurred without the presence of the SCDF).



- ▶ The degree of wave runup and risk of SCDF overtopping reduces as particle size is increased. For particles of  $D_{50} = 10$  mm or greater, overtopping of the SCDF is not predicted to occur under the simulated 1:20 year storm event. It is recommended, however, that further wave overtopping analysis is undertaken in order to identify any combinations of extreme waves and water levels that would lead to SCDF overtopping, as only one event has been modelled for each grain size. More particle sizes could also be assessed (for example, ranging between  $D_{50} = 10$ -80 mm) in order to identify the optimal grain size in terms of cost-benefit ratio for overtopping and erosion protection.
- ▶ During the decommissioning phase, the SCDF under RCP4.5 conditions showed a similar response as to that at the end of the operational phase. Erosion of the SCDF crest is predicted to occur during the BfE storm with RCP4.5 SLR during both 2120 and 2140 sea levels using the XBeach2D sand model, but not the 1:20 year NE or SE storms. During the 2140 SLR, the crest height was reduced to approximately 5.8 m ODN, but still remained higher than the elevation of the coastal path behind the SCDF crest. However, tests of the SCDF in XBeach-G using medium pebbles ( $D_{50} = 10$  mm) showed no crest lowering up to 2140 under RCP4.5 with the 1:20 year NE storm.
- ▶ Under RCP8.5 conditions, erosion of the SCDF crest in front of the Adaptive Design is predicted to occur during both modelled storm events at 2120 and 2140 sea level with the 1:20 year NE storm using the XBeach 2D sand model. During the 2140 SLR, the crest height was reduced to approximately 6 m ODN, but remained higher than the elevation of the coastal path behind the SCDF crest. However, tests of the Adaptive Design in XBeach-G using medium pebbles ( $D_{50} = 10$  mm) showed no crest lowering up to 2140 under RCP8.5 with the 1:20 year NE storm. For the BfE storm with RCP8.5, the SCDF crest in front of the Adaptive Design is predicted to erode back to the edge of the coastal path, at approximately 5.2 m ODN. The smallest remaining beach volume was to the north with 38 m<sup>3</sup>/m (18% of initial beach volume) but on average 54% of the pre-storm subaerial SCDF beach volume remains.
- ▶ The simulations predicted relatively minor and patchy differences in the beach morphology north and south of the SCDF, caused by the presence of the SCDF. With the receded shoreline, sediment eroded from the SCDF was predicted to feed the beach areas immediately north and south of the SCDF, but further modelling of multi-decadal longshore transport and shoreline change would be required to better understand the cumulative influence of the SCDF on the adjacent shorelines.
- ▶ Particle size is a very important consideration in the design of the SCDF. Using very coarse sand/fine pebbles ( $D_{50} = 2$  mm) resulted in 3-6 times less volumetric erosion of the SCDF (above 0 m ODN) than coarse sand ( $D_{50} = 0.8$  mm), while medium pebbles ( $D_{50} = 10$  mm) resulted in 3-9 times less SCDF erosion, and very coarse pebbles ( $D_{50} = 40$  mm) resulted in 3-12 times less SCDF erosion. With fine cobbles ( $D_{50} = 80$  mm) 18-35 times less erosion of the SCDF was predicted than with coarse sand. For example, the storm erosion demand on the SCDF during the modelled 1-in-20 year NE storm (2099 sea level), was -37 m<sup>3</sup>/m with the coarse sand ( $D_{50} = 0.8$  mm), -14 m<sup>3</sup>/m with very coarse sand/fine pebbles ( $D_{50} = 2$  mm), -14 m<sup>3</sup>/m with medium pebbles ( $D_{50} = 10$  mm), -12 m<sup>3</sup>/m with very coarse pebbles ( $D_{50} = 40$  mm), and -2 m<sup>3</sup>/m with cobbles ( $D_{50} = 80$  mm).
- ▶ Not only has the modelling demonstrated that the reduced mobility of pebbles (and fine cobbles, were a cobble layer to be used and exposed) resists storm erosion far more effectively than coarse sand, it has also shown that large particles reduce wave runup elevation by increasing infiltration and exfiltration of water from the beach face. Large particles therefore provide multiple benefits to the long-term resilience of the SCDF, but further numerical modelling or, ideally, full scale physical modelling is recommended to provide a better understanding of the potential benefit of increasing SCDF particle size within the coarse end of the naturally occurring grain size spectrum. Physical modelling in full-scale facilities such as that conducted by Bayle et al. (2020) is recommended to avoid scaling issues.

## 6 References

---

- Almeida, L. P., Masselink, G., Russell, P. E. and Davidson, M. A. 2015. Observations of gravel beach dynamics during high energy wave conditions using a laser scanner. *Geomorphology*, **228**, 15-27.
- Bayle, P. M., Blenkinsopp, C. E., Conley, D., Masselink, G., Beuzen, T. and Almar, R. 2020. Performance of a dynamic cobble berm revetment for coastal protection, under increasing water level. *Coastal Engineering*, **159**, 103712.
- BEEMS Technical Report TR523. *Sizewell C Coastal Processes Monitoring and Mitigation Plan*. Cefas, Lowestoft.
- BEEMS Technical Report TR531. *Storm Response Modelling – Preliminary evidence toward setting volumetric thresholds for SCDF recharge*. Cefas, Lowestoft.
- BEEMS Technical Report TR543. *Modelling of the Temporary and Permanent Beach Landing Facilities at Sizewell C*. Cefas, Lowestoft.
- BEEMS Technical Report TR544. *Preliminary design and maintenance requirements for the Sizewell C Soft Coastal Defence Feature*. Cefas, Lowestoft.
- Blair, T. C. and McPherson, J. G. 1999. Grain-size and textural classification of coarse sedimentary particles. *Journal of Sedimentary Research*, **69**, (1), 6-19.
- Bolle, A., Mercelis, P., Roelvink, D., Haerens, P. and Trouw, K. 2011. Application and validation of XBeach for three different field sites. *Coastal Engineering Proceedings*, **1**, 40.
- Brooks, S. M. and Spencer, T. 2012. Shoreline retreat and sediment release in response to accelerating sea level rise: Measuring and modelling cliffline dynamics on the Suffolk Coast, UK. *Global and Planetary Change*, **80-81**, 166-179.
- Bruun, P. 1954. *Coast erosion and the development of beach profiles*. US Beach Erosion Board.
- Courant, R., Friedrichs, K. and Lewy, H. 1928. Über die partiellen Differenzengleichungen der mathematischen Physik. *Mathematische annalen*, **100**, (1), 32-74.
- Daly, C., Roelvink, D., van Dongeren, A., de Vries, J. v. T. and McCall, R. 2012. Validation of an advective-deterministic approach to short wave breaking in a surf-beat model. *Coastal Engineering*, **60**, 69-83.
- Elsayed, S. M. and Oumeraci, H. 2017. Effect of beach slope and grain-stabilization on coastal sediment transport: An attempt to overcome the erosion overestimation by XBeach. *Coastal Engineering*, **121**, 179-196.

Kinsela, M. A., Morris, B. D., Linklater, M. and Hanslow, D. J. 2017. Second-pass assessment of potential exposure to shoreline change in New South Wales, Australia, using a sediment compartments framework. *Journal of Marine Science and Engineering*, **5**, (4), 61.

Lindemer, C. A., Plant, N. G., Puleo, J. A., Thompson, D. M. and Wamsley, T. V. 2010. Numerical simulation of a low-lying barrier island's morphological response to Hurricane Katrina. *Coastal Engineering*, **57**, (11-12), 985-995.

Longuet-Higgins, M. S. and Stewart, R. W. 1962. Radiation stress and mass transport in gravity waves, with application to 'surf beats'. *Journal of Fluid Mechanics*, **13**, 481-504.

Longuet-Higgins, M. S. and Stewart, R. W. 1964. Radiation stresses in water waves; a physical discussion, with applications. Deep Sea Research and Oceanographic Abstracts. Elsevier.

Lowe, J. A., Bernie, D., Bett, P.E., Brichenno, L., Brown, S., Calvert, D., Clark, R.T., Eagle, K.E., Edwards, T., Fosser, G., Fung, F., Gohar, L., Good, P., Gregory, J., Harris, G.R., Howard, T., Kaye, N., Kendon, E.J., Krijnen, J., Maisey, P., McDonald, R.E., McInnes, R.N., McSweeney, C.F., Mitchell, J.F.B., Murphy, J.M., Palmer, M., Roberts, C., Rostron, J.W., Sexton, D.M.H., Thornton, H.E., Tinker, J., Tucker, S., Yamazaki, K., and Belcher, S. 2018. *UKCP18 Science Overview report*. Met Office, Exeter.

Masselink, G., McCall, R., Poate, T. and van Geer, P. 2014. Modelling storm response on gravel beaches using XBeach-G. *Proceedings of the ICE-Maritime Engineering*,

McCall, R. T. 2015. *Process-based modelling of storm impacts on gravel coasts*. University of Plymouth, UK.

McCall, R. T., De Vries, J. S. M. V. T., Plant, N. G., Van Dongeren, A. R., Roelvink, J. A., Thompson, D. M. and Reniers, A. 2010. Two-dimensional time dependent hurricane overwash and erosion modeling at Santa Rosa Island. *Coastal Engineering*, **57**, 668-683.

McCall, R. T., Masselink, G., Poate, T. G., Roelvink, J. A. and Almeida, L. P. 2015. Modelling the morphodynamics of gravel beaches during storms with XBeach-G. *Coastal Engineering*, **103**, 52-66.

McCall, R. T., Masselink, G., Poate, T. G., Roelvink, J. A., Almeida, L. P., Davidson, M. and Russell, P. E. 2014. Modelling storm hydrodynamics on gravel beaches with XBeach-G. *Coastal Engineering*, **91**, 231-250.

McCarroll, R. J., Castelle, B., Brander, R. W. and Scott, T. 2015. Modelling rip current flow and bather escape strategies across a transverse bar and rip channel morphology. *Geomorphology*, **246**, 502-518.

McCarroll, R. J., Masselink, G., Valiente, N. G., Scott, T., Wiggins, M., Kirby, J.-A. and Davidson, M. 2021. A rules-based shoreface translation and sediment budgeting tool for estimating coastal change: ShoreTrans. *Marine Geology*, **435**, 106466.

McMillan, A., Batstone, C., Worth, D., Tawn, J., Horsburgh, K. and Lawless, M. 2011. *Coastal flood boundary conditions for UK mainland and islands. Design sea levels*. Environment Agency and Defra, February 2011. ISBN SC060064/TR2: Design sea levels

Nairn, R. B., Roelvink, J. A. and Southgate, H. N. 1991. Transition zone width and implications for modelling surfzone hydrodynamics. *Coastal Engineering* 1990. 68-81.

Nederhoff, C. M., Lodder, Q. J., Boers, M., Den Bieman, J. P. and Miller, J. K. 2015. Modeling the effects of hard structures on dune erosion and overwash: A case study of the impact of Hurricane Sandy on the New Jersey coast. In: *The Proceedings of the Coastal Sediments 2015*. World Scientific.

NNB Generation Company (SZC) Limited 2020. Sizewell Coastal Geomorphology and Hydrodynamics: Synthesis for Environmental Impact Assessment (MSR1 – Edition 4).

NNB Generation Company (SZC) Limited 2021a. *Environmental Statement Addendum, Volume 1, Chapter 2 Main Development Site*.

NNB Generation Company (SZC) Limited 2021b. *Sizewell C Coastal Defences Design Report*.

Pender, D. and Karunaratna, H., 2013. A statistical-process based approach for modelling beach profile variability. *Coastal Engineering*, 81, pp.19-29.

Phillips, O. M. 1977. The dynamics of the upper ocean.

Poate, T., McCall, R. and Masselink, G. 2016. A new parameterisation for runup on gravel beaches. *Coastal Engineering*, 117, 176-190.

Roelvink, D. and Reniers, A. 2011. A guide to modeling coastal morphology. *Advances in Coastal Engineering*. 12,

Roelvink, D., Reniers, A., Van Dongeren, A., Van Thiel de Vries, J., Lescinski, J. and McCall, R. 2010. XBeach model description and manual. *Delft University of Technology, User Manual, Delft, The Netherlands*,

Roelvink, D., Reniers, A., Van Dongeren, A. P., de Vries, J. v. T., McCall, R. and Lescinski, J. 2009. Modelling storm impacts on beaches, dunes and barrier islands. *Coastal Engineering*, 56, 1133-1152.

Roelvink, D. R., A. 1993. Dissipation in random wave groups incident on a beach. *Advances in Coastal Engineering*, 19, 127-150.

Schambach, L., Grilli, A. R., Grilli, S. T., Hashemi, M. R. and King, J. W. 2018. Assessing the impact of extreme storms on barrier beaches along the Atlantic coastline: Application to the southern Rhode Island coast. *Coastal Engineering*, 133, 26-42.

Simmons, J. A., Splinter, K. D., Harley, M. D. and Turner, I. L. 2019. Calibration data requirements for modelling subaerial beach storm erosion. *Coastal Engineering*, 152, 103507.

Splinter, K. D. and Palmsten, M. L. 2012. Modeling dune response to an East Coast Low. *Marine Geology*, 329, 46-57.

Sutherland, J., Brampton, A., Motyka, G., Blanco, B. and Whitehouse, R. 2005. *Beach lowering in front of coastal structures: research scoping study*. Environment Agency, Bristol.

Svendsen, I. A. 1984. Wave heights and set-up in a surf zone. *Coastal engineering*, **8**, 303-329.

Van Dongeren, A., Bolle, A., Vousdoukas, M. I., Plomaritis, T., Eftimova, P., Williams, J., Armaroli, C., Idier, D., Van Geer, P. and Van Thiel de Vries, J. 2009. MICORE: dune erosion and overwash model validation with data from nine European field sites. *Proceedings of coastal dynamics*.

Van Rijn, L. C. 2007a. Unified view of sediment transport by currents and waves. I: Initiation of motion, bed roughness, and bed-load transport. *Journal of Hydraulic engineering*, **133**, (6), 649-667.

Van Rijn, L. C. 2007b. Unified view of sediment transport by currents and waves. II: Suspended transport. *Journal of Hydraulic Engineering*, **133**, (6), 668-689.

Vousdoukas, M. I., Ferreira, Ó., Almeida, L. P. and Pacheco, A. 2012. Toward reliable storm-hazard forecasts: XBeach calibration and its potential application in an operational early-warning system. *Ocean Dynamics*, **62**, (7), 1001-1015.

**SCDF MODELLING**  
**NOT PROTECTIVELY MARKED**

**Coastal Marine  
Applied Research**



# **Storm erosion modelling of the Sizewell C Soft Coastal Defence Feature using the XBeach modelling suite**

## **Appendices**



## Appendix A Grain size classification

| PARTICLE LENGTH (d <sub>t</sub> ) |        |        |     | GRADE       | CLASS          | FRACTION    |                   |
|-----------------------------------|--------|--------|-----|-------------|----------------|-------------|-------------------|
| km                                | m      | mm     | φ   |             |                | Unlithified | Lithified         |
| 1075                              |        |        | -30 | very coarse | Megalith       | Megagravel  | Mega-conglomerate |
| 538                               |        |        | -29 | coarse      |                |             |                   |
| 269                               |        |        | -28 | medium      |                |             |                   |
| 134                               |        |        | -27 | fine        |                |             |                   |
| 67.2                              |        |        | -26 | very fine   |                |             |                   |
| 33.6                              |        |        | -25 | very coarse | Monolith       |             |                   |
| 16.8                              |        |        | -24 | coarse      |                |             |                   |
| 8.4                               |        |        | -23 | medium      |                |             |                   |
| 4.2                               |        |        | -22 | fine        |                |             |                   |
| 2.1                               |        |        | -21 | very fine   |                |             |                   |
| 1.0                               | 1048.6 |        | -20 | very coarse | Slab           |             |                   |
| 0.5                               | 524.3  |        | -19 | coarse      |                |             |                   |
| 0.26                              | 262.1  |        | -18 | medium      |                |             |                   |
|                                   | 131.1  |        | -17 | fine        |                |             |                   |
|                                   | 65.5   |        | -16 | very coarse | Block          |             |                   |
|                                   | 32.8   |        | -15 | coarse      |                |             |                   |
|                                   | 16.4   |        | -14 | medium      |                |             |                   |
|                                   | 8.2    |        | -13 | fine        |                |             |                   |
|                                   | 4.1    | 4096   | -12 | very coarse | Boulder        | Gravel      | Conglomerate      |
|                                   | 2.0    | 2048   | -11 | coarse      |                |             |                   |
|                                   | 1.0    | 1024   | -10 | medium      |                |             |                   |
|                                   | 0.5    | 512    | -9  | fine        |                |             |                   |
|                                   | 0.25   | 256    | -8  | coarse      | Cobble         |             |                   |
|                                   |        | 128    | -7  | fine        |                |             |                   |
|                                   |        | 64     | -6  | very coarse | Pebble         |             |                   |
|                                   |        | 32     | -5  | coarse      |                |             |                   |
|                                   |        | 16     | -4  | medium      |                |             |                   |
|                                   |        | 8      | -3  | fine        |                |             |                   |
|                                   |        | 4      | -2  |             | Granule        |             |                   |
|                                   |        | 2      | -1  |             |                |             |                   |
|                                   |        | 1      | 0   | very coarse | Sand           | Sand        | Sandstone         |
|                                   |        | 0.50   | 1   | coarse      |                |             |                   |
|                                   |        | 0.25   | 2   | medium      |                |             |                   |
|                                   |        | 0.125  | 3   | fine        |                |             |                   |
|                                   |        | 0.063  | 4   | very fine   | Silt           | Mud         | Mudstone or Shale |
|                                   |        | 0.031  | 5   | coarse      |                |             |                   |
|                                   |        | 0.015  | 6   | medium      |                |             |                   |
|                                   |        | 0.008  | 7   | fine        |                |             |                   |
|                                   |        | 0.004  | 8   | very fine   | Clay<br>↓<br>? |             |                   |
|                                   |        | 0.002  | 9   |             |                |             |                   |
|                                   |        | 0.001  | 10  |             |                |             |                   |
|                                   |        | 0.0005 | 11  |             |                |             |                   |
|                                   |        | 0.0002 | 12  |             |                |             |                   |
|                                   |        | 0.0001 | 13  |             |                |             |                   |

Figure A-1. Modified Udden-Wentworth grain size classification, from Blair and McPherson (1999).

## Appendix B Calibration and Validation

### B.1 Calibration and Validation Forcing Conditions

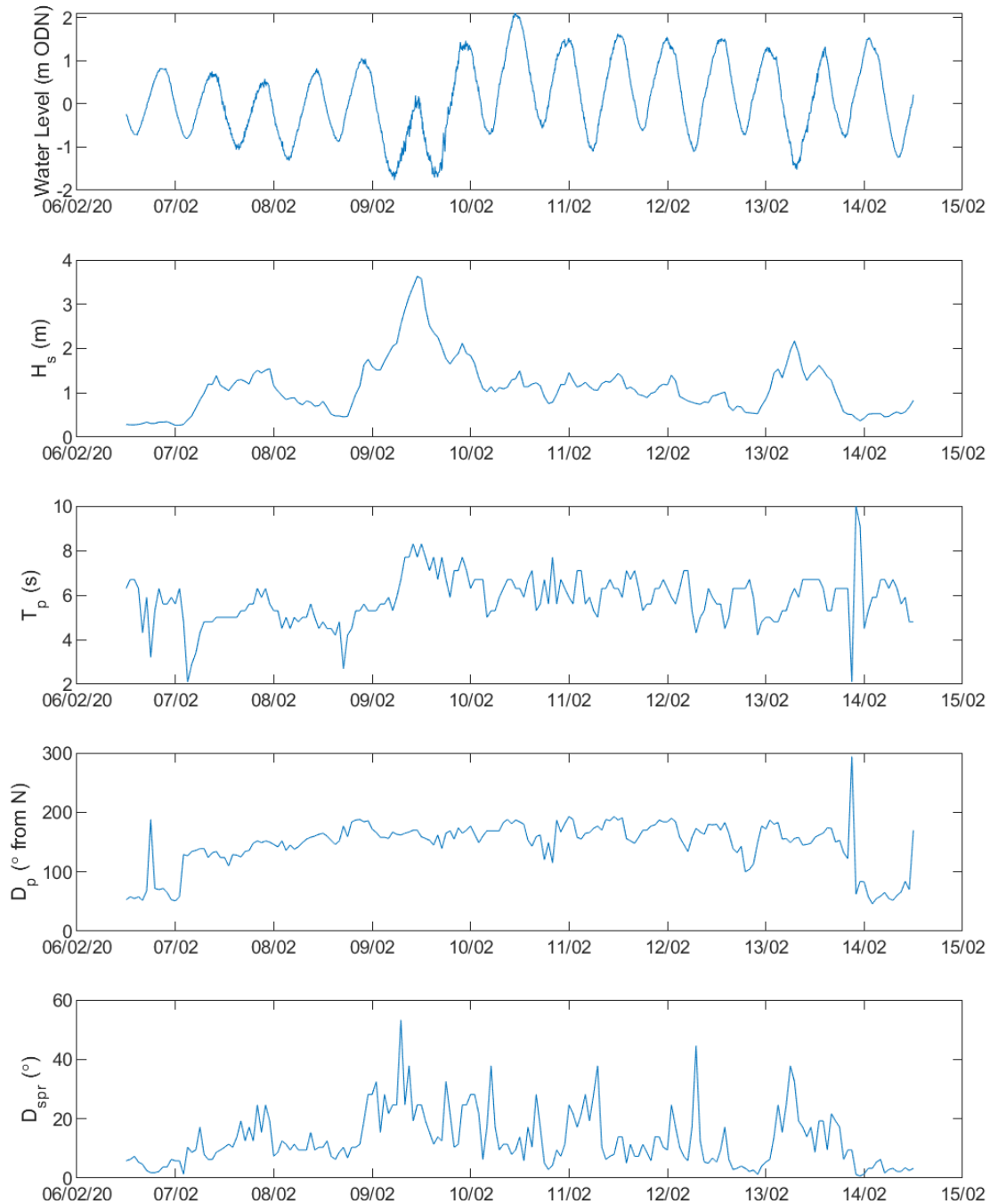


Figure B-1. Calibration ("May Storm") water level and wave forcing conditions.

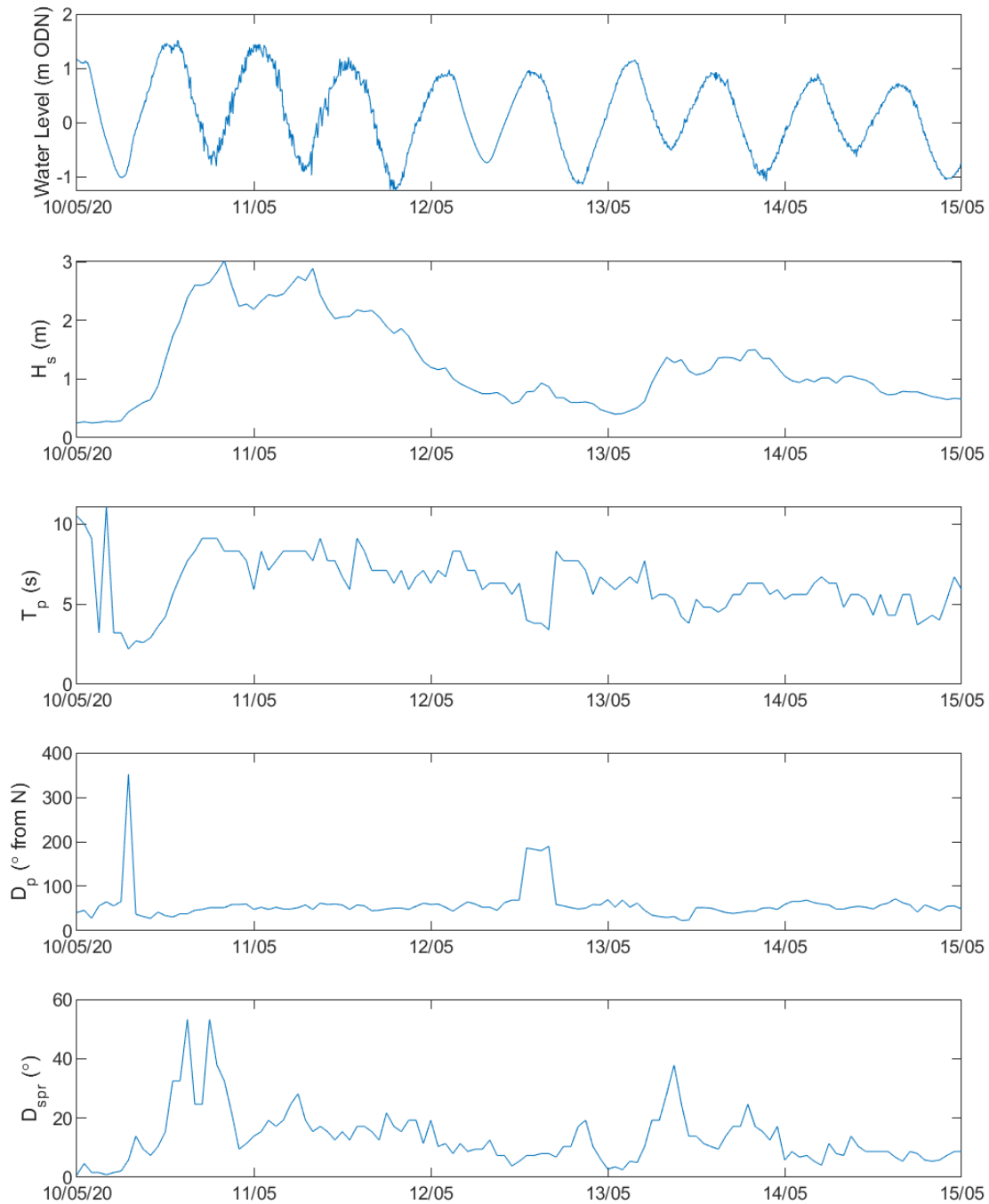


Figure B-2. Validation ("Storm Ciara") water level and wave forcing conditions.

## B.2 Calibration and Validation Statistics

Table B-1. Model Brier Skill Scores (BSS) and Root Mean Squared Error (RMSE) for the 2D XBeach-S calibration and validation model simulations. BSS calculated using modelled post-storm bed elevations assessed against measured post storm bed levels and using pre-storm measured bed levels as the baseline comparison for BSS.

| Model Run                | Brier Skill Score | RMSE (m) |
|--------------------------|-------------------|----------|
| Calibration "May Storm"  | -8.88             | 1.05     |
| Validation "Storm Ciara" | -1.35             | 1.44     |

## Appendix C Volumetric Change Maps

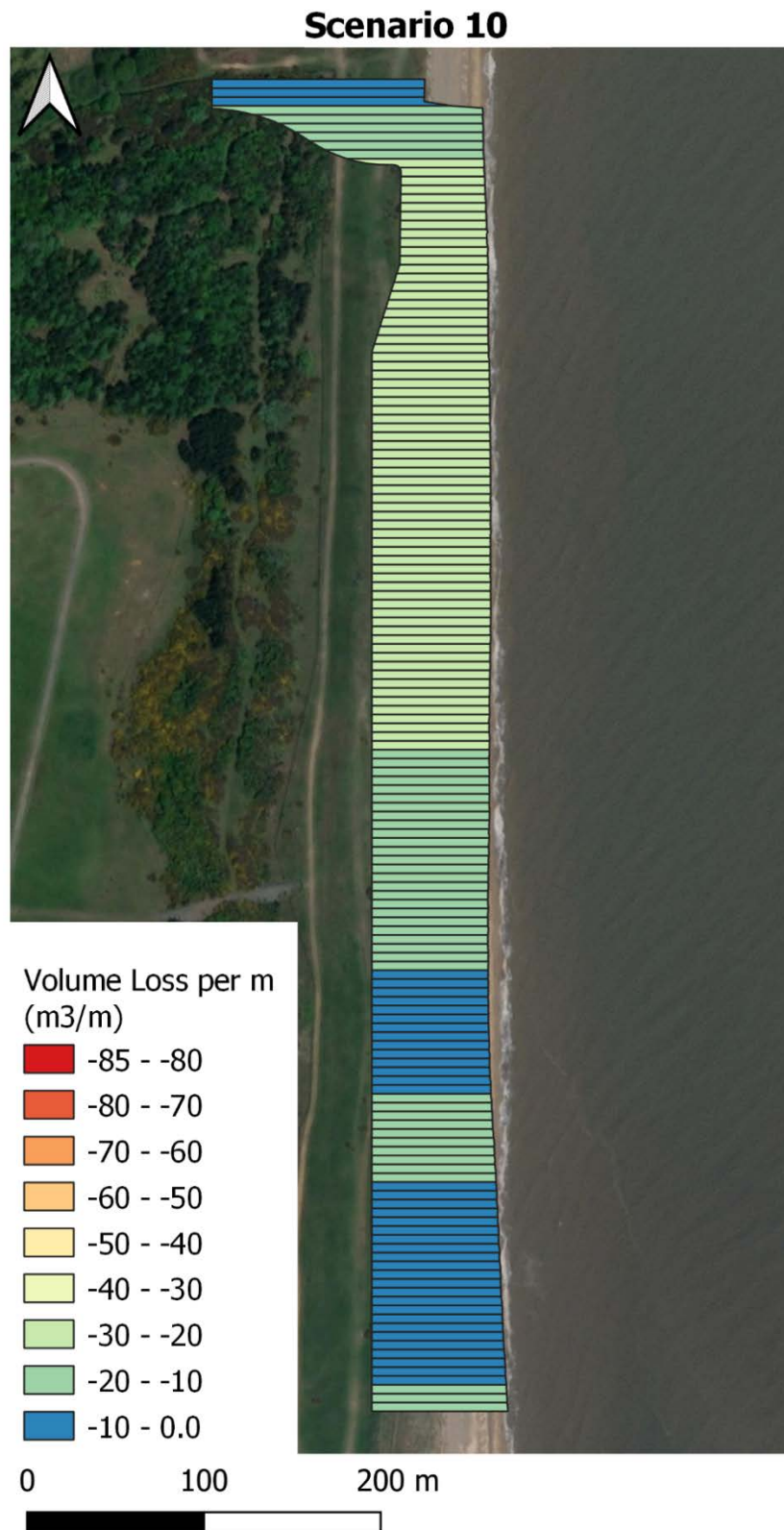


Figure C-3. Beast from the East storm, 2018 Sea Level – volume loss per m at each polygon across the location of the SCDF for the SCDF with present shoreline case.

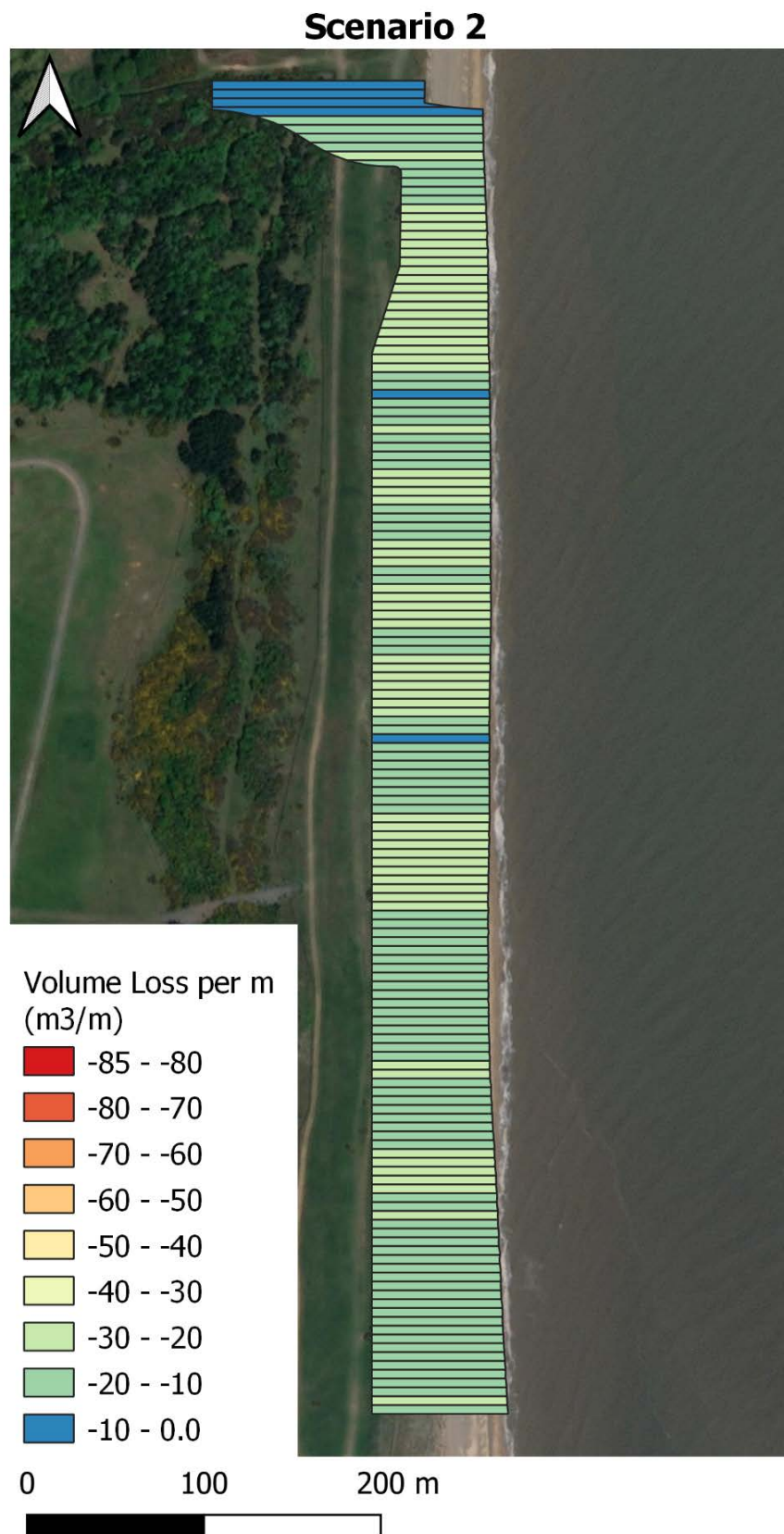


Figure C-4. North East 1-in-20 year storm, Present Sea Level – volume loss per m at each polygon across the location of the SCDF for the SCDF with present shoreline case.



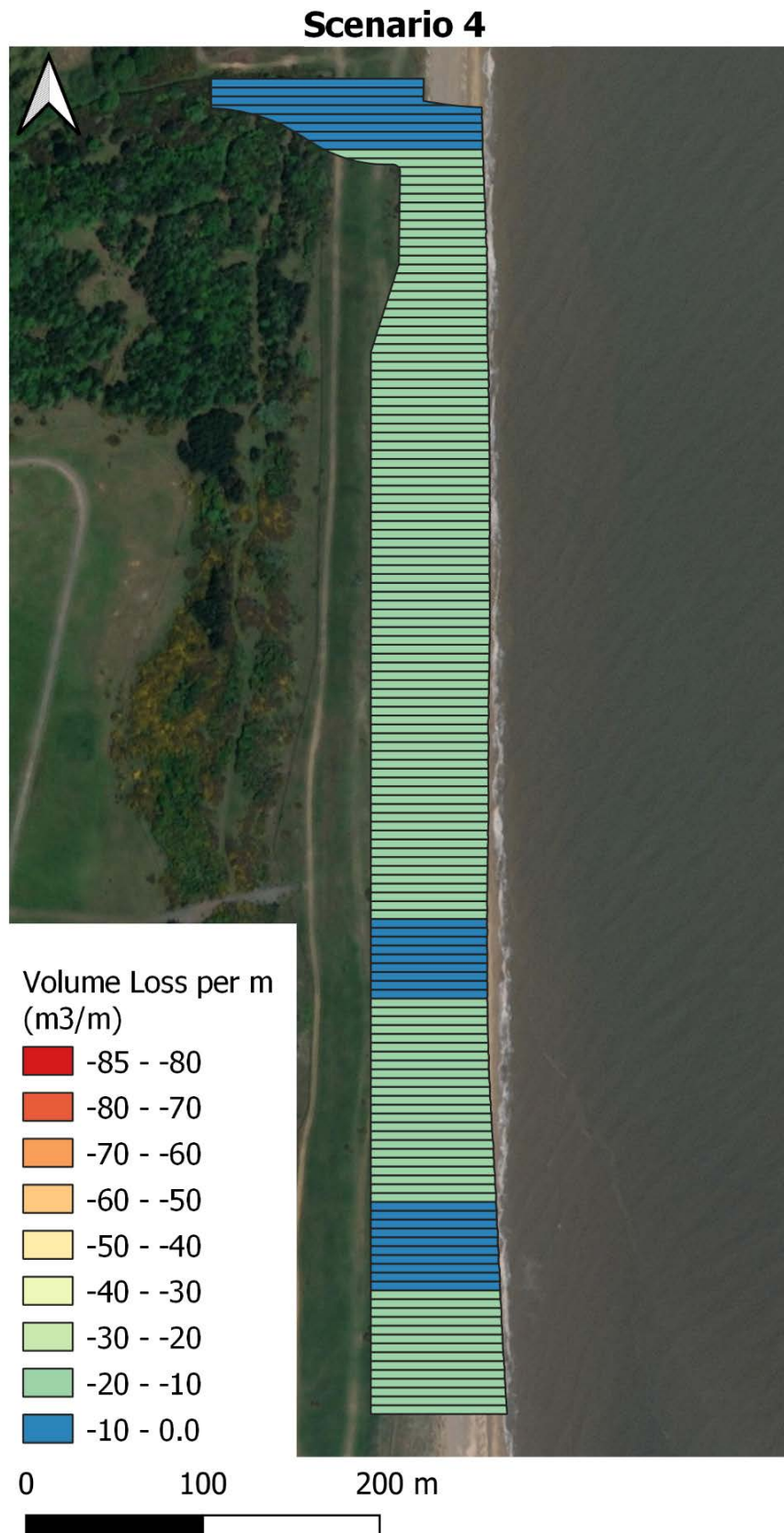


Figure C-5. South East 1-in-20 year storm, Present Sea Level – volume loss per m at each polygon across the location of the SCDF for the SCDF with present shoreline case.

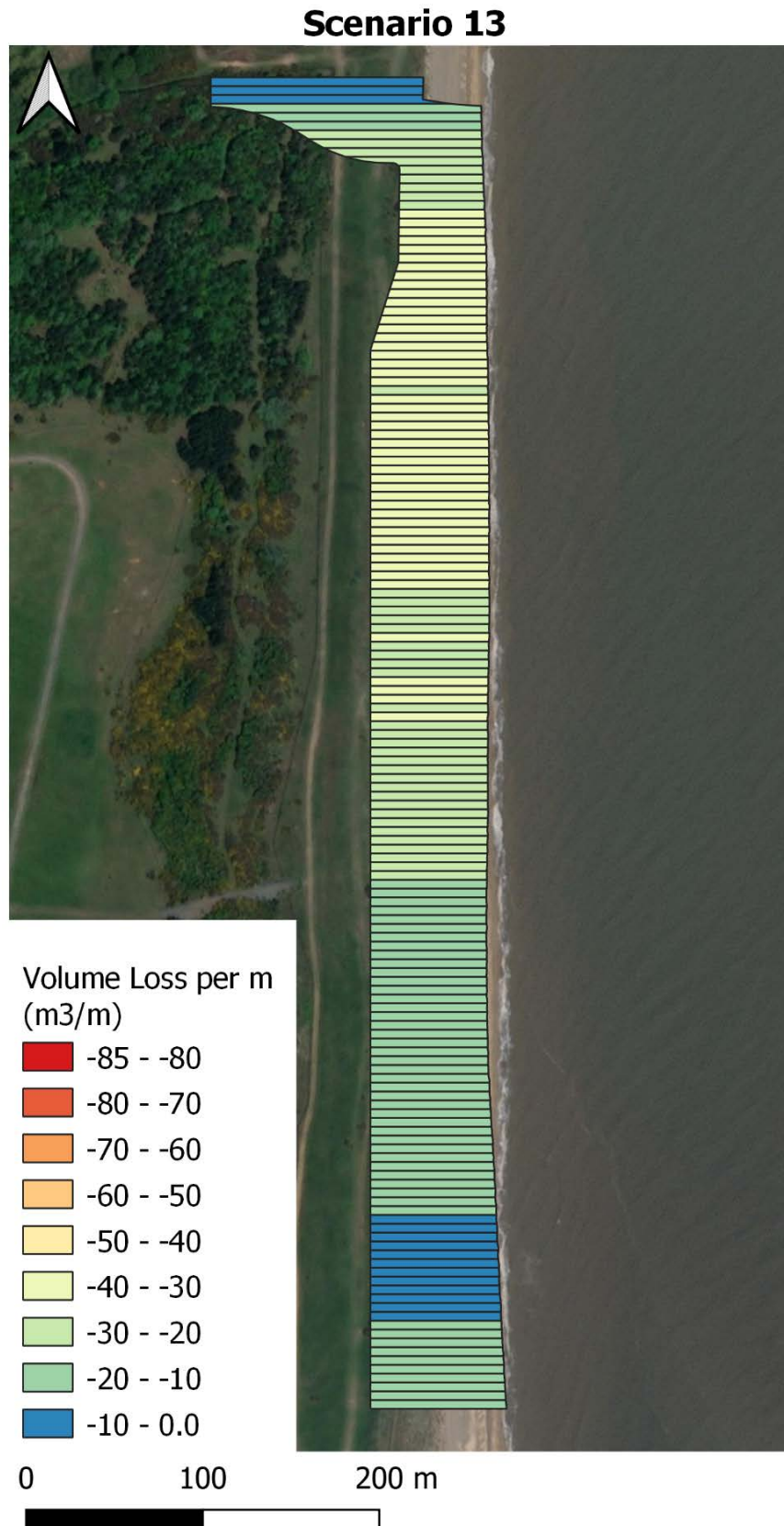


Figure C-6. Beast from the East storm, 2069 Sea Level – volume loss per m at each polygon across the location of the SCDF for the SCDF with present shoreline case.

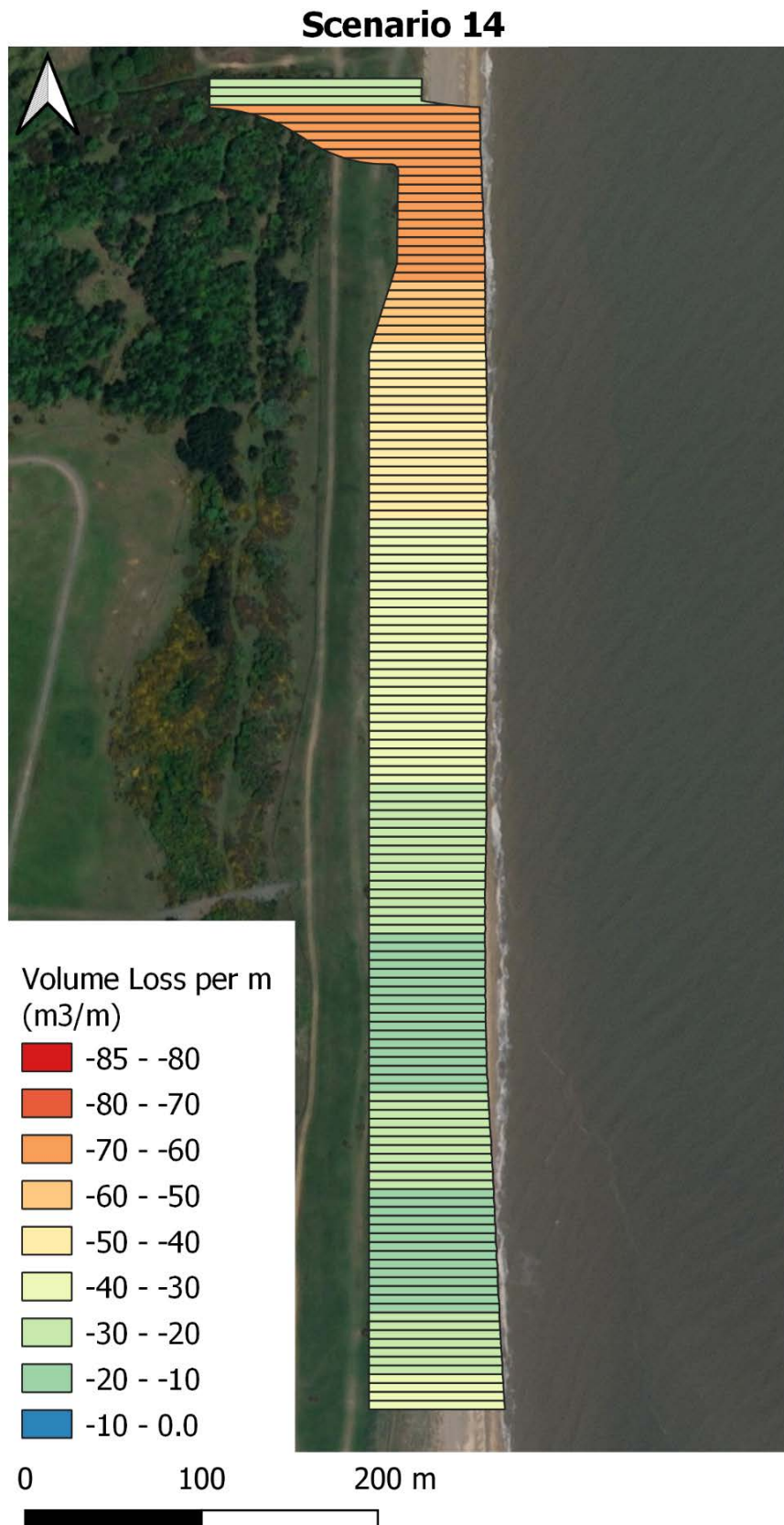


Figure C-7. Beast from the East storm, 2069 Sea Level – volume loss per m at each polygon across the location of the SCDF for the SCDF with future eroded shorelines case.

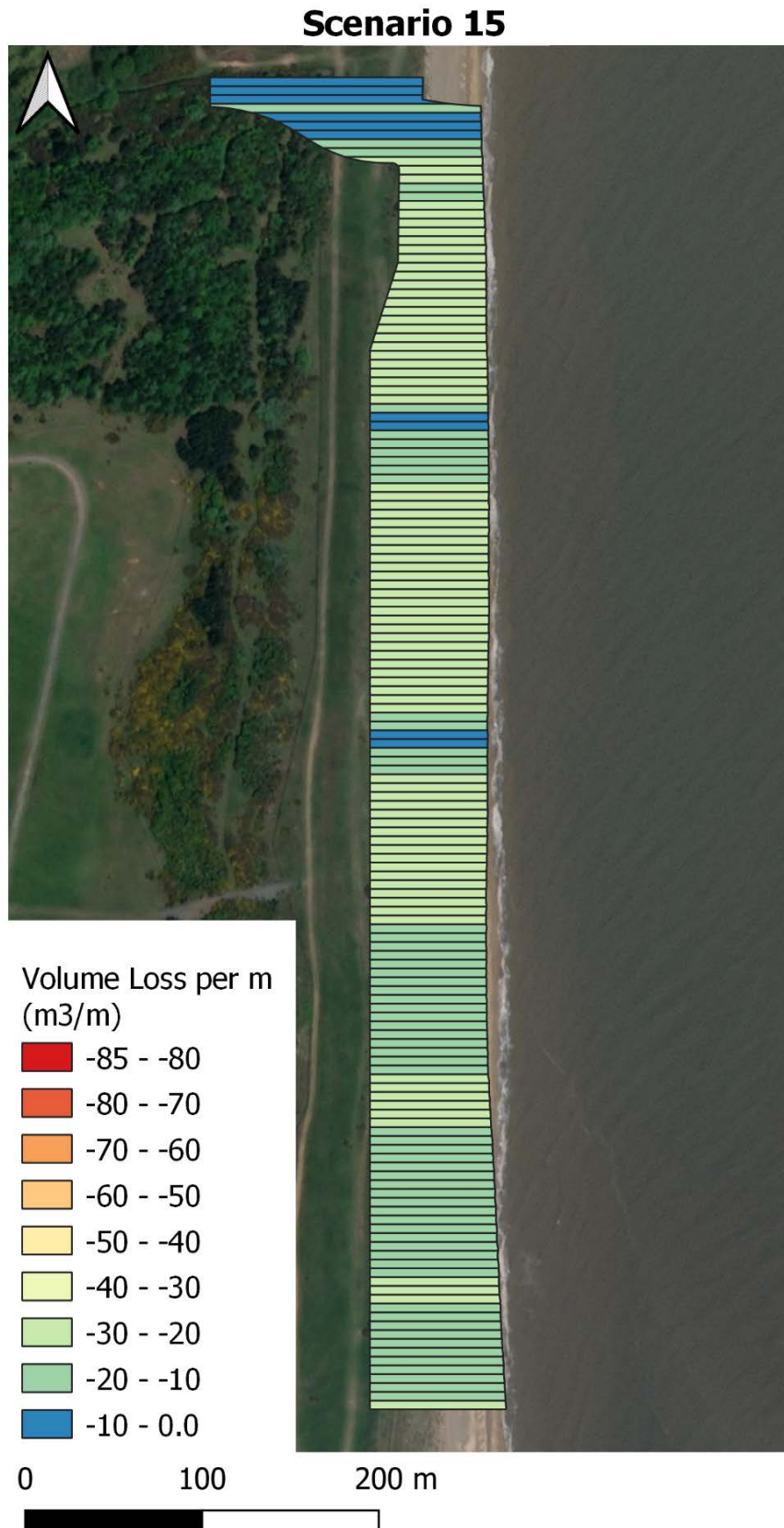


Figure C-8. North East 1-in-20 year storm, 2069 Sea Level – volume loss per m at each polygon across the location of the SCDF for the SCDF with present shoreline case.



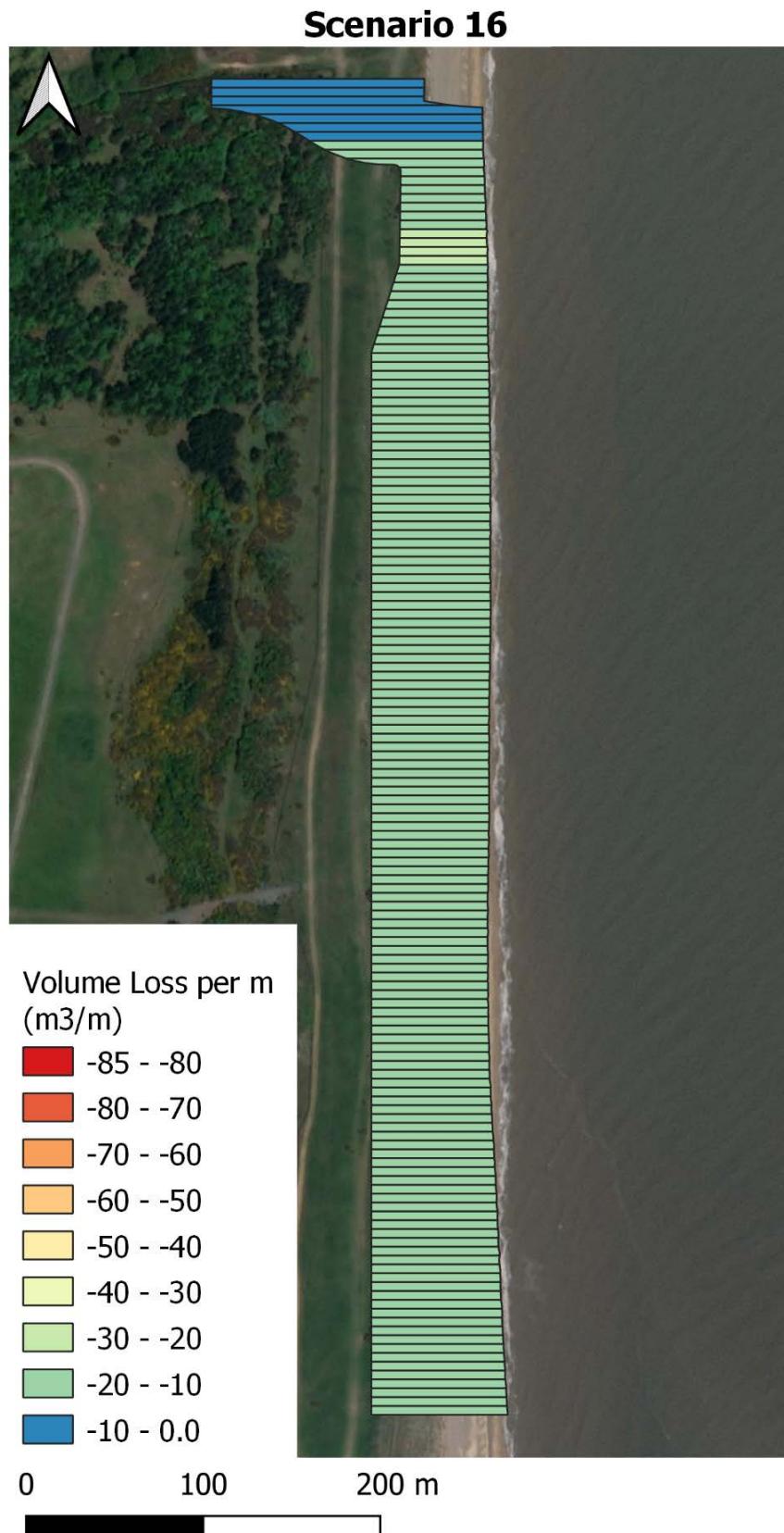


Figure C-9. South East 1-in-20 year storm, 2069 Sea Level – volume loss per m at each polygon across the location of the SCDF for the SCDF with present shoreline case.

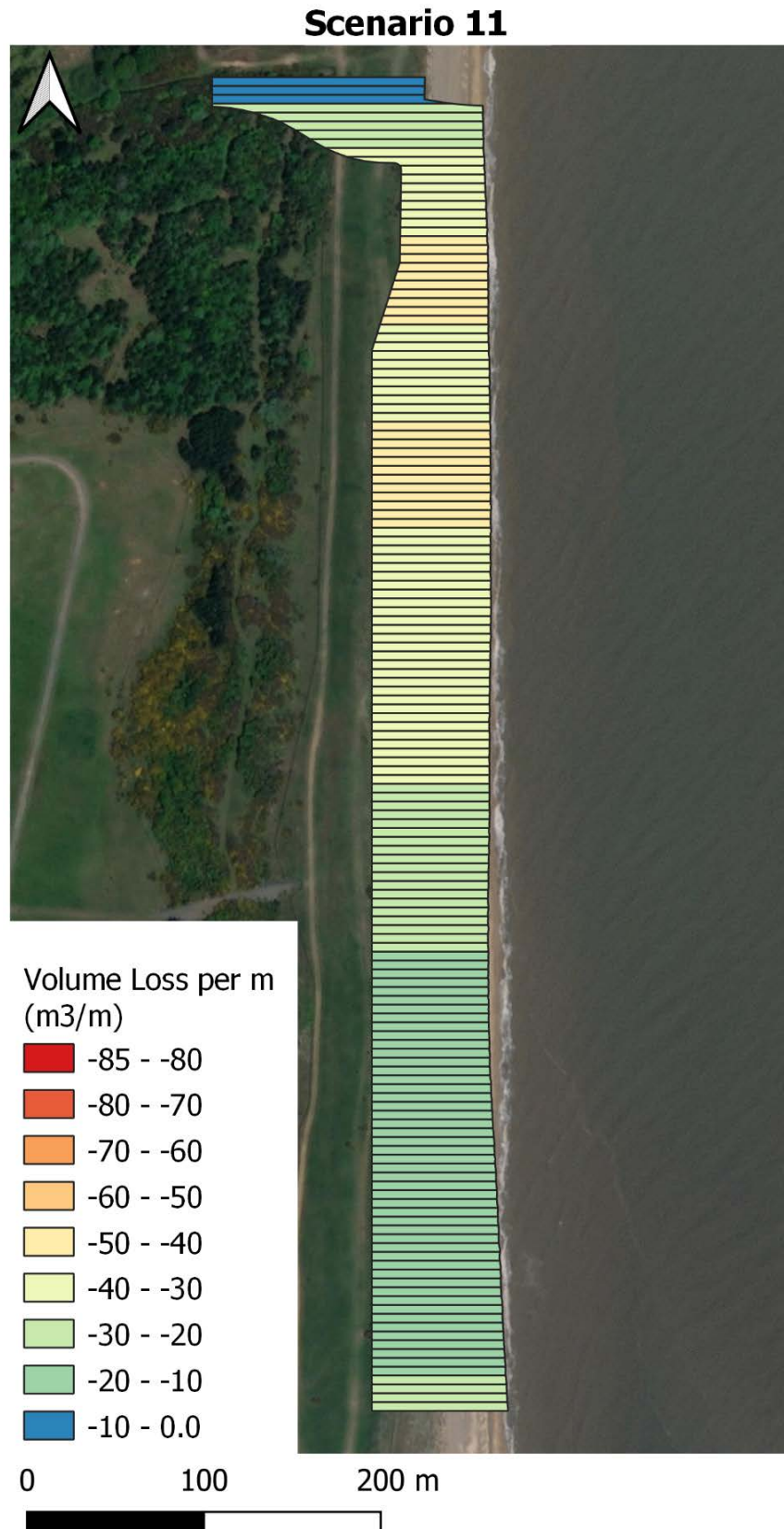


Figure C-10. Beast from the East storm, 2099 Sea Level – volume loss per m at each polygon across the location of the SCDF for the SCDF with present shoreline case.



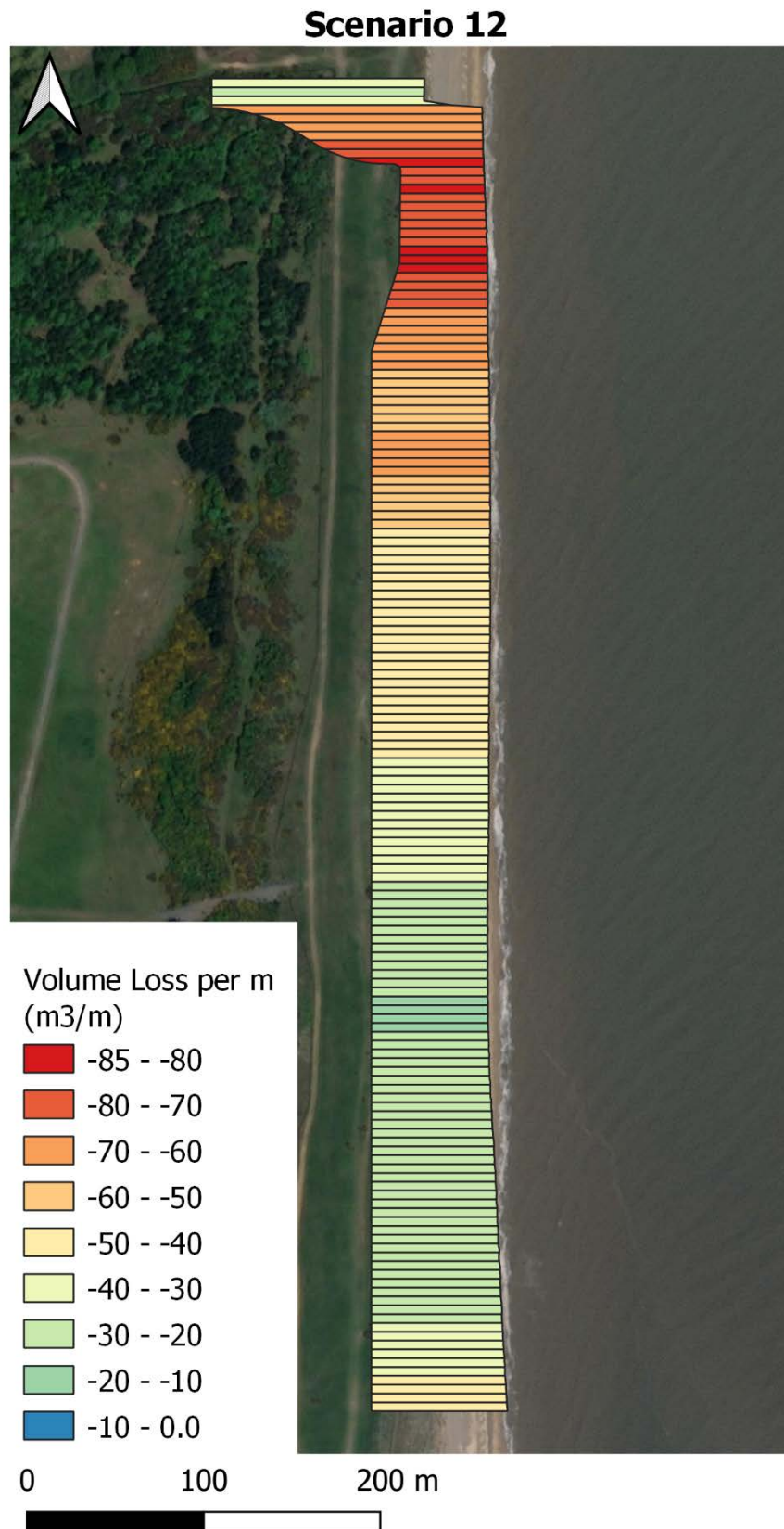


Figure C-11. Beast from the East storm, 2099 Sea Level – volume loss per m at each polygon across the location of the SCDF for the SCDF with future eroded shorelines case.

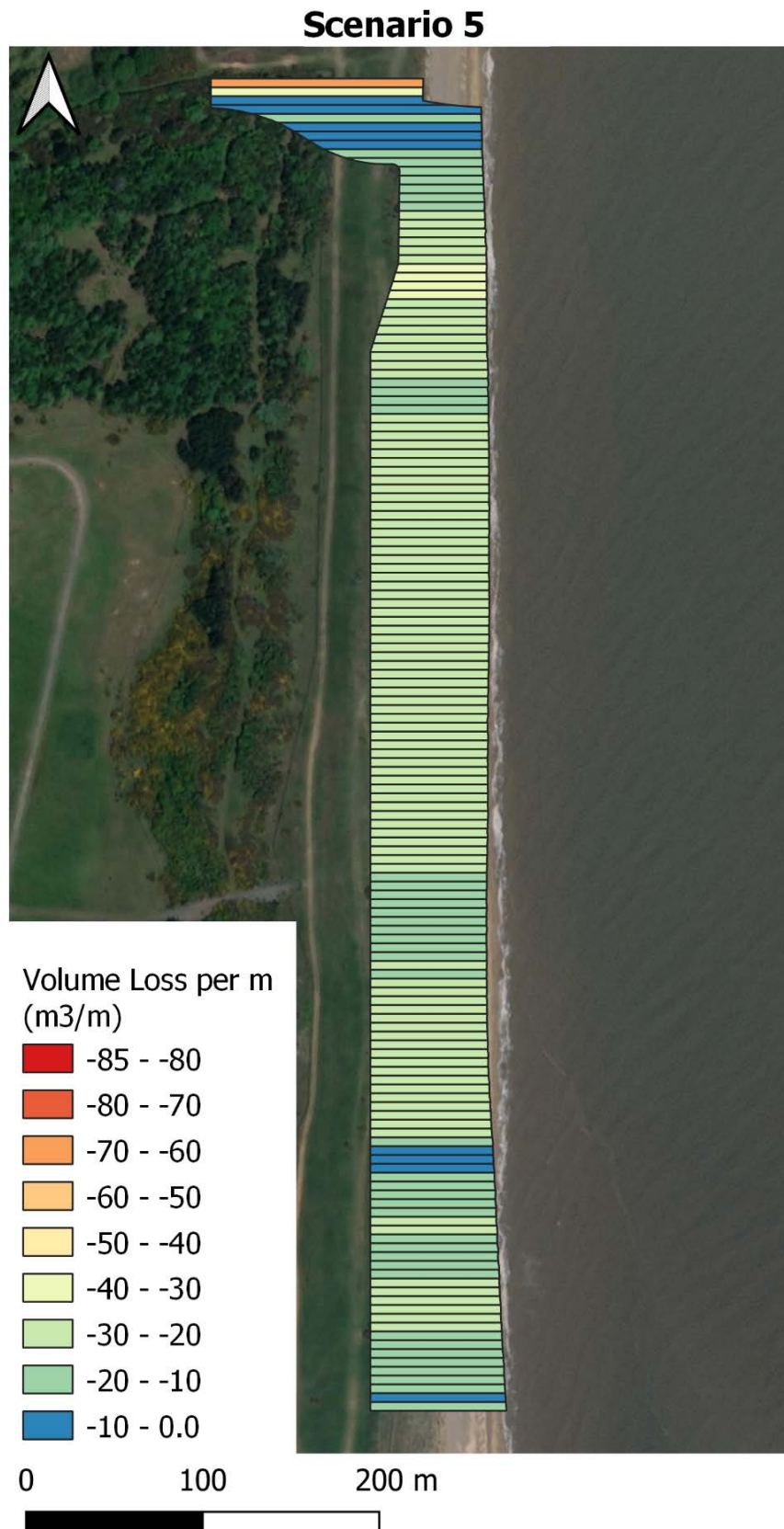


Figure C-12. North East 1-in-2020 year storm, 2099 Sea Level – volume loss per m at each polygon across the location of the SCDF for the SCDF with present shoreline case.

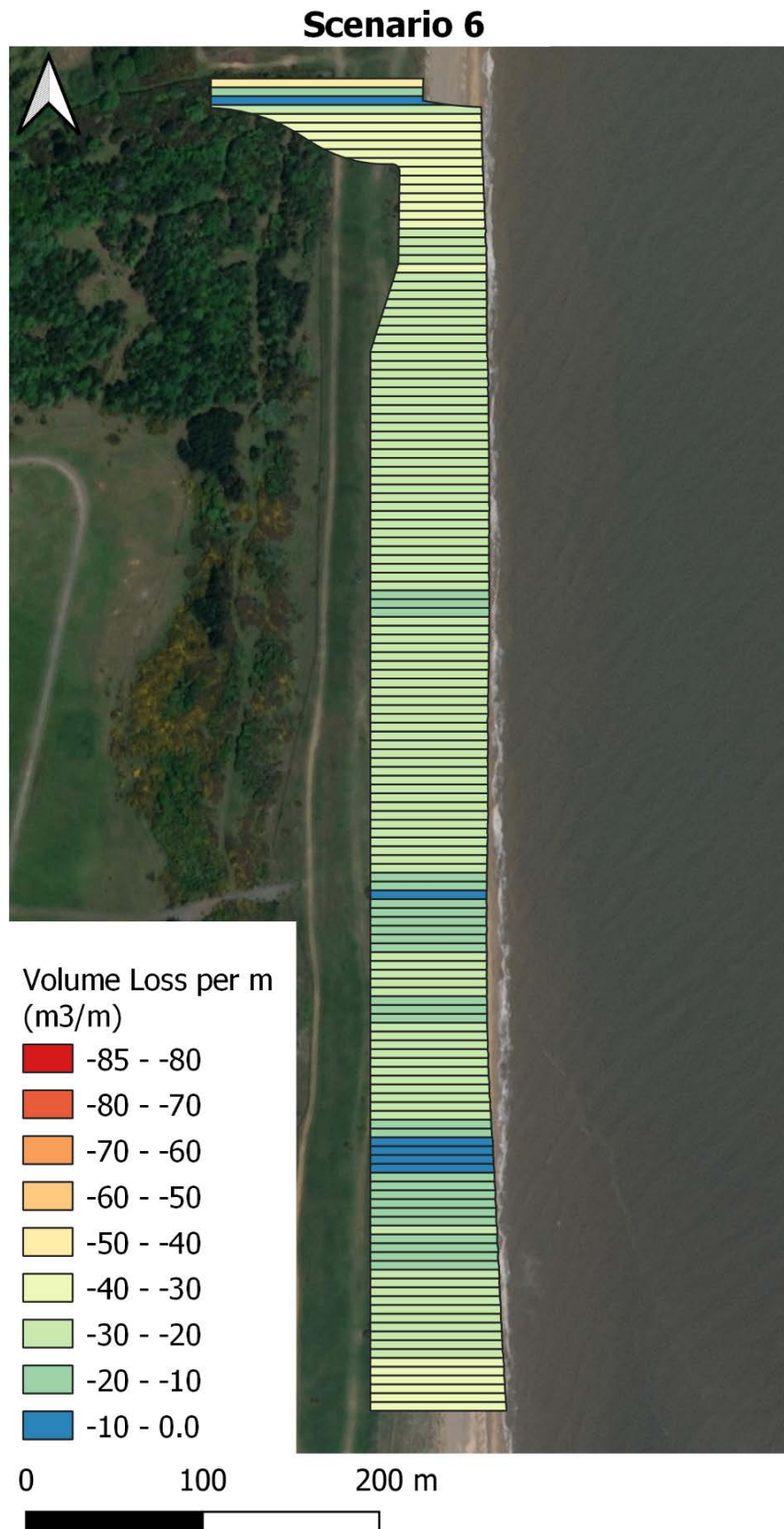


Figure C-13. North East 1-in-20 year storm, 2099 Sea Level – volume loss per m at each polygon across the location of the SCDF for the SCDF with future eroded shorelines case.

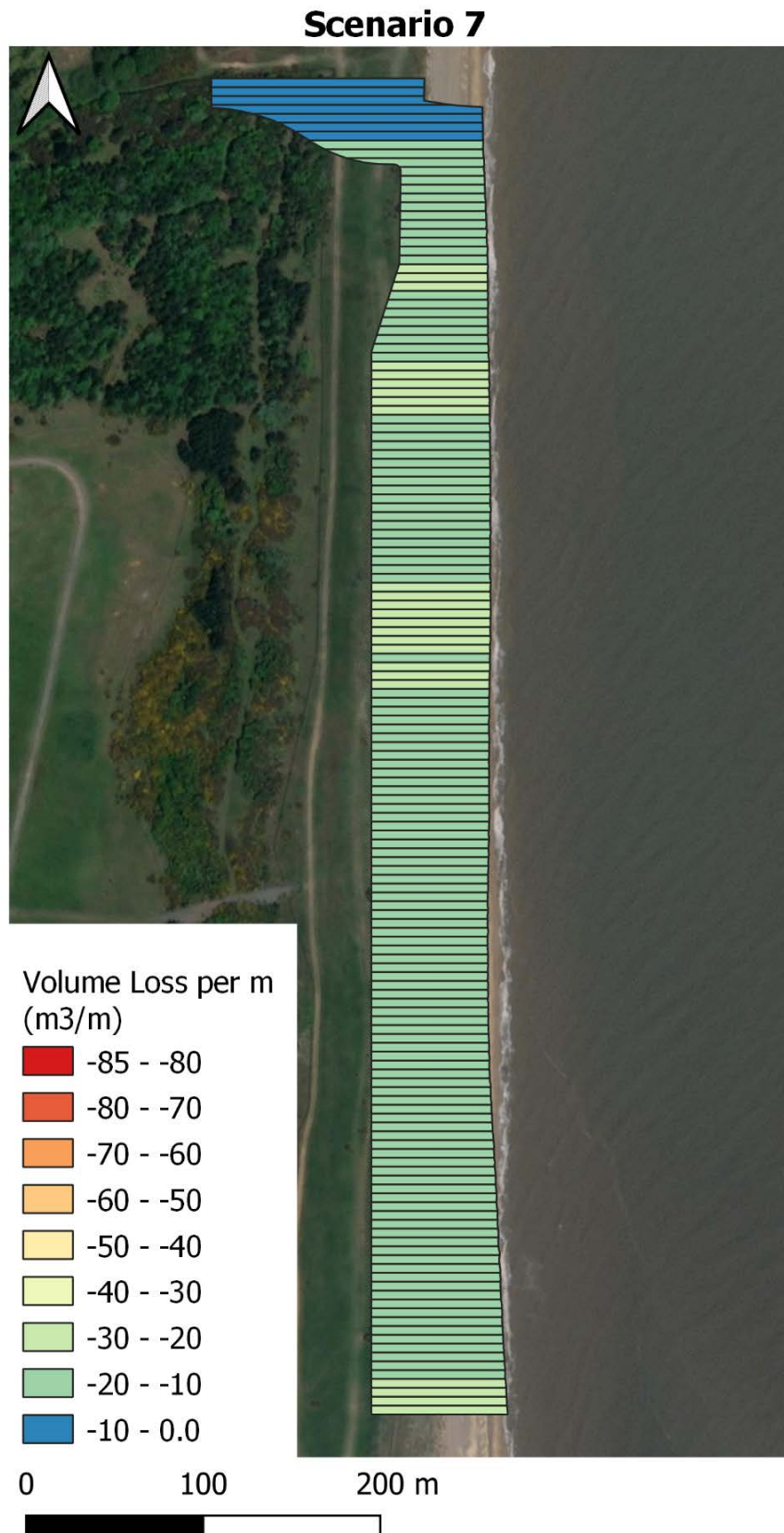


Figure C-14. South East 1-in-20 year storm, 2099 Sea Level – volume loss per m at each polygon across the location of the SCDF for the SCDF with present shoreline case.



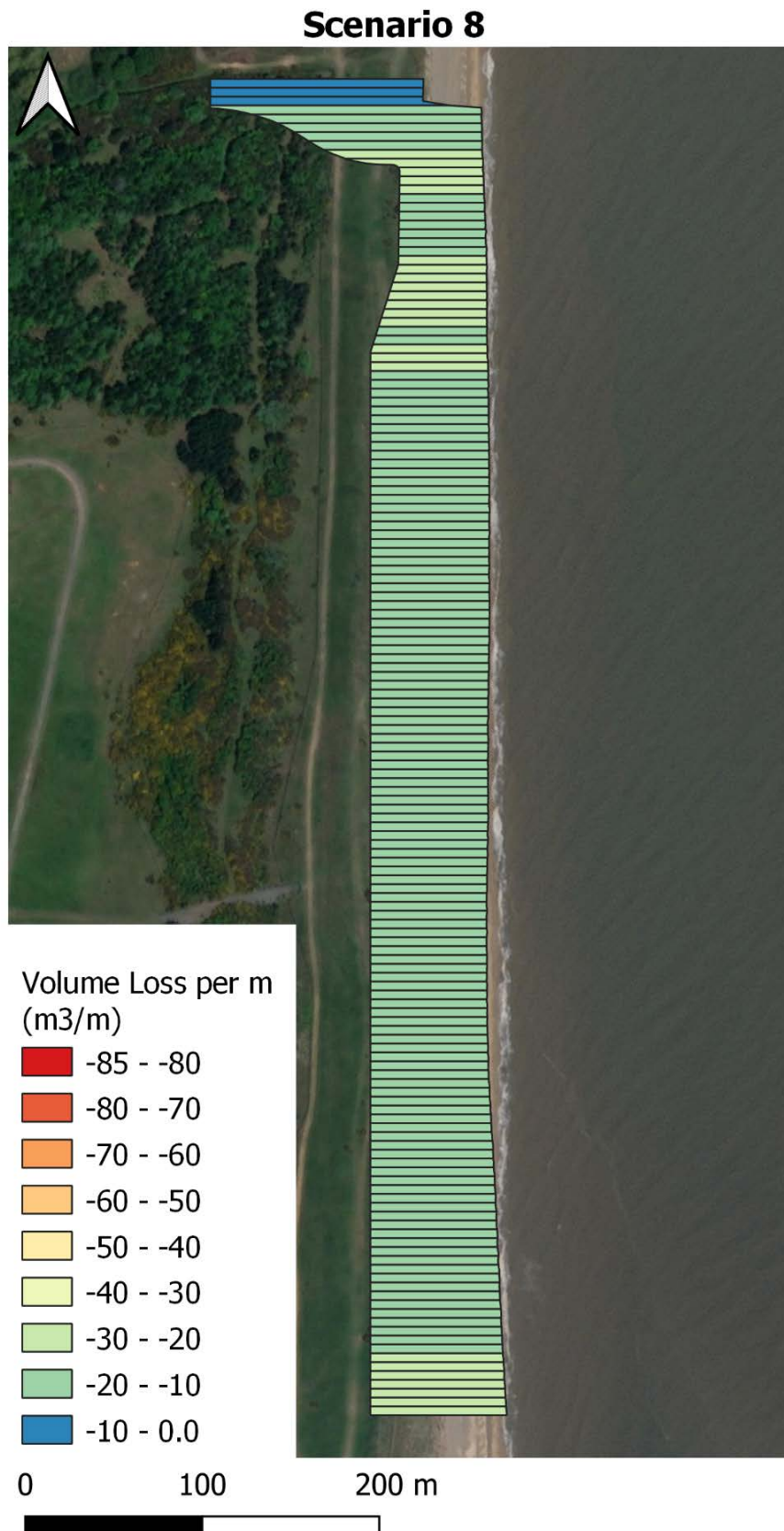


Figure C-15. South East 1-in-20 year storm, 2099 Sea Level – volume loss per m at each polygon across the location of the SCDF for the SCDF with future eroded shorelines case.

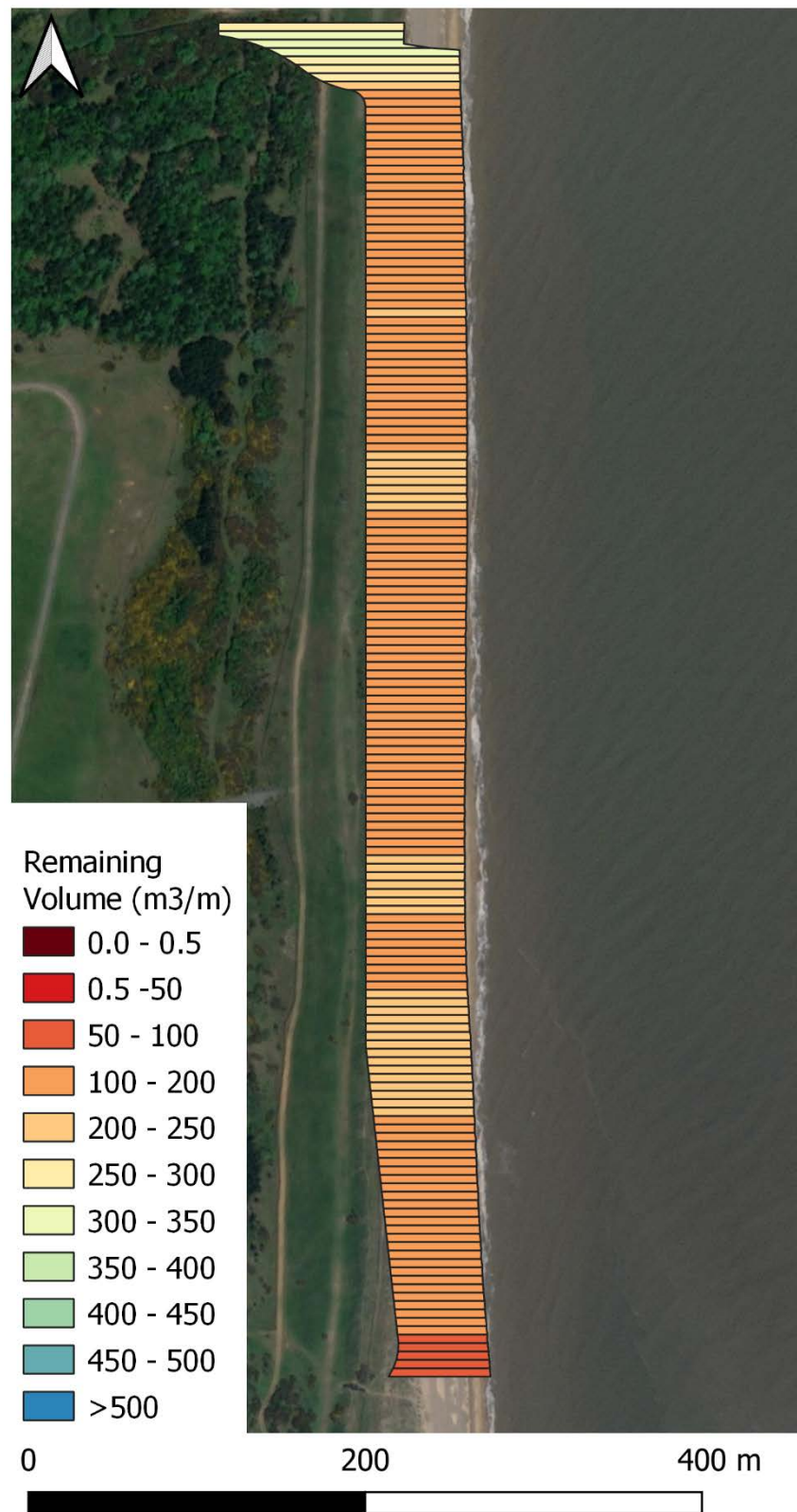


Figure C-16: North East 1-in-20 year storm, RCP4.5 2120 Sea Level – volume loss per m at each polygon across the location of the SCDF for the SCDF with future eroded shorelines case.





Figure C-17: North East 1-in-20 year storm, RCP8.5 2120 Sea Level – volume loss per m at each polygon across the location of the SCDF for the SCDF with the Adaptive Design and future eroded shorelines case.

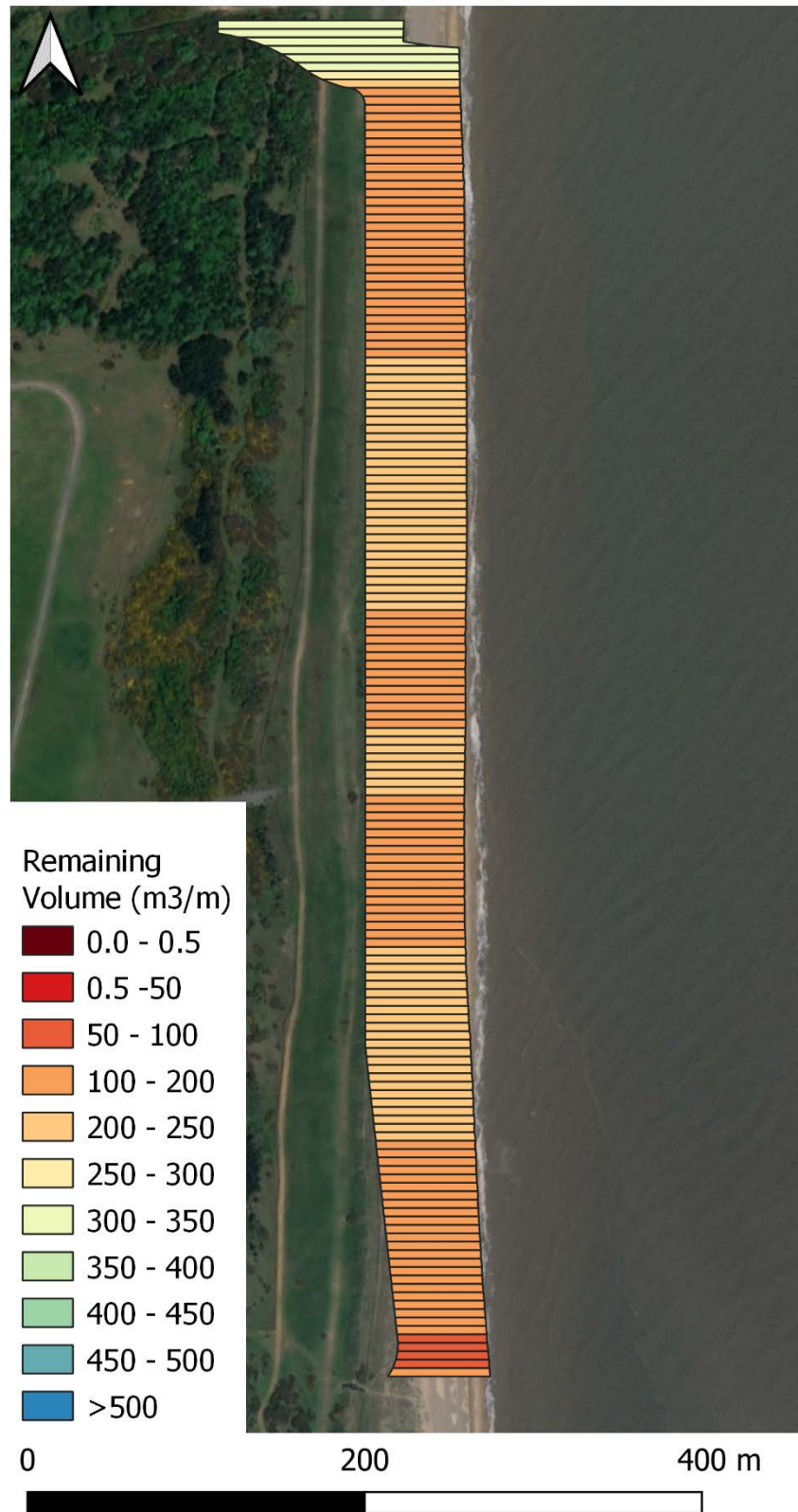


Figure C-18: South East 1-in-20 year storm, RCP4.5 2120 Sea Level – volume loss per m at each polygon across the location of the SCDF for the SCDF with future eroded shorelines case.



Figure C-19: South East 1-in-20 year storm, RCP4.5 2140 Sea Level – volume loss per m at each polygon across the location of the SCDF for the SCDF with future eroded shorelines case.



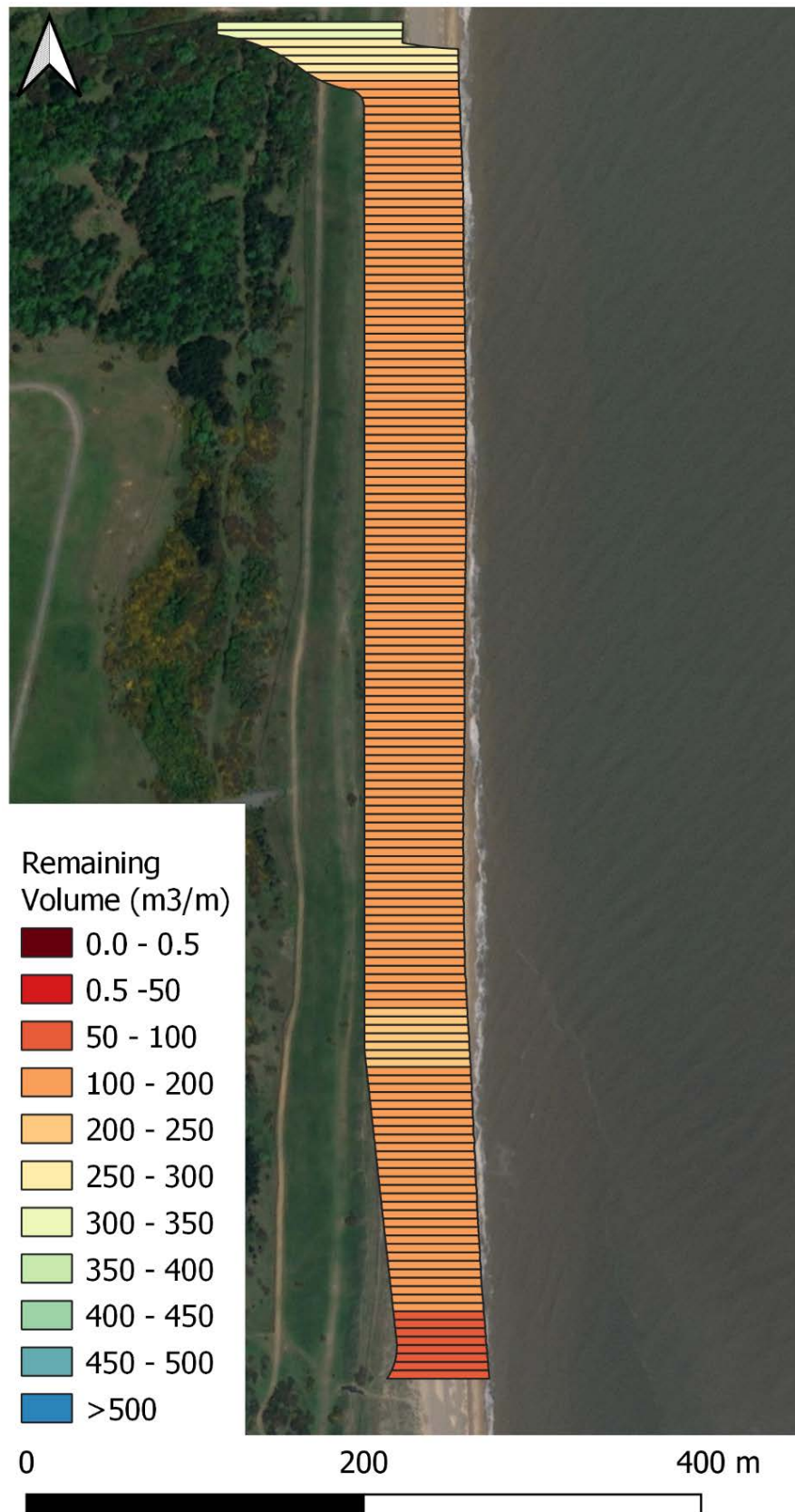


Figure C-20: BfE storm, RCP4.5 2120 Sea Level – volume loss per m at each polygon across the location of the SCDF for the SCDF with future eroded shorelines case.

## Appendix D Wave runup results

### D.1 Wave runup results

Table D-1. 2% exceedance and maximum wave run-up values ( $R_{2\%}$  and  $R_{max}$ , respectively) and end-of-simulation crest heights at three locations ( $Y_1$ ,  $Y_2$ ,  $Y_3$ ) from the 2D simulations. Values are highlighted in red where  $R_{2\%}$  exceeds the end crest height and highlighted in orange where  $R_{max}$  exceeds the end crest height. Runup heights were assessed both with present-day shorelines ('SCDF') and with future eroded shorelines ('SCDF Future').

| Scen. No. | Description                                    | Profile (all values are in mODN) |           |       |           |           |       |           |           |       |
|-----------|--|----------------------------------|-----------|-------|-----------|-----------|-------|-----------|-----------|-------|
|           |  | Y1                               |           |       | Y2        |           |       | Y3        |           |       |
|           |  | $R_{2\%}$                        | $R_{max}$ | Crest | $R_{2\%}$ | $R_{max}$ | Crest | $R_{2\%}$ | $R_{max}$ | Crest |
| 2         | 1-in-20 year storm, NE, present SL - SCDF      | 3.17                             | 3.59      | 4.24  | 3.15      | 3.99      | 6.52  | 2.98      | 3.14      | 5.25  |
| 4         | 1-in-20 year storm, SE, present SL -SCDF       | 2.84                             | 2.97      | 4.24  | 2.67      | 2.80      | 6.52  | 2.75      | 2.83      | 5.25  |
| 5         | 1-in-20 year storm, NE, 2099 SLR - SCDF        | 3.77                             | 4.00      | 3.61  | 3.96      | 4.31      | 6.52  | 3.77      | 4.04      | 5.25  |
| 6         | 1-in-20 year storm, NE, 2099 SLR – SCDF future |                                  |           |       | 3.83      | 4.33      | 6.51  |           |           |       |
| 7         | 1:20 yr storm, SE, 2099 SLR - SCDF             | 3.49                             | 3.69      | 4.24  | 3.44      | 3.57      | 6.52  | 3.39      | 3.46      | 5.25  |
| 8         | 1:20 yr storm, SE, 2099 SLR - SCDF future      |                                  |           |       | 3.45      | 3.68      | 6.51  |           |           |       |
| 10        | BfE storm, E, present SL - SCDF                | 1.60                             | 2.37      | 4.24  | 1.68      | 2.54      | 6.52  | 1.54      | 2.42      | 5.25  |
| 11        | BfE storm, E, 2099 SLR - SCDF                  | 2.32                             | 3.96      | 4.22  | 2.41      | 3.35      | 6.52  | 2.26      | 3.04      | 5.25  |
| 12        | BfE storm, E, 2099 SLR – SCDF Future           |                                  |           |       | 2.41      | 3.70      | 6.51  |           |           |       |
| 13        | BfE storm, E, 2069 SLR - SCDF                  | 2.00                             | 2.79      | 4.24  | 2.10      | 3.99      | 6.52  | 1.94      | 2.75      | 5.25  |
| 14        | BfE storm, E, 2069 SLR – SCDF Future           |                                  |           |       | 2.08      | 3.14      | 6.51  |           |           |       |
| 15        | 1-in-20 year storm, NE, 2069 SLR - SCDF        | 3.57                             | 3.65      | 3.89  | 3.62      | 4.00      | 6.52  | 3.36      | 3.56      | 5.25  |
| 16        | 1-in-20 year storm, SE, 2069 SLR -SCDF         | 3.30                             | 3.62      | 4.24  | 3.19      | 3.26      | 6.52  | 3.16      | 3.21      | 5.25  |

Table D-2. 2% exceedance and maximum wave run-up values ( $R_{2\%}$  and  $R_{max}$ , respectively) and end-of-simulation SCDF crest height from the 1D XBeach-S and XBeach-G simulations. Values are highlighted in red if  $R_{2\%}$  exceeds the crest height and highlighted in orange where  $R_{max}$  exceeds the end crest height.

| Scen. No. | Description                                 | Grain size (mm)                  | $R_{2\%}$ (mODN) | $R_{max}$ (mODN) | Crest end (mODN) |
|-----------|---|----------------------------------|------------------|------------------|------------------|
| 1-1D      | 1-in-20 year storm, NE, 2021 SLR (XBeach-S) | $D_{50} = 0.8$<br>$D_{90} = 1.5$ | 3.33             | 3.85             | 6.53             |
| 2-1D      | 1-in-20 year storm, NE, 2021 SLR (XBeach-S) | $D_{50} = 2$ $D_{90} = 3$        | 3.30             | 3.79             | 6.53             |
| 3-1D      | 1-in-20 year storm, NE, 2021 SLR (XBeach-G) | $D_{50} = 2$ $D_{90} = 3$        | 4.44             | 6.01             | 6.53             |
| 4-1D      | 1-in-20 year storm, NE, 2021 SLR (XBeach-G) | $D_{50} = 10$ $D_{90} = 15$      | 4.31             | 5.78             | 6.53             |
| 5-1D      | 1-in-20 year storm, NE, 2021 SLR (XBeach-G) | $D_{50} = 40$ $D_{90} = 60$      | 4.07             | 5.46             | 6.53             |
| 6-1D      | 1-in-20 year storm, NE, 2021 SLR (XBeach-G) | $D_{50} = 80$ $D_{90} = 120$     | 3.96             | 6.15             | 6.53             |
| 7-1D      | 1-in-20 year storm, NE, 2069 SLR (XBeach-S) | $D_{50} = 0.8$<br>$D_{90} = 1.5$ | 3.83             | 4.41             | 6.53             |
| 8-1D      | 1-in-20 year storm, NE, 2069 SLR (XBeach-S) | $D_{50} = 2$ $D_{90} = 3$        | 3.85             | 4.36             | 6.53             |
| 9-1D      | 1-in-20 year storm, NE, 2069 SLR (XBeach-G) | $D_{50} = 2$ $D_{90} = 3$        | 4.77             | 6.46             | 6.53             |
| 10-1D     | 1-in-20 year storm, NE, 2069 SLR (XBeach-G) | $D_{50} = 10$ $D_{90} = 15$      | 4.67             | 6.22             | 6.53             |
| 11-1D     | 1-in-20 year storm, NE, 2069 SLR (XBeach-G) | $D_{50} = 40$ $D_{90} = 60$      | 4.47             | 5.84             | 6.53             |
| 12-1D     | 1-in-20 year storm, NE, 2069 SLR (XBeach-G) | $D_{50} = 80$ $D_{90} = 120$     | 4.35             | 6.14             | 6.53             |
| 13-1D     | 1-in-20 year storm, NE, 2099 SLR (XBeach-S) | $D_{50} = 0.8$<br>$D_{90} = 1.5$ | 4.30             | 5.09             | 6.53             |
| 14-1D     | 1-in-20 year storm, NE, 2099 SLR (XBeach-S) | $D_{50} = 2$ $D_{90} = 3$        | 4.28             | 4.96             | 6.53             |
| 15-1D     | 1-in-20 year storm, NE, 2099 SLR (XBeach-G) | $D_{50} = 2$ $D_{90} = 3$        | 5.09             | 6.54             | 6.53             |
| 16-1D     | 1-in-20 year storm, NE, 2099 SLR (XBeach-G) | $D_{50} = 10$ $D_{90} = 15$      | 4.99             | 6.41             | 6.53             |
| 17-1D     | 1-in-20 year storm, NE, 2099 SLR (XBeach-G) | $D_{50} = 40$ $D_{90} = 60$      | 4.79             | 6.10             | 6.53             |



| Scen.<br>No. | Description                                 | Grain size<br>(mm)           | $R_{2\%}$<br>(mODN) | $R_{max}$<br>(mODN) | Crest<br>end<br>(mODN) |
|--------------|---|------------------------------|---------------------|---------------------|------------------------|
| 18-1D        | 1-in-20 year storm, NE, 2099 SLR (XBeach-G) | $D_{50} = 80$ $D_{90} = 120$ | 4.68                | 6.13                | 6.53                   |

## Appendix E 2D Hydrodynamic Results

---

### E.1 2D Hydrodynamic Results – SCDF compared to SCDF-future

---

#### E.1.1 Beast from the East Storm, 2069 Sea Level

The Beast from the East Storm, 2069 Sea Level Rise results averaged over the entire simulation for the SCDF and SCDF future case are presented here. Figure E-1Figure E-10 – Figure E-3 show the average wave height results. Figure E-4 – Figure E-6 show the current speed/ velocity results. Figure E-7 – Figure E-9 show the bed shear stress and sediment flux results.

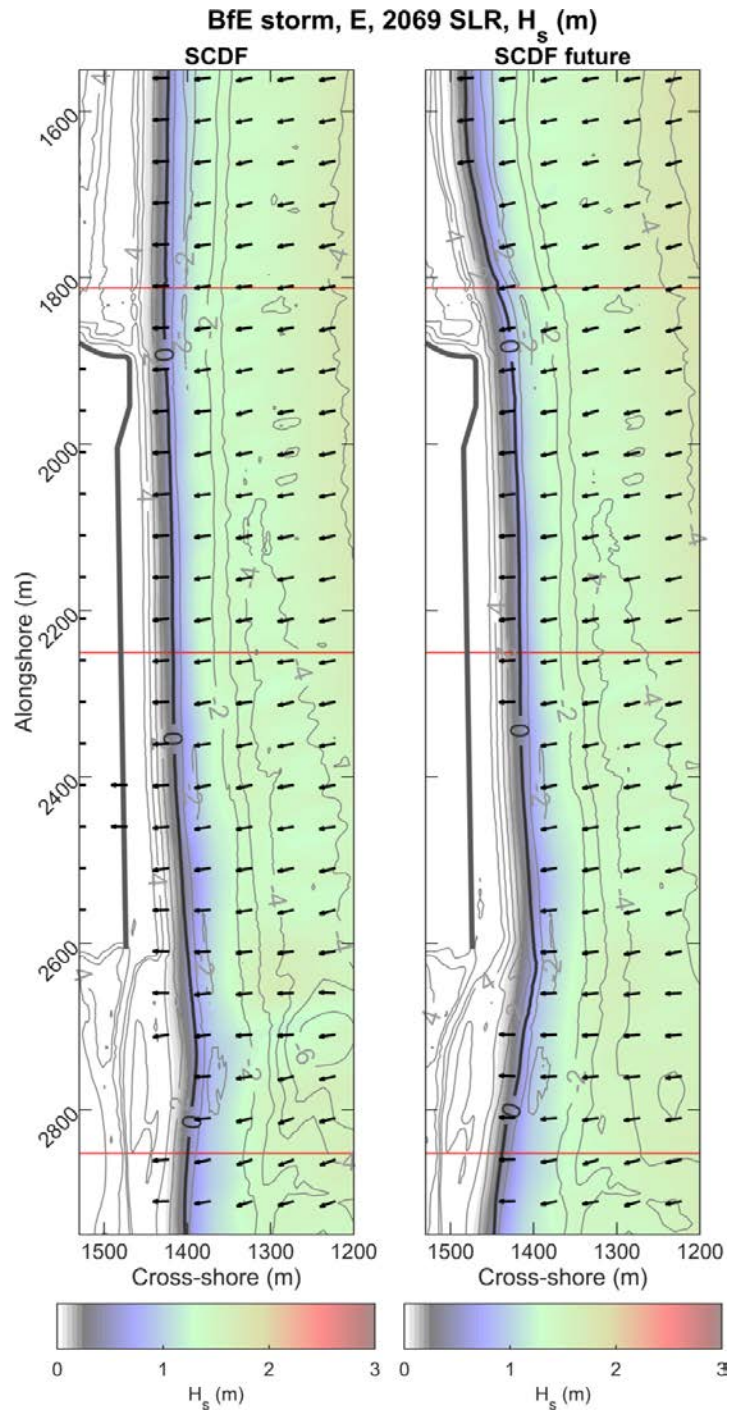


Figure E-1. Beast from the East storm, 2069 Sea Level – 2D average wave heights over the simulation for the SCDF (left) and SCDF-future (right). The red lines indicate the locations of the cross-sectional plots presented in the figure below.

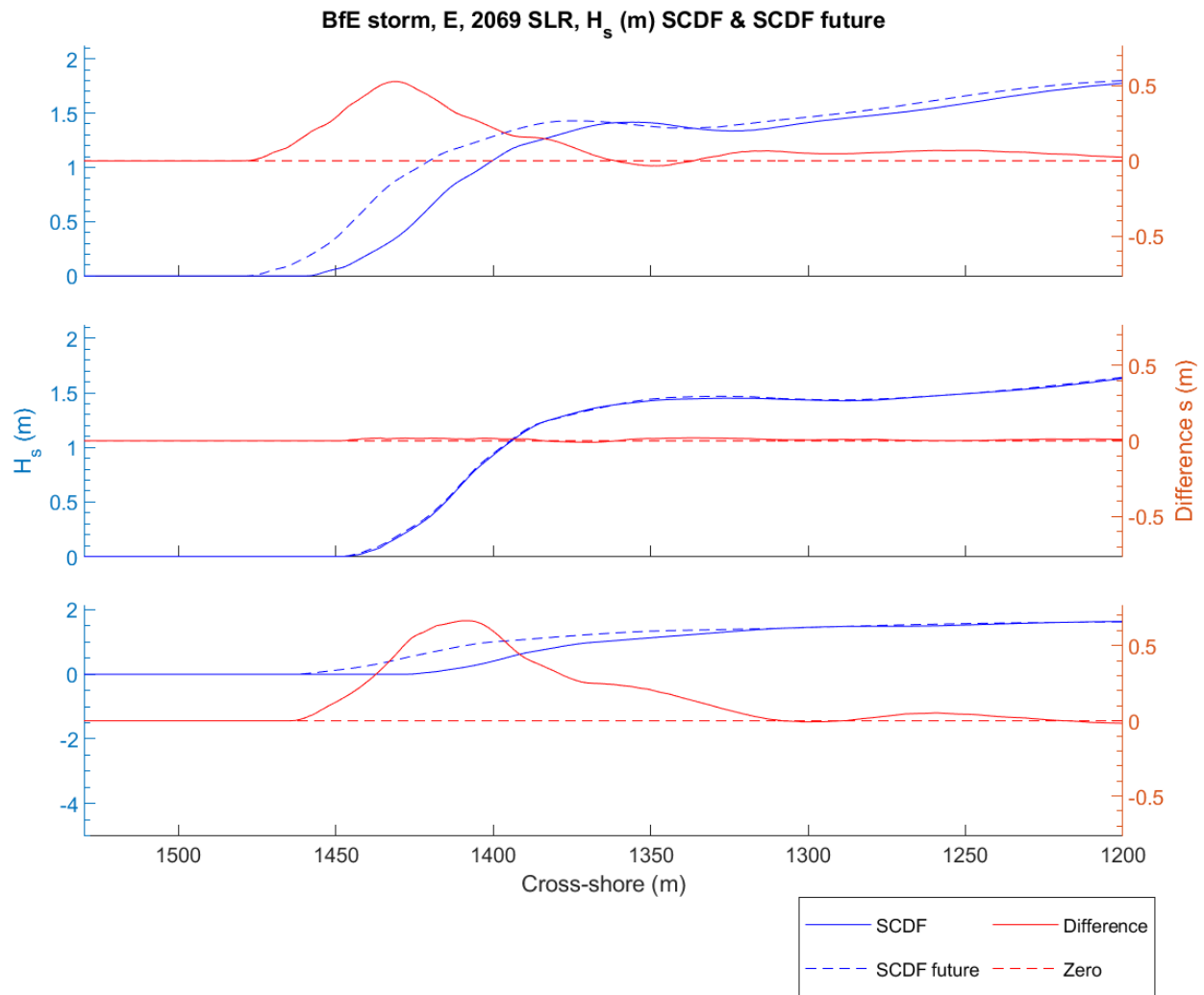


Figure E-2. Beast from the East storm, 2069 Sea Level – Average wave height over the simulation for the SCDF, SCDF-future and the difference between the SCDF and SCDF-future average wave height. Plots show profiles  $Y_1$  (top),  $Y_2$  (middle) and  $Y_3$  (bottom), indicated as red lines in the figure above.

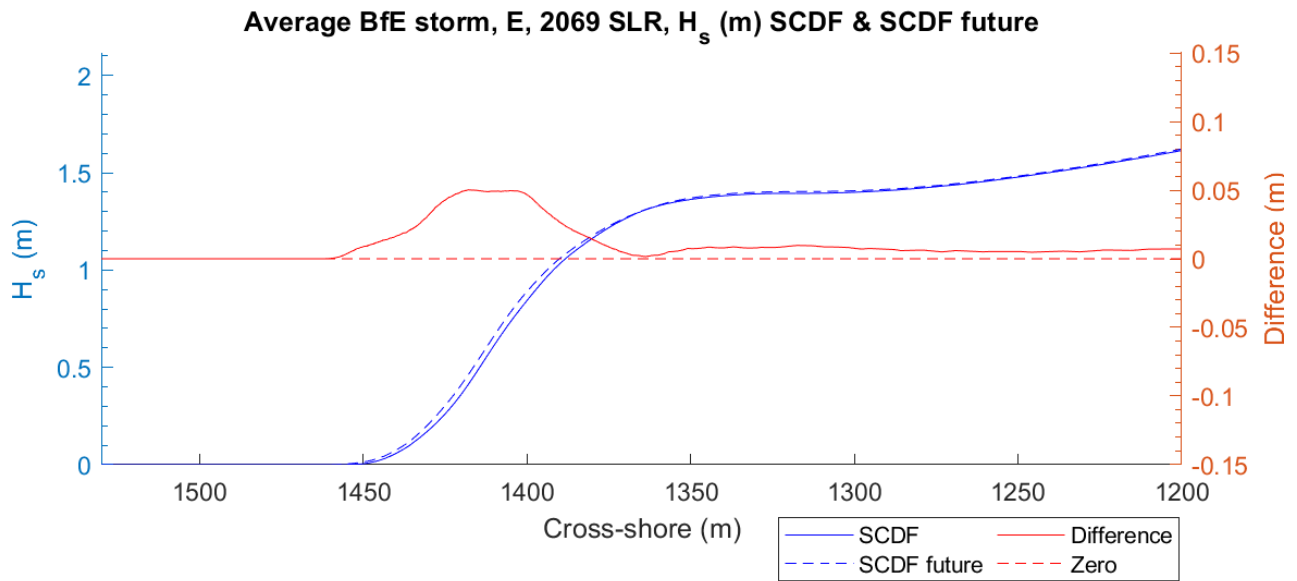


Figure E-3. Beast from the East storm, 2069 Sea Level – Average wave heights over the simulation for the SCDF and SCDF-future averaged along the frontage of the SCDF ( $Y_{average}$ ), and the difference between the SCDF and SCDF-future average wave heights.



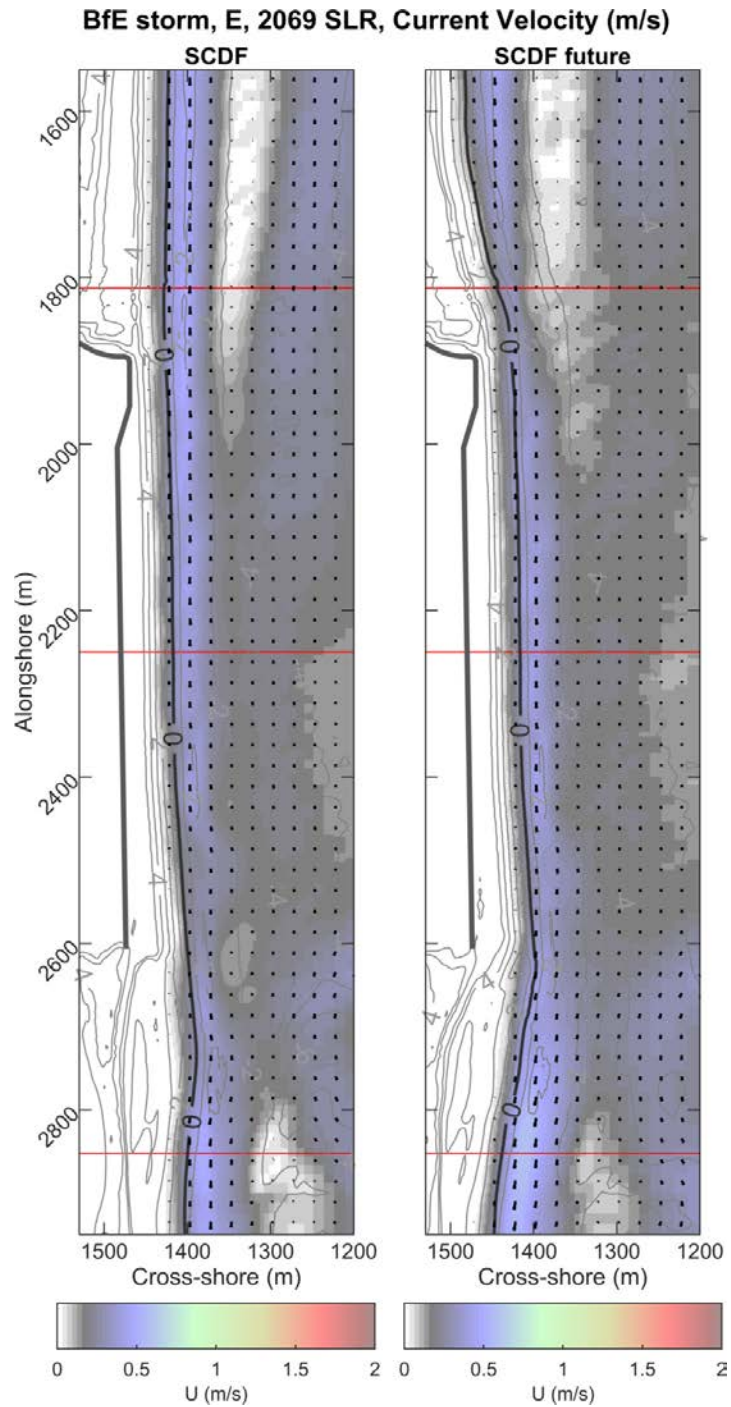


Figure E-4. Beast from the East storm, 2069 Sea Level – 2D average current velocities over the simulation for the SCDF (left) and SCDF-future (right). The red lines indicate the locations of the cross-sectional plots presented in the figure below.

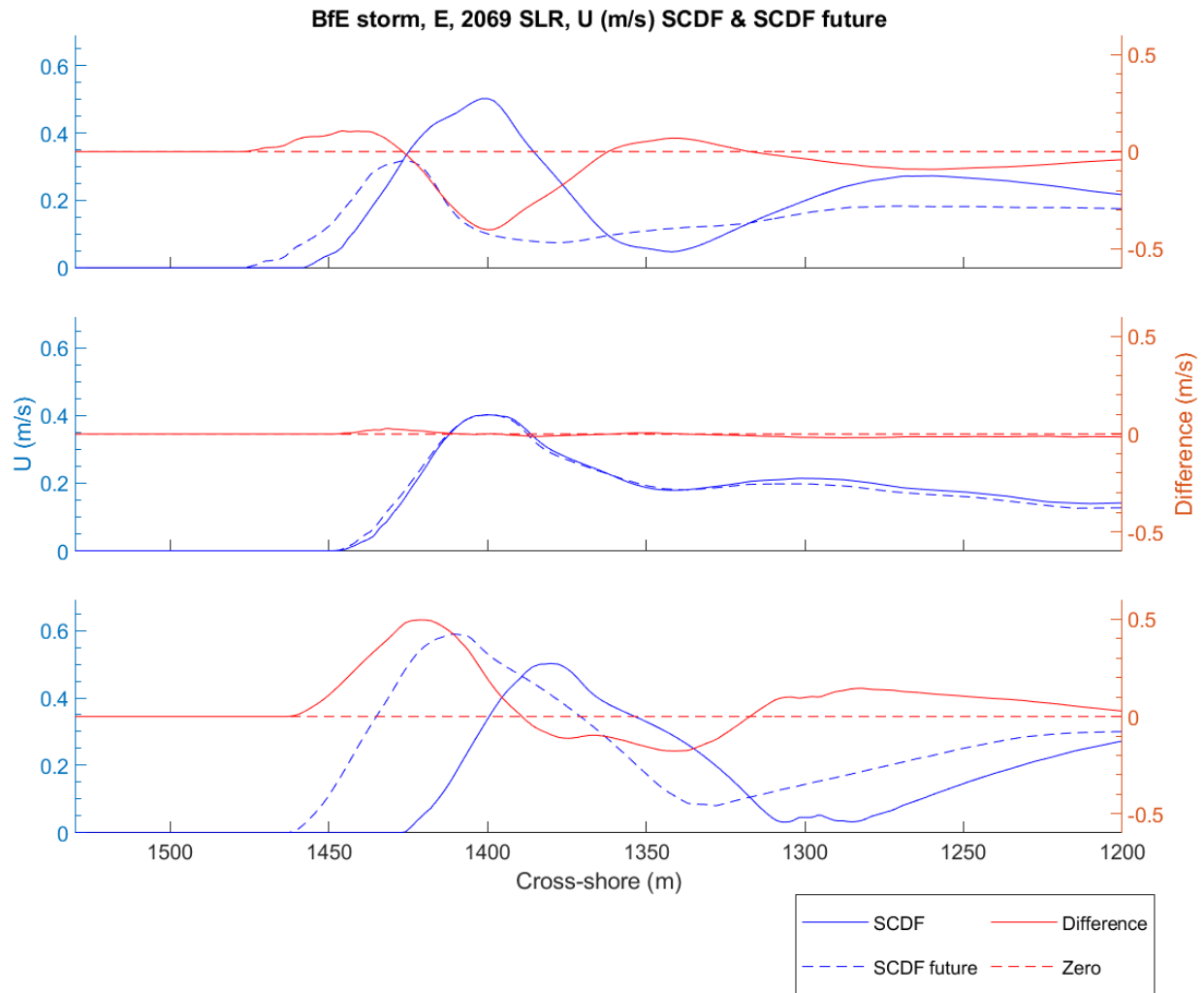


Figure E-5. Beast from the East storm, 2069 Sea Level – Average current speeds over the simulation for the SCDF, SCDF-future and the difference between the SCDF and SCDF-future average current speeds. Plots show profiles Y<sub>1</sub> (top), Y<sub>2</sub> (middle) and Y<sub>3</sub> (bottom), indicated as red lines in figure above.

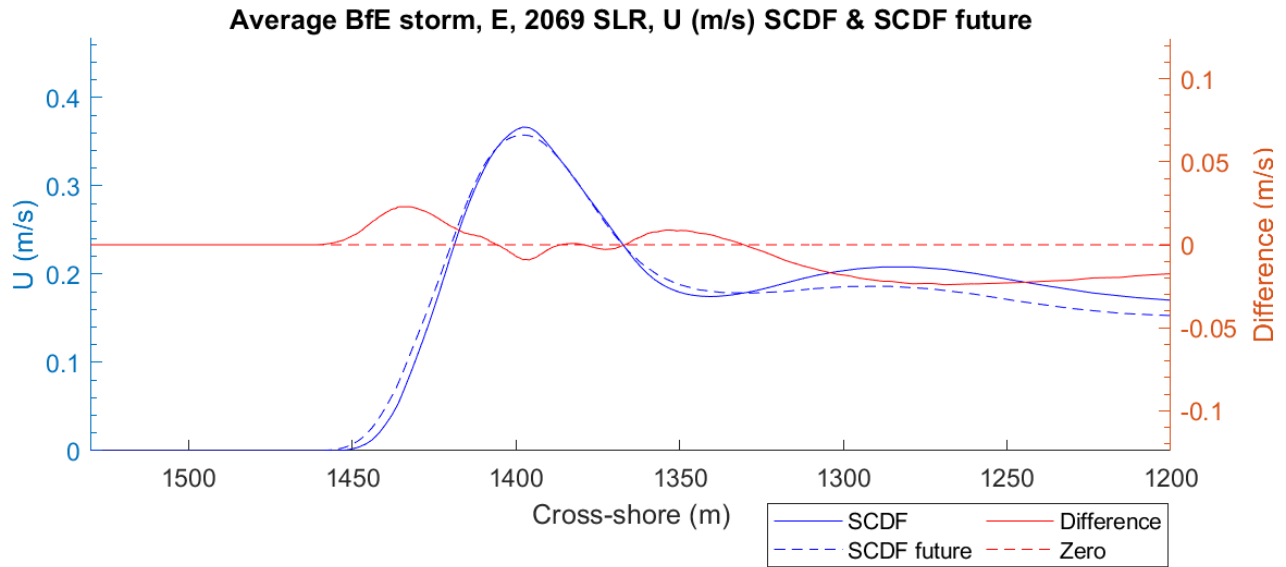


Figure E-6. Beast from the East storm, 2069 Sea Level – Average current speeds over the simulation for the SCDF and SCDF-future averaged along the frontage of the SCDF ( $Y_{average}$ ), and the difference between the SCDF and SCDF-future average current speeds.

BfE storm, E, 2069 SLR, Bed Shear Stress ( $\text{N/m}^2$ ) and Sediment Flux ( $\text{m}^2/\text{s}$ )

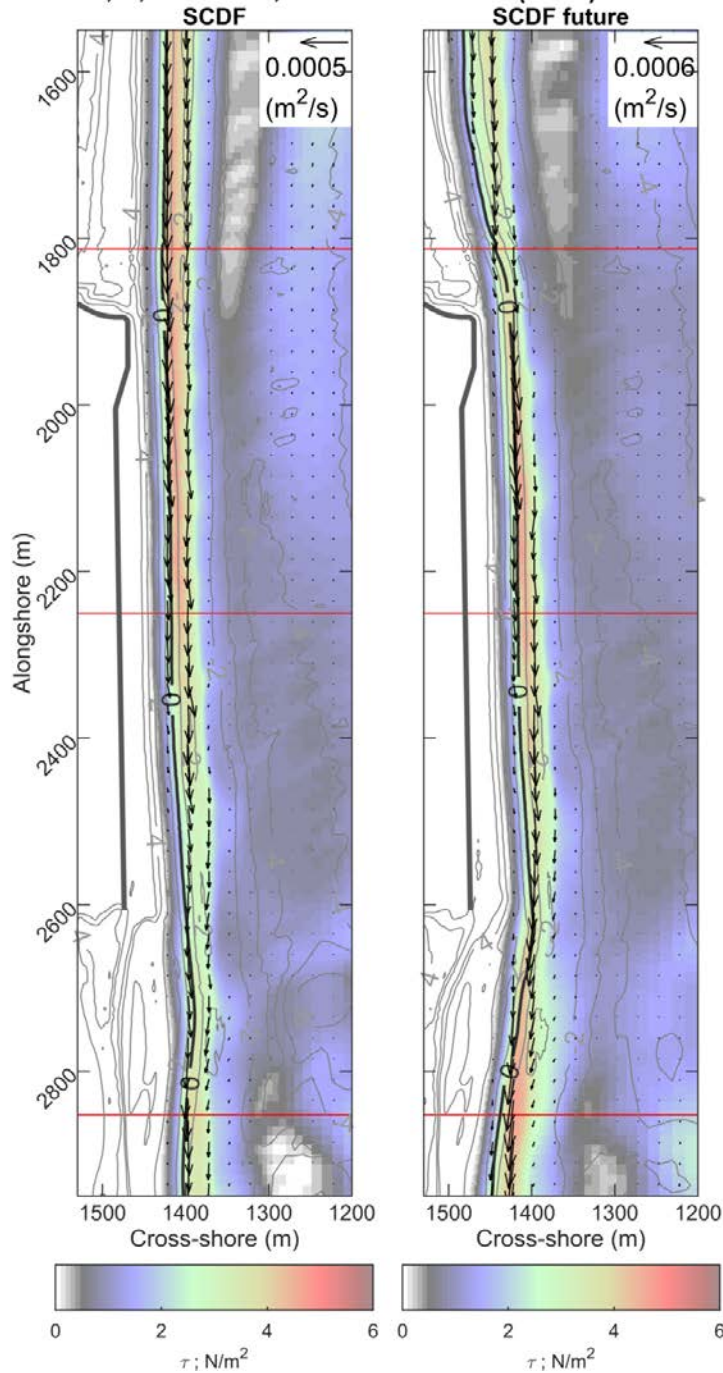


Figure E-7. Beast from the East storm, 2069 Sea Level – 2D average bed shear stress and sediment flux over the simulation for the SCDF (left) and SCDF-future (right). The red lines indicate the locations of the cross-sectional plots presented in the figure below.

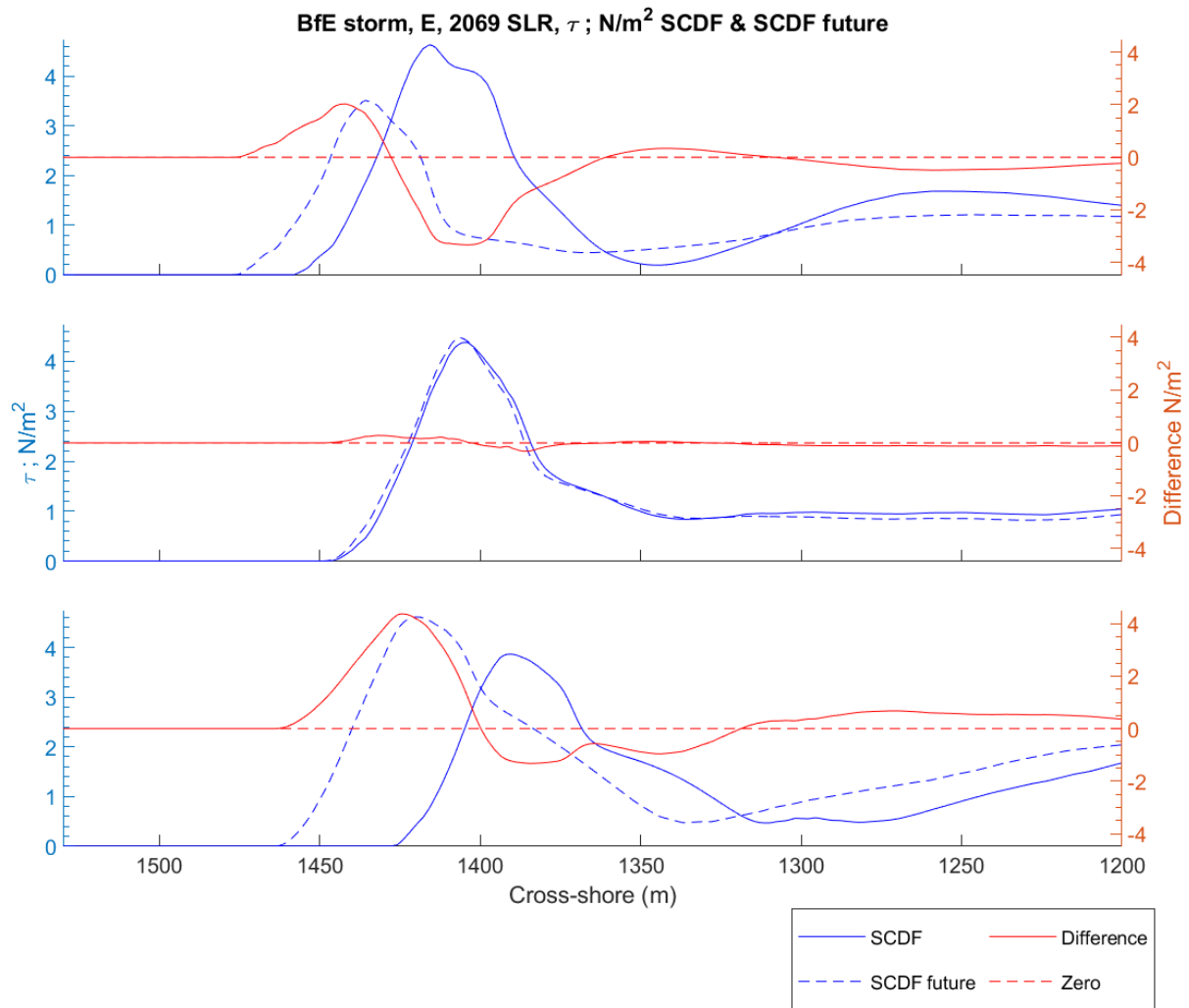


Figure E-8. Beast from the East storm, 2069 Sea Level – Average bed shear stress over the simulation for the SCDF, SCDF-future and the difference between the SCDF and SCDF-future average bed shear stress. Plots show profiles  $Y_1$  (top),  $Y_2$  (middle) and  $Y_3$  (bottom), indicated as red lines in the figure above.

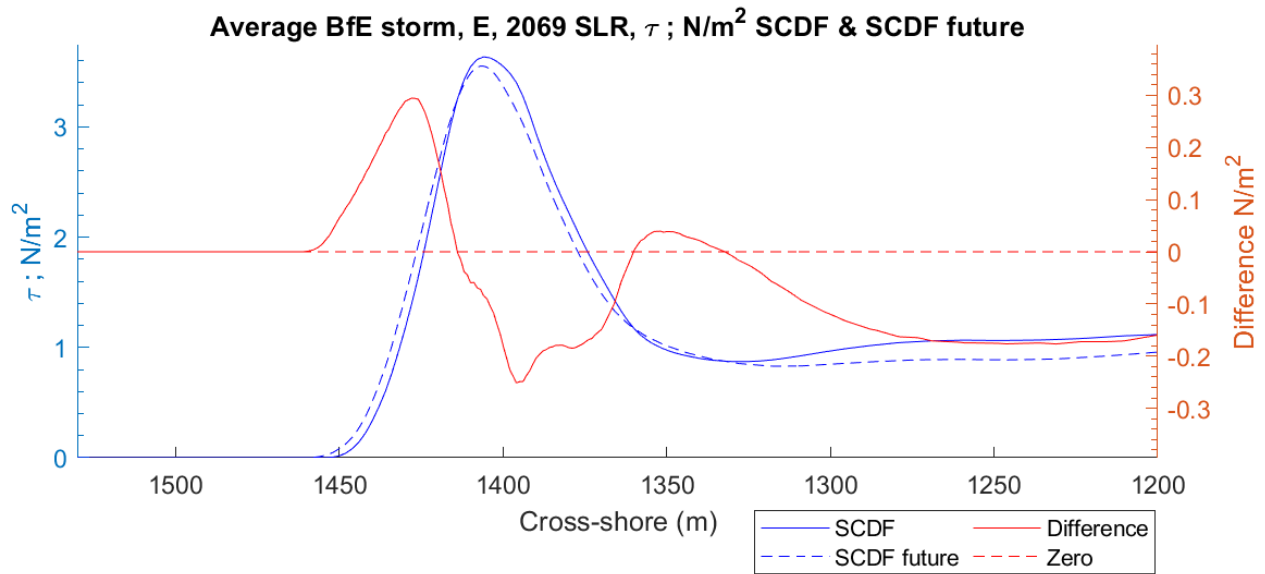


Figure E-9. Beast from the East storm, 2069 Sea Level – Average bed shear stress over the simulation for the SCDF and SCDF-future averaged along the frontage of the SCDF ( $Y_{average}$ ), and the difference between the SCDF and SCDF-future average bed shear stress.

### E.1.2 Beast from the East Storm, 2099 Sea Level

The Beast from the East Storm, 2099 Sea Level Rise results averaged over the entire simulation for the SCDF and SCDF future case are presented here. Figure E-10 – Figure E-12 show the average wave height results. Figure E-13 – Figure E-15 show the current speed/ velocity results. Figure E-16 – Figure E-18 show the bed shear stress and sediment flux results.



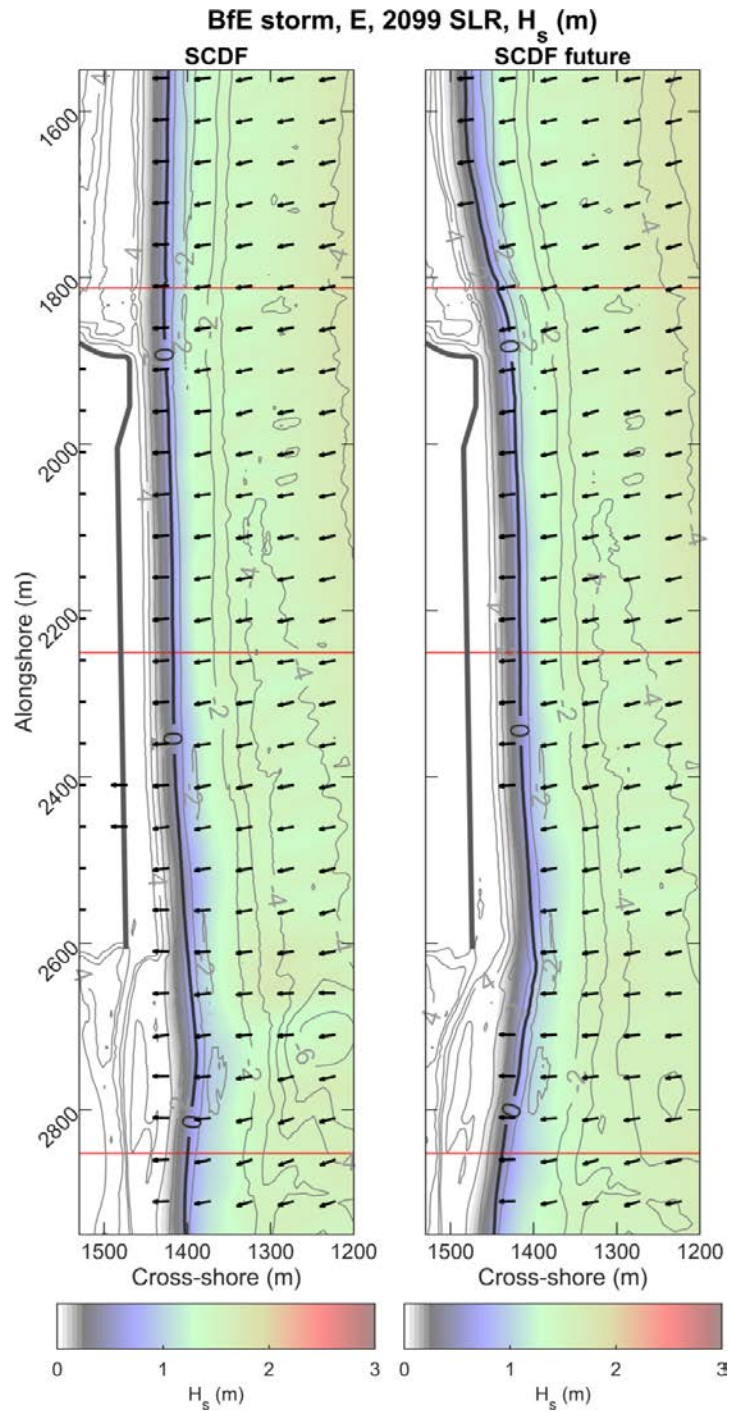


Figure E-10. Beast from the East storm, 2099 Sea Level – 2D average wave heights over the simulation for the SCDF (left) and SCDF-future (right). The red lines indicate the locations of the cross-sectional plots presented in the figure below.

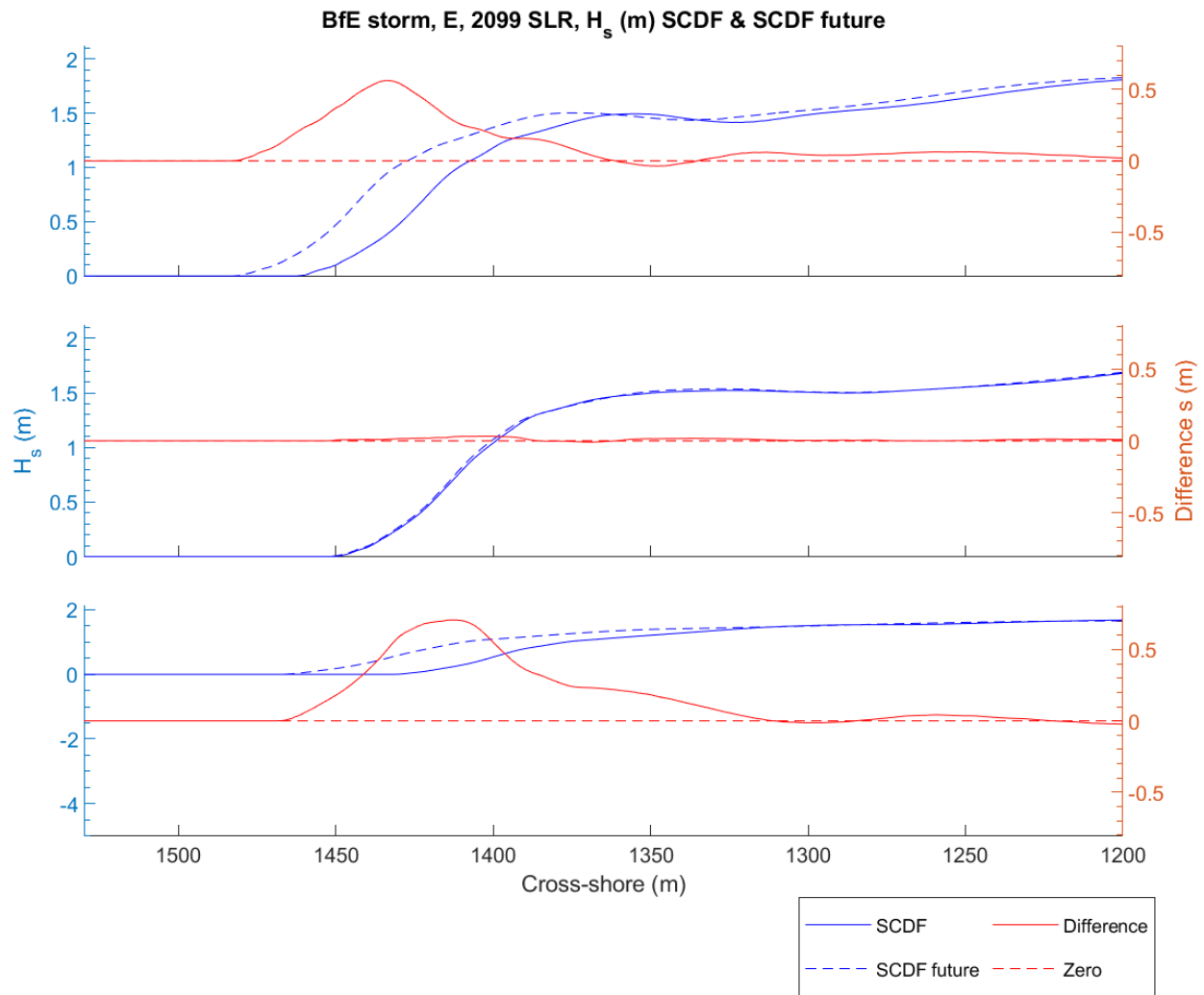


Figure E-11. Beast from the East storm, 2099 Sea Level – Average wave height over the simulation for the SCDF, SCDF-future and the difference between the SCDF and SCDF-future average wave height. Plots show profiles  $Y_1$  (top),  $Y_2$  (middle) and  $Y_3$  (bottom), indicated as red lines in the figure above.

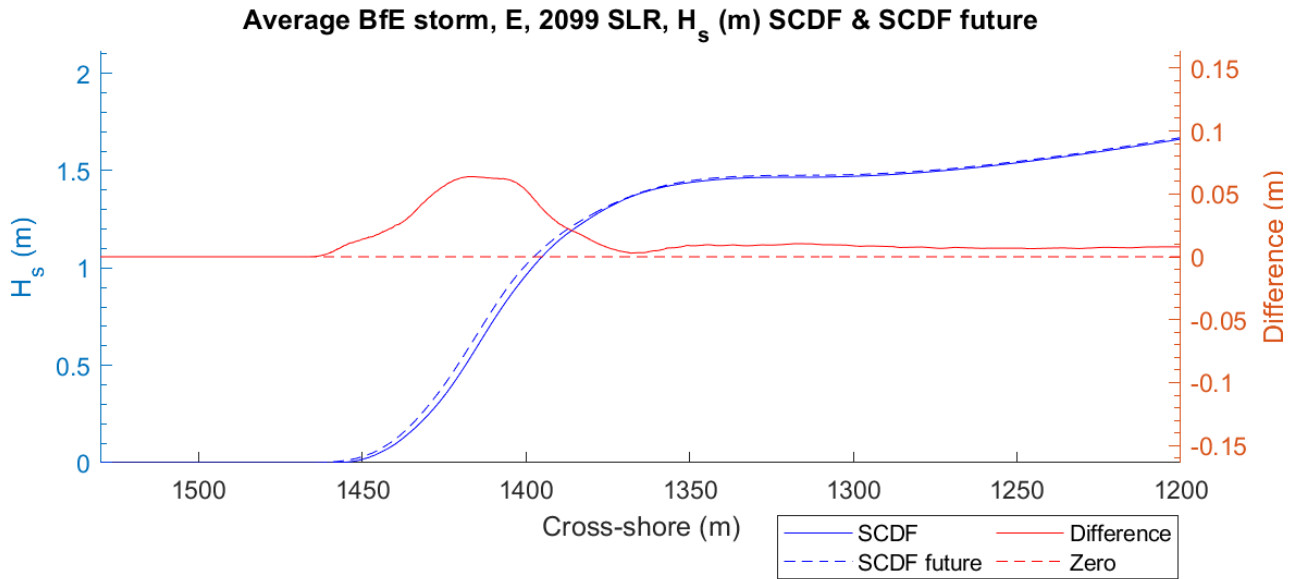


Figure E-12. Beast from the East storm, 2099 Sea Level – Average wave heights over the simulation for the SCDF and SCDF-future averaged along the frontage of the SCDF ( $Y_{average}$ ), and the difference between the SCDF and SCDF-future average wave heights.

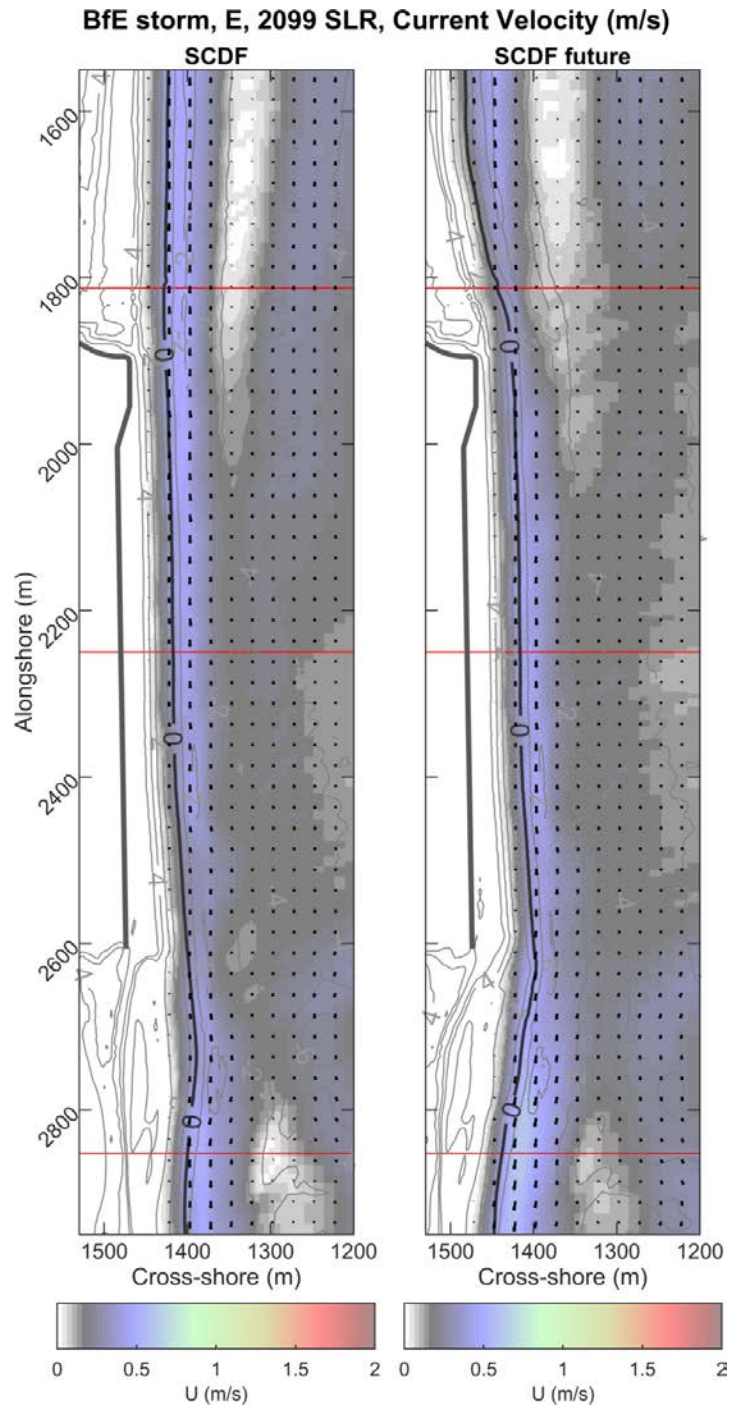


Figure E-13. Beast from the East storm, 2099 Sea Level – 2D average current velocities over the simulation for the SCDF (left) and SCDF-future (right). The red lines indicate the locations of the cross-sectional plots presented in the figure below.

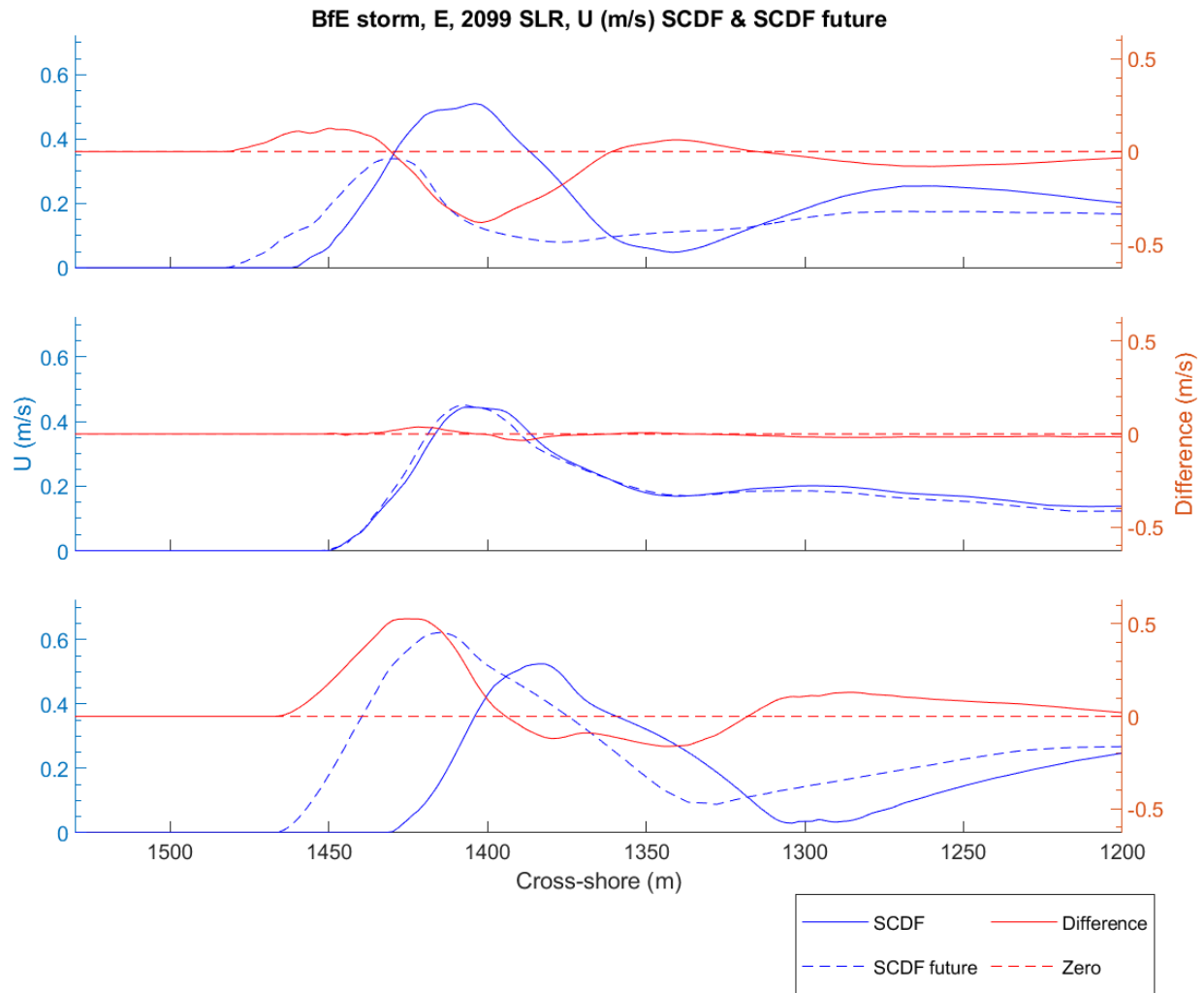


Figure E-14. Beast from the East storm, 2099 Sea Level – Average current speeds over the simulation for the SCDF, SCDF-future and the difference between the SCDF and SCDF-future average current speeds. Plots show profiles  $Y_1$  (top),  $Y_2$  (middle) and  $Y_3$  (bottom), indicated as red lines in figure above.

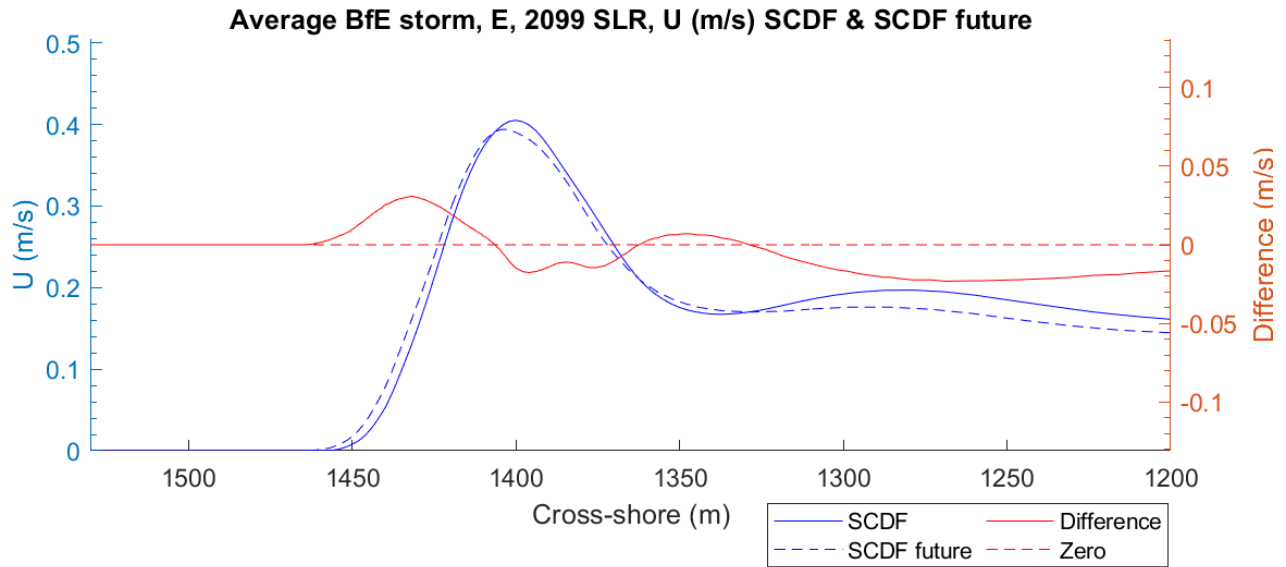


Figure E-15. Beast from the East storm, 2099 Sea Level – Average current speeds over the simulation for the SCDF and SCDF-future averaged along the frontage of the SCDF ( $Y_{average}$ ), and the difference between the SCDF and SCDF-future average current speeds.



BfE storm, E, 2099 SLR, Bed Shear Stress ( $\text{N/m}^2$ ) and Sediment Flux ( $\text{m}^2/\text{s}$ )

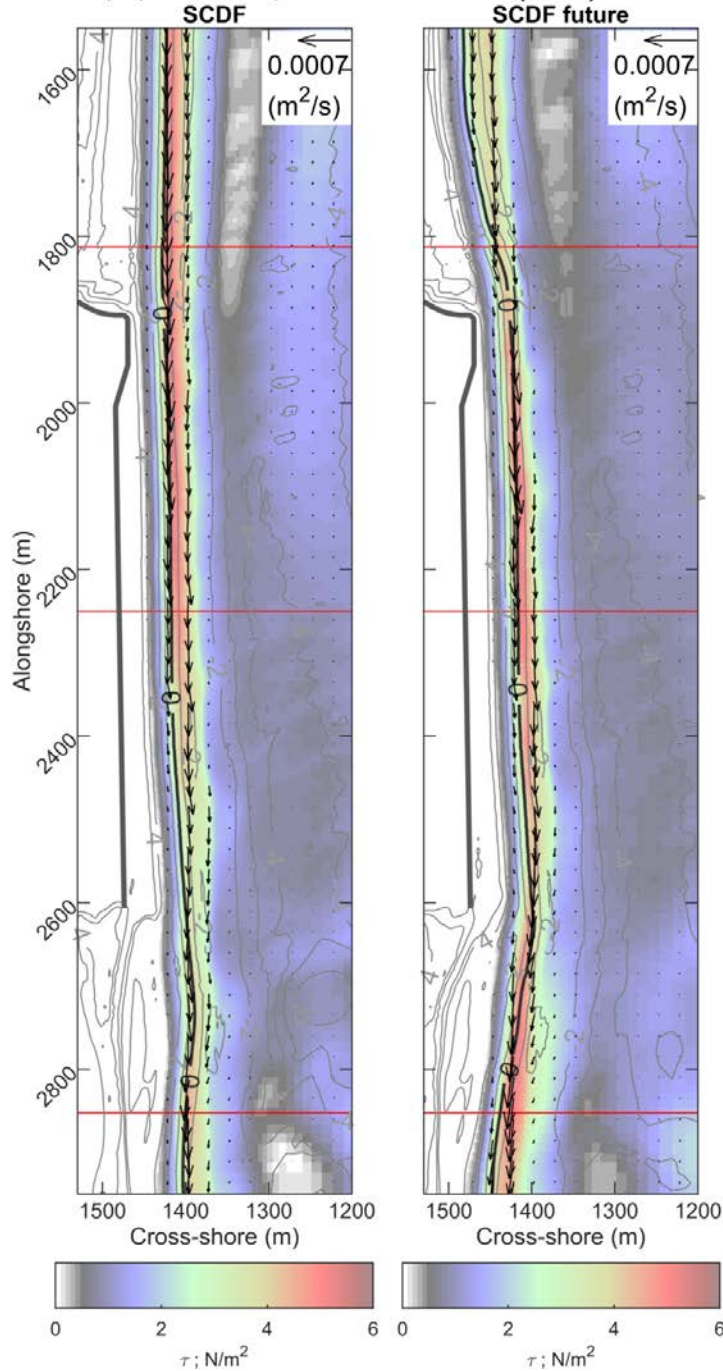


Figure E-16. Beast from the East storm, 2099 Sea Level – 2D average bed shear stress and sediment flux over the simulation for the SCDF (left) and SCDF-future (right). The red lines indicate the locations of the cross-sectional plots presented in the figure below.

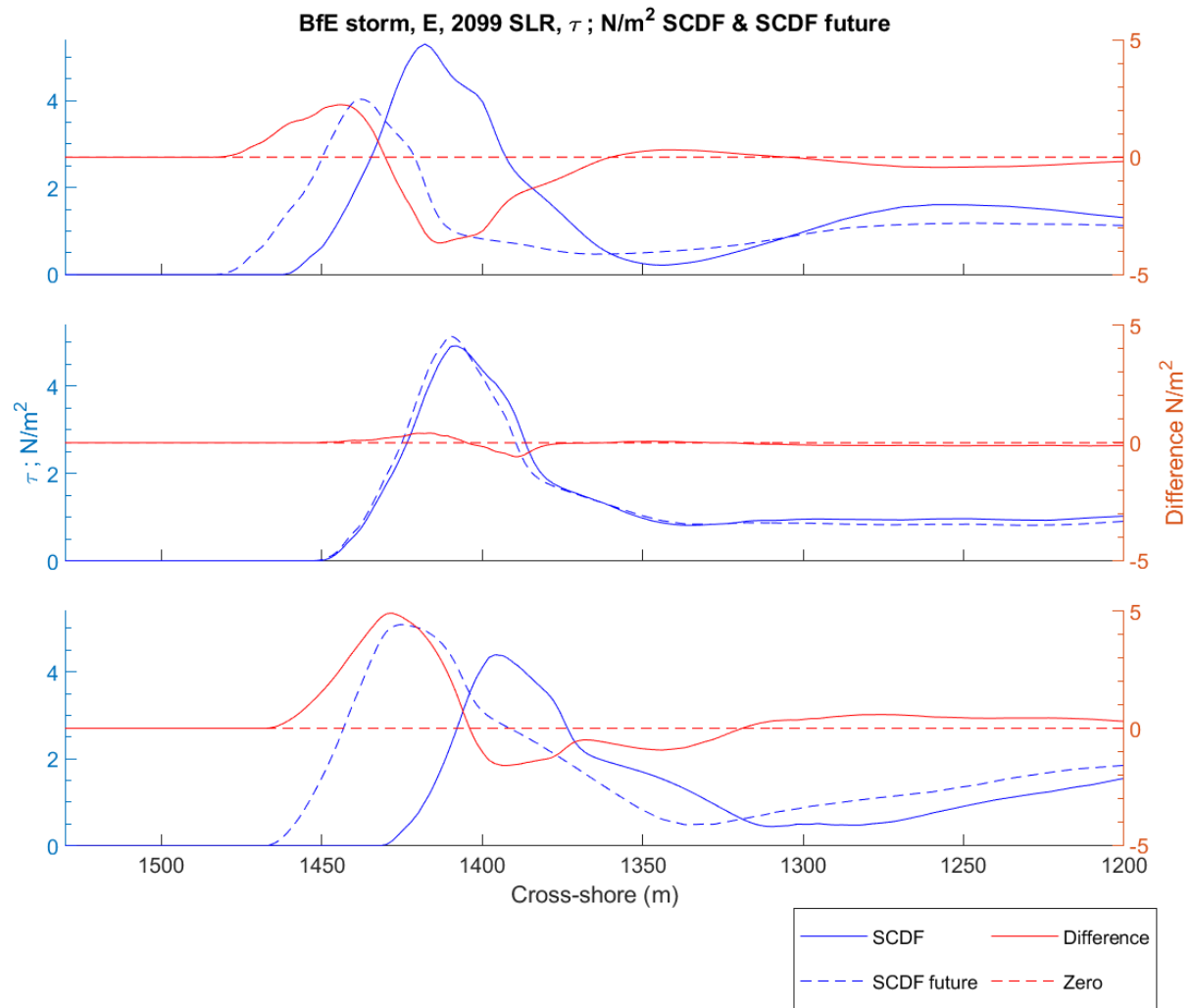


Figure E-17. Beast from the East storm, 2099 Sea Level – Average bed shear stress over the simulation for the SCDF, SCDF-future and the difference between the SCDF and SCDF-future average bed shear stress. Plots show profiles  $Y_1$  (top),  $Y_2$  (middle) and  $Y_3$  (bottom), indicated as red lines in the figure above.

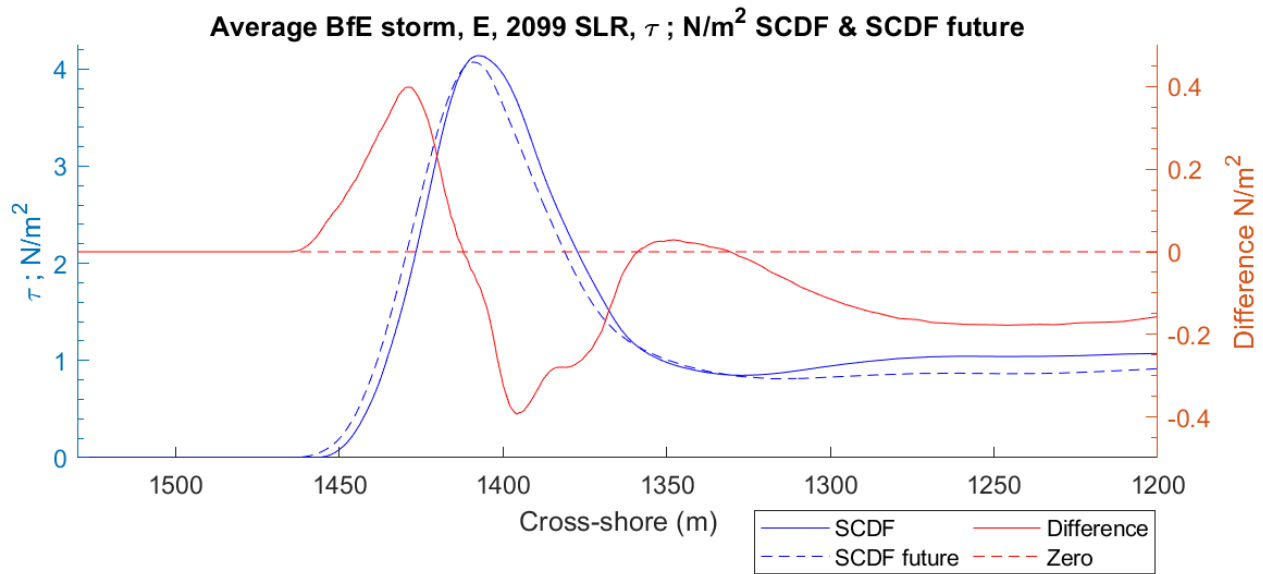


Figure E-18. Beast from the East storm, 2099 Sea Level – Average bed shear stress over the simulation for the SCDF and SCDF-future averaged along the frontage of the SCDF ( $Y_{average}$ ), and the difference between the SCDF and SCDF-future average bed shear stress.

### E.1.3 North East 1-in-20 Year Storm, 2099 Sea Level

The North East 1-in-20 Year Storm, 2099 Sea Level Rise results averaged over the entire simulation for the SCDF and SCDF future case are presented here. Figure E-19 – Figure E-21 show the average wave height results. Figure E-22 – Figure E-24 show the current speed/ velocity results. Figure E-25 – Figure E-27 show the bed shear stress and sediment flux results.

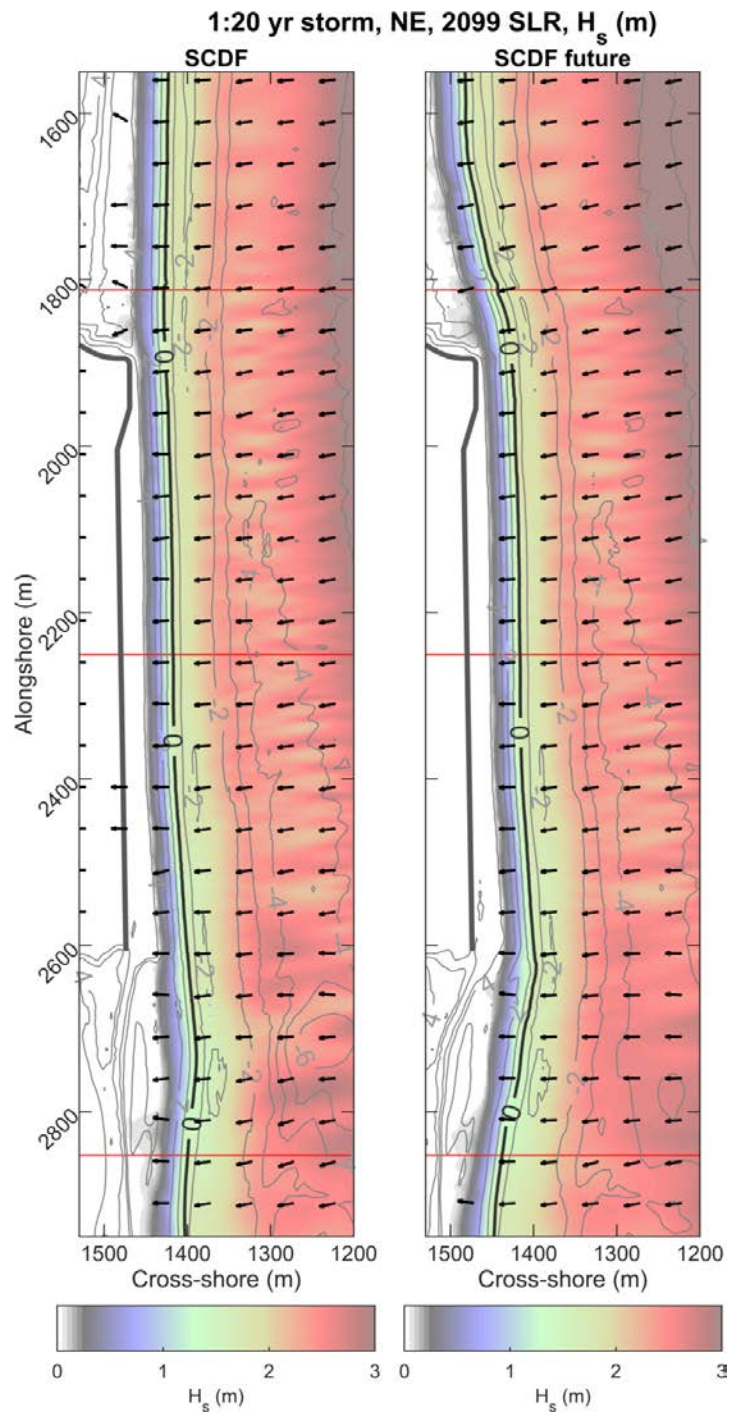


Figure E-19. North East 1-in-20 year storm, 2099 Sea Level – 2D average wave heights over the simulation for the SCDF (left) and SCDF-future (right). The red lines indicate the locations of the cross-sectional plots presented in the figure below.

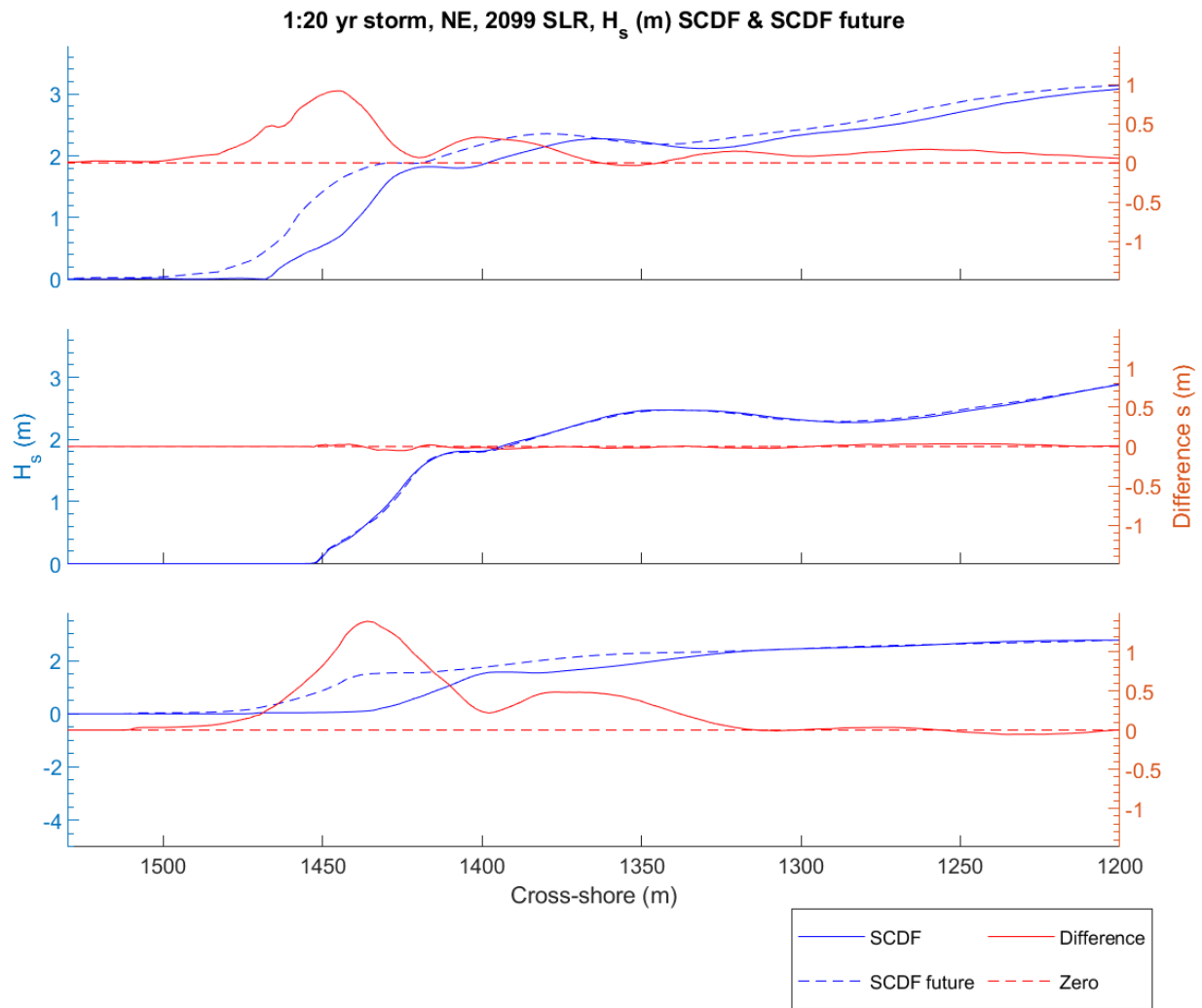


Figure E-20. North East 1-in-20 year storm, 2099 Sea Level – Average wave height over the simulation for the SCDF, SCDF-future and the difference between the SCDF and SCDF-future average wave height. Plots show profiles Y<sub>1</sub> (top), Y<sub>2</sub> (middle) and Y<sub>3</sub> (bottom), indicated as red lines in the figure above.

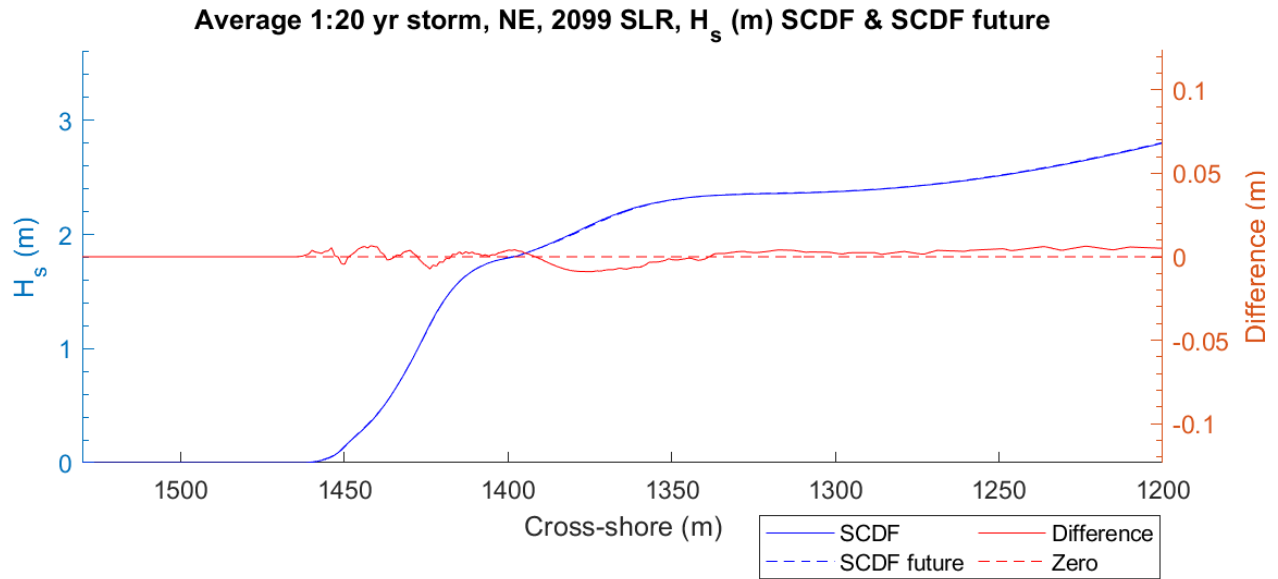


Figure E-21. North East 1-in-20 year storm, 2099 Sea Level – Average wave heights over the simulation for the SCDF and SCDF-future averaged along the frontage of the SCDF ( $Y_{average}$ ), and the difference between the SCDF and SCDF-future average wave heights.



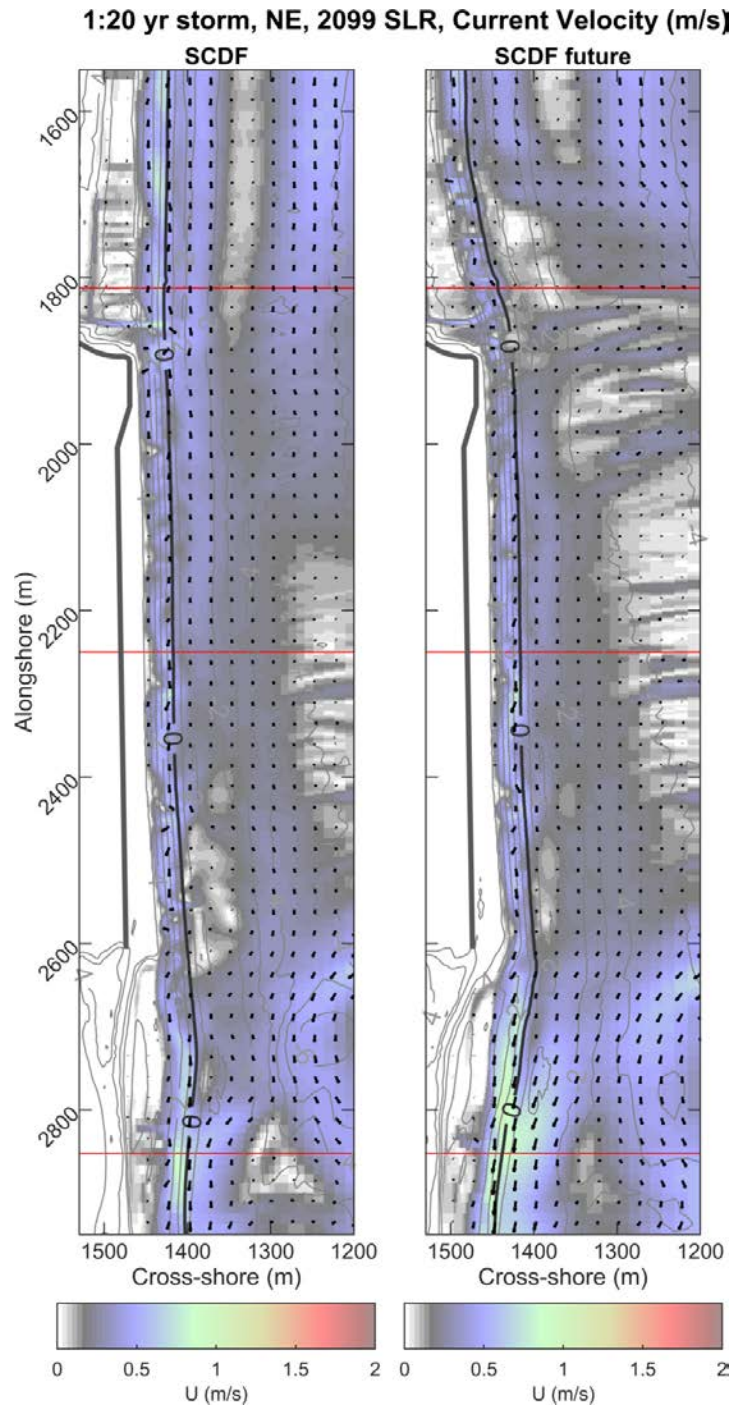


Figure E-22. North East 1-in-20 year storm, 2099 Sea Level – 2D average current velocities over the simulation for the SCDF (left) and SCDF-future (right). The red lines indicate the locations of the cross-sectional plots presented in the figure below.

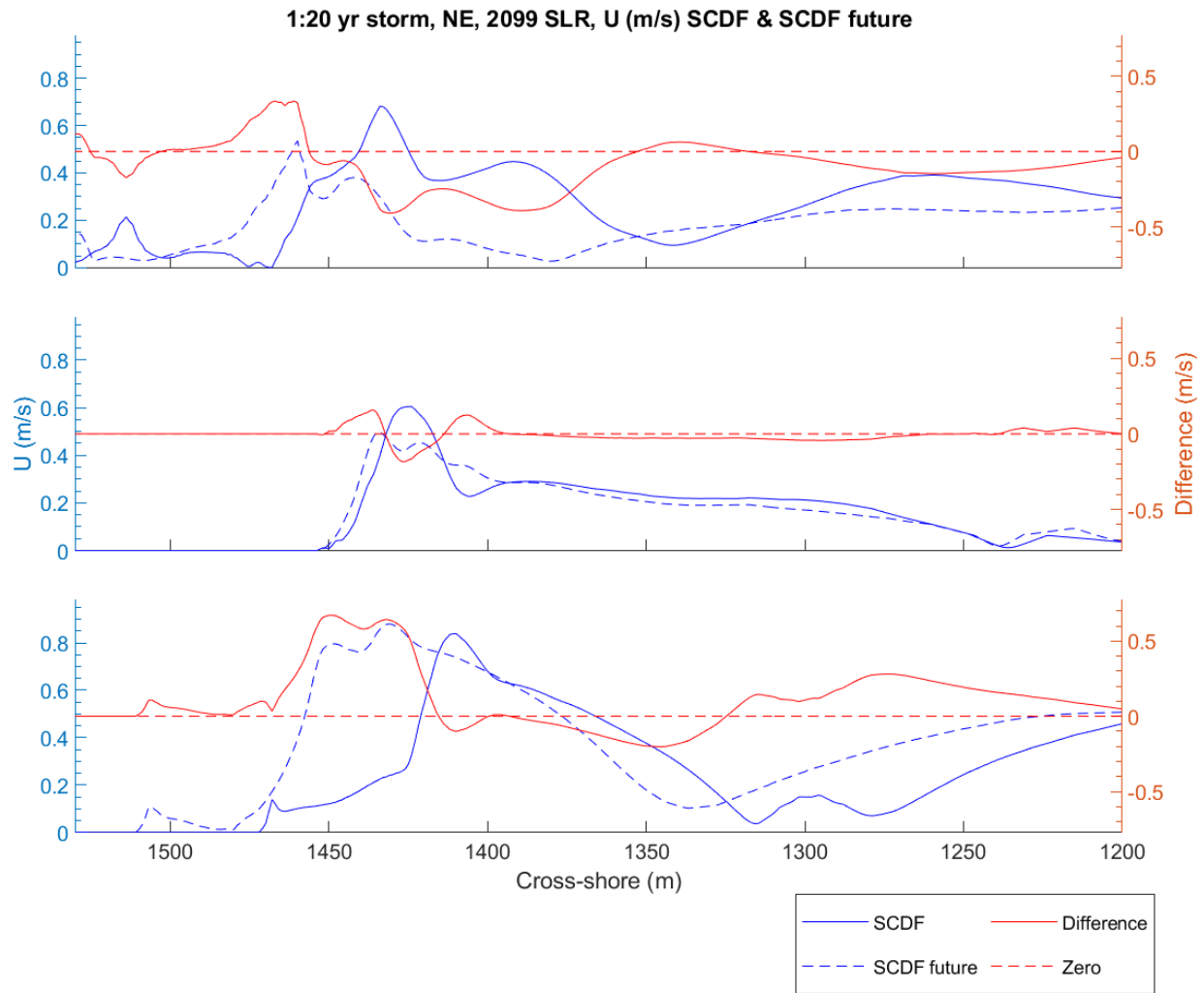


Figure E-23. North East 1-in-20 year storm, 2099 Sea Level – Average current speeds over the simulation for the SCDF, SCDF-future and the difference between the SCDF and SCDF-future average current speeds. Plots show profiles  $Y_1$  (top),  $Y_2$  (middle) and  $Y_3$  (bottom), indicated as red lines in figure above.

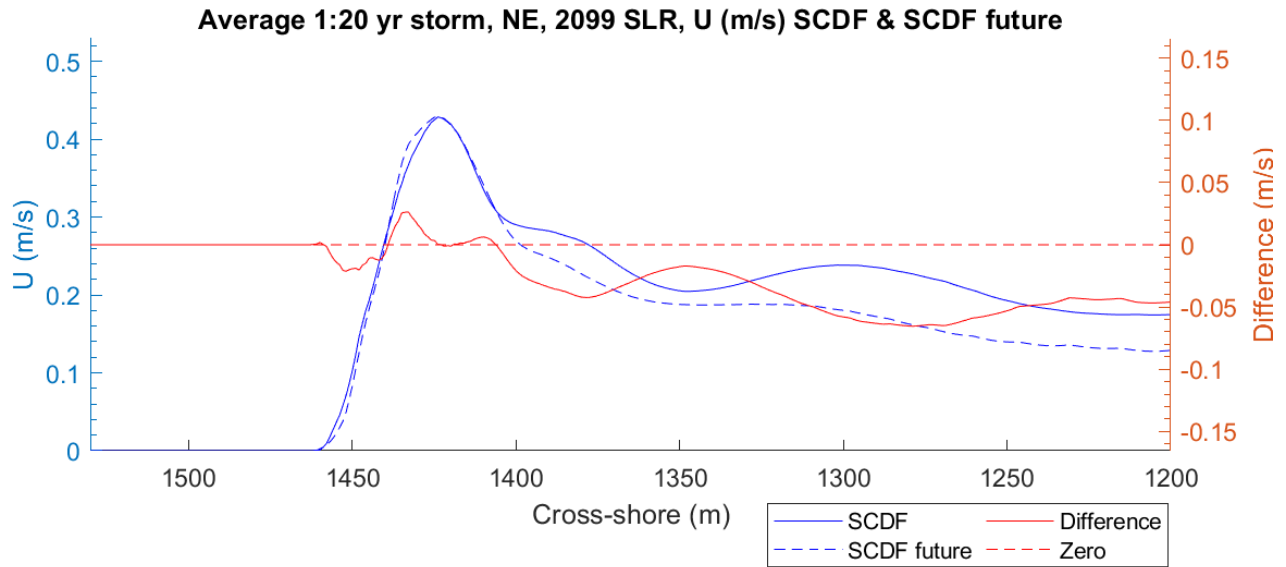


Figure E-24. North East 1-in-20 year storm, 2099 Sea Level – Average current speeds over the simulation for the SCDF and SCDF-future averaged along the frontage of the SCDF ( $Y_{average}$ ), and the difference between the SCDF and SCDF-future average current speeds.

1:20 yr storm, NE, 2099 SLR, Bed Shear Stress ( $\text{N/m}^2$ ) and Sediment Flux ( $\text{m}^2/\text{s}$ )

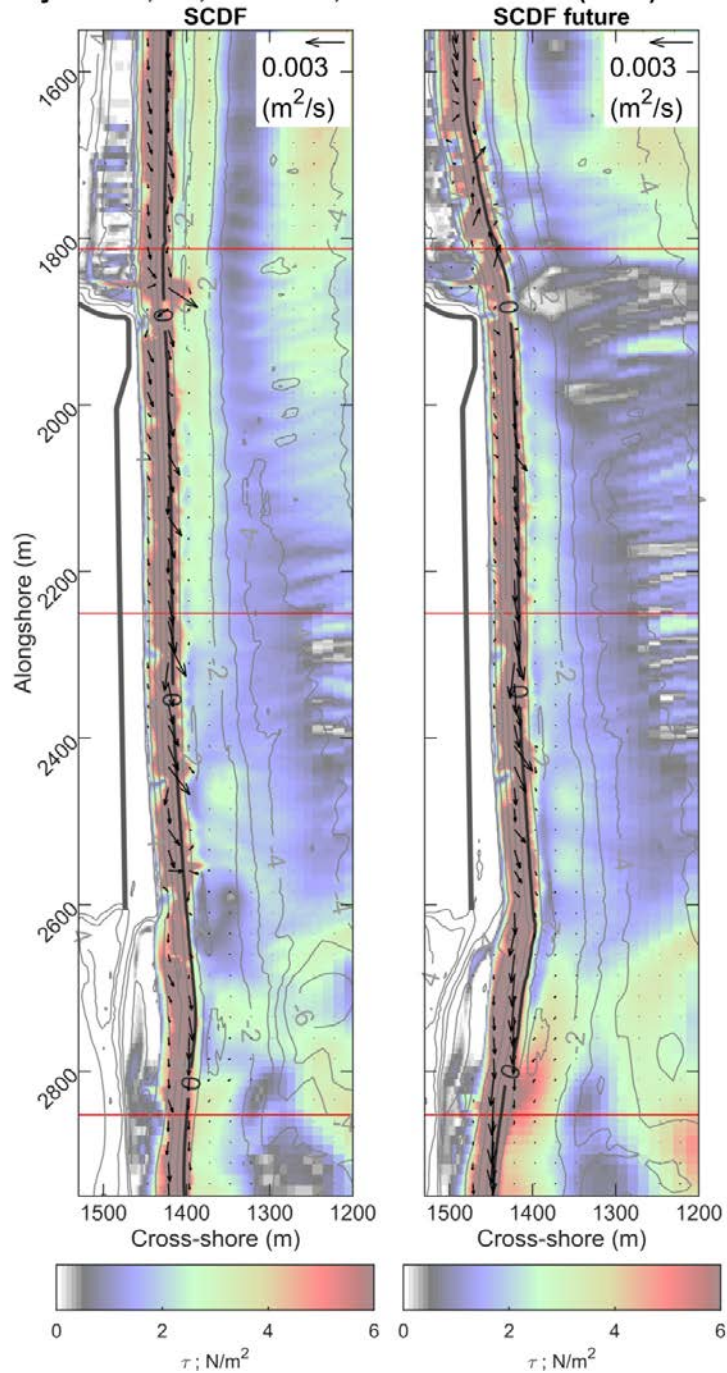


Figure E-25. North East 1-in-20 year storm, 2099 Sea Level – 2D average bed shear stress and sediment flux over the simulation for the SCDF (left) and SCDF-future (right). The red lines indicate the locations of the cross-sectional plots presented in the figure below.

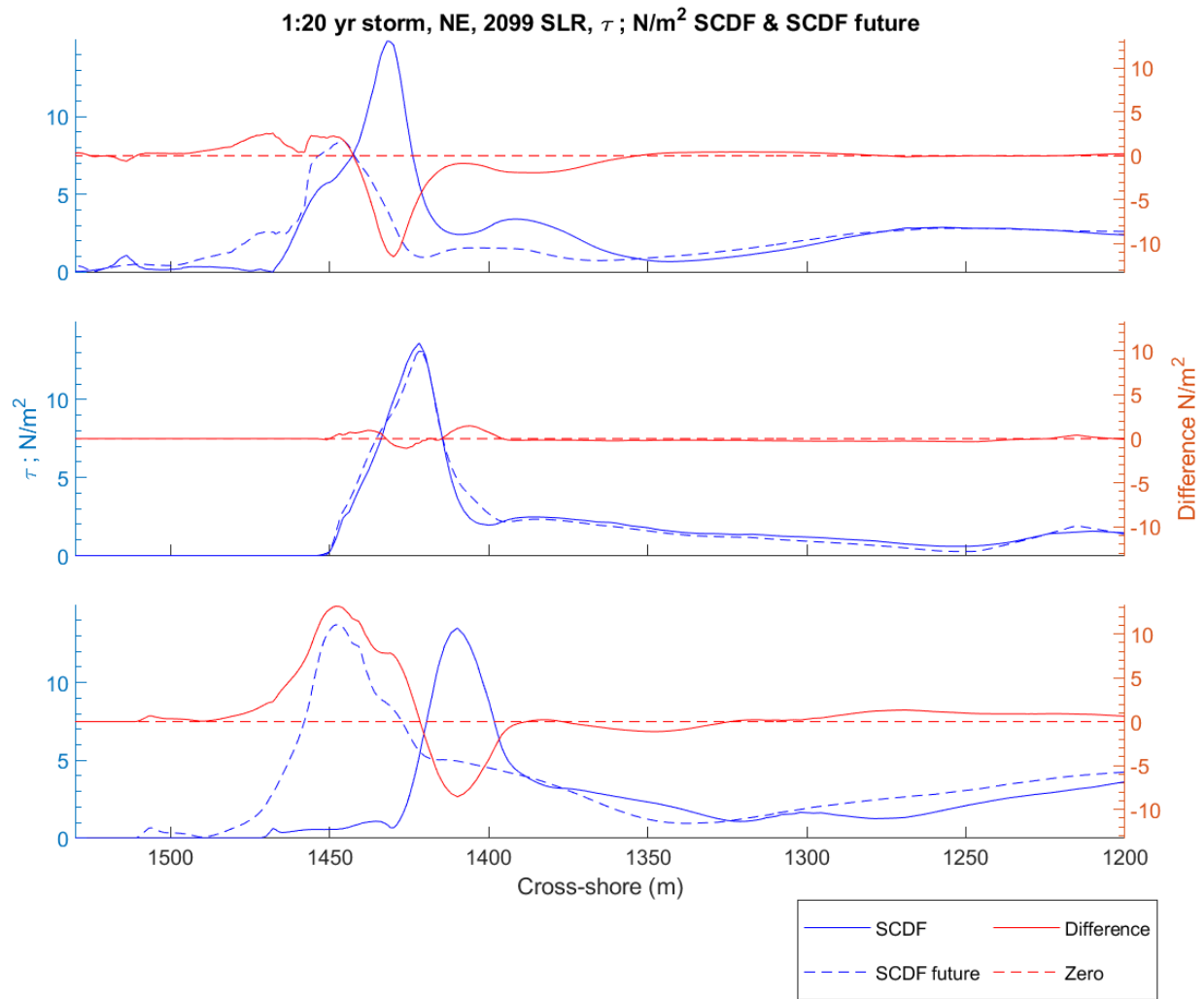


Figure E-26. North East 1-in-20 year storm, 2099 Sea Level – Average bed shear stress over the simulation for the SCDF, SCDF-future and the difference between the SCDF and SCDF-future average bed shear stress. Plots show profiles Y<sub>1</sub> (top), Y<sub>2</sub> (middle) and Y<sub>3</sub> (bottom), indicated as red lines in the figure above.

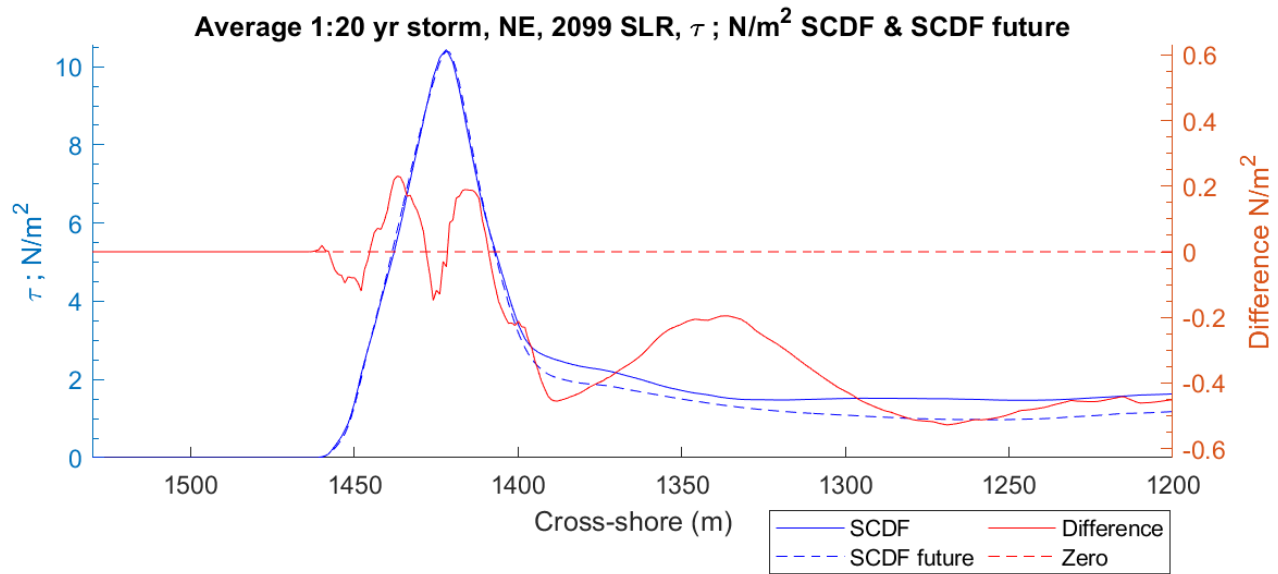


Figure E-27. North East 1-in-20 year storm, 2099 Sea Level – Average bed shear stress over the simulation for the SCDF and SCDF-future averaged along the frontage of the SCDF ( $Y_{\text{average}}$ ), and the difference between the SCDF and SCDF-future average bed shear stress.

#### E.1.4 South East 1-in-20 Year Storm, 2099 Sea Level

The South East 1-in-20 Year Storm, 2099 Sea Level Rise results averaged over the entire simulation for the SCDF and SCDF future case are presented here. Figure E-28 – Figure E-30 show the average wave height results. Figure E-31 – Figure E-33 show the current speed/ velocity results. Figure E-34 – Figure E-36 show the bed shear stress and sediment flux results.



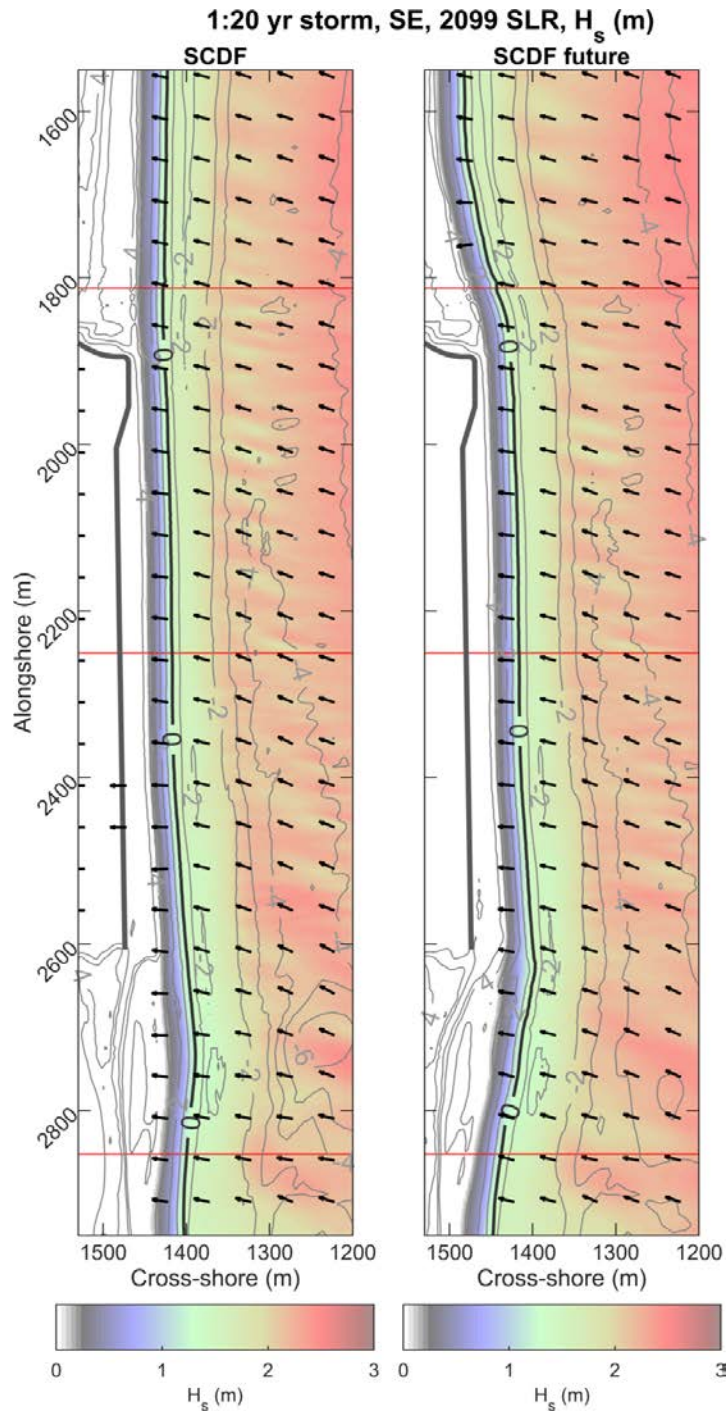


Figure E-28. South East 1-in-20 year storm, 2099 Sea Level – 2D average wave heights over the simulation for the SCDF (left) and SCDF-future (right). The red lines indicate the locations of the cross-sectional plots presented in the figure below.

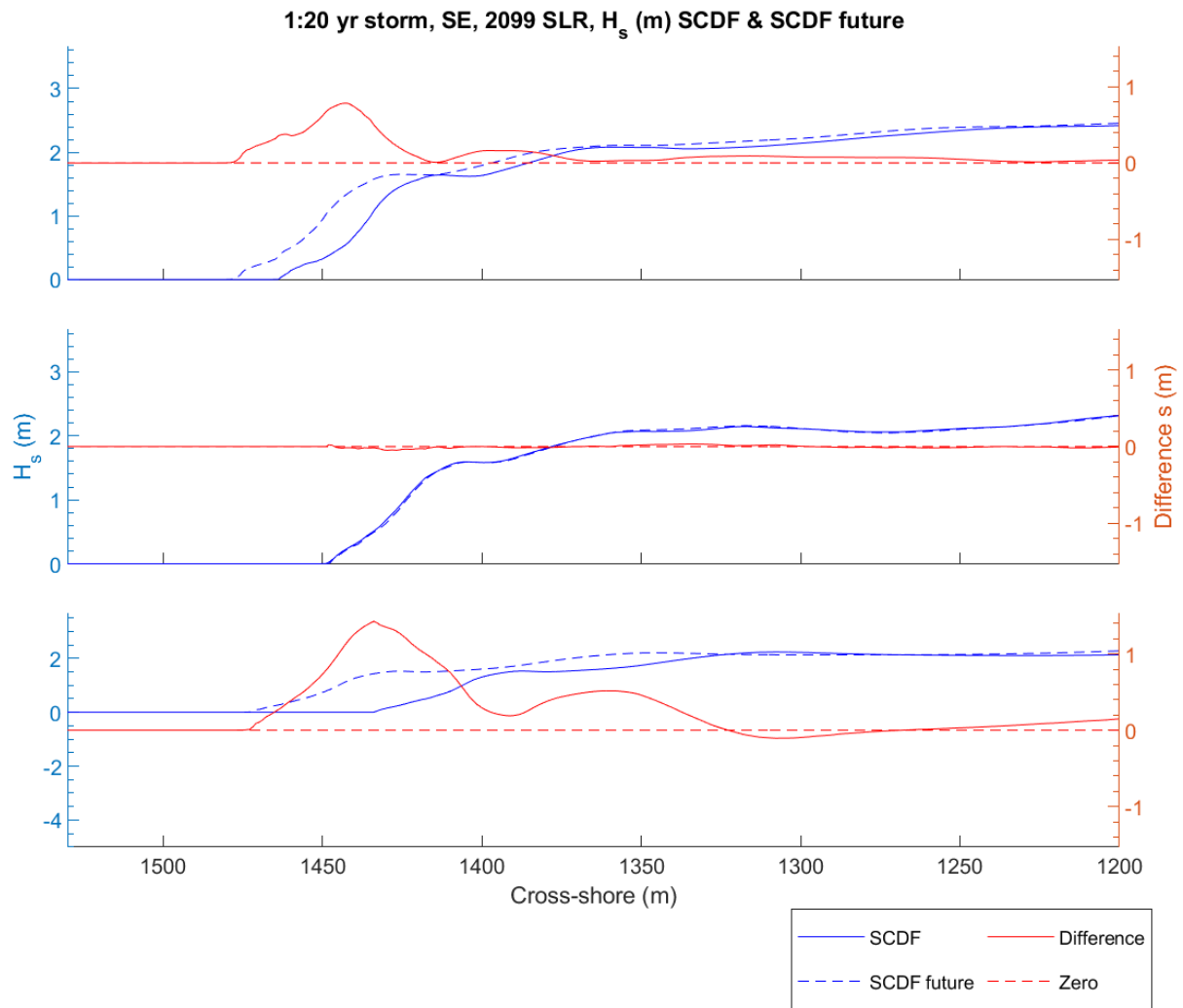


Figure E-29. South East 1-in-20 year storm, 2099 Sea Level – Average wave height over the simulation for the SCDF, SCDF-future and the difference between the SCDF and SCDF-future average wave height. Plots show profiles  $Y_1$  (top),  $Y_2$  (middle) and  $Y_3$  (bottom), indicated as red lines in the figure above.

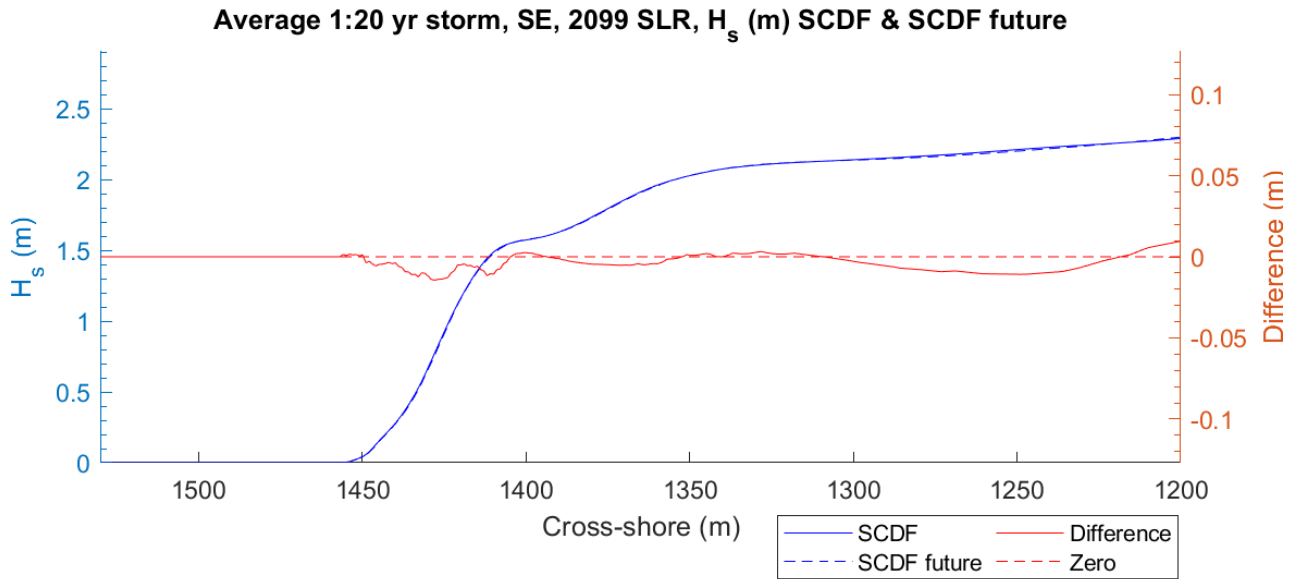


Figure E-30. South East 1-in-20 year storm, 2099 Sea Level – Average wave heights over the simulation for the SCDF and SCDF-future averaged along the frontage of the SCDF ( $Y_{average}$ ), and the difference between the SCDF and SCDF-future average wave heights.

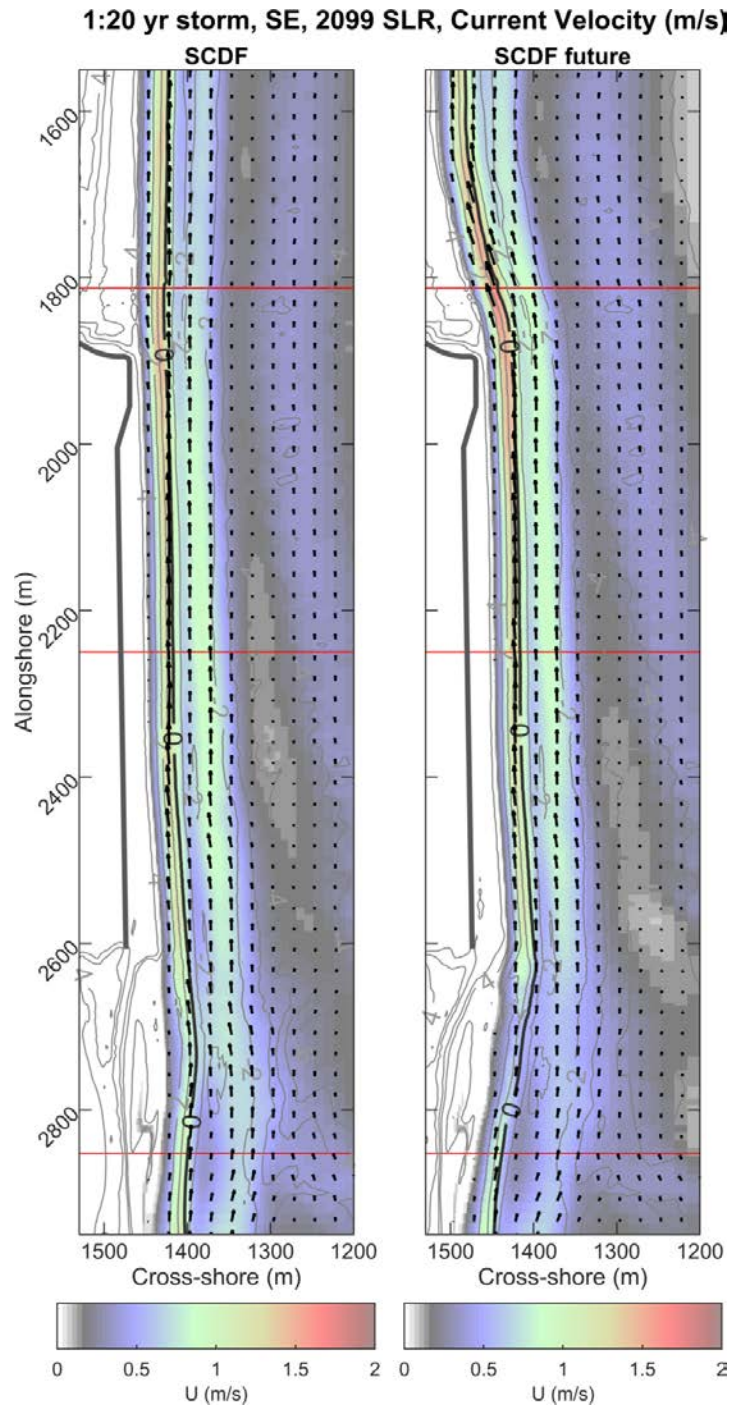


Figure E-31. South East 1-in-20 year storm, 2099 Sea Level – 2D average current velocities over the simulation for the SCDF (left) and SCDF-future (right). The red lines indicate the locations of the cross-sectional plots presented in the figure below.

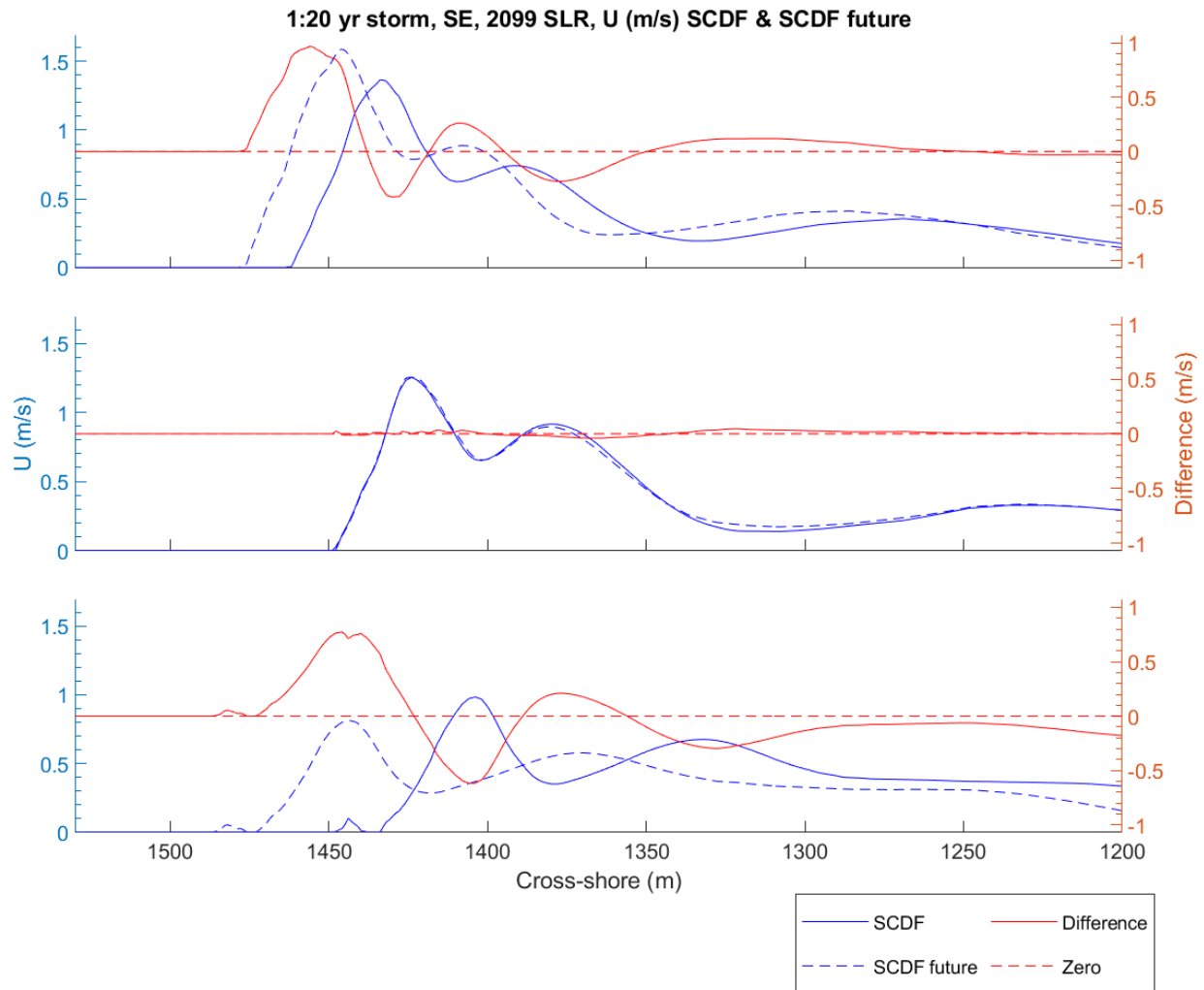


Figure E-32. South East 1-in-20 year storm, 2099 Sea Level – Average current speeds over the simulation for the SCDF, SCDF-future and the difference between the SCDF and SCDF-future average current speeds. Plots show profiles  $Y_1$  (top),  $Y_2$  (middle) and  $Y_3$  (bottom), indicated as red lines in figure above.

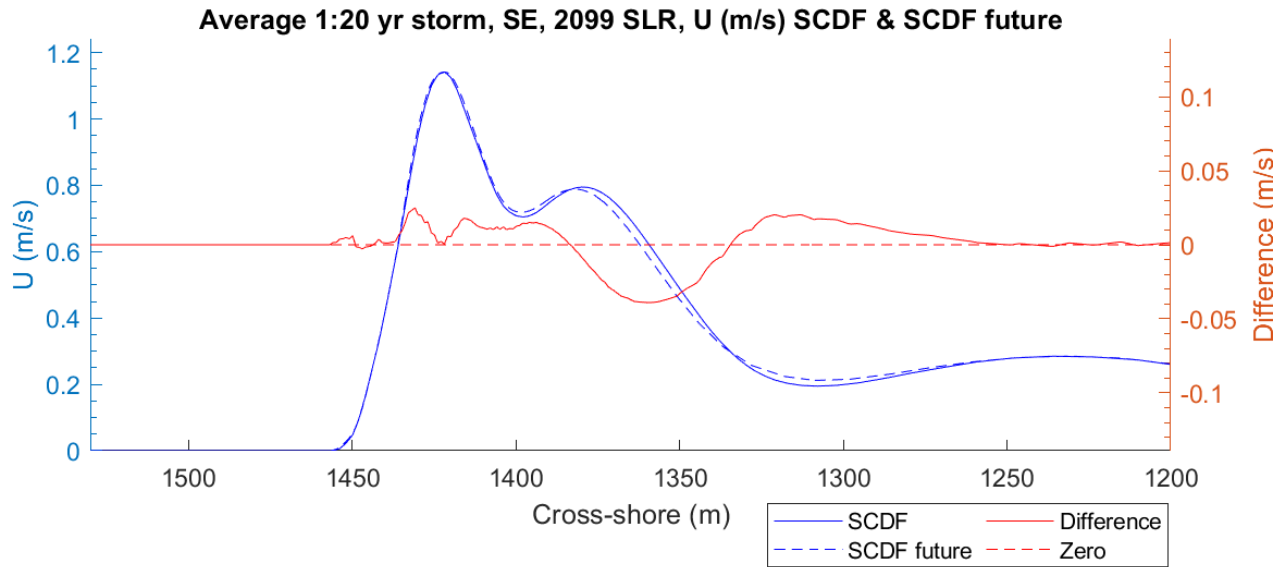


Figure E-33. South East 1-in-20 year storm, 2099 Sea Level – Average current speeds over the simulation for the SCDF and SCDF-future averaged along the frontage of the SCDF ( $Y_{average}$ ), and the difference between the SCDF and SCDF-future average current speeds.



1:20 yr storm, SE, 2099 SLR, Bed Shear Stress ( $\text{N/m}^2$ ) and Sediment Flux ( $\text{m}^2/\text{s}$ )

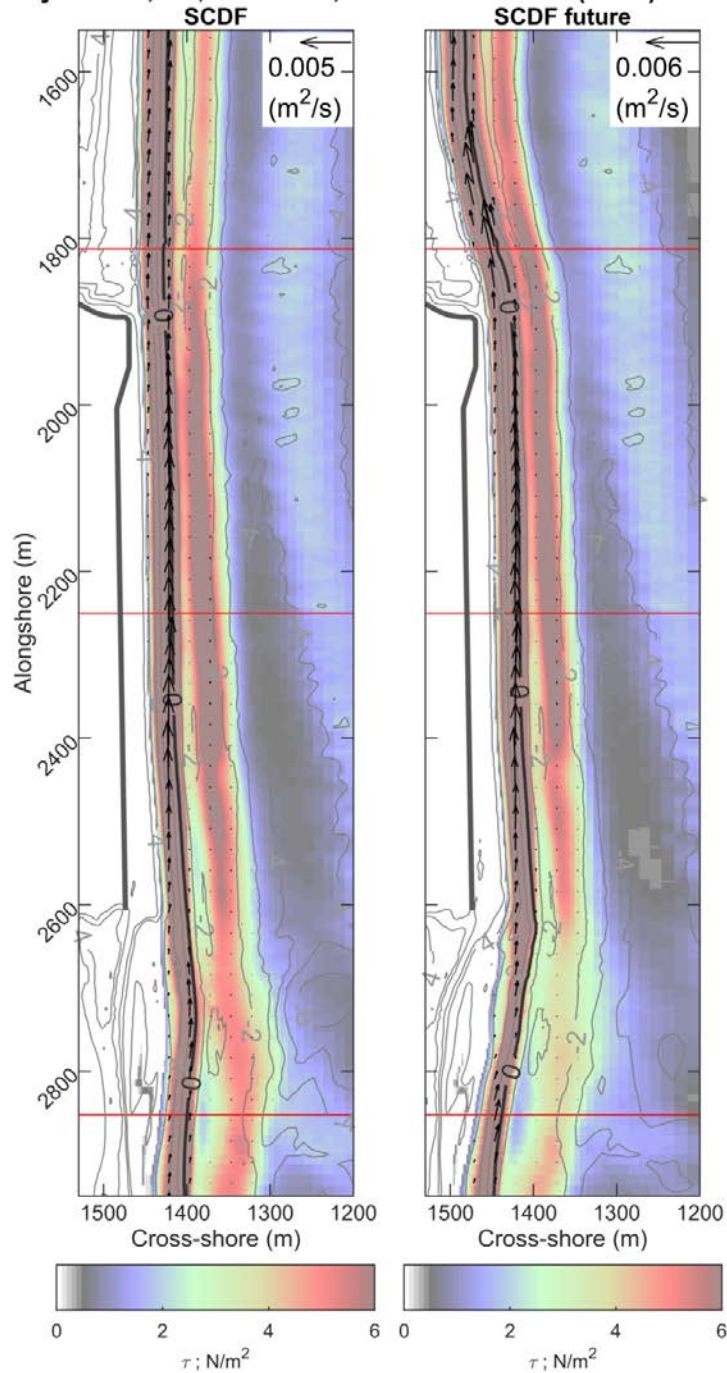


Figure E-34. South East 1-in-20 year storm, 2099 Sea Level – 2D average bed shear stress and sediment flux over the simulation for the SCDF (left) and SCDF-future (right). The red lines indicate the locations of the cross-sectional plots presented in the figure below.

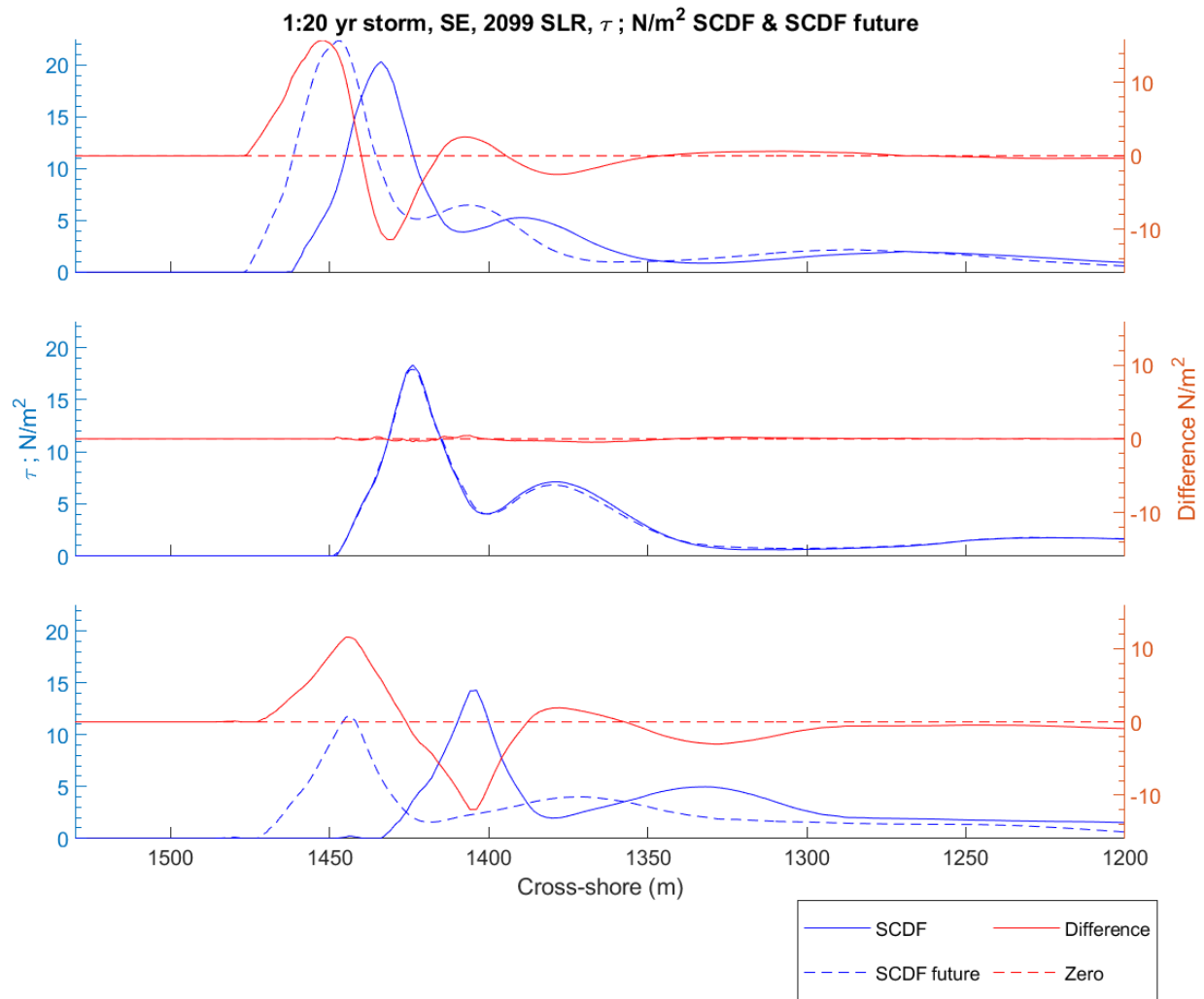


Figure E-35. South East 1-in-20 year storm, 2099 Sea Level – Average bed shear stress over the simulation for the SCDF, SCDF-future and the difference between the SCDF and SCDF-future average bed shear stress. Plots show profiles  $Y_1$  (top),  $Y_2$  (middle) and  $Y_3$  (bottom), indicated as red lines in the figure above.

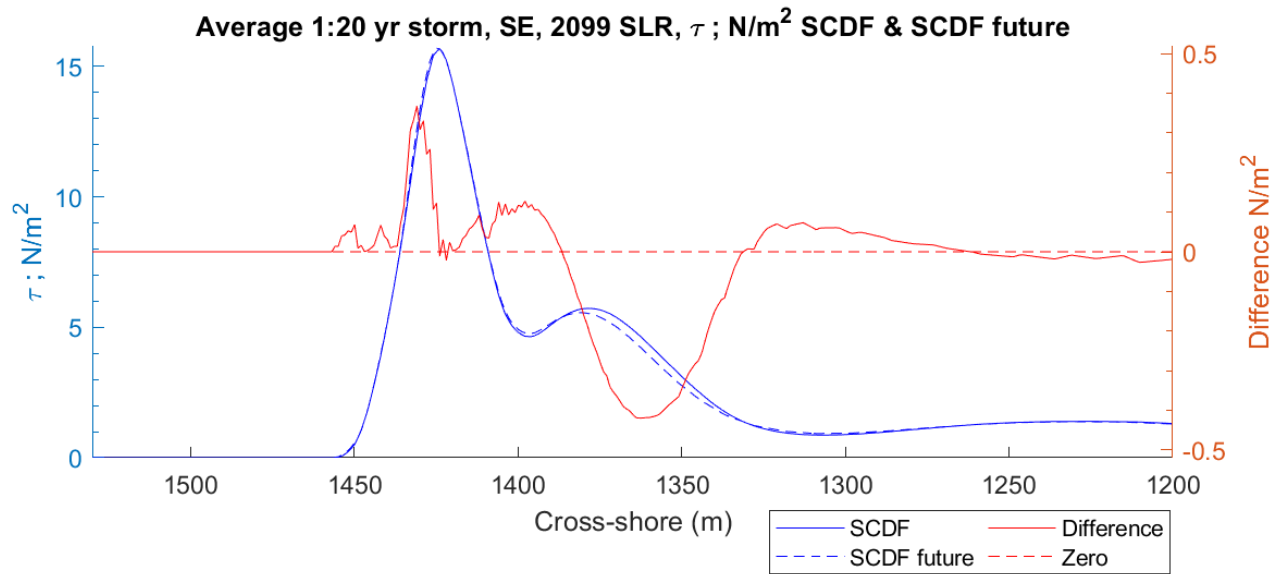


Figure E-36. South East 1-in-20 year storm, 2099 Sea Level – Average bed shear stress over the simulation for the SCDF and SCDF-future averaged along the frontage of the SCDF ( $Y_{\text{average}}$ ), and the difference between the SCDF and SCDF-future average bed shear stress.